Complement, Antimicrobial, and Neutrophil Responses to *Neisseria gonorrhoeae*

Evan R. Lamb
Robins, Iowa

Bachelor of Science, University of Iowa, May 2019

A Dissertation presented to the Graduate Faculty
of the University of Virginia in Candidacy for the Degree of
Doctor of Philosophy

Department of Microbiology, Immunology, and Cancer Biology
University of Virginia

May 2025

ABSTRACT

Neisseria gonorrhoeae (the gonococcus, Gc) is a Gram-negative bacterium and causative agent of the sexually transmitted infection gonorrhea. Gonorrhea is an urgent public health threat with rising incidence rates and detrimental effects on health and fertility. Gc colonizes its obligate human host at mucosal surfaces where it encounters a robust innate immune defense response including the complement system and neutrophils. However, Gc has evolved many mechanisms to evade killing by the human immune system. Moreover, Gc is rapidly becoming resistant to all classes of antibiotics used to combat this pathogen. Understanding the interplay between these opposing forces will be critical to developing new therapeutics and vaccines against this threat.

A major function of the complement system is to generate 10-11nm membrane attack complex pores (MAC) comprised of components C5b-C9 which directly kill Gram-negative pathogens. Here, I found that MAC deposition disrupted both the gonococcal outer and inner membranes and broadly enhanced the activities of antibiotics as well as host-derived antimicrobials. MAC deposition re-sensitized a multidrug-resistant Gc isolate to clinically relevant antibiotics. I also found that complement complexes lacking C9 (2-4nm pores) were capable of anti-gonococcal bactericidal activity and increased activities of antimicrobials <2nm in diameter but that larger antimicrobials >4.5nm in diameter remained ineffectual. These findings shed further light on the biology and multifunctional capacity of the MAC to control bacterial pathogens.

Immune control of Gc is also mediated by neutrophils, the first responders to infected mucosa. Interactions with pathogens or soluble factors at the neutrophil surface are critical for neutrophil activation and functions. To characterize neutrophil responses to inflammatory stimuli, I led the design of a designed a 22-color spectral flow cytometry panel profiling primary human neutrophil surface markers for phagocytosis, degranulation, migration, and chemotaxis. Care was taken to maximize panel adaptability to broad research questions in the field of neutrophil biology. This panel revealed that neutrophils exhibit conserved responses to known activating agents and Gc. However, the primary neutrophils demonstrated both intra- and inter-donor variability. Neutrophil activation correlated with infectious dose and number of Gc associated per neutrophil as determined by imaging flow cytometry. Multidimensional analyses identified neutrophil subpopulations in response to Gc infection and showed gonococci expressing opacity-associated adhesins more readily associated with neutrophils.

Neutrophil interactions with mucosal pathogens occur at an epithelial surface which the neutrophils must traverse to engage the adhered bacteria. To this end, we examined a Transwell filter support system with an endocervical epithelial layer, infecting Gc, and migrating primary human neutrophils. Preliminary results showed transmigration across an infected epithelium in response to an as of yet unidentified bacterial stimulatory factor. Transepithelial migration was also observed to decrease neutrophil bactericidal activity against Gc compared to a non-transmigration model.

Taken together, results from this work expand understanding on how cooperative innate immune effectors respond to and kill Gc. Complement complexes with and without C9 can both control Gc and enhance antimicrobial activity against this increasingly antibiotic-resistant pathogen. Gc induces heterogenic neutrophil activation and phagocytosis of the infecting bacteria with to be discovered impact on Gc viability. Understanding these phenomena can advance therapeutic developments that exploit complement-antimicrobial synergy to combat multidrug-resistant Gc and promote neutrophil subpopulations which better combat gonococci.

ACKNOWLEDGEMENTS

I want to express my deepest gratitude to everyone who helped make this work possible and supported me along this journey.

To the members of the Criss Lab – Aimee, Allie, Amaris, Amy, Asya, Cami, Chris, Ian G., Ian L., Jocelyn, Keena, Lacie, Mary G., and Mary B. – thank you so much for your friendship, mentorship, and compassion. You all made coming into lab a joy and helped to make the tough days brighter. Alison, thank you for your deep dedication to your lab members. You always strove to support our science, our training, and us as individuals.

Thank you to the scientific community at UVA for its commitment to fostering trainees and advancing biomedical research. Thank you to the members of my thesis committee – Melissa Kendall, Loren Erickson, Molly Hughes, and Anne Sperling – our meetings were productive and inspiring. Thank you to those in the Microbiology, Immunology, and Cancer Biology Department and with UVA's Medical Scientist Training Program for all the mentorship and support along the way – specifically Dean Kedes, Mariano Garcia-Blanco, Judith Woodfolk, Ashley Woodard, Lucy Pemberton, Kate Creveling, Jennifer Hamlin, and all the members of GermJam (née CKAD).

Thank you to our many collaborators and colleagues who made this work possible. Mike Solga, Taylor Harper, and Lesa Campbell in the Flow Cytometry Core Facility were essential in my training and in conducting this science. Ron Taylor, Sanjay Ram, and Anna Blom were our gurus on the complement system

throughout this work; Anne Jerse and J. Alex Duncan and their lab members were a joy to work with on our vaccine-related projects.

Thank you to my mentor at the University of Iowa – Linda McCarter – your support and inspiration is why I chose to become a scientist.

Thank you to my family, especially my parents John and Martha Lamb for supporting me in this endeavor, encouraging me to be a nerd and follow my dreams, and for loving me unconditionally. To my friends near and far, to those who stood by me in the tranches of Undergrad, Grad School, and Med School – I wouldn't have made it here without you. To my best friend – AJ Santiago – you have been the best partner and support system I could ask for. I'm excited to start the next chapter with you by my side.

TABLE OF CONTENTS

FIGURES

TABLES

ABBREVIATIONS

1°	primary
Adh	Adhered
AF	AlexaFluor
ATCC	American Type Culture Collection
AUC	Area Under the Curve
Az	Azithromycin
BSA	Bovine Serum Albumin
BUV	Brilliant Ultraviolet
BV	Brilliant Violet
C’	Complement
C4BP	C4b-Binding Protein
CAMP	Cationic Antimicrobial Peptide
CCM	Carcinoembryonic Antigen-Related Cell Adhesion Molecule
CDC	Centers for Disease Control and Prevention
CEACAM	Carcinoembryonic Antigen-Related Cell Adhesion Molecule
CFU	Colony Forming Unit
CHIM	Controlled Human Infection Model
CLSI	Clinical & Laboratory Standards Institute
CR	Complement Receptor
CRIg	Complement Receptor of the Immunoglobulin superfamily
CRO	Ceftriaxone
CRP	C-reactive protein
CTB	CellTrace Blue

CTY	CellTrace Yellow
CyTOF	Cytometry by time-of-flight
Da	Daltons
DGI	Disseminated Gonococcal Infection
Doxy	Doxycycline
DoxyPEP	Doxycycline Post-Exposure Prophylaxis
DPBS	Dulbecco's Phosphate-Buffered Saline
DPBSG	Dulbecco's Phosphate-Buffered Saline with glucose
ECM	Extracellular matrix
EGASP	Enhanced Gonococcal Antimicrobial Surveillance Programme
EPT	Expedited Partner Therapy
FB	Factor B
FBS	Fetal Bovine Serum
FcR	Fc Receptor
FD	Factor D
fHbp	Factor H binding protein
FITC	Fluorescein isothiocyanate
FMO	Fluorescence Minus One
fPR	Formyl Peptide Receptor
FQ	Fluoroquinolone
FSC	Forward Scatter
GASP	Gonococcal Antimicrobial Surveillance Program
Gc	Gonococcus, *Neisseria gonorrhoeae*
GCB	Gonococcal Base (Media)

GCBL	Gonococcal Base Liquid (Media)
GISP	Gonococcal Isolate Surveillance Project
GPCR	G protein-coupled receptor
HBSS	Hank's Balanced Salt Solution
HI	Heat Inactivation, Heat Inactivated
hpi	hours post-infection
HSPG	Haparan sulfate proteoglycan
HXA_3	Hepoxilin A_3
IAP	Integrin-associated protein
ICAM	Intercellular adhesion molecule
Ig	Immunoglobulin
IL	Interleukin
IM	Intramuscular
ITAM	Immunoreceptor tyrosine-based activation motif
ITIM	Immunoreceptor tyrosine-based activation motif
kDa	Kilodaltons
KDO	3-deoxy-D-manno-octulosonic acid
KSFM	Keratinocyte serum-free media
LOS	Lipooligosaccharide
LOX	Lipoxygenase
LPS	Lipopolysaccharide
LTB_4	Leukotriene B_4
MAC	Membrane Attack Complex
MASP	Mannose-associated serine protease
MBL	Mannose-binding lectin

MFI	Median Fluorescence Intensity
MIC	Minimum Inhibitory Concentration
MIP	Macrophage Infectivity Potentiator-like protein
MMLV	Moloney murine leukemia virus
MMP	Matrix mtalloprotease
MOI	Multiplicity of infection
MOPS	3-(N-morpholino)propanesulfonic acid
MPO	Myeloperoxidase
m-YFP	membrane-Yellow Fluorescent Protein
NAAT	Nucleic Acid Amplification Tests
NANA	N-acetylneuraminic acid
NFY	NovaFluor Yellow
NFY700	NovaFluor Yellow 700
NHBA	Neisserial Heparin Binding Antigen
NHS	Normal Human Serum
NIR	Near-infrared
NPN	1-N-phenylnapthylamine
OMCI	*Ornithodoros moubata* Complement Inhibitor
OMV	Outer Membrane Vesicle
Opa	Opacity-associated protein
P.IA	Porin 1B
P.IB	Porin IA
PBS	Phosphate-Buffered Saline
PEA	Phosphatidylethanolamine
PEP	Post-exposure prophylaxis
PFA	Paraformaldehyde
PI	Protein I

PID	Pelvic Inflammatory Disease
PII	Protein II
PIII	Protein III
PKC	Protein Kinase C
PLA2	Phospholipase-A_2
PLC	Phospholipase C
PMA	Phorbol 12-myristate 13-acetate
PMF	Proton Motive Force
PMN	Polymorphonuclear Leukocyte
PPNG	Penicillinase-producing *Neisseria gonorrhoeae*
PTX	Pentraxin
Rmp	Reduction modifiable protein
ROS	Reactive Oxygen Species
RPMI	Roswell Park Memorial Institute Medium
SAP	Serum amyloid P
SBA	Serum Bactericidal Assay
SEM	Scanning Electron Microscopy
SIRP	Signal-regulatory protein
SSC	Side Scatter
STI	Sexually Transmitted Infection
TAN	Tumor-associated neutrophil
TIV	Tag-it Violet
TLR	Toll-like Receptor
TM	Transmigrated
UK	United Kingdom
UMAP	Uniform Manifold Approximation and Projection
US	United States

Vn	Vitronectin
VSV-G	Vesicular stomatitis virus glycoprotein
WHO	World Health Organization
WT	Wildtype, wild-type
YFP	Yellow Fluorescent Protein
ZNIR	Zombie Near-infrared

1 INTRODUCTION

1.1 *Neisseria gonorrhoeae* & gonococcal infections

1.1.1 Clinical manifestations & epidemiology.

Neisseria gonorrhoeae (the Gonococcus, Gc) is the causative agent of the sexually transmitted infection (STI) gonorrhea, disseminated gonococcal infections (DGI), and resulting clinical sequelae.[1] Gonorrhea is most frequently acquired through close sexual contact, with primary infection sites being mucosa of the urogenital tract, anorectum, and oropharynx.[2] Gonorrhea can also present as an ocular infection particularly through vertical transmission at childbirth (*ophthalmia neonatorum*).[1,3]

Signs and symptoms of local gonorrhea include pain/discomfort, dysuria, and a purulent exudate/discharge.[4] For urogenital infections, symptom onset generally occurs 1-6 days after exposure.[5] However, many individuals remain asymptomatic. Oropharyngeal and anorectal infections seldom result in appreciable signs or symptoms. Urogenital infections in men, in which the urethra is the primary infection site, are symptomatic in 80% of cases. In women, in which the cervix is the primary infection site, upwards of 50% of cases remain asymptomatic (Fig. 1A).[1,5] The asymptomatic nature of many infections presents a barrier to diagnosis and treatment without routine testing of sexually active individuals.

In the absence of prompt treatment, bacteria can ascend from primary infection sites to the uterus, fallopian tubes, peritoneal cavity, epididymis, and testes causing inflammation, tissue damage, and scarring. Resulting damage can

present as Pelvic Inflammatory Disease (PID), ectopic pregnancies, epididymitis/orchitis, and infertility. Furthermore, bacteria can disseminate via the bloodstream to distal tissues causing septic arthritis, and rarely, endocarditis and meningitis. Gc infection can also increase susceptibility to HIV infection due to epithelial damage and immune cell recruitment.

Gonorrhea is the second most prevalent bacterial STI with an estimated 82-100 million cases annually worldwide and 600,000 reported cases in the United States in 2023.[3,6] In the US, gonorrhea incidence rates have been increasing for the past decade with a peak at 214 cases per 100,000 people in 2021. Although, cases decreased slightly in 2022 and 2023 with most recent rates at 179.5 cases per 100,000 people (Fig. 1B).[6] Gonorrhea rates are disproportionately elevated in high-risk populations including men who have sex with men, sex workers, and racial minorities.[6] Low- and middle-income countries also report higher gonorrhea incidence on average.[7]

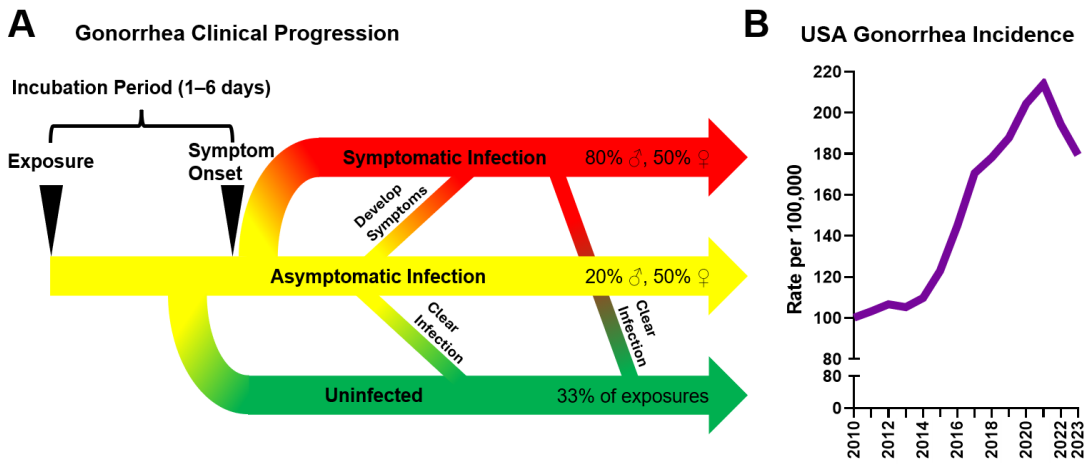

Figure 1. Gonorrhea clinical progression and incidence

(A) Schematic summarizing gonorrhea clinical progression following initial exposure. Infection may present with symptoms or remain asymptomatic. Men (♂) are more likely to present with recognizable symptoms (80%) compared to asymptomatic infection (20%), whereas women (♀) present with or without symptoms at roughly equal rates (50%). Incubation period, the time between exposure and onset of first symptoms, estimated at 1-6 days in cases which develop symptoms. Approximately one quarter of asymptomatic infections have been documented to progress to symptomatic infection with another quarter estimated to clear within one year. Schematic adapted from Lovett and Duncan, 2019.[5] (B) Incidence rate of gonorrhea reported to the CDC from 2010 to 2023. Peak incidence was recorded in 2021 at 214 cases per 100,000 total United States population.

1.1.2 Microbiology of the gonococcus.

Gc is a fastidious Gram-negative diplococcus (Fig. 2A) and bacterial pathogen of its obligate human host.[8] Gc infection is routinely diagnosed by Nucleic Acid Amplification Tests (NAATs) on specimens from suspected infection sites. Bacterial culturing may also be conducted in low resource situations, suspected treatment failure, or disseminated infection/bacteremia.[9] Culturing is predominantly conducted with CO_2-supplemented chocolate agar-based mediums (erythrocyte-lysed blood agar) containing antibiotics (vancomycin, nystatin, colistin, trimethoprim) to select against non-*Neisseria* species found at collection sites.[10,11] Gc colonies isolated on these agar mediums (Thayer-Martin media, Martin-Lewis media) can be further characterized by Gram-stain, oxidase-positivity, and catalase positivity.[4,8,12]

As a Gram-negative bacterium, the gonococcal cell/cytoplasm is bounded by a three-layered envelope of the 1) cytoplasmic/inner membrane, 2) periplasm with cell wall, and 3) outer membrane (Fig. 2).[13] The inner membrane is composed of a phospholipid bilayer and associated proteins which are crucial for maintaining the proton motive force (PMF) of the cell.[14,15] The periplasmic space between the diderm membranes contains 1-2 peptidoglycan layers of the cell wall which confer structure and integrity to the bacterial cell.[16] The outer membrane of *Neisseria* species contains phospholipids and an outer leaflet of lipooligosaccharide (LOS) along with many outer membrane-embedded proteins. These proteins include many factors crucial for gonococcal virulence, physiology, and are promising vaccine candidates.

The major outer membrane proteins of Gc were historically classified as Proteins I, II, and III (PI-III)[17] which correspond to Porin, Opacity-associated proteins (Opa), and reduction modifiable protein (Rmp; Fig. 2B).[18] Together, these proteins constitute >60% of the cell's outer membrane protein repertoire.[17]

Porin (PI, PorB) is the most abundant gonococcal outer membrane protein (32-39 kDa) which forms trimeric β-barrel pores through the outer membrane allowing passive diffusion of solutes <1.4 kDa.[17,19,20] Porin can also enhance host-cell adhesion and invasion. Two porin variants have been described in Gc termed Porin 1A and Porin 1B (P.IA, P.IB). DGI cases are enriched in P.IA-expressing isolates with P.IB being more common in localized/PID infections.[21] This may be due to P.IA's capacity to enhance epithelial cell invasion and the greater capacity of P.IA to bind host-derived complement inhibitors (described in detail later). Porin has been linked to immune system evasion by suppressing the oxidative burst[22], degranulation, actin polymerization, and receptor expression of neutrophils[23]; blocking phagosome maturation in macrophages[24]; and inhibiting dendritic cell-T cell interactions.[25-27] Neisserial Porin has also been reported to both induce and repress apoptosis in host cells[28-31], translocate to host cells causing either activating or apoptosis-inducing ion flux[29,30], and stimulate host cells via Toll-like Receptor 2 (TLR2).[32,33] Discrepancies in these studies may be linked to cell-type, porin variant, and porin conformations (native versus aggregate).

Opa proteins (PII) are a group of outer membrane proteins which form β-barrels containing four unstructured and highly variable extracellular loops.[17,34] Many different Opa variants have been described in Gc with any given isolate

containing at least 10 distinct *opa* loci and expressing 9 to 11 unique Opa proteins.[35-37] Opa proteins are phase-variable, meaning any individual Opa protein can be expressed in an 'ON/OFF' manner. As a result, individual Gc isolates can express no Opa proteins (Opa-), one Opa variant, or multiple Opa variants simultaneously.[38,39] Opa phase variation is achieved by slipped-strand mispairing of CTCTT repeats in the 5' coding region of the *opa* genetic loci. Changes to the number of coding-strand pentamers in the transcribed *opa* gene can place downstream codons in or out of frame, resulting in translation-level presence or absence of expression.[39-41] The variable Opa protein expression pattens influence Gc adhesion to other gonococci and to a variety of host cell-types.[42] Most Opa-Opa interactions between gonococci present as opaque/refractive colony phenotypes when viewed through a bottom-lit stereomicroscope allowing discrimination between Opa-expressing (Opa+) and Opa- colonies.[38,43-45] Most Opa proteins have been shown to bind carcinoembryonic antigen-related cell adhesion molecule family proteins (CEACAMs; CCMs).[46,47] Opa proteins can bind CEACAM-1, -5, and -6 on epithelial cells, thereby enhancing adherence and colonization at mucosal surfaces. Adhesion via CEACAMs can also decrease epithelial cell exfoliation, further supporting the gonococcal niche. On immune cells, such as neutrophils, Opa proteins can bind CEACAM-1, -3, and -6.[39,48] Through these ligand-receptor interactions, Opa-expressing bacteria are more likely to associate with neutrophils resulting in greater phagocytosis and Gc death.[38,39,49] Interestingly, CEACAM-3 on neutrophils contains an immunoreceptor tyrosine-based activation motif (ITAM) which is thought to enhance neutrophil

activation and bactericidal capacity.[49,50] CEACAM-1 engagement also enhances Opa+ Gc association with host cells. However, CEACAM-1 contains an immunoreceptor tyrosine-based inhibitory motif (ITIM) which has been shown to suppress leukocyte activity but its role in neutrophils is less well defined.[51] Results from animal models[52] or natural or Controlled Human Infection Models (CHIM) indicate that Opa+ Gc are selected for during infection. Specifically, Opa proteins that bind CEACAM-1 are enriched in isolates as an infection progresses compared to CEACAM-3-binding Opa proteins, possibly due to the ITIM versus ITAM motifs of their binding partners.[53,54] Opa proteins also interact with heparan sulfate proteoglycans (HSPGs) which enhance invasion into epithelial cells and are hypothesized to bind other host proteins such as the complement inhibitor vitronectin (discussed later).[55,56] In this work, frequent use is made of strain FA1090 Gc which have had all *opa* genes deleted to create a constitutively Opa- strain and a constitutively Opa+ strain with a single Opa protein, OpaD, reintroduced into its native locus with removal of 5' pentameric repeats.[38]

Rmp (PIII) is a 44 kDa OmpA-like protein with a reported periplasmic domain and short surface-exposed residue tract.[57-60] Rmp associates with Porin in the outer membrane at a ratio of three Porin per Rmp molecule. Unlike many other gonococcal surface factors, Rmp does not exhibit appreciable variation among isolates, and conserved surface-exposed epitopes can elicit antibody responses with broad recognition.[18,58,59,61] Anti-Rmp antibodies are protective toward the bacteria as they block the activity of otherwise bactericidal antibodies such as those raised against Porin or LOS (possible mechanisms discussed later).[62-65] The

presence of such blocking antibodies was first appreciated in individuals who had been exposed to/infected with Gc many times.[63] Moreover, anti-Rmp IgG can enhance Gc colonization in murine models of infection.[66] The anti-Rmp antibodies may in part explain why prior gonococcal infection, not merely a prior STI or high-risk behavior, is one of the greatest risk factors/determinants for a new gonococcal infection.[67,68] The role of Rmp antibodies in vaccine-elicited responses remains to be fully explored. However, efforts to generate immunity with outer membrane vesicle (OMV) based vaccines using Rmp mutant strains is underway.[69]

The gonococcal surface is also decorated with proteins with additional important functions or, as of yet, uncharacterized roles (some discussed in greater detail later). Among these are Type IV Pili which aid the bacterium in initial adherence to host epithelia, twitching motility, and uptake of environmental DNA.[70,71] Pili are formed by many protein subunits including an inner-membrane localized platform and ATPases, an outer-membrane pore (PilQ), and pilin subunits which form the principal filament structure of the pilus. The pilus filament is made of the major pilin subunit, PilE, as well as minor subunits (PilC, PilH-L).[72-74] The Type IV Pilus is phase variable meaning a variety of piliation types and unpiliated Gc can be found.[45,75] However, piliation is required for infection as pilus binding to host epithelia enables a bacterium to close the distance and reach the epithelial cell surface where tight, intimate association can occur via factors such as Opa-CEACAM binding.[1,76] Furthermore, the major pilin subunit is antigenically variable in which silent *pilS* loci on the Gc chromosome can recombine with the expressed *pilE* locus, generating epitope diversity and thereby evading antibody

responses.[77-79] Pili function by extending the filament up to multiple cell-lengths from the cell surface (1-2μm on average), allowing the pilus to bind host cells or DNA, then retract the pilus to pull the bacterium closer to host cells or DNA to the bacterial surface in a ‘grappling hook-like’ manner.[80]

Finally, the outer membrane contains abundant LOS, the gonococcal analog to lipopolysaccharide (LPS) of other Gram-negative bacteria.[35] Like LPS, LOS contains a membrane-anchoring lipid A and inner core of 2-keto-3-deoxy-D-manno-octulosonic acid (KDO) and heptose residues. Branching off the inner core are three outer core saccharide chains, however unlike LPS, LOS lacks repeating O-antigens beyond the core saccharide chains.[35,81,82] The LOS structure is under the control of phase variable LOS glycosyltransferases and phosphoethanolamine (PEA) transferase which modulate the core saccharide residues and can add PEA to lipid A, respectively.[81,83] LOS can also be sialylated by the constitutively expressed LOS sialyltransferase (Lst)[84] which caps LOS chains with sialic acid, a molecular mimicry mechanism to suppress the host immune response and recruit host complement inhibitors.[85,86]

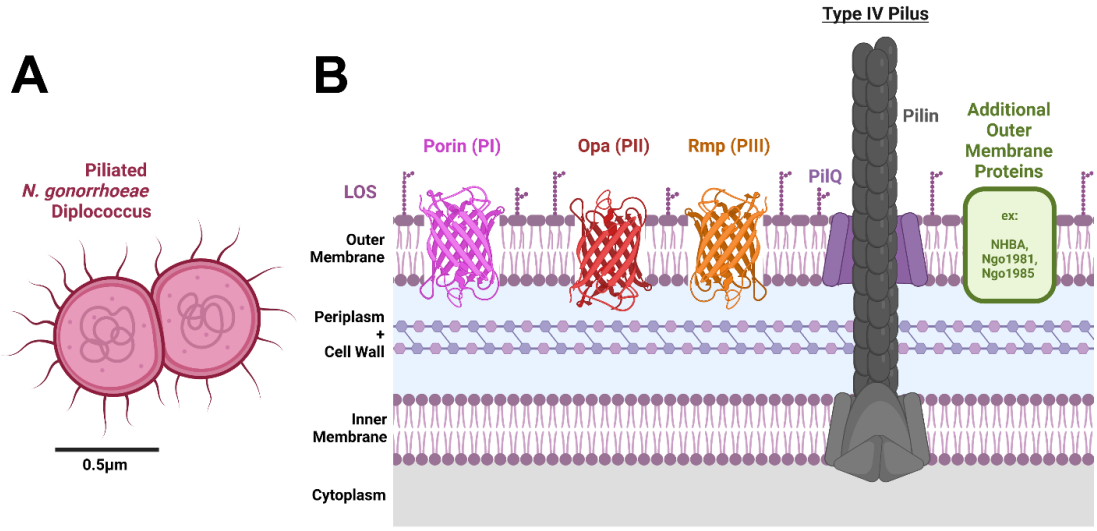

Figure 2. *Neisseria gonorrhoeae* morphology, envelope, and surface structures

(A) Gc is routinely identified through microscopic evaluation in specimens as a small, Gram-negative diplococcus with an individual cell being approximately half a micron in diameter. (B) The Gram-negative cell envelope consists of a surface-exposed outer membrane with lipooligosaccharide (LOS) in the outer leaflet, a periplasm which contains the peptidoglycan cell wall, and an inner membrane phospholipid bilayer which encompasses the bacterial cytoplasm. The outer membrane contains many surface proteins including Porin (PI) channels, opacity-associated proteins (Opa, PII), reduction modifiable protein (Rmp, PIII), among others. The gonococcal surface may also be decorated with Type IV Pili which span the bacterial envelope in which pilin subunits pass through the outer membrane by a pore formed by PilQ.

1.2 Treatments for gonorrhea & antimicrobial resistance

1.2.1 Therapeutic regimens against gonococcal infections.

The United States Centers for Disease Control and Prevention (US CDC) currently recommends a single 500mg intramuscular (IM) dose of the extended-spectrum cephalosporin ceftriaxone as the frontline therapy for uncomplicated cases of gonorrhea in adults, adolescents, and pregnant women.[87,88] This recommendation was enacted in 2020 to replace the prior guideline of 250mg IM ceftriaxone with 1g oral azithromycin (a macrolide) dual-therapy due to increasing isolates (>5%) with azithromycin resistance.[88,89] Dual-therapy had initially been introduced in 2010 with the purposes of 1) treating the Gc infection, 2) avoiding resistance via antibiotics with different mechanisms of action, and 3) treating *Chlamydia trachomatis* co-infection.[89] The current guidelines include treatment with a doxycycline regimen if concurrent chlamydia is identified via positive Gc-Chlamydia NAAT testing.[87,88] The dose doubling from 250mg to 500mg ceftriaxone was in response threats of cephalosporin resistance in part by increasing the free ceftriaxone concentration at the pharynx, a key site in resistance determinant acquisition.[88,90-93]

Specific situations call for alternative gonorrhea treatment regimens and prophylaxis. A 1g ceftriaxone dose is indicated in individuals over 300lbs and daily in DGI cases until the infection is cleared.[87,88] For children <45kg 20-50mg/kg dosing is suggested.[87] In individuals with cephalosporin sensitivities, a 240mg IM dose of the aminoglycoside gentamicin is recommended alongside 2g azithromycin.[87] 800mg oral cefixime can be given as expedited partner therapy

(EPT) in which partners of the primary patient are treated without being directly seen by a physician.[87,94] To prevent *ophthalmia neonatorum*, pregnant women should be screened and treated, and prophylactic erythromycin ointment given <24h after birth to all newborns.[87,95] Post-exposure prophylaxis in adults includes 200mg oral doxycycline (DoxyPEP) within 72h after sexual contact as recommended by the US CDC in June, 2024.[87,96] DoxyPEP shows strong efficacy (70-90%) in preventing chlamydia and syphilis but is less effective against Gc infection. Some studies find decreasing gonorrhea rates by upwards of 50% while others find modest yet significant increases.[96-100]

1.2.2 Epidemiology of drug-resistant gonorrhea.

Gc is rapidly acquiring resistance determinants against most antibiotic classes (Fig. 3A,B).[101,102] The threat of drug-resistant Gc has prompted creation of dedicated efforts and task forces including the WHO's Gonococcal Antimicrobial Surveillance Programme (GASP)[101] and CDC's Gonococcal Isolate Surveillance Project (GISP)[103] to monitor resistance trends. Gonococcal resistance to penicillin and tetracycline antibiotics (e.g. doxycycline) was reported only 1-2 decades after introduction of these antibiotics and has remained at or above 10% of all isolates.[104,105] Resistance to fluoroquinolone antibiotics (e.g. ciprofloxacin) was rapidly reported after introduction and increased in the US from near 0% of isolates in 2000 to ~15% in 2007, prompting the CDC to caution against cephalosporin use against gonorrhea.[87,88,106] Ciprofloxacin resistance rates have continued to rise and are now above 30%. Macrolide resistance, as monitored by decreased azithromycin susceptibility, reached high levels in the

early 2000's globally and spiked above 5% in the US in 2019, prompting cessation of azithromycin use as first-line dual-therapy in 2020 (Fig. 3A).[88,104,107] The Clinical Laboratory Standards Institution (CLSI) in the US sets the decreased azithromycin susceptibility breakpoint at 1µg/mL as determined by minimum inhibitory concentration (MIC).[107] Isolates with resistance levels 256-times greater than this breakpoint have been identified.[104,108]

Increased gonococcal fluoroquinolone resistance led to cephalosporins being the only frontline antibiotics (± combination therapy) recommended against gonorrhea.[106,109] Cefixime, an oral cephalosporin, had been the drug of choice in other countries until resistance rates (MIC>0.25µg/mL) increased across isolates, reaching upwards of 30% in some locales and treatment failures began to arise.[104] In the US, the CDC stopped recommending cefixime around 2011 when resistance rates reached 1.4% (Fig. 3A).[88,109] Ceftriaxone has since been the mainstay of treatment with elevated MIC rates less than 0.4% in the US. However, ceftriaxone-resistant strains have been on the rise globally.[110] The first cases of gonorrhea with elevated ceftriaxone MICs were reported in Japan in 2006 (0.5µg/mL) and 2010 (4µg/mL). The 2010 isolate was characterized as strain H041 which is used extensively in this body of work.[110,111] Ceftriaxone resistant strains have continued to spread, being subsequently identified in France, Spain, the UK, Australia, Southeast Asia, and recently in the US.[104] Globally, ceftriaxone resistance rates from 2015-2022 have averaged 0.8% of isolates but can exceed 38% in certain locales as observed in Cambodia by the WHO Enhanced GASP (EGASP) 2022 Report (Fig. 3A).[112,113]

This alarming rise in antimicrobial resistance has placed Gc among the highest-priority pathogens to combat by developing and bringing to market new pharmaceuticals, novel therapeutic strategies, and vaccines. Two prominent investigatory therapeutics are zoliflodacin and gepotidacin which have shown promise in recent phase 3 clinical trials (clinicaltrials.gov NCT03959527 & NCT04010539, respectively).[114-117] Both orally dosed regimens met the endpoint of non-inferiority versus IM ceftriaxone plus oral azithromycin, cured >95% of infections, and showed *in vitro* activity against Gc strains resistant to other classes of antibiotics.[118,119] Zoliflodacin is a first-in-class spiropyrimidinetrione which acts on the GyrB topoisomerase II (Fig. 3B).[116,118] Gepotidacin is a first-in-class triazaacenaphthylene which targets the DNA gyrase GyrA and ParC topoisomerase IV (Fig. 3B).[115] Both compounds act at different sites on their targets than each other or fluoroquinolones and show no evidence of cross-resistance.[120] However, mutations in GyrB and ParC which confer zoliflodacin and gepotidacin resistance, respectively, can be selected for *in vitro* after incubation with sublethal concentrations.[118,121] This is particularly a concern regarding pharyngeal Gc infections in which treatment failure may result due to lower tissue bioavailability.

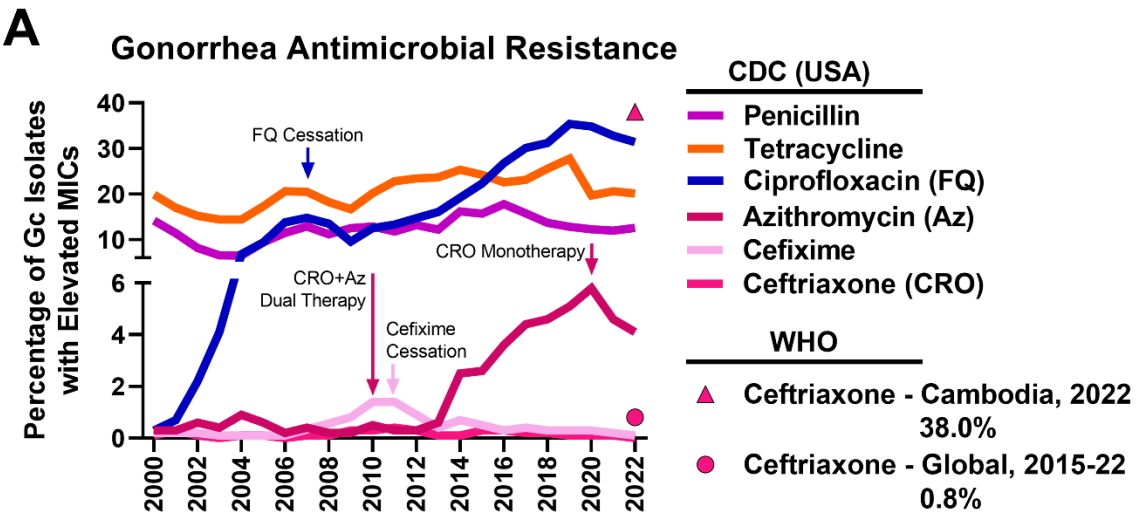
A
Gonorrhea Antimicrobial Resistance
Percentage of Gc Isolates with Elevated MICs
FQ Cessation
CRO Monotherapy
CRO+Az Dual Therapy
Cefixime Cessation
CDC (USA)
Penicillin
Tetracycline
Ciprofloxacin (FQ)
Azithromycin (Az)
Cefixime
Ceftriaxone (CRO)
WHO
Ceftriaxone - Cambodia, 2022 38.0%
Ceftriaxone - Global, 2015-22 0.8%

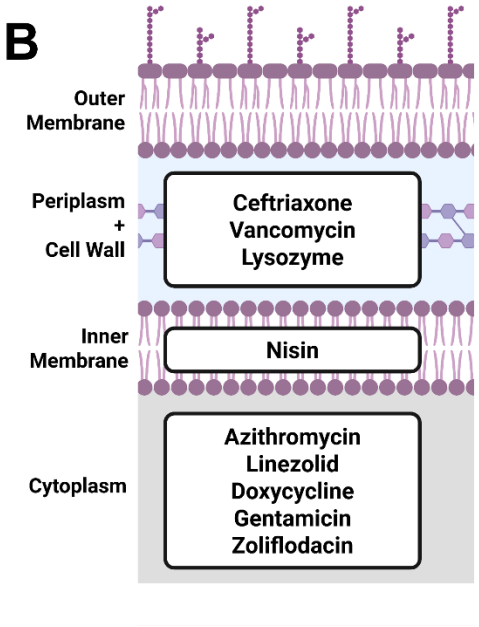
B
Outer Membrane
Periplasm + Cell Wall
Ceftriaxone
Vancomycin
Lysozyme
Inner Membrane
Nisin
Cytoplasm
Azithromycin
Linezolid
Doxycycline
Gentamicin
Zoliflodacin

Figure 3. Timeline of antimicrobial resistance in gonorrhea isolates

(A) Percentage of tested Gc isolates with elevated MIC levels in the United States as reported by the CDC or globally as reported by the WHO from 2000 to 2022. Antibiotics belong to the following antibiotic classes: penicillin, beta-lactam; tetracycline is the namesake for its antibiotic class and is a correlate for doxycycline resistance; ciprofloxacin, fluoroquinolone (FQ); azithromycin (Az), macrolide; cefixime and ceftriaxone (CRO), cephalosporin beta-lactams. Cambodia data presented from the Enhanced Gonococcal Antimicrobial Surveillance Programme (EGASP) of the WHO. Recommendations against fluoroquinolone and cefixime as therapies were issued in 2007 and 2011, respectively. Dual-therapy with ceftriaxone and azithromycin was recommended as the primary treatment regimen in 2010 but discontinued in favor of ceftriaxone monotherapy in 2020. (B) Location of action within the gonococcal cell for antimicrobials used in this body of work. Periplasm/Cell Wall, ceftriaxone, vancomycin, lysozyme; Inner Membrane, nisin; Cytoplasm, azithromycin, linezolid, doxycycline, gentamicin, zoliflodacin.

1.2.3 Mechanisms of antibiotic resistance in Gc.

Gc possesses numerous antibiotic resistance mechanisms, both acquired and intrinsic (Fig. 4). The rapid rise in antibiotic resistance in this pathogen has been linked to its natural competence to DNA uptake, allowing ready acquisition of new resistance alleles/genes. Gc exists in polymicrobial contexts at mucosal infection sites which enables transformation of novel DNA from other organisms. Commensal *Neisseria* species, common pharyngeal residents, are thought to be a natural source for antibiotic resistance in Gc as they are exposed to sublethal antibiotic concentrations in the context of treating other infections.[104,122,123] Acquired resistance determinants in Gc are both chromosomal and plasmid-based in nature.[104,124]

Plasmid-borne resistance in Gc is primarily conveyed via beta-lactamases, enzymes which degrade beta-lactam antibiotics in the extracellular or periplasmic space.[125] The TEM-1 (class A) beta-lactamases produced by Gc confer resistance to penicillin and ampicillin. These isolates are termed penicillinase-producing *Neisseria gonorrhoeae* (PPNGs).[124]

Resistance to other beta-lactam antibiotics and additional antibiotic classes are generally chromosomally encoded and mediated by non-cleavage-based mechanisms. A common mechanism is to acquire altered alleles for antibiotic targets, reducing drug-target interactions while preserving the biologic activity of the altered gene product. The most extensively characterized target is the penicillin-binding protein PBP2-transpeptidase.[124,126] This enzyme is responsible for peptidoglycan cross-linking and is the target of beta-lactam

antibiotics, notably ceftriaxone.[104] Alterations to the *penA* gene, encoding PBP2, can confer high-level ceftriaxone resistance.[104,111] More than 480 unique *penA* alleles have been described.[124,127] These are classified as mosaic, semi-mosaic, and non-mosaic based on origin and number of resultant amino acid substitutions.[124,128] Mosaic *penA* alleles (such as that of H041) confer the greatest ceftriaxone resistance and contain upwards of 60 amino acid alterations from the wild-type allele. Gc acquires mosaic alleles via recombination with commensal *Neisseria* species. Semi-mosaic alleles contain ~20-30 amino acid alterations whereas non-mosaic alleles possess fewer than 13 alterations and are mostly localized to the C-terminus.[124] In addition to PBP2-conferred beta-lactam resistance, Gc can commonly acquire macrolide resistance via altered 23S rRNA, L22 and L4 ribosomal proteins; fluoroquinolone resistance via altered DNA gyrases/topoisomerases (GyrA, ParC, ParE); tetracycline resistance via altered S10 ribosomal protein; spectinomycin resistance via altered 16S rRNA and 5S ribosomal protein; and aminoglycoside resistance via altered elongation factor G.[124]

In addition to altering antibiotic targets, Gc can acquire resistance by altering the channels which allow antibiotics to bypass the Gram-negative outer membrane.[110,111,124] The outer membrane is a significant, intrinsic determinant of antimicrobial resistance as it blocks permeation by compounds that are too large (>600 Da) or too electrostatically unfavorable.[129,130] Gram-negative bacteria make use of porins (i.e. PorB in Gc) in the outer membrane to facilitate solute diffusion. These porins also accommodate antibiotics, increasing access to their

targets. Amino acids substitutions in the channel of PorB (*penB* mutants) can decrease Gc susceptibility to penicillins, cephalosporins, and tetracyclines.[131] Mutations in PilQ (*penC* mutants), the outer membrane pore through which the gonococcal Type IV Pili filaments protrude, can also confer penicillin and tetracycline resistance. However, PilQ mutations have thus far only been isolated in the laboratory setting as PilQ is required for proper pilus function and natural infection.[132,124]

Gc can also express efflux pump systems which export harmful compounds out of the bacterial cytoplasm and/or periplasm to the extracellular space.[15] The most prominent gonococcal efflux apparatus is the MtrCDE system which is highly expressed in many drug-resistant isolates including H041.[110,133] Increased expression is commonly achieved by mutations in the regulatory protein MtrR or in the MtrR-binding region upstream of *mtrCDE*.[133,134] MtrD forms an inner membrane PMF-powered transport protein, MtrE forms an outer membrane channel, and MtrC bridges the bilayer-spanning apparatus.[15] The MtrCDE system effluxes macrolides, beta-lactams including cephalosporins, and tetracyclines, as well as host-derived compounds such as cathelicidins bile salts, and progesterone.[15] MtrE is also associated with the MacAB-MtrE efflux system, which is known to export macrolides, and the FarAB-MtrE system which exports host-derived fatty acids. The NorM and MtrF efflux systems are localized to the inner membrane and efflux fluoroquinolone and sulfonamide antibiotics, respectively.[15] As they export both antibiotics and host-derived antimicrobials, the role of efflux pumps in Gc pathogenesis is thought to occur both in subverting

therapeutic regimens and overcoming host immune responses enabling gonococcal colonization.[15,135,136]

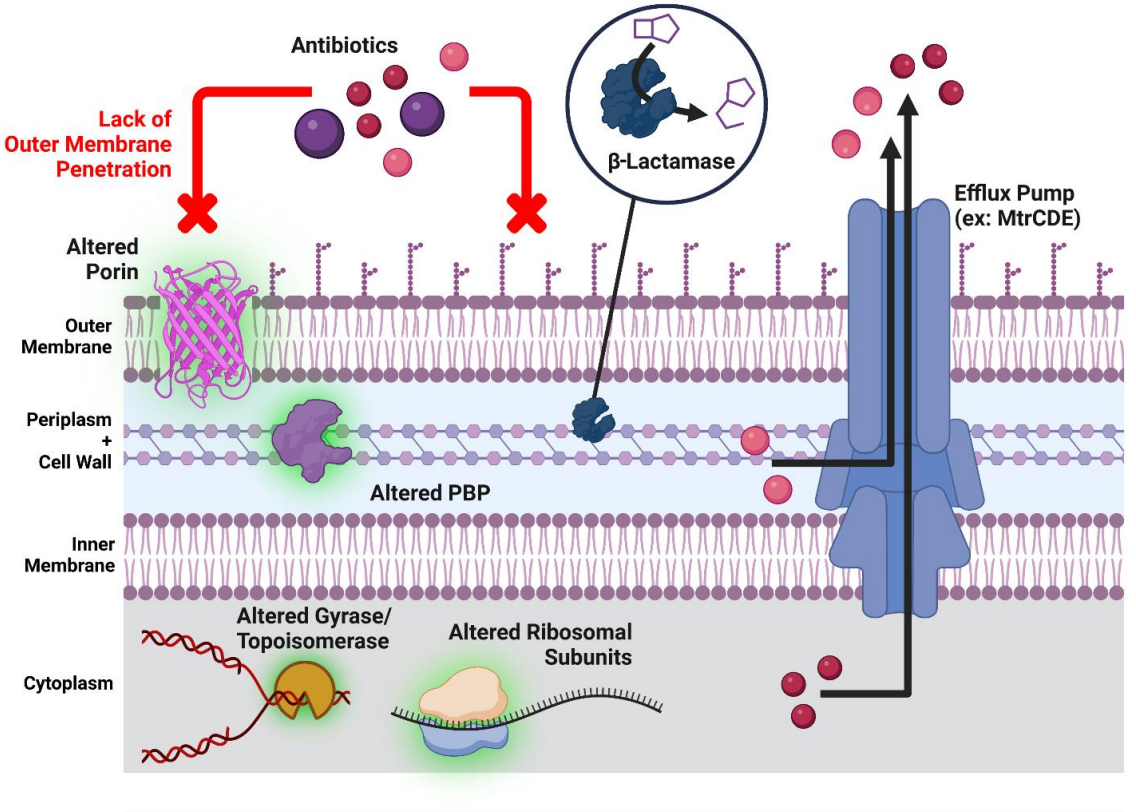

Figure 4. Mechanisms of antibiotic resistance in *N. gonorrhoeae*

Gc possesses many mechanisms which can work in concert and can function against multiple antibiotic classes. The outer membrane prevents diffusion of many antibiotics into the periplasm or cytoplasm, precluding access to their targets. Porin in the outer membrane can be altered to decrease antibiotic diffusion through these pores. Beta-lactams can be degraded by secreted beta-lactamases. Antibiotic targets (e.g. penicillin-binding proteins, DNA gyrases and topoisomerases, and ribosomal units) can be altered to decrease antibiotic binding/activity. Antibiotics can also be actively exported from the cytoplasm or periplasm by efflux pumps such as the MtrCDE system.

1.3 Immune responses to Gc

Gc encounters the forces of innate and adaptive immunity at mucosal surfaces of primary infection as well as in the bloodstream and distal sites when disseminated.[1,21] Innate immune responses are first-line general defenses against a broad array of potential pathogens.[21,137-142] Among these defenses are the complement system, phagocytes including neutrophils, and secreted antimicrobial compounds, factors which are the principal subjects of investigation in this work. Other notable innate defenses against Gc are mucus/epithelial barriers against dissemination, host nutrient-sequestering factors[143], and commensal microbes that occupy would-be Gc niches.[52,144-146] The specific and acquired adaptive immune system against Gc is limited but includes T-cell and B-cell responses with the latter producing IgG, IgM, and IgA antibodies. These immunoglobulins can be elicited by prior Gc infection or be cross-reactive against Gc if elicited by similar commensal species.[62,63,147]

1.3.1 The complement cascade: activation, effector functions, & Gc resistance.

1.3.1.1 Complement pathways and activation.

The complement system (Fig. 5) is a repertoire of more than 50 core proteins, related factors, receptors, and inhibitors.[21,137-142] Complement systems have a deep evolutionary history, present in animal life as phylogenetically disparate from humans as sea squirts/tunicates (conserved within the phylum Chordata).[148] In humans complement proteins are most abundant in serum where they circulate to body sites as an innate immune mechanism against

invading pathogens.[21,142,149,150] Core complement components sequentially activate/recruit one another in an enzymatic cascade to deposit complement products on targeted cells and to release soluble signaling factors.[21,142,151] Complement is canonically divided into three pathways based on initial activation steps and components.[138,142]

The Classical Pathway is initiated by IgG or IgM binding to their cognate antigens. Membrane-localization of antigens more robustly activates classical complement as it supports antibody clustering and conformations which recruit the first core complement component, C1q. IgM is a more effective recruiter and activator of C1q than IgG due to its pentameric structure and enhanced antigen avidity. Among the IgG subclasses, differential Fc-region structure and glycosylation determine complement activation with IgG3 being the most potent, followed by IgG1 then IgG2 with IgG4 stimulating very little complement activation.[152,153] Engineering antibodies to express different Fc-region subclasses, to be multimerized (pentamers or hexamers), or to express chimeric Fc-regions matching host complement source can increase their complement fixation capacity.[154-156] In addition to immunoglobulins, pentraxin-family proteins can recruit C1q and induce complement activity. Pentraxins include pentraxin-1 through -3 as well as the acute phase proteins serum amyloid P (SAP) and C-reactive protein (CRP) a common clinical diagnostic marker for inflammatory processes.[157,158] Following C1q recruitment, C1r is activated followed by C1s in an autocatalytic cascade to form the C1 complex.[21]

The Lectin Pathway is activated by host lectin proteins binding their cognate glycan moieties on targets. Predominant lectins include mannose-binding lectin (MBL) and ficolins.[21] These high-avidity proteins recruit mannose-associated serine protease 1 and 2 (MASP1, MASP2), the lectin pathway's equivalent of C1r and C1s, respectively.

C1 complexes and lectin-MASP complexes cleave complement components C4 then C2 to generate membrane-localized C4b and C2b which then associate to form the 'classical C3 convertase' (C4bC2b, historically C4bC2a). C3 convertases cleave component C3 into C3a and C3b, the keystone step in complement activation onto which all complement activation pathways converge.[21]

To generate C3a and C3b, the final canonical complement pathway, the Alternative Pathway, relies on spontaneous hydrolysis of soluble C3 upon H_2O incorporation as C3-H_2O. This then allows Factor B to bind the C3 product and Factor D to subsequently form the 'soluble alternative C3 convertase' (C3(H_2O)Bb).[21] This generates more C3b which can be either in suspension where it can form more soluble C3 convertases, or it can bind nearby membranes. Membrane-bound C3b (from any of the pathways) can then associate with Factor B and be cleaved by Factor D, generating the 'membrane-bound alternative C3 convertase' (C3bBb). Through Factor B association and cleavage, the alternative C3 convertases form a feedforward amplification-loop to generate more C3b.[159] Because spontaneous C3 hydrolysis from the Alternative Pathway alone results in background C3b generation and little bactericidal

activity, the principal role of the Alternative Pathway is believed to be its amplification capacity of membrane-bound C3b.[21,159,160]

Ultimately, membrane-bound C3b associates with either the classical or alternative membrane-bound C3 convertases to form the next enzymatic complex in the cascade: the C5 convertase (C4bC2bC3b or C3bBbC3b, respectively).[21] These complexes cleave component C5 into soluble C5a fragments and C5b which associates with nearby membranes. C5b is the first component of the 'terminal' complement components, C5b-C6-C7-C8-C9. Components C5b-C9 ultimately associate to form lytic pores in lipid bilayers which can lyse the targeted cells.[161] As an immune response, complement-mediated cell lysis is directed against pathogens (Gram-negative bacteria, enveloped viruses, and protozoal parasites) and malignant host-cells.[162,163] Dedicated and detailed discussion of terminal complement complex generation, functions, and mechanisms are presented in subsequent sections.

Many processes in the complement cascade are highly regulated to prevent off-target effects and damage to host tissues. Auto-antibodies, inhibitor deficiencies, and many other causes can lead to over-activation of the core complement cascade and produce serious pathologies in nearly every organ system.[164,165] The function of membrane-bound C3b can be modulated, based on cognate receptor recognition, through cleavage into degradation products (iC3b, C3c, C3d, C3dg) by specific complement inhibitors and general proteases.[21,166] Negative regulators of complement are discussed later in their relation to *Neisseria* immune evasion.[21] A notable positive regulator is the host protein

properdin which supports complement activity by stabilizing alternative C3 and C5 convertases.[21]

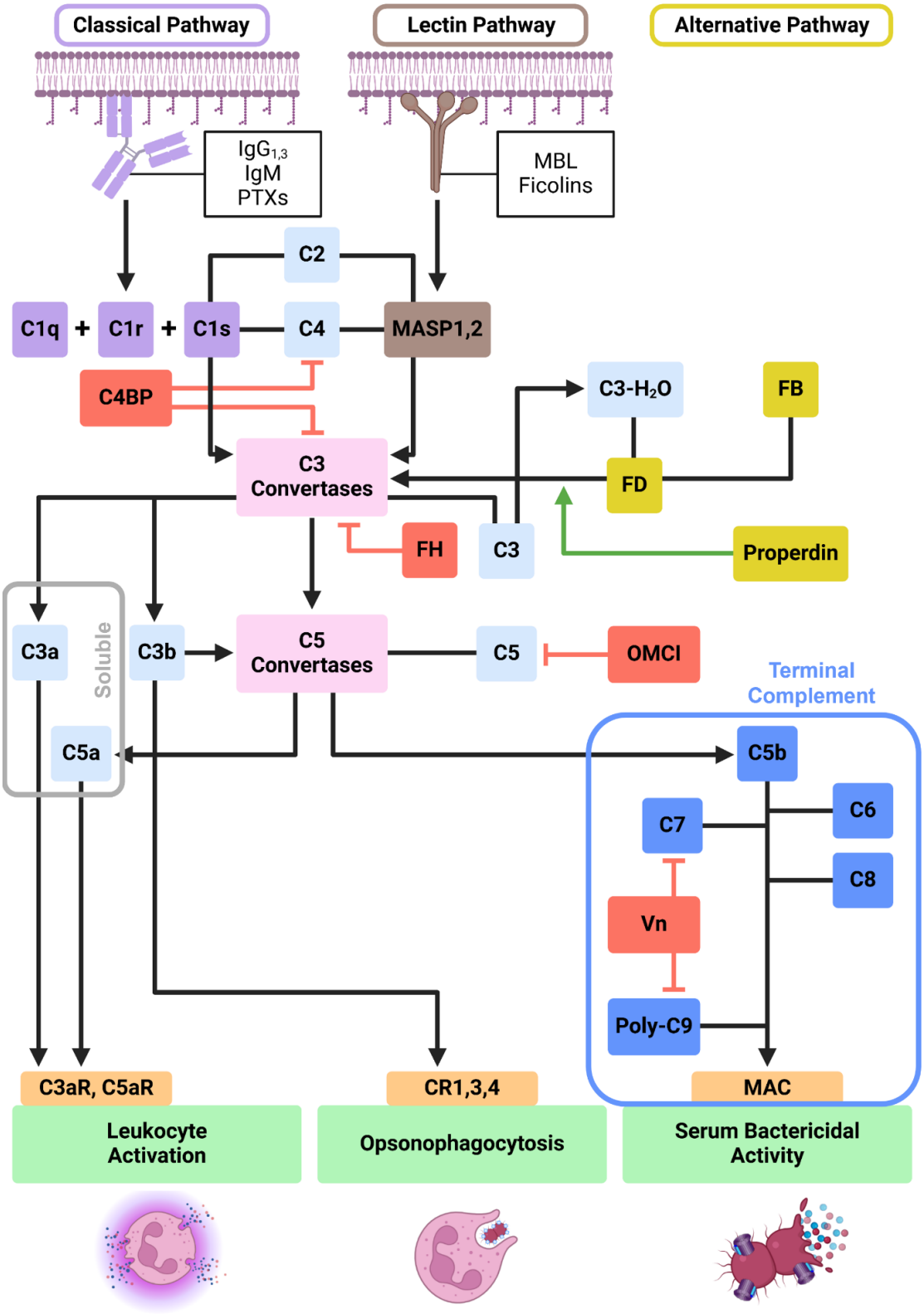
Classical Pathway
Lectin Pathway
Alternative Pathway
IgG1,3
IgM
PTXs
MBL
Ficolins
C2
C1q
C1r
C1s
C4
MASP1,2
C4BP
C3-H2O
FB
C3
Convertases
FD
FH
C3
Properdin
C3a
Soluble
C3b
C5
Convertases
C5
OMCI
Terminal
Complement
C5a
C5b
C6
C7
C8
Vn
Poly-C9
C3aR, C5aR
CR1,3,4
MAC
Leukocyte
Activation
Opsonophagocytosis
Serum Bactericidal
Activity

Figure 5. Pathways of the complement cascade and effector functions

The serum-derived complement cascade can be canonically activated by three pathways: Classical, Lectin, and Alternative. The Classical Pathway is activated upon surface binding by IgG, IgM, or pentraxins (PTXs), whereas The Lectin Pathway is activated by mannose-binding lectin (MBL) or ficolins. The Classical and Lectin Pathways lead to C1 complex or MASP recruitment, respectively, to cleave complement components C4 and C2 which form the 'classical' C3 convertase. Classical C3 convertase formation is blocked by the host-derived soluble inhibitor C4b-Binding Protein (C4BP). The Alternative Pathway is activated spontaneously by component C3 'tickover' into C3-H_2O which allows Factor B (FB) binding and cleavage by Factor D (FD) to form 'alternative' C3 convertases. Formation and persistence of alternative C3 convertases is enhanced by properdin. These C3 convertases cleave C3 into C3a and C3b. C3b binds C3 convertases to form C5 convertases which cleave component C5 into C5a and C5b. C5 cleavage is blocked by the inhibitor OMCI. C3a and C5a are soluble anaphylatoxins which activate leukocytes by binding their cognate receptors (C3aR, C5aR). In addition to forming C5 convertases, C3b can also serve as an opsonin ligand for complement receptors (CR1, CR3, CR4) to enhance opsonophagocytic uptake of targeted cargo. C5b initiates terminal complement deposition by recruiting components C6, C7, C8, and C9 which polymerizes (Poly-C9) to form the membrane attack complex (MAC). The MAC promotes serum bactericidal activity. Terminal complement can be inhibited by binding of the soluble host inhibitor vitronectin (Vn) to C9 subunits or C7-containing precursors.

1.3.1.2 Complement opsonization & opsonophagocytosis.

Opsonization refers to decoration of cells, particles, or aggregates with proteins (opsonins) that enhance interactions of the decorated target with other cells expressing receptors specific for the opsonin.[138,165] The most common and extensively studied opsonization interactions are between immunoglobulins and Fc-region receptors (FcR's) and between complement products and cognate complement receptors (CR's).[167,168] Opsonization by complement promotes pathogen clearance through enhanced phagocytic uptake by leukocytes such as neutrophils and macrophages in an effector function known as opsonophagocytosis. Bacterial pathogens with membrane bound C3b or degradation products are more readily recognized by host immune cells. Predominant CR's expressed by neutrophils (and monocytes/macrophages) during bacterial infection are complement receptor 1 (CR1) and complement receptor 3 (CR3).[142,167] These CRs recognize C3b and iC3b, respectively, to enhance neutrophil-pathogen association.[169] Complement receptor 4 (CR4), which recognizes iC3b, is expressed on neutrophils under prolonged/systemic inflammatory processes such as sepsis but is abundant during homeostasis on monocytes/macrophages and is a classic dendritic cell marker[169]. Complement receptor 2 (CR2) is expressed on B-cells and enhances their activation by serving as a co-receptor/co-stimulator with iC3b, C3d and C3dg binding.[169] Finally, complement receptor of the immunoglobulin family (CRIg, also known as VSIG4) is expressed on tissue-resident macrophages to promote immunohomeostasis by clearing opsonized bacteria or byproducts.[169]

The roles of CR's in *Neisseria* infection and clearance are scantly studied with the exception of CR3. CR3 is a heterodimeric integrin which binds diverse substrates and is expressed on epithelial cells in addition to leukocytes.[169,170] CR3 is shown to be an important adhesin in opsonophagocytosis of Gc, in which it promotes 'silent' phagocytic uptake by neutrophils.[171] It can also serve as a receptor to enhance Gc adherence to epithelial cells by binding iC3b, Porin, Pili, and LOS.[2,172]

1.3.1.3 Leukocyte activation & recruitment: anaphylatoxins.

The C3 and C5 convertases cleave their substrates to generate C3b and C5b which progress through the core complement cascade. In this process, smaller soluble fragments C3a and C5a are also generated.[142] These products are termed anaphylatoxins and increase local inflammation. The fragment C4a is sometimes included among the anaphylatoxins but its bioactivity is far less than C3a and C5a.[173] The anaphylatoxins increase smooth muscle contraction, vasodilation, vascular permeability, and potently stimulate degranulation by mast cells and platelets to yield their namesake 'anaphylaxis' like activity.[21,173] They also serve as chemoattractants to recruit circulating leukocytes to inflamed tissues.[174] These leukocytes are simultaneously activated by anaphylatoxin recognition to promote antimicrobial effector functions including reactive oxygen species generation, degranulation, phagocytosis, and adhesin upregulation in neutrophils, monocytes, and macrophages. Leukocyte chemoattraction and activation is achieved through binding anaphylatoxins to their cognate receptors, C3aR and C5aR1, two G protein-coupled receptors (GPCRs) which activate the

MAP Kinase and phospholipase C (PLC) pathways in myeloid cells.[174] A second C5a receptor, C5aR2 formerly C5L2, is co-expressed with C5aR1 on immune cells. This receptor's function is less well understood but has been proposed to counteract C5aR1 signaling as a decoy receptor for C5a or to increase β-arrestin-mediated internalization/silencing of C5aR1.[175,176]

1.3.1.4 Serum bactericidal activity: terminal complement.

Serum bactericidal activity results from terminal complement deposition which directly kills bacteria in the absence of cellular actors. Canonically, terminal complement killing is achieved through generation of pore-forming complexes of components C5b-C9 in the outer membrane of Gram-negative bacteria (Fig. 5,6).[21,161] However, the exact bactericidal mechanism of terminal complement complexes remains enigmatic.[161]

Measuring terminal complement activity, via serum bactericidal assays (SBAs), is a commonplace method to identify susceptibility of different bacterial species, strains, or isolates to complement-mediated killing, and to identify complement-fixing ability of different serum sources (e.g. immunized versus un-immunized sera). SBA protocols include antibody, complement, and bacterial strain(s) of interest.[177-180] Serum is used as the complement source with or without exogenous purified complement components. Antibodies may either be added exogenously or native to the serum being tested. Serum lacking intrinsic complement activity via heat-inactivation (56°C for 30min) should be included as a control.[181] However, the degree of bacterial death which constitutes 'bactericidal' activity is not broadly agreed upon and variation in antibody and

serum concentrations, diluent buffers used, time of complement challenge, etc. make comparisons between studies complicated. In the field of meningococcal vaccinology, 50% killing from the inoculum is accepted as bactericidal.[179]

1.3.1.5 Terminal complement complexes: the membrane attack complex.

Terminal complement components sequentially associate at a targeted outer membrane of Gram-negative bacteria (Fig. 6).[151] The multi-layered meshwork of the cell wall in Gram-positive bacteria prevents ready association of terminal complement components within their cytoplasmic membrane. At a Gram-negative outer membrane, convertase-generated soluble C5b is captured by C6, with the nascent C5b-C6 complex then being bound by C7.[182] C5b-C7 is lipophilic and loosely associates with the outer membrane leaflet. When C8 incorporates, a conformational rearrangement secures the C5b-C8 complex into and penetrates the outer membrane.[151,161] Membrane-embedded C5b-C8 can then recruit a C9 monomer which undergoes a similar structural rearrangement as C8 in which it 'unfurls' its transmembrane α-helix domains to create β-hairpin staves which span the outer membrane.[151,161,183,184] This new conformation can then recruit the next C9 monomer resulting in C9 polymerization. Ultimately, up to 18 C9 copies can be incorporated into the final terminal complement structure, the membrane attack complex (MAC).[183-185]

When fully formed, the MAC is comprised of complexed C5b, C6, C7, C8 (one copy each), and polymerized C9 (12-18 copies). The fully polymerized C5b-C9 complex creates an outer membrane-spanning pore with an inner diameter of 10-11nm and penetrates the outer membrane through approximately 5nm long

transmembrane domains of C6-C9. (Fig. 6A).[151,161,185,186] Throughout the remainder of this document, ‘MAC’ will refer to this fully-polymerized complex. However, precursor terminal complement complexes have been reported, including those in which no C9 or multi/oligomerized C9 have been incorporated. Incomplete complexes can form ‘arc’ like structures on their own and can associate with one another forming heterogenous terminal complement multimers of varying structures (Fig. 6B).[187] These precursors are also thought to occur in the presence of full MAC complexes provided there is sufficient C9.

In addition to C9-bearing precursors, C5b-C8 units embed within membranes in the absence of C9 or in C9-limited situations.[187] A single entity of complexed C5b-C8 can either recruit C9 as described above or can aggregate with other C5b-C8 units to form what is referred to in this document as a C5b-C8 complex. This terminal complement complex contains three to four C5b-C8 units on average and forms biologically active pores within the membrane of approximately 2-4nm in diameter (Fig. 6C).[154,187-191] However, the role of incomplete or alternate terminal complement complexes during homeostasis, inflammation, or infection is poorly studied, as is their occurrence *in vivo* for complement-competent or complement-deficient individuals.

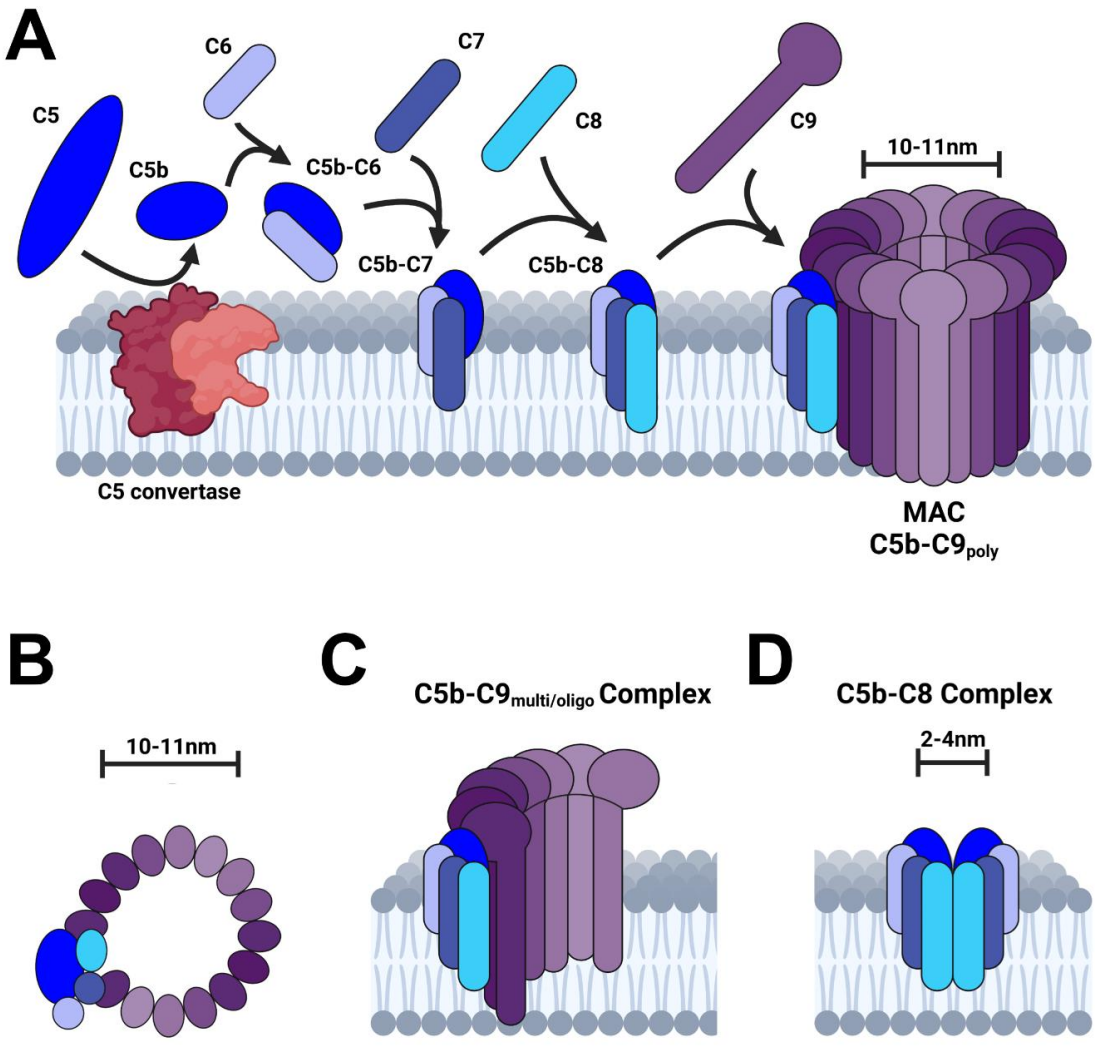
A
C5
C6
C7
C8
C9
C5b
C5b-C6
C5b-C7
C5b-C8
10-11nm
C5 convertase
MAC
C5b-C9poly
B
10-11nm
C
C5b-C9multi/oligo Complex
D
C5b-C8 Complex
2-4nm

Figure 6. Formation of terminal complement complexes

(A) Membrane-bound C5 convertases cleave complement component C5, generating C5b which then associates with components C6 and C7 to form a soluble C5b-C7 precursor complex. C5b-C7 can then recruit component C8 and embed within the membrane. C5b-C8 can next recruit component C9 which polymerizes with other C9 monomers in the membrane to form the membrane attack complex (MAC; C5b-$C9_{poly}$). A fully formed MAC contains 12-18 C9 units and forms a membrane-spanning pore with an inner diameter of approximately 10-11nm (B). Precursor complexes without a fully formed C9 pore can also be identified as ‘arc-like’ structures or conglomerates (C). Complexed C5b-C8 can also associate with other complexed C5b-C8 entities to form C5b-C8 complexes which are reported to form pores with diameters of approximately 2-4nm (D).

1.3.1.6 MAC-mediated bactericidal activity: possible mechanisms.

Complement-mediated lysis has been extensively studied against erythrocytes, other collaterally damaged host cell types, malignant cells, and artificial liposomes which all possess one lipid membrane separating their cytosol from the environment. In these systems, MAC generation can disrupt the membrane leading to osmotic lysis[189], vital component loss, and influx of toxic/pro-apoptotic compounds[154], ultimately leading to death in the cellular models. Gram-negative bacteria, however, possess two lipid membranes which delineate the intra- and extracellular compartments (Fig. 2). The structural limitations imposed by the approximate 5nm length of MAC transmembrane domains prevent the complex from spanning two distinct lipid bilayers.[151,161,192] This suggests that the MAC cannot directly disrupt structures in the bacterial cell deeper than the outer membrane, specifically, the inner membrane. Despite this, inner membrane disruption has been shown to be necessary for MAC-mediated killing of Gram-negative bacteria.[161,182,183,193]

Multiple, non-exclusive hypotheses have been proposed to rectify the physical discrepancies between MAC localization, inner membrane damage, and bacterial death (Fig. 7).[161] Similar to osmolysis of single-membraned targets, the MAC may disrupt bacterial osmotic stability allowing water influx to the cytoplasm, increasing turgor pressure, and resulting in lysis by inner membrane damage (Fig. 7A). The MAC pore may also result in the leakage of vital periplasmic or cytoplasmic factors through the MAC pore itself and/or via the inner membrane damage it causes (Fig. 7B). Similarly, destabilization of the

outer or inner membranes could perturb the PMF of a bacterial cell either by hydrogen ion leakage through the outer membrane or via gradient dissipation across the inner membrane (Fig. 7C). In bacteria which require the PMF to respire and grow, a sustained PMF insult could lead to eventual death or a 'viable-but-non-culturable' state if investigation relies on colony growth.

In a converse to vital factor efflux, the MAC pore may serve as a conduit for toxic factor influx (Fig. 7D). Serum bactericidal activity has long been suggested to be caused by the MAC allowing periplasmic access of the serum-derived host enzyme lysozyme which degrades peptidoglycan cell walls.[194,195] Evidence for this includes true lysis of bacterial cells/their cell walls only in the presence of serum/lysozyme but not with purified complement components alone. However, bacterial death can still occur in the absence of lysozyme suggesting that inner membrane damage and cell wall damage are uncoupled in MAC-mediated cell death.[161,194-196] Chapter 2 describes how the MAC enables access of lysozyme and antibiotics into Gc. Alongside lysozyme, MAC-mediated influx of other factors has also focused on C9 itself as an inner membrane-damaging agent (Fig. 7D). This has been proposed as either transiting through the outer membrane-embedded pore or by releasing from the outer membrane to penetrate the inner membrane. Data suggest against this hypothesis as 1) MAC-associated C9 is tightly complexed and unlikely to disassociate and diffuse to the inner membrane, 2) unfurling of C9 into β-hairpin staves occurs once membrane associated and prior conformational change is unlikely to promote transmembrane integration, 3) native C9 prior to conformational changes at 63

kDa and 10.4nm at maximum diameter is likely too large for the 10-11 nm MAC and Gram-negative peptidoglycan meshwork (pore size ~2-3nm, passage by <50 kDa proteins) to accommodate efficiently.[16,161,192]

Other ways in which MAC is thought to induce bacterial death include MAC-mediated lipid exchanged between the outer and inner membranes as a result of or along with membrane perturbation (Fig. 7E), similar to what has been observed with polymyxin B or other amphipathic/detergent like compounds.[161] The MAC may also (over)stimulate envelope-damage stress responses from outer membrane damage, buildup of periplasmic precursors, or disruption of cell wall-membrane linkages, ultimately leading to inner membrane disruption, vesiculation, and cell death (Fig. 7F).[161] The MAC was also suggested to penetrate both the outer and inner membranes simultaneously at cell-division-related sites in which both membranes were closely juxtaposed. This would have allowed the MAC to span a shorter lipid confluence. These sites were also hypothesized to occur at specific locations on a Gram-negative cell such as a pole/septum of recent or imminent division. However, this hypothesis appears to be untrue based upon analyses of flux into or out of the periplasm/cytoplasm of different compounds and microscopy showing these outer-inner membrane confluences to be artifactual and which show the MAC deposits regularly across Gram-negative surfaces.[161,192] Although, studies of MAC localization across the cellular landscape are generally conducted with excess complement meaning ‘preferential’ incorporation sites may have been masked. These proposed

processes may work in tandem or in concert making it difficult to forensically ascertain the most proximal cause of death.

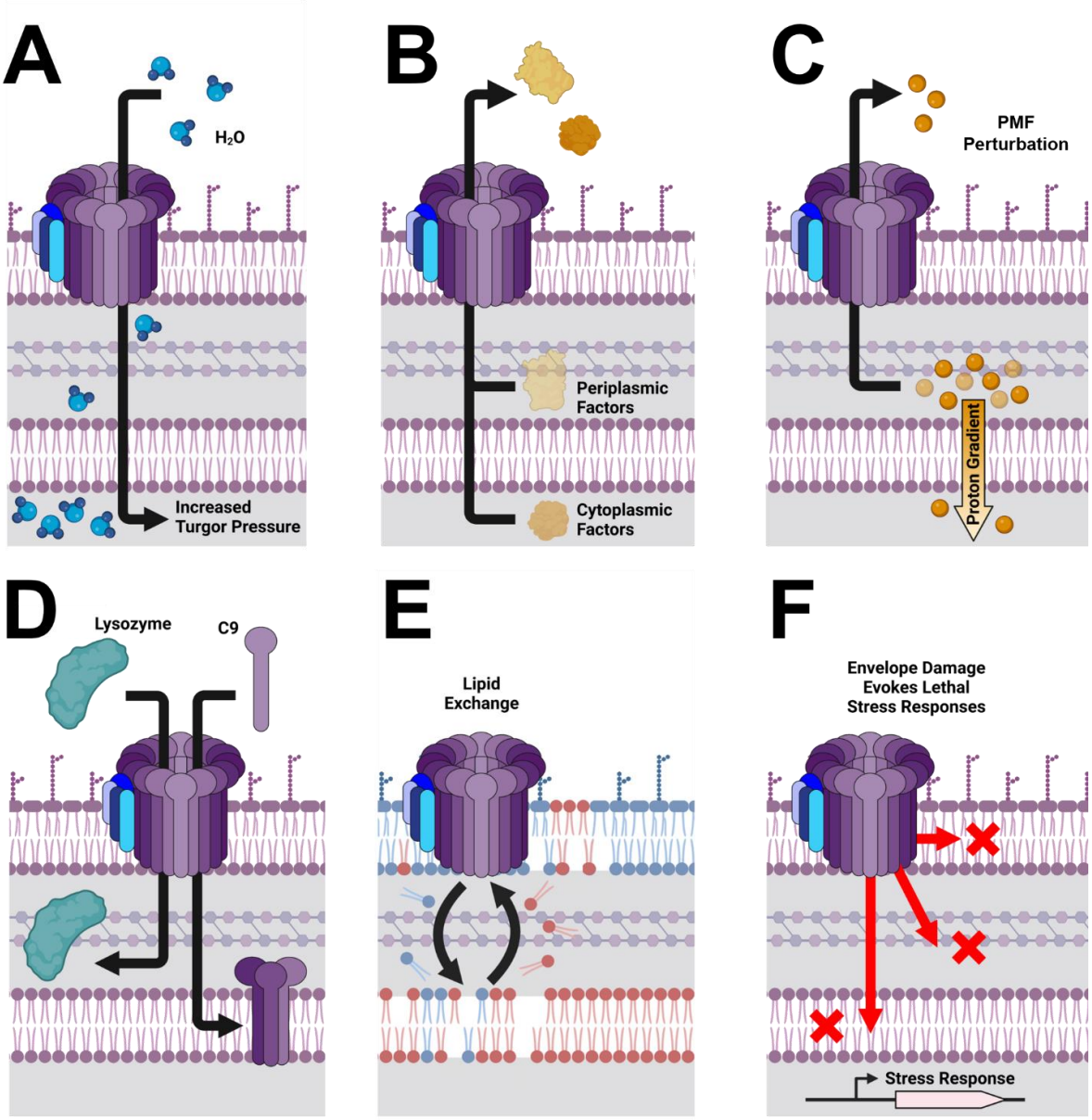
A
H_2O
Increased
Turgor Pressure
B
Periplasmic
Factors
Cytoplasmic
Factors
C
PMF
Perturbation
Proton Gradient
D
Lysozyme
C9
E
Lipid
Exchange
F
Envelope Damage
Evokes Lethal
Stress Responses
Stress Response

Figure 7. Hypothesize mechanisms of MAC-mediated Gram-negative cell death

Schematics of proposed mechanisms underlying MAC-mediated killing which may act in concert. (A) The MAC pore promotes osmosis of water into the bacterial cell, increasing osmotic/turgor pressure which ruptures the cell. (B) The MAC promotes leakage of bacterial factors from the periplasm or cytoplasm which are required for cell survival. (C) The MAC allows leakage of protons from the periplasm which dissipates the proton motive force (PMF). (D) The MAC allows toxic compounds such as antimicrobials (e.g. lysozyme) or membranolytic C9 to access regions of the bacterial cell beyond the outer membrane to exert their bactericidal effects. (E) The MAC disrupts lipid membrane homeostasis leading to membrane perturbation and exchange of phospholipid species between the outer and inner membranes. (F) The MAC damages the Gram-negative envelope which is sensed by the bacterium thereby initiating a maladaptive or programmed cell death stress response.

1.3.1.7 Complement component synthesis & tissue abundance.

Most complement components are primarily synthesized by the liver and secreted into systemic circulation to achieve abundant serum concentrations.[195,197] Under homeostatic conditions, complement concentrations in serum achieve levels of 60µg/mL (C6, C9), 200µg/mL (C5), and upwards of 2,000µg/mL (C3).[198] Serum concentrations of some complement components can increase 2-3-fold during inflammation due to increased hepatocyte production of these acute phase proteins. Therefore, diminished liver synthetic function, such as occurs during cirrhosis, can result in functional or acquired complement deficiencies.[21,137,198] Some complement components such as C1q, C6, and C7, are synthesized largely or entirely by extrahepatic sources and secreted into systemic circulation or locally.[198-200] Non-hepatocyte complement-producing cells include epithelia, endothelia, fibroblasts, and immune cells.[197,201] Immune cells are important complement sources with macrophages/monocytes secreting significant levels of C1q, C3, C4, C5, Factor B, and properdin.[197,200,202] Mast cells are also an appreciable source of local C3 and C5. Neutrophils in circulation and those recruited to sites of inflammation are sources of C2, C3, C4, and C5 upon degranulation. Neutrophils also synthesize and secrete significant properdin levels.[197,200,202]

Complement abundance and activity at tissues is varied and under-investigated in most cases. During homeostasis, tissue complement activity is less than that of serum, but inflammation inducing immune cell recruitment, serum transudate, and local synthesis may considerably increase complement

component concentrations and activity at inflamed sites.[149,150] Relevant to Gc infection, tissues of the reproductive tract have been shown to produce complement, with epithelial cells increasing synthesis in inflamed conditions.[203] Complement activity at the homeostatic cervix is estimated at approximately 10% that of serum and neutrophils exposed to Gc synthesize C2, C3, C4, C5 and properdin.[149] The impact of hormones and menstrual cycle on complement synthesis and abundance at reproductive tissues is poorly understood and warrants greater investigation.

1.3.1.8 Complement resistance in *Neisseria*.

Many Gc strains/isolates have evolved to resist complement-mediated killing (serum resistance) through diverse mechanisms (Fig. 8).[21] This underscores the pressure exerted against Gc by human complement and the importance of complement in controlling Gc infection. Many, but not all, complement resistance mechanisms are specific to human complement factors contributing in part to the human specificity of this pathogen.[21,204]

Many Gc surface factors are phase or antigenically variable including Opa, Pili, etc. as detailed in prior sections. Additionally, surface-modifying enzymes such as LgtD which adds a terminal GalNAc residue to LOS can be phase variable, further altering the gonococcal surface landscape. By varying the surface-exposed antigens and/or epitopes, Gc can evade antibody-mediated complement activation. Non-variable Rmp can prevent effective antibody-mediated complement activation through blocking antibody recruitment.[63] These antibodies are elicited in individuals with prior Gc exposure and enhance Gc

colonization in murine models.[66] It is possible that complement evasion by anti-Rmp antibodies is mediated by steric hinderance of antibodies directed against other surface epitopes, such as Porin which is closely associated with Rmp in the outer membrane. Anti-Rmp antibodies recognizing different Rmp epitopes have variable levels of blocking capacity with some even being bactericidal, lending support for this model. However, analysis of C3 and C9 deposition by anti-Rmp antibody binding shows variable results with some studies showing decreased complement deposition on bacteria and others showing that blocking antibodies induce greater complement deposition. These antibodies may be promoting complement deposition at a distance from the outer membrane which prevents proper incorporation of bactericidal components.[21,57,62,63] In *N. meningitidis*, capsule production is a potent source of complement resistance by preventing effective antibody recognition/complement deposition, although Gc lacks a capsule.[21]

Hosts produce numerous soluble complement inhibitor proteins to prevent off-target damage by regulating multiple stages in the complement cascade (Fig. 5).[21,142,165] However, Gc has evolved to exploit these inhibitors by recruiting them to its surface, thereby protecting the pathogen from complement. Gc Porin recruits C4b-Binding Protein (C4BP) to block the Classical Pathway C3 convertase function by binding and inhibiting C4b (Fig. 5).[21,205] C4BP is recruited by approximately 90% of P.IA-expressing isolates and approximately 20% of P.IB-expressing isolates. Gonococcal P.IA can also recruit Factor H (without sialylated LOS unlike P.IB, see below), a key inhibitor of the Alternative Pathway

by blocking C3 convertases (Fig. 5).[21] These observations in part explain why P.IA-expressing Gc have a greater capacity to disseminate via the bloodstream. Some Gc isolates can also recruit the soluble host factor vitronectin (Vn) which can bind to and block both soluble C5b-C7 complexes and C9, thereby inhibiting MAC formation.[21,191] The bacterial factor which recruits Vn to the Gc surface has not been fully demonstrated but evidence suggests that some Opa variants are likely involved.[21,52,53] Please see Chapter 5 for data on Vn-Gc interactions.

The above methods used to achieve serum resistance have been historically termed ‘stable serum resistance’ as these mechanisms persist following gonococcal passaging on media. In contrast, other isolates exhibited ‘unstable’ or transient serum resistance which was lost after passaging on laboratory media. It was identified that this resistance was conferred by Gc decorating surface factors such as LOS with host-scavenged sialic acid (N-acetylneuraminic acid, NANA).[21,85] Passaging isolates on media without sialic acid therefore abrogated the resistance potential. LOS sialylation principally serves to recruit host Factor H to limit complement activation and enables P.IB Factor H recruitment. Sialylation can also mask surface epitopes, further limiting antibody and MBL recognition.[21,85]

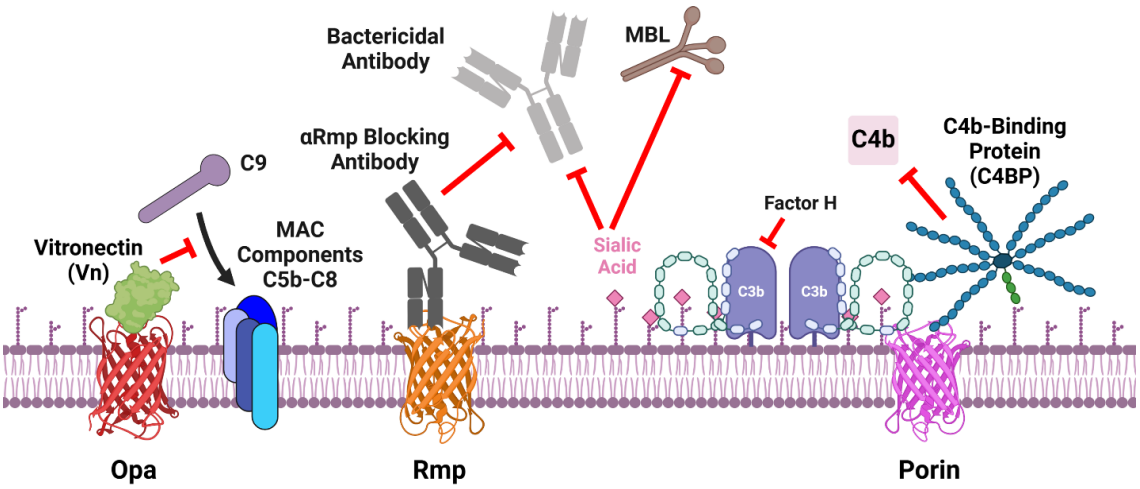

Figure 8. Surface-recruited mechanisms of gonococcal complement resistance

Gc has evolved many mechanisms to evade complement-mediated killing including recruitment of host-derived vitronectin to inhibit terminal complement deposition and membrane attack complex (MAC) formation (hypothesized to be recruited by Opa proteins), Rmp being recognized by antibodies which block the bactericidal activity of other antibodies, decoration of lipooligosaccharide with sialic acid which prevents antibody and mannose-binding lectin (MBL) recognition, sialic acid recruitment of host-derived Factor H to inhibit the Alternative Pathway, and recruitment of the host-derived Classical Pathway inhibitor C4b-Binding Protein (C4BP) by Porin. Not shown: phase and antigenic variation of surface antigens to prevent antibody recognition.

1.3.1.9 Complement deficiencies and susceptibility to *Neisseria* infections.

Another line of reasoning to support complement's important role in controlling *Neisseria* is that individuals with complement deficiencies are at a significantly greater risk for acquiring gonococcal and meningococcal infections.[21,137,198,206] Proximal complement deficiencies (i.e. of components acting prior to C5) show a strong link to infections by encapsulated organisms (e.g. *N. meningitidis*, *Streptococcus pneumoniae*, *Haemophilus influenzae*) and to autoimmune diseases (e.g. lupus syndromes, hemolytic anemias).[21,137,198,206] Throughout the complement cascade, deficiencies can result from inherited or acquired etiologies. Acquired deficiencies can be a result of defects in synthesis (e.g. chronic liver disease), consumptive depletion (e.g. multiple myeloma, vasculitides, nephritic syndromes), or from processes which deplete protein from serum (e.g. nephrotic syndromes, enteropathies). Acquired complement deficiencies can also result from the use of complement inhibiting pharmaceuticals such as the anti-C5 antibody eculizumab used clinically to treat paroxysmal nocturnal hemoglobinuria and atypical hemolytic uremic syndrome.[21,137,198,206] Linking complement deficiencies to *Neisseria*, upwards of half of all individuals with a homozygotic complement deficiency will eventually develop at least one *Neisseria* infection in their lifetime.[21,198]

Deficiencies in terminal complement components, whether genetic or pharmacologic, are almost exclusively associated with infections by *Neisseria* species. Individuals with terminal complement deficiencies are predisposed to

invasive meningococcal disease and DGI. Inherited complement deficiencies vary in their severity based on the affected component, homozygosity, and whether the mutation depletes all of the component or lowers its abundance/functionality. Approximately 5-10% of all meningococcal disease cases have an underlying deficiency in terminal complement and complement-deficient patients have a 41% recurrence rate of infection.[198] Individuals with terminal complement deficiencies are 1,000- to 10,000-fold more susceptible to invasive meningococcal disease and upwards of 300-fold more susceptible to gonococcal infections.[21,137,198,206] For example, patients receiving eculizumab therapy have a 2,000-fold greater risk for invasive meningococcal disease, prompting a black-box warning on its use requiring vaccination against *N. meningitidis* prior to administering the antibody.[21] On average, deficiencies in C7 produce a 10,000-fold increased risk of acquiring meningococcal disease compared to matched wild-type C7 controls. C5, C6, and C8 deficiencies also incur similar susceptibilities. Interestingly, C9 deficient individuals are approximately 10-fold less susceptible than those with deficiencies in C5-C8, possibly owing to the ability C5b-C8 terminal complement complexes to kill meningococci in the absence of C9 (see Chapter 2 for data with Gc and further discussion).[21,137,190,198,206] Despite the lower risk compared to C5-C8 deficiencies, C9 deficiencies still confer an approximate 1,400-fold increased risk for *N. meningitidis* infection. Prevalence of complement deficiencies varies by components and study population. For example, C9-deficiency in the broader United States population is estimated at 0.03% (1/3,300 people) whereas C9-

deficiency reaches 0.1% (1/1,000 people) in Japan.[198] In addition to terminal complement, deficiencies in properdin (the only X-linked complement gene) of the alternative pathway is also strongly linked to meningococcal disease.[21,198]

Invasive meningococcal disease in these patients is reported to be less lethal than in complement-replete patients with a mortality rate per 1,000 episodes of 1.5 compared to 19, respectively.[21,198] It has also been suggested that complement deficient patients have milder disease episodes, but severity can be difficult to assess.[21,198] The lower lethality and possible lower severity has been linked to decreased terminal complement-mediated lysis of the Gram-negative bacteria, resulting in less LPS endotoxin release and hence a less active immune response.

Studies on complement deficiencies and infection by other *Neisseria* species including Gc are less common than those on meningococcal disease. However terminal complement deficiencies predispose to DGI and result in upwards of 300-fold increased risk for gonococcal infections broadly defined as well as increase risk of bacteremia from otherwise commensal *Neisseria*.[21,198,206,207] The lower susceptibility of Gc infection compared to meningococcal disease may be due to a lack of investigation into this topic or the many asymptomatic Gc infections which avoid detection. In meningococcal disease, the calculated increase in risk is inversely proportional to the incidence rate in a study population. In regions with sporadic cases of meningococcal disease (1 case/100,000 people), infections with complement deficiencies are more likely to occur compared to those with intact complement. In contrast, areas

with epidemic *N. meningitidis* (35 cases/100,000 people) result in many more infections across the entire population, possibly masking the impact of complement deficiencies.[198] This line of reasoning may in part explain the discrepancies in calculated susceptibility increases between *N. meningitidis* and Gc infections (currently ~200 reported gonorrhea cases/100,000 people in the United States).[3] The biology of these two pathogens, sites of infection, and disease presentations may also play a significant role. In murine models of Gc infection in which active complement clears Gc, inhibition of C5, C7, or homozygous C9 deletion abrogate complement-mediated killing to increase bacterial loads and infection duration.[156,208]

1.3.2 Neutrophils: function, recruitment, and Gc evasion.

1.3.2.1 Neutrophil recruitment & transmigration.

Neutrophils (often synonymized with polymorphonuclear leukocytes, PMNs) are granulocytic myeloid cells with significant roles in innate immunity to pathogens.[146,209-211] They can be differentiated from other leukocytes based on their granular content and segmented, multi-lobed nuclei.[212] At homeostasis, neutrophils are the most abundant circulating leukocyte at approximately 40-60% of all white blood cells with nearly 1e11 produced in the human body each day. Following maturation in the bone marrow, neutrophils are deployed into the bloodstream where they patrol for sites of inflammation caused by invading pathogens or sterile host-inflammation.[209-211]

In the absence of inflammatory signals, neutrophils pass from arteries through capillaries then veins for their short lifespan estimated between 12 hours

and 6 days.[209-211,213] However, inflammation can recruit neutrophils (Fig. 9) from the circulation at post-capillary venules. Inflammatory factors which stimulate neutrophils and promote recruitment include a variety of chemotactic cytokines, inflammatory lipids (e.g. eicosanoids; prostaglandins, leukotrienes), bacteria-derived formylated-peptides, and complement-derived anaphylatoxins (Fig. 9).[167,214-216] Inflammation promotes margination of the neutrophils and increased surface adhesins so that they associate with endothelia of vessel walls. The neutrophils then 'roll' along the endothelium until tighter adherence is achieved.[217] Neutrophil-endothelial interactions are mediated by surface receptors and ligands which display increased surface expression due to inflammatory stimuli. Cytokines such as IL-1, TNFα, and IL-8 derived by stromal, endothelial, epithelial, and/or local immune cells promote neutrophil selectin surface expression and modifications to sialyl-Lewis^X moieties that bind endothelial receptors including CD34, E-selectin, and P-selectin. Inflammatory signals stimulate surface expression of neutrophilic integrins which bind cognate ligands including intercellular adhesion molecule 1 (ICAM-1, CD54) to promote neutrophil migration across the endothelium (transendothelial migration).[209-211,217,218]

Neutrophils can then engage pathogens within the stromal space beyond the endothelium containing abundant extracellular matrix (ECM) or further continue to cross the basement membrane and epithelium at a site of infection via transepithelial migration where they can engage apically adhered pathogens (Fig. 9).[216,219,220] Transepithelial migration is particularly relevant for mucosal

pathogens like Gc in which they colonize the apical surface of diverse epithelial cells. The transmigration process across endocervical epithelial cells is induced by a primary chemotactic gradient derived by the epithelial cells (hepoxilin-A_3, HXA_3) followed by a feed-forward loop of a neutrophil-secreted secondary chemotactic gradient (leukotriene-B4, LTB_4).[216] The transmigration process and exposure to the many stimulatory signals has been linked to increased neutrophil activity against pathogens, although exact mechanisms underlying this augmentation are unclear.[221-223] Following the migratory process and engagement with pathogens, neutrophils can then release from the epithelial surface into the luminal space where they, along with any pathogenic cargo, can be eliminated.[219]

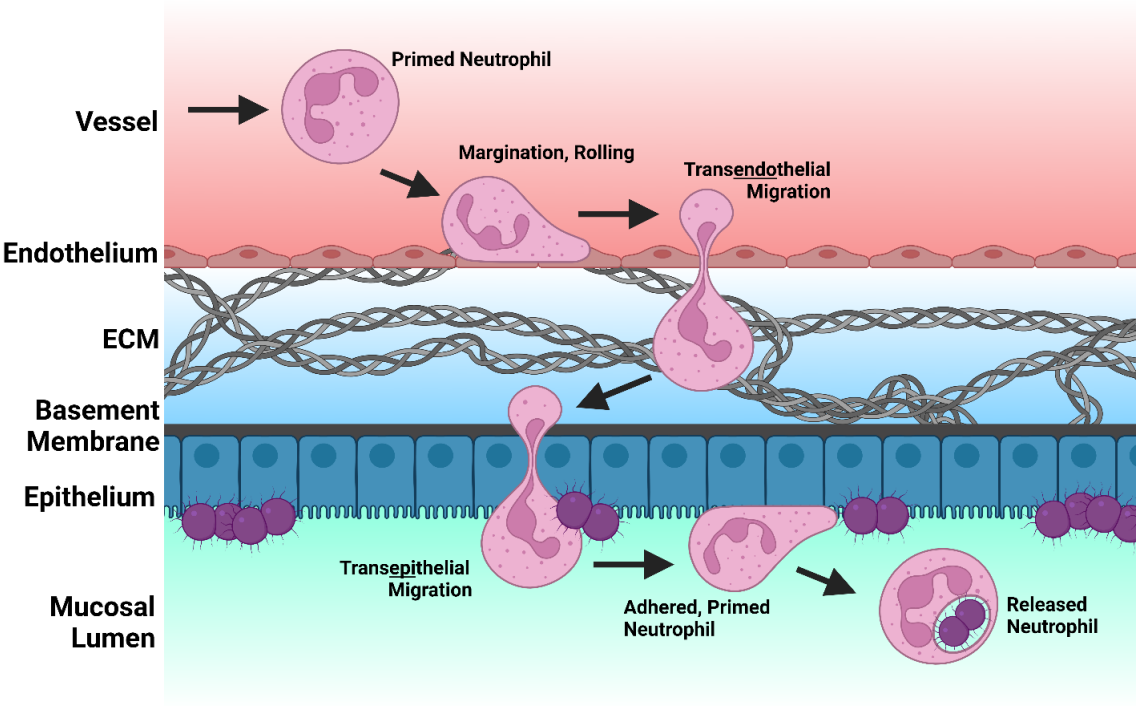

Figure 9. Neutrophil recruitment and transmigration

Schematic of neutrophil recruitment during a mucosal infection from the vasculature, across the endothelium by transendothelial migration, through the underlying stroma and extracellular matrix (ECM), and across the basement membrane and epithelium by transepithelial migration. PMNs are recruited by numerous chemoattractants and priming agents released by pathogens and host cells. These factors can also promote vascular permeability as well as vasodilation which marginates neutrophils to the vessel wall where they roll along the endothelial cells prior to migration. After reaching the apical surface of the epithelium, neutrophils eventually release and are shed into the mucosal lumen. Shown here is a simple columnar epithelium such as that of the endocervix.

1.3.2.2 Neutrophil antimicrobial activities.

Neutrophils possess numerous antimicrobial functions with the goal of clearing invading pathogens. These innate immune cells synthesize a vast repertoire of antimicrobial proteins with different properties and mechanisms of action.[209-213] Antimicrobials are synthesized during neutrophil maturation and are pre-loaded into membrane-bound granules.[212] As professional phagocytes, neutrophils engage and internalize pathogens through phagocytosis which can be enhanced by opsonin deposition on targeted cargo (see section 1.2.1.2).[142] Once internalized, the neutrophil can direct antimicrobial-laden granules to the phagosome where membrane fusion exposes phagocytosed bacteria to antimicrobials. Granules can also be mobilized to the neutrophil plasma membrane causing antimicrobials to degranulate into the external milieu.[211,212]

Neutrophil granules are classified into subsets based upon their contents and order of sequential mobilization.[212,224,225] Upon stimulation, neutrophils first direct secretory vesicles to the plasma membrane which are enriched in adhesins and receptors for chemotaxis/further activation. These include CR1, CR3, FcγRIII, CD14, formylated peptide receptors (fPR), etc. Neutrophils next mobilize tertiary then secondary granules (a.k.a. gelatinase and specific granules, respectively), subsets which are synthesized as a continuum during granulopoiesis. These contain variable amounts of adhesins and receptors that further aid in migration/activation, ECM-degrading compounds including the matrix metalloproteases (MMPs) and collagenase, and antimicrobials such as lysozyme, lipocalin, and lactoferrin. They also contain the membrane-

incorporated NADPH-oxidase which generates the reactive oxygen species (ROS) hydrogen peroxide. Finally, neutrophils fuse primary (a.k.a. azurophilic) granules to the targeted membrane, releasing additional soluble antimicrobials. These include the serine proteases (cathepsin G, neutrophil elastase, and proteinase 3), cationic antimicrobial peptides (CAMPs; defensins, bactericidal permeability-increasing protein, azurocidin), and the cathelicidin LL-37 as well as other antimicrobials also found in the prior granule subsets. Primary granules also contain myeloperoxidase (MPO), and enzyme that converts hydrogen peroxide produced by NADPH-oxidase into the more potent ROS hypochlorous acid.[212,224,225] ROS and antimicrobial compounds can reach extremely high concentrations within the small volume of neutrophil phagosomes, presenting a considerable assault against phagocytosed pathogens.[226]

Neutrophils can also exert antimicrobial activity by generating neutrophil extracellular traps or NETs.[227] This occurs when neutrophils extrude their nuclear (or mitochondrial) DNA into the environment. The extracellular DNA can entangle pathogens and expose them to high concentrations of antimicrobials such as elastase, lactoferrin, and citrullinated histones which also exert bactericidal activity.[227,228]

1.3.2.3 Neutrophil surface marker expression & diversity.

Different cell types express unique repertoires of surface-exposed antigens comprising receptors, adhesins, enzymes, etc. which influence how they interact with neighboring cells and substrates. Neutrophil surface markers can vary widely in their presence and expression levels between resting, primed,

and activated states.[214,229-233] However, the presence/absence of certain markers and/or the relative abundance provide valuable information on neutrophil stimulation.

Mature neutrophils possess many surface antigens also found on other leukocyte populations. Classic neutrophil markers include CD15, CD16, and CD11b.[234] Low or absent expression of other surface markers can enable differentiation of neutrophils from other cell types such as monocytes (CD14, HLA), eosinophils (CD49d, Siglec-8), basophils (CD123), natural killer cells (CD56), and dendritic cells (CD11c, CD209).[234-236] Cells expressing CD11b, CD16, and CD66b have been characterized as >99% neutrophils via flow cytometry.[237] Flow cytometric analysis of whole blood can also delineate neutrophil-containing granulocyte populations from monocytes, erythrocytes, and lymphocytes based on forward and side scatters (FSC, SSC) which roughly correspond to overall cell size and cellular complexity/granularity, respectively.[234,235]

Upon stimulation, many surface markers are upregulated on the neutrophil plasma membrane. Increased abundance is largely due to granule mobilization and fusion with the plasma membrane to expose preformed membrane proteins.[225] Markers found in different granule/vesicle subsets can indicate certain granule mobilization, for example CD63 and CD66b are markers of primary and secondary granule degranulation, respectively.[212,225] In cases of prolonged neutrophil activation, such as in sepsis, markers which are otherwise absent (e.g. CD64) can be identified on the surface as biomarkers of exhaustive

stimulation.[168] Other markers decrease in surface expression as neutrophils are stimulated. These include CD62L (L-selectin) and CD16 which are cleaved from the surface by proteases (e.g. ADAM17) which are released as neutrophils are primed/activated in a process termed ectodomain shedding.[238-240] Other markers are endocytosed during neutrophil activation thereby decreasing their surface levels. This is particularly observed with chemokine receptors, such as the aforementioned C5aR1 and fPR, as a mechanism to prevent overstimulation.[176,241]

Cytometric analysis of neutrophil morphology, surface markers, and transcriptional profiles show ontogenetic and functional diversity of these innate cell types. As neutrophils mature, they increase abundance of markers such as CD16 and CD35 while decreasing CD33. CD10 is a marker of mature, segmented neutrophils as opposed to the band cell precursors with less potent antimicrobial activity.[242] Band cell release into circulation can be increased during infection and is used clinically as an indicator of inflammation. As neutrophils age, their function can also be modulated with senescent neutrophils (CXCR4+) showing a predisposition to NET release.[242] Neutrophil heterogeneity has also been studied in the tumor microenvironment in which tumor associated neutrophils (TANs) can play either anti- or pro-tumor roles.[232] However, the basis of neutrophil heterogeneity, functional impact, and surface markers of different subsets remain to be defined and represent an important avenue for future investigations.[229-233,242,243]

1.3.2.4 Gc subversion of neutrophil effector functions.

Gc has evolved numerous mechanisms to combat and evade the antimicrobial effector functions of neutrophils. By subverting neutrophil-mediated killing, Gc gains access to otherwise inhospitable niches in its human host.[12,146,228,244]

Gc infection includes both extracellular bacteria adhered to the apical surface of colonized epithelia and Gc located intracellularly within neutrophil phagosomes. Gc possesses multiple mechanisms to avoid 1) association with neutrophils, 2) subsequent internalization, and 3) killing once internalized. To avoid neutrophil binding and internalization, Gc can avoid opsonization by antibodies and/or complement through the mechanisms discussed above including phase variation and complement inhibition. Gc can also limit neutrophil phagocytosis by recruiting host C4BP and sialylating its LOS through complement-independent mechanisms.[48,85] Gc has also been reported to bind the trailing uropod of neutrophils via Type IV Pili to avoid the phagocytic leading edge.[245] A major mechanism of non-opsonic phagocytosis is though interactions of Gc Opa with neutrophil CCMs. Gc that express CCM-3 binding Opa more readily associate with and are internalized by PMNs. Conversely, Gc which lack Opa expression through phase variation or genetic deletion are less readily bound or internalized by neutrophils.[38,39,48] Neutrophils that interact with Opa-negative Gc also display lower levels of stimulation and granule fusion with the phagosome.[49,246] Phagosome maturation is also suppressed by Gc phagocytosed in a ‘silent’ CR3-dependent manner.[171]

Unlike Opa-expressing Gc, Opa-negative Gc do not evoke an oxidative burst from neutrophils. The underlying mechanism for this suppression is currently unknown but the NADPH-Oxidase cytosolic subunits (p40, p47, p67) are not recruited to phagosomes containing Opa-negative Gc.[247] Gc also produces ROS detoxifying enzymes including catalases, superoxide dismutases, and glutathione peroxidases as well as enzymes which repair damaged proteins and DNA.[202,247,248] However, deletion of these factors singly or together does not produce survival disadvantages in Gc even when a robust oxidative burst is elicited, suggesting that ROS is dispensable for anti-gonococcal activity.[146,247]

Non-oxidative antimicrobials are also evaded by Gc. As described previously, the outer membrane itself is a barrier to many antibacterial factors, and compounds that do penetrate this defense can be exported by efflux pumps.[15,129,130,136,249] Other protective factors including lysozyme inhibitors have also been described.[249-251] Gc has also evolved to overcome the nutrient limitations that neutrophils attempt to impose by transferrin, lactoferrin, calprotectin, etc. This is achieved through TonB-dependent transporters which pirate essential transition metals like iron and zinc from human metal-sequestering proteins.[143] It has also been proposed that lactate produced by neutrophils when stimulated can also be used as a carbon source by Gc.[8,252,253] Gc can overcome NET-mediated killing by producing a DNA-degrading nuclease.[254]

1.3.2.5 Experimental models of Gc-neutrophil interactions.

Gc is an obligate human pathogen that has evolved to specifically exploit human factors for its survival and colonization.[1,146] Gc fails to bind homologous factors from other species such as complement inhibitors, metal-sequestering proteins as nutrient sources, and Gc Opa bind cognate CCM receptors only on species closely related to humans.[143,146,255,256] Therefore, infection in non-human *in vivo* models is difficult to achieve and does not fully recapitulate the hallmarks of human Gc infection. Moreover, studying human neutrophil biology and host-pathogen interactions is challenging due to neutrophils being terminally differentiated, short-lived, genetically intractable, and readily stimulated during isolation procedures for *in vitro*/*ex vivo* experimentation.[146,220,257,258] Multiple models of Gc-neutrophil interactions exist with caveats and nuances to interpretations, and efforts are underway to develop new models to address current shortcomings.

Non-human *in vivo* animal models of Gc infection are inherently limited yet provide valuable information on the concerted immune responses against Gc. Depending on the specific system, they also include factors such as hormones, mucus, and epithelia which greatly influence pathogenesis. Historically, chimpanzee infection models showed symptomatic colonization (Gc binds chimp Factor H, C4BP, and CCMs) but this model was discontinued due to cost, availability, and ethical concerns.[259] Currently, *in vivo* murine models are the most commonly used animal systems to investigate Gc pathogenesis and interactions with neutrophils.[260-262] In wild-type BALB/c mice, inoculated Gc can

colonize the lower genital tract during the short pro-estrus stage of the estrous cycle and exogenously dosed 17β-estradiol can increase colonization up to 9-12 days. Antibiotics (streptomycin, vancomycin, trimethoprim) are also included in this model to control commensal microflora and enhance colonization.[260,261] In this estradiol-treated murine model, neutrophils are recruited to the lower genital tract. Upper genital tract infection can be simulated by transcervical Gc inoculation, in which neutrophils can eventually be identified in the endometrial lumen.[146,260] Interestingly, estradiol-treated C57BL/6 mice can also be colonized with Gc, but the innate immune response is not robustly elicited.[263] It should be noted that estradiol itself is immunosuppressive and alters receptor and soluble factor levels. Transgenic murine models have also been used and are being advanced for Gc infection studies including mice with humanized transferrin, lactoferrin, calprotectin, Factor H, C4BP, and CCMs to supply host-specific factors exploited by Gc.[146]

Murine and human neutrophils share many characteristics yet differ in key regards which influence studies on murine neutrophil-Gc interactions.[146,167,213] Perhaps most notably is that murine neutrophils lack the ITAM-containing CCM-3 which is bound by some Gc Opa proteins and is required for the oxidative burst and primary granule exocytosis.[38,49,146,213] Unlike in humans, murine neutrophils produce no FcαR or ITAM-containing Siglec-14, but do express stimulatory FcγRIII and FcγRIV and inhibitory FcγRIIb.[167,213] Murine neutrophils are also released into systemic circulation comparatively earlier in their maturation process compared to human neutrophils (although many *ex vivo* murine studies

isolate bone marrow-derived neutrophils regardless of maturity).[213,264] Murine neutrophils also produce NADPH-Oxidase activity and MPO levels roughly one quarter to half that of human neutrophils and fail to synthesize α-defensins, azurocidin, and bactericidal permeability-increasing protein found in human primary granules.[146,213,265] The genetic tractability of murine neutrophils, those isolated from transgenic mice, and immortalized neutrophil-like human cell lines provides increased utility despite the caveats.[266]

In vivo studies of human Gc infection and the roles of neutrophils come from natural infections and the controlled human infection model of male volunteers.[146,267-269] Human infection studies suggest a selective pressure for Gc that bind CCM-1 over CCM-3[54] and show differences in males and females.[268] The controlled human infection model allows for inoculation of characterized strains for analysis of phase variation, gene products essential for infection, and both soluble and cellular immune responses. The controlled model has also been used to explore candidate vaccines.[270,271] This model is limited to only 5 days post inoculation or at first sign of symptoms and, due to potential sequelae, male volunteers only.[267] Tissue explant models of *ex vivo* cervixes and fallopian tubes have also been utilized to examine a variety of cell types in their native architecture.[272,273] These models, however, lack tissue resident or recruited immune cells.

With the above considerations and limitations in mind, *in vitro* studies of purified primary human neutrophils from the circulation are frequently interrogated for their anti-gonococcal activity. Studies of isolated neutrophils and

Gc alone have yielded many of the important findings discussed above.[43,274-276] However, unless specifically included for investigations, these *in vitro* assays often omit key elements of the infectious milieu. These can include serum components, sources of sialic acid, hormones, and a variety of endo/epithelial cell types and underlying stroma on which Gc adhere and through which neutrophils must transmigrate. Therefore, efforts to more closely model native infections *in vitro* are being pursued. For example, this work makes extensive use of a primary human neutrophil infection model in which neutrophils are pre-treated with IL-8 and adhered so as to mimic a primed, post-recruitment state that would be observed at infected mucosa.[43]

Building toward this end, biomimetic models have garnered greater interest among the Gc scientific community and in the fields of other STIs and/or obligate human pathogens such as *N. meningitidis.* These models seek to recapitulate native infections by incorporating additional cell types (including immune cells) from either primary or immortalized sources in 3-dimensional architectures with fluid flow, ECM, mucus, microbiota, etc.[146,273,277,278] No model will fully represent what occurs during a natural *in vivo* infection and different components are incorporated depending on the specific processes being investigated. Chapter 4 of this work discusses a tripartite Gc-neutrophil-endocervical Transwell system which was used to investigate neutrophil transmigration and its impacts on anti-gonococcal activity.[216]

1.4 Gonococcal Vaccines

1.4.1 Gc evasion of adaptive immunity.

Gc is adept at suppressing the adaptive immune arm in addition to evading the innate system. As mentioned above, Gc can avoid recognition by antibodies directed against specific epitopes through phase and antigenic variation of surface components, sialylation of LOS epitopes, as well as shedding OMV 'decoys'. Gc also produces an IgA_1 protease which has been proposed to cleave mucosal IgA_1 antibodies as an avoidance mechanism. However, this function has been questioned as this exoenzyme cleaves non-specific substrates including LAMP1, TNF Receptor II, human chorionic gonadotropin, etc., making its role in pathogenesis less certain.[279-282]

Gc interaction with antigen presenting cells such as monocytes and dendritic cells can induce NLRP3 inflammasome and cathepsin B-mediated pyronecroptosis, increased PDL-1 and PDL-2 expression to induce apoptosis of PD1-expressing cells (e.g. CD4+ T cells), and prevent dendritic cell stimulation of CD4+ T cells.[30,283] Direct interaction of Gc with lymphocytes via Opa and ITIM-containing CCM-1 results in reduced T cell Receptor signaling, T and B cell proliferation, and antibody production in addition to inducing B cell death.[25,27,284,285]

Gc induces cytokine secretion which skews the immune response away from a protective Th1 to an ineffectual Th17 programme. Gc-elicited TGF-β and IL-10 directly inhibit Th1 cells and indirectly by promoting Treg differentiation and functions.[284] IL-6 production during Gc infection further skews toward a Th17-

predominant response.[286] Exogenous introduction of microencapsulated IL-12 has been shown to be protective against Gc in the murine vaginal colonization model by overcoming Th17 skewing through promotion of a Th1 programme.[287]

1.4.2 History of gonococcal vaccine efforts.

As a result of Gc suppression of adaptive immunity, and the diversity of epitopes which can be expressed or silenced by the bacteria, long-lived immunity is not elicited against natural or experimental infections.[262,288,289] Prior clinical trials have been conducted with heat-killed whole gonococci as an immunization in the early 1970's which resulted in no greater protection compared to controls.[271] Candidate vaccines with purified pilin subunits have showed protection only against Gc expressing homologous pilin antigens but no protection against different pilin subunits in controlled human infection models (1980's) or natural infection (1990's).[271,289] Vaccine candidates prepared from Gc outer membrane fractions likewise showed no protection over placebo. Data suggest that the lack of protection may be in part due to blocking antibodies elicited by outer membrane Rmp, an important consideration for future vaccine development.[69] In recent years, exciting data has emerged showing cross-protection of OMV-based serogroup B meningococcal vaccines against Gc. However, the mechanisms underlying this protection are as of yet unclear.

1.4.3 Reactivity and protection of meningococcal vaccines against Gc.

Seminal studies out of New Zealand showed that gonorrhea incidence significantly declined in regions which had undergone active vaccination efforts against a serogroup B meningococcal outbreak (vaccine efficacy of

approximately 31%).[290] Comparatively, chlamydia cases showed no such trend, suggesting specific cross-reactivity of meningococcal vaccine-elicited immunity against Gc. The vaccine investigated in this retrospective study, MeNZB, was based on OMVs derived from the outbreak-specific serogroup B *N. meningitidis*. Efforts across the globe with other OMV-based vaccines have shown similar results with an estimated 30-40% efficacy of these vaccines against gonorrhea over the timespan examined.[291,292]

The most thoroughly investigated vaccine now is the 4-component meningococcal serogroup B OMV vaccine 4CMenB (trade name Bexsero) produced commercially by GSK (formerly GlaxoSmithKline). This vaccine contains the MeNZB OMVs as well as 3 other recombinant antigens. The recombinant additives are surface expressed in *N. meningitidis* and include NadA, Factor H binding protein (fHbp), and *Neisseria* Heparin Binding Antigen (NHBA). NHBA and fHbp are also fused to other immunogenic meningococcal proteins, GNA1030 and GNA2091, respectively.[292] Gc expresses surface-exposed NHBA and outer membrane proteins with appreciable homology to those found in the meningococcal OMVs (Porin, Opa, PilQ, BamA, MtrE).[292,293] However, Gc-expressed fHbp is not surface exposed and Gc does not express a NadA homolog. Immunization with 4CMenB elicits Gc-binding antibodies in mice and humans that result in complement-mediated bactericidal activity and opsonophagocytic killing with neutrophils as well as reduces Gc colonization in the murine genital tract.[177,293,294] However, the contribution of these vaccine-elicited antibodies to Gc control *in vivo* is not fully understood and correlates of

protection for candidate gonorrhea vaccines have not yet been established.[177,180] Discussion of findings related to complement-mediated activities of vaccine-elicited antibodies can be found in Chapter 5.

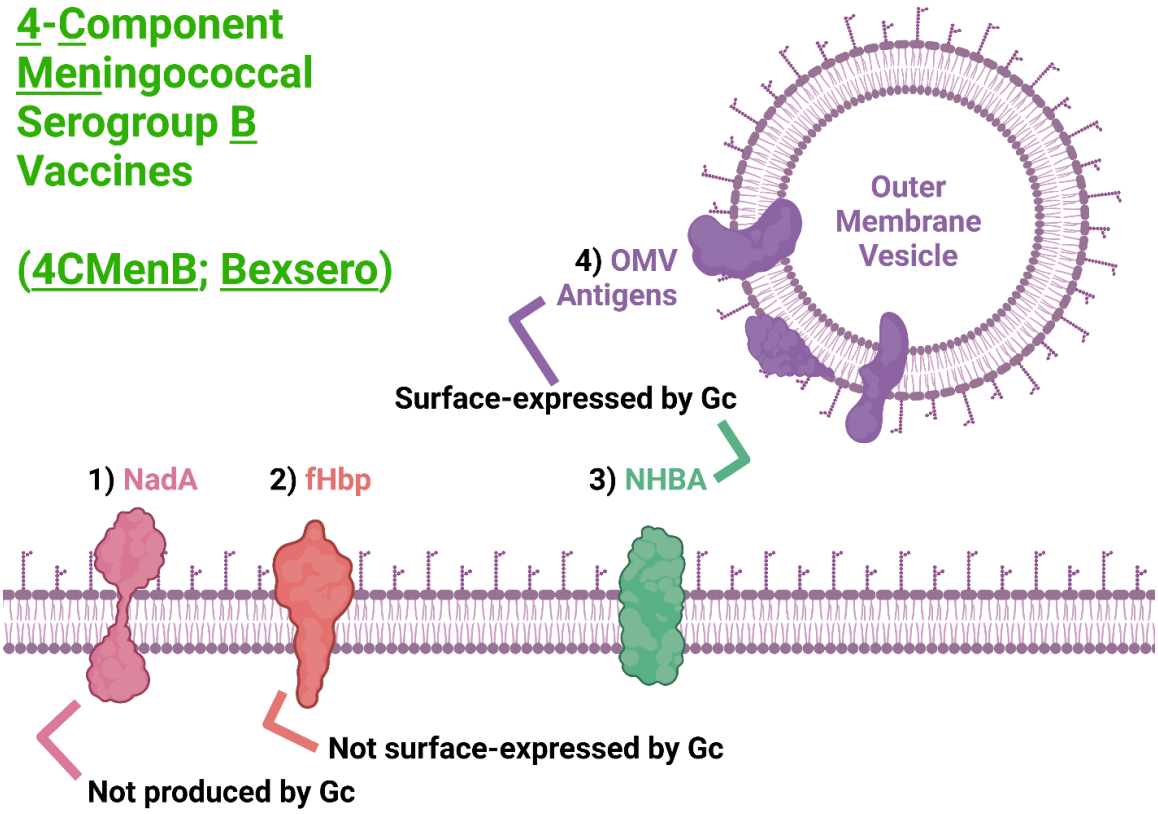

Figure 10. Constituents of 4-component meningococcal serogroup B vaccines

4-component vaccines against meningococcal disease caused by serogroup B *N. meningitidis* (e.g. 4CMenB, Bexsero) include recombinant meningococcal 1) NadA, 2) Factor H Binding Protein (fHbp), and 3) *Neisseria* Heparin Binding Antigen (NHBA), as well as 4) isolated outer membrane vesicles (OMVs). NHBA and fHBP are each fused to another immunogenic meningococcal protein. Gc lacks a NadA homolog and does not express a surface-exposed fHbp homolog. Gc has been shown to express NHBA on its surface. OMVs contain a variety of antigens with appreciable homology to those found in Gc.

1.5 Dissertation goals

The work presented here was initiated by a desire to better understand the many fascinating and incompletely understood effectors of the innate immune system with which Gc must contend. Complement, especially terminal complement, has an intimate association with the pathogenic *Neisseria* although how the MAC exerts its effects is not fully understood. Recent publications showing the potential for MAC-mediated enhancement of antimicrobial therapy against Gram-negatives inspired deeper investigation into the increasingly antibiotic-resistant gonococcus (Chapter 2). We sought to expand upon prior findings by more thoroughly characterizing the array of potentiated antimicrobials, their sites of action, as well as the role of C9 in this process.

Prior to focusing in on complement-related projects, early efforts to interrogate neutrophil-Gc-epithelial interactions in a Transwell system with transepithelial migration yielded intriguing results (Chapter 4). Neutrophil heterogeneity appreciated in this system sparked ambitions to design a spectral flow cytometry panel to characterize primary human neutrophil activation states and surface expression for phagocytic receptors, degranulation, migration, and chemotaxis (Chapter 3). We desired to establish a panel which was adaptable to many applications in neutrophil biology.

We are hopeful that results from these efforts advance the fields of *Neisseria* complement, and neutrophil biology with implications for therapeutic and vaccine development.

2 Terminal complement complexes with or without C9 potentiate antimicrobial activity against *Neisseria gonorrhoeae*

This chapter is a modified version of the previously published article: Lamb EL, and Criss AK. Terminal complement complexes with or without C9 potentiate antimicrobial activity against *N. gonorrhoeae*. (2025). mBio.

Contributors:

Evan Lamb – Conceptualization, Methodology, Analysis, Investigation, Authorship, Validation, Visualization, Funding Acquisition.

Alison Criss – Conceptualization, Methodology, Analysis, Authorship, Funding Acquisition, Project Administration.

2.1 Introduction

The complement system is a predominant arm of innate immunity that is a front-line defense for combating pathogens.[21,137-142] Complement components are abundant in serum and found at most tissues and mucosal surfaces.[2,149,150,295] Complement activation is robustly initiated by IgG and IgM binding, and the resulting catalytic cascade promotes effector functions including leukocyte activation and opsonophagocytosis of C3b-labeled targets by phagocytes.[2,21,142,296] Complement directly kills pathogens by forming membrane attack complex (MAC) pores in target membranes.[21,185,192,195]

The MAC is generated by progressive membrane insertion of the terminal complement components C5b through C8 and subsequent polymerization of C9, resulting in 10-11nm pores.[161,185,192,297] The 5nm C9 transmembrane domains are not predicted to span beyond the Gram-negative outer membrane to targets deeper in the bacterial cell.[161,192] However, in *Escherichia coli*, outer membrane disruption alone is insufficient to drive bacterial death by the MAC, whereas inner membrane disruption is essential.[161,182,183,193] Therefore, foundational biologic questions remain as to how the MAC promotes bactericidal activity. Furthermore, C5b-C8 complexes, without poly-C9, can themselves cluster in membranes, forming smaller pores (~2-4nm) that lyse liposomes and erythrocytes, and kill nucleated cells. Effects and mechanisms of C5b-C8 complexes on Gram-negative bacteria remain to be fully investigated.[154,187-191]

Deficiencies in the complement system result in increased susceptibility to certain infections.[21,137] In particular, deficiencies in C5 through C9 result in a

1,000- to 10,000-fold increased risk for invasive meningococcal disease by *Neisseria meningitidis* and >300-fold increased susceptibility to local and disseminated infection by *N. gonorrhoeae*.[21,206] In turn, pathogenic *Neisseria* attempt to evade complement-mediated killing by hijacking host-derived complement inhibitors C4b-binding protein, factor H, sialic acid, and vitronectin, evading antibody recognition by phase and antigenic variation, and meningococcal capsule production.[21,35,52,204,298-303]

N. gonorrhoeae (the gonococcus, Gc) causes an estimated 82-100 million cases of gonorrhea annually worldwide.[3,6,304] Gonorrhea is an urgent public health threat due to rapidly rising case numbers along with increasing antibiotic resistance.[6,101,102,305,306] Gc infection is characterized by mucosal inflammation, resulting in an influx of neutrophils and serum transudate.[1] If left untreated, or if treatment is ineffective due to antibiotic resistance, collateral tissue damage can cause serious sequelae including pelvic inflammatory disease, ectopic pregnancy, endocarditis, and infertility.[1,21]

Gonococci have been isolated that are resistant to all classes of antibiotics that have been used for treatment, including macrolides, fluoroquinolones, tetracyclines, and beta-lactams. Extensively-drug resistant Gc with lowered susceptibility to extended spectrum cephalosporins are circulating worldwide.[101,102,306] Resistance is conferred by mutation of the antibiotic's target, reduced uptake via mutations in the outer membrane porin, and increased efflux pump production.[15,110,111,133] As in other Gram-negatives, the outer membrane is a barrier preventing access to deeper sites in the bacterial cell.[110,131,250,307,308]

MAC-mediated disruption of the outer membrane can enhance bactericidal activity of antimicrobials against Gram-negative bacteria.[196,309,310] In this model of MAC-mediated potentiation, antimicrobials that are excluded by the outer membrane gain access to the inside of the bacterial cell by traversing through the MAC pore, similar to pharmacologic strategies of enhancing antibiotic activity by combining them with membrane-disrupting compounds.[311-313] However, it is unclear whether MAC-mediated potentiation is conferred by antimicrobial transit through channels formed by the MAC pore or by generalized membrane perturbation.[314] The ability of C5b-C8 complexes to potentiate antimicrobials has also not been tested.

Given these observations and the importance of complement to control *Neisseria*, we investigated how sublethal MAC deposition affected Gc susceptibility to curated antimicrobials. We demonstrate that MAC damages both the gonococcal outer and inner membranes and enhances antibiotic activity at each layer of the Gram-negative cell. Moreover, the MAC re-sensitizes a multidrug-resistant Gc strain to clinically relevant antibiotics. C9-deficient serum promotes membrane damage and anti-gonococcal activity of antibiotics but does not potentiate the activity of host-derived lysozyme, implicating C5b-C8 in forming size-restricted pores in Gc. Our results reveal differences in how terminal complement restricts Gc compared with other Gram-negative bacteria and help explain how terminal complement deficiencies uniquely sensitize individuals to *Neisseria*, suggesting novel host-targeting therapeutic approaches to help combat drug-resistant gonorrhea.

2.2 Results

2.2.1 Human serum kills Gc via terminal complement component deposition.

A serum bactericidal assay (SBA) was adapted to interrogate MAC disruption and antimicrobial potentiation of Gc.[177] Gc was incubated with anti-lipooligosaccharide IgM, followed by addition of Ig-depleted pooled human serum as complement source; serum can contain antibodies that cross-react with Gc antigens, even in individuals with no prior Gc exposure.[147] Titrating both serum and IgM concentrations resulted in significant, reproducible concentration-dependent Gc killing (Fig. 11A,B). 410ng/mL anti-Gc IgM and 2-3% serum yielded non-significant yet detectable killing (sublethal). Serum that was heat-inactivated (HI) or treated with the C5-specific inhibitor OMCI (*Ornithodoros moubata* complement inhibitor) fully lost bactericidal activity (Fig. 11A-C).[181,310,315] By imaging flow cytometry, C3b, C7, and C9 were on the surface of Gc incubated with IgM and active, but not HI serum (Fig. 11D-G). We conclude that Gc is susceptible to classical complement-mediated killing via the MAC in a serum- and antibody-concentration dependent manner.[179]

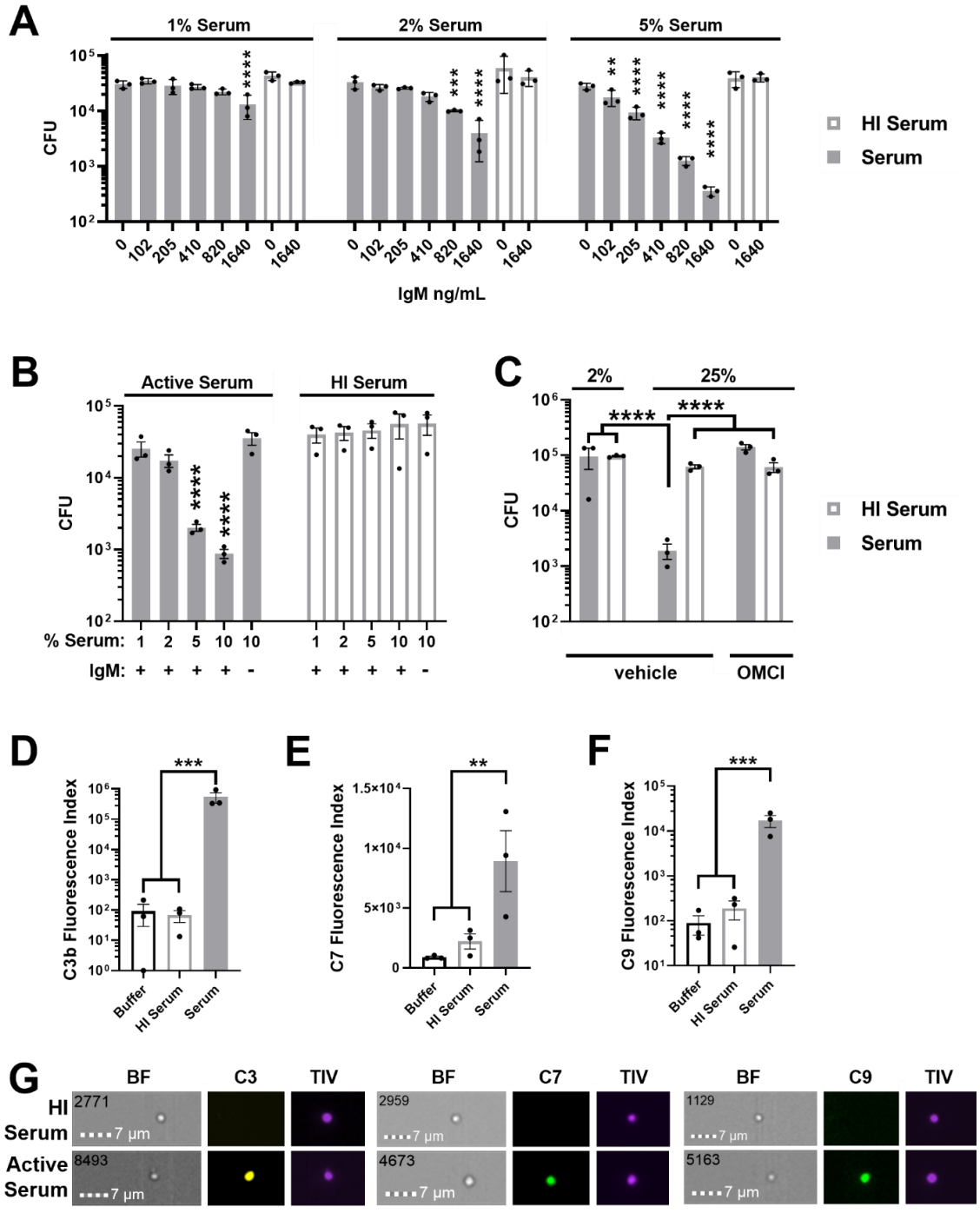
A
1% Serum
2% Serum
5% Serum
CFU
IgM ng/mL
HI Serum
Serum
B
Active Serum
HI Serum
% Serum:
IgM:
C
2%
25%
vehicle
OMCI
D
C3b Fluorescence Index
Buffer
HI Serum
Serum
E
C7 Fluorescence Index
F
C9 Fluorescence Index
G
BF
C3
TIV
C7
C9
HI Serum
Active Serum
7 µm

Figure 11. IgG/M-depleted human serum exhibits MAC-mediated bactericidal activity against Gc

(A) FA1090 Gc was pre-incubated with increasing concentrations of anti-Gc IgM 6B4, followed by incubation with active or heat-inactivated (HI) IgG/M-depleted human serum at 1, 2, or 5% final concentration. (B) FA1090 Gc was pre-incubated without antibody or with 410ng/mL anti-Gc IgM, then challenged with increasing concentrations of IgG/M-depleted human serum. (C) FA1090 Gc was incubated with 410ng/mL anti-Gc IgM and indicated serum concentrations with 20µg/mL of the C5 inhibitor OMCI or vehicle. In (A-C), CFU were enumerated from serial dilutions. (D-G) H041 Gc was treated with IgM for 30 min, then incubated with 2% (D) or 50% (E,F) IgG/M-depleted serum for 2hr, followed by staining and imaging flow cytometry for C3 (D), C7 (E), or C9 (F). Data are presented as Fluorescence Index (median fluorescence intensity * percent positive). (G), Representative micrographs from imaging flow cytometry of C3b, C7, and C9 binding to individual Gc. The scale bar is in the lower lefthand corner. The upper lefthand number indicates the event number of single, focused Gc out of 10,000 total events. BF = brightfield, TIV = Tag-it Violet counterstain. Error bars are standard error of the mean. Significance was determined by 1-way ANOVA with Tukey's multiple comparisons on Log_{10}-transformed data versus 0ng/mL IgM in HI serum at indicated serum percentages (A), vs. 10% HI serum without IgM (B), or as indicated by comparison bars (C-F). **=p<0.01, ***=p<0.001, ****=p<0.0001.

2.2.2 The MAC disrupts both the gonococcal outer and inner membranes.

The SBA conditions above were used to assess complement disruption of Gc outer and inner membranes. 1-N-phenylnapthylamine (NPN) fluoresces only upon integration into the inner membrane, following outer membrane disruption.[313,316] NPN fluorescence was significantly increased in Gc in an active complement-dependent manner (Fig. 12A). Sytox Green fluoresces upon DNA intercalation, after disruption of both outer and inner membranes.[161,310] Gc incubated with active serum, but not HI serum or buffer, showed increased Sytox fluorescence over 2hr (Fig. 12B). Endpoint Sytox Green fluorescence and area under the curve (AUC) were significantly increased in Gc exposed to active serum (Fig. 12C). We conclude that active complement damages both gonococcal outer and inner membranes.

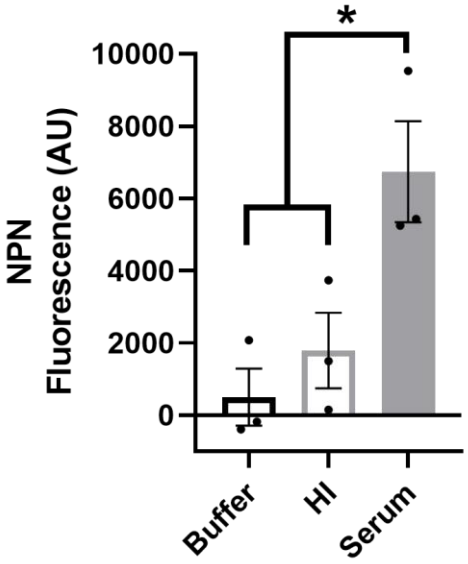
*
10000
8000
6000
4000
2000
0
NPN
Fluorescence (AU)
Buffer
HI
Serum

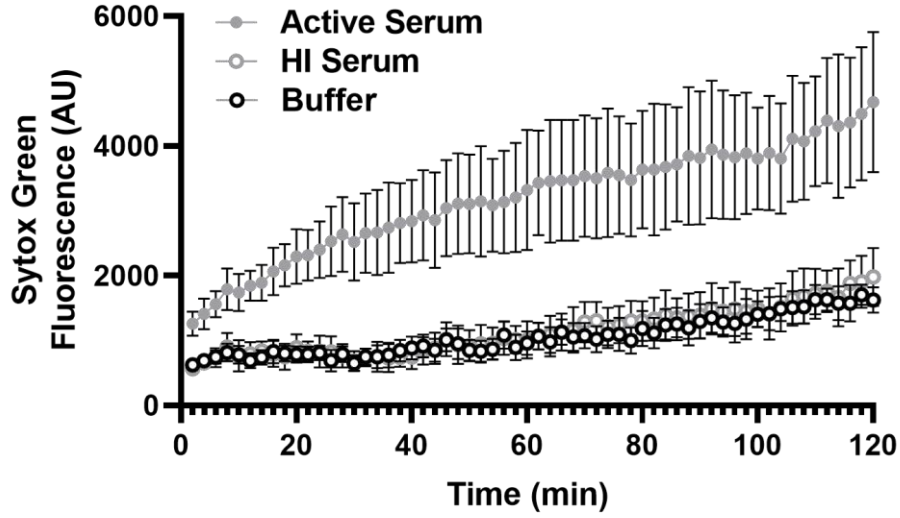
6000
4000
2000
0
Sytox Green
Fluorescence (AU)
Active Serum
HI Serum
Buffer
0
20
40
60
80
100
120
Time (min)

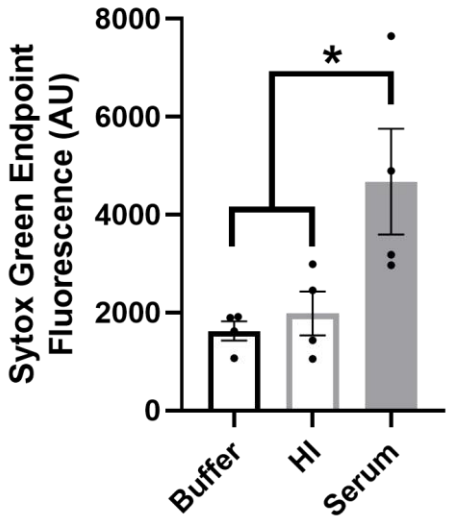
*
8000
6000
4000
2000
0
Sytox Green Endpoint
Fluorescence (AU)
Buffer
HI
Serum

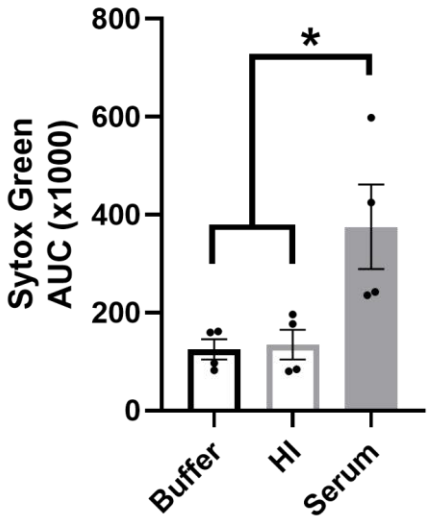
*
800
600
400
200
0
Sytox Green
AUC (x1000)
Buffer
HI
Serum

Figure 12. The MAC disrupts the gonococcal outer and inner membranes

(A-B) Gc was pre-incubated with anti-Gc IgM followed by incubation with active serum, heat-inactivated (HI) serum, or buffer and assessed for NPN (A) or Sytox Green fluorescence (B). NPN experiments used 1-81-S2/S-23; Sytox experiments, strain H041. (C) Sytox Green data from (B) displayed as fluorescence value at the end of the 2-hour incubation and calculated area under the curve (AUC) over 2 hours. Error bars are standard error of the mean. Significance was determined by 1-way ANOVA with Tukey's multiple comparisons. *=$p<0.05$.

2.2.3 The MAC potentiates antimicrobial activity of classically Gram-positive antibiotics.

To ascertain if the MAC can enhance antimicrobial activity, we developed a modified SBA in which IgM- and serum-opsonized Gc was subsequently challenged with antibiotics or host-derived antimicrobials. As proof of concept, we assessed how MAC deposition affected the susceptibility of Gc to antibiotics that are not generally effective against Gram-negative bacteria due to poor penetration of the outer membrane coupled with active efflux: vancomycin, nisin, and linezolid.[196,311,317]

Vancomycin targets D-Ala-D-Ala linkages of peptidoglycan. Treating FA1090 Gc with 3μg/mL vancomycin and 2% active serum reduced viability by 5,327-fold. In comparison, the viability of Gc exposed to 2% active serum alone reduced by 3.7-fold; when exposed to the same concentrations of vancomycin and HI serum, viability reduced 304-fold (Fig. 13A). The statistically significant, greater-than-additive effect of active serum and antibiotic was calculated as a potentiation index, defined as the ratio of antibiotic killing in the presence of active serum versus HI serum (see Methods). A potentiation index >1.0 indicates a greater-than-additive effect from combining antibiotic and active serum. The calculated potentiation index of 3μg/mL vancomycin in 2% serum was 4.7 (Fig. 13A, Table 1). Incubation with OMCI abrogated vancomycin potentiation (potentiation index of 0.83) and was no different from incubation with HI serum, showing potentiation of vancomycin was dependent on terminal complement (Fig. 13A, Table 1). Potentiation was measured over active serum and

vancomycin concentrations in 2-way titration experiments (Fig. 13B). Active serum also potentiated vancomycin's activity against the unrelated Gc strain MS11 (Figure 14, Table 1).

Given that complement causes Gc inner membrane damage (Fig. 12B,C), we next tested classically-Gram-positive antibiotics that target either lipid II in the inner membrane (nisin) or ribosomes in the cytoplasm (linezolid). In HI serum, nisin and linezolid had minimal effect on Gc viability at 100 and 50 μg/mL, respectively (Fig. 13C,D). The anti-gonococcal activities of nisin and linezolid were significantly increased with active serum (Fig. 13C,D) and reduced to HI serum levels when OMCI was added, indicating MAC dependence (Fig. 13C). Potentiation indexes for nisin and linezolid were 3.7 and 8.6, respectively (Table 1).

Vancomycin potentiation was independently measured using overnight broth microdilution assays for MIC determination. Addition of 2.5% active serum reduced the MIC from 5-10μg/mL to 0.078-0.123μg/mL, a 40- to 128-fold decrease (Fig. 13E). MIC broth microdilution experiments similarly demonstrated that active serum potentiated nisin activity (Fig. 15). Taken together, these data show that the MAC potentiates the activity of antibiotics that otherwise have limited activity against Gc. The use of three antibiotics with different targets and mechanisms of action emphasizes that the MAC can enable antibiotic access to all topological layers of the Gc cell.

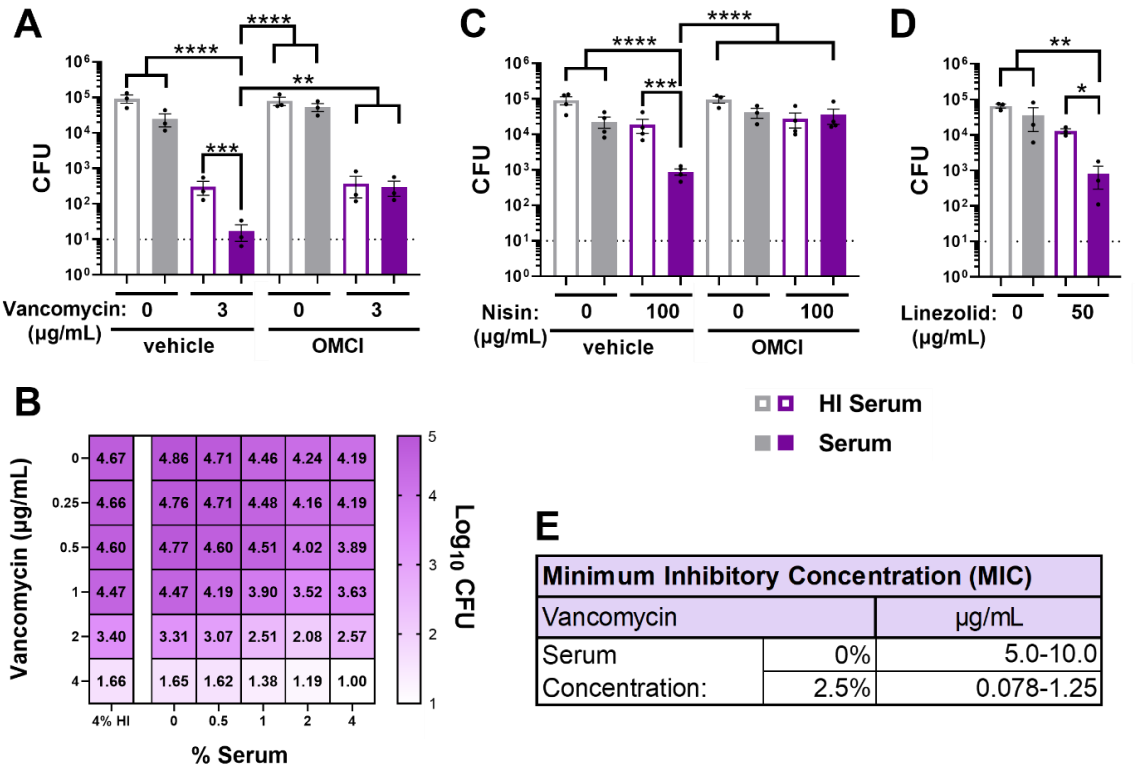

Figure 13. The MAC potentiates antimicrobial activity of classically Gram-positive antibiotics that act at all layers of the gonococcal cell.

(A-D) FA1090 Gc was preincubated with anti-Gc IgM followed by incubation with 2% (A,C), 3% (D), or indicated concentration (B) of IgG/M-depleted human serum with or without heat inactivation (HI). Gc was then incubated with the indicated antibiotic, and CFU were enumerated. Where indicated, serum was first incubated with the C5 inhibitor OMCI (20μg/mL) or vehicle. Error bars are standard error of the mean. Significance was determined by 1-way ANOVA with Tukey's multiple comparisons on Log_{10}-transformed data. *=p<0.05, **=p<0.01, ***=p<0.001, ****=p<0.0001. Dotted line represents minimum reportable CFUs. (E) FA19 Gc assayed via 16-hour minimum inhibitory concentration (MIC) broth microdilution assay over a range of vancomycin concentrations in GCBL alone or supplemented with 2.5% IgG/M-depleted human serum.

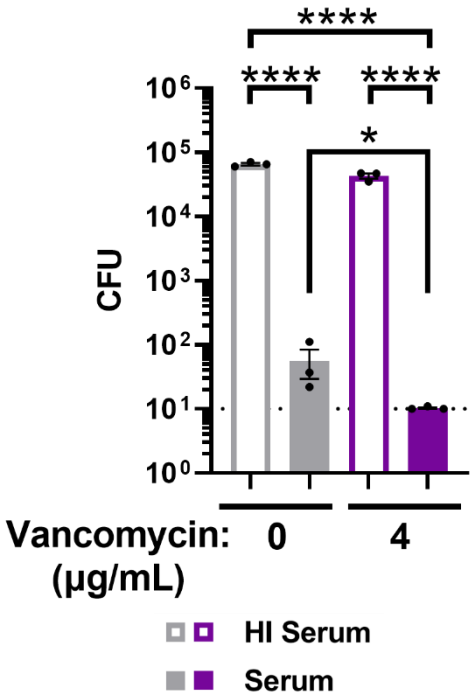

Figure 14. Vancomycin activity is potentiated in the MS11 strain of Gc.

MS11 Gc preincubated with anti-gonococcal IgM followed by incubation with 2% IgG/M-depleted human serum with or without heat-inactivation (HI), and subsequent incubation with vancomycin or vehicle for CFU enumeration. Error bars are standard error of the mean. Significance was determined by 1-way ANOVA with Tukey's multiple comparisons on Log_{10}-transformed data. *=$p<0.05$, ****=$p<0.0001$. Dotted line represents minimum reportable CFUs.

Gc Strain

Minimum Inhibitory Concentration (MIC)		
Nisin		µg/mL
Serum Concentration:	0%	50-100
	2.5%	0.39-0.78

FA19

Minimum Inhibitory Concentration (MIC)		
Ceftriaxone		ng/mL
Serum Concentration:	0%	8.0-16.0
	2.5%	0.0625

MS11

Minimum Inhibitory Concentration (MIC)		
Ceftriaxone		ng/mL
Serum Concentration:	0%	2.0-8.0
	2.5%	0.0625-0.25

FA1090

Minimum Inhibitory Concentration (MIC)		
Ceftriaxone		ng/mL
Serum Concentration:	0%	0.25-0.5
	2.5%	0.03125-0.0625

FA19

Figure 15. Minimum inhibitory concentrations of nisin and ceftriaxone are decreased by serum across multiple Gc strains.

Additional Gc strains were assayed via broth microdilution assays over a range of nisin or ceftriaxone concentrations in media alone or supplemented with 2.5% IgG/M-depleted human serum as above.

Table 1: Potentiation Indexes				
Antimicrobial (µg/mL)	% IgG/M-depl Serum	Potentiation Index	Potentiation Index with OMCI	Gc Strain
Vancomycin (3)	2	**4.7**	**0.83**	FA1090
Nisin (100)	2	**3.7**	**0.33**	FA1090
Linezolid (50)	3	**8.6**	-	FA1090
Vancomycin (4)	2	**3.6**	-	MS11
Azithromycin (4)	2	**174.5**	**0.90**	H041
Ceftriaxone (4)	2	**12.5**	**0.68**	H041
Zoliflodacin (0.125)	2	**9.7**	-	H041
Doxycycline (4)	2	**99.8**	-	H041
Gentamicin (10)	2	**4.8**	-	H041
Lysozyme (1,000)	2	**3.8**	**1.0**	FA1090
	% C9-reconst Serum			
Azithromycin (4)	1	**535.1**	-	H041
Lysozyme (1,000)	1	**9.3**	-	H041
Ceftriaxone (4)	1	**9.3**	-	H041
Nisin (100)	1	**8.7**	-	H041
	% C9-depl Serum			
Azithromycin (4)	1	**120.7**	-	H041
Lysozyme (1,000)	1	**0.95**	-	H041
Ceftriaxone (4)	1	**8.0**	-	H041
Nisin (100)	1	**1.9**	-	H041

Table 1. Potentiation indexes

OMCI = C5 inhibitor, 20µg/mL.

2.2.4 The MAC enhances frontline and novel antibiotic activity against multidrug-resistant Gc.

Frontline antibiotic regimens for gonorrhea are ceftriaxone alone or with azithromycin, depending on local recommendations, yet resistance to these and other antibiotics is increasing.[102] We determined if MAC-mediated potentiation can restore sensitivity of multidrug-resistant Gc to antibiotics using strain H041, the first isolate reported with elevated ceftriaxone resistance. H041 displays decreased susceptibility to other antibiotics, including azithromycin.[110,318] H041 Gc exposed to 2% active serum and 4μg/mL azithromycin had a 1,295-fold decrease in viability (Fig. 16A). This was a statistically significant enhancement over the effect of azithromycin alone (2% HI serum, 7.4-fold viability decrease) or when OMCI was added (Fig. 16A), resulting in a potentiation index of 174.5 (Table 1). By two-way titration, potentiation occurred over a range of azithromycin and serum concentrations (Fig. 16B). Ceftriaxone at 4μg/mL was significantly more potent at Gc killing in 2% active serum compared to HI serum, with a potentiation index of 12.5; potentiation was abrogated with OMCI (Fig. 16C).

By broth microdilution, the average MIC for azithromycin dropped in the presence of 2.5% active serum by 22-fold (0.0078-0.016μg/mL without serum vs. 0.0002-0.0078μg/mL with serum) (Fig. 16D). Adding serum decreased the ceftriaxone MIC by 125-250-fold, from 1μg/mL to 0.004-0.008μg/mL, which is below the 0.25μg/mL susceptibility breakpoint for Gc (Fig. 16E).[319] Serum also potentiated ceftriaxone against multiple Gc strains (Fig. 15). We conclude that

MAC deposition renders Gc more sensitive to clinically relevant antibiotics, reducing MICs below breakpoints for drug-resistant strains.[107,319]

The first-in-class antibiotic zoliflodacin, a DNA topoisomerase inhibitor, is a promising new therapeutic for gonorrhea (ClinicalTrials.gov ID NCT03959527).[320] 2% active serum significantly enhanced the activity of 0.125μg/mL zoliflodacin against H041 Gc, with a potentiation index of 9.7 (Fig. 17A, Table 1). Serum also potentiated the activity of doxycycline, currently recommended for post-exposure prophylaxis by the CDC despite a high frequency of circulating resistance in Gc[99,321,322], and gentamicin, currently recommended for uncomplicated urogenital infection with ceftriaxone-resistant Gc or in patients with cephalosporin sensitivity.[87,323,324] For H041 Gc with 2% active serum compared with HI serum, 4μg/mL doxycycline reduced bacterial viability 317-fold with a potentiation index of 99.8, and 10μg/mL gentamicin reduced viability 1,656-fold with a potentiation index of 4.8 (Fig. 17B,C; Table 1). Thus, new antibiotics and antibiotic treatment regimen for gonorrhea can be potentiated with human serum.

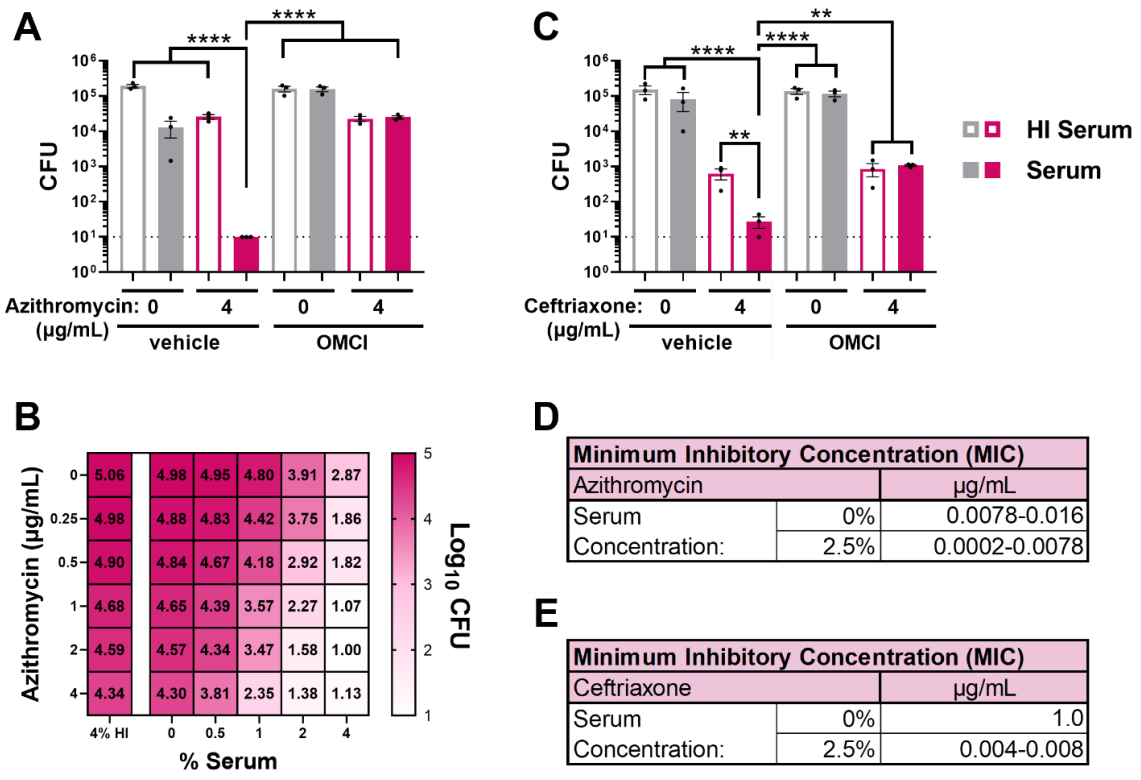

Minimum Inhibitory Concentration (MIC)		
Azithromycin		µg/mL
Serum Concentration:	0%	0.0078-0.016
	2.5%	0.0002-0.0078

Minimum Inhibitory Concentration (MIC)		
Ceftriaxone		µg/mL
Serum Concentration:	0%	1.0
	2.5%	0.004-0.008

Figure 16. MAC-dependent increase in sensitivity and susceptibility of multidrug-resistant Gc to front-line antibiotics

(A-C) H041 Gc was pre-incubated with anti-Gc IgM followed by incubation with 2% (A,C) or indicated concentration (B) of IgG/M-depleted human serum, with or without heat-inactivation (HI). Gc was then incubated with the indicated antibiotic, and CFU were enumerated. Where indicated, serum was first incubated with the C5 inhibitor OMCI (20µg/mL) or vehicle. Error bars are standard error of the mean. Significance was determined by 1-way ANOVA with Tukey's multiple comparisons on Log_{10}-transformed data. **=p<0.01, ****=p<0.0001. Dotted line represents minimum reportable CFUs. (D,E) FA19 Gc (D) or H041 Gc (E) were assayed over a range of azithromycin or ceftriaxone concentrations in GCBL alone or supplemented with 2.5% IgG/M-depleted human serum.

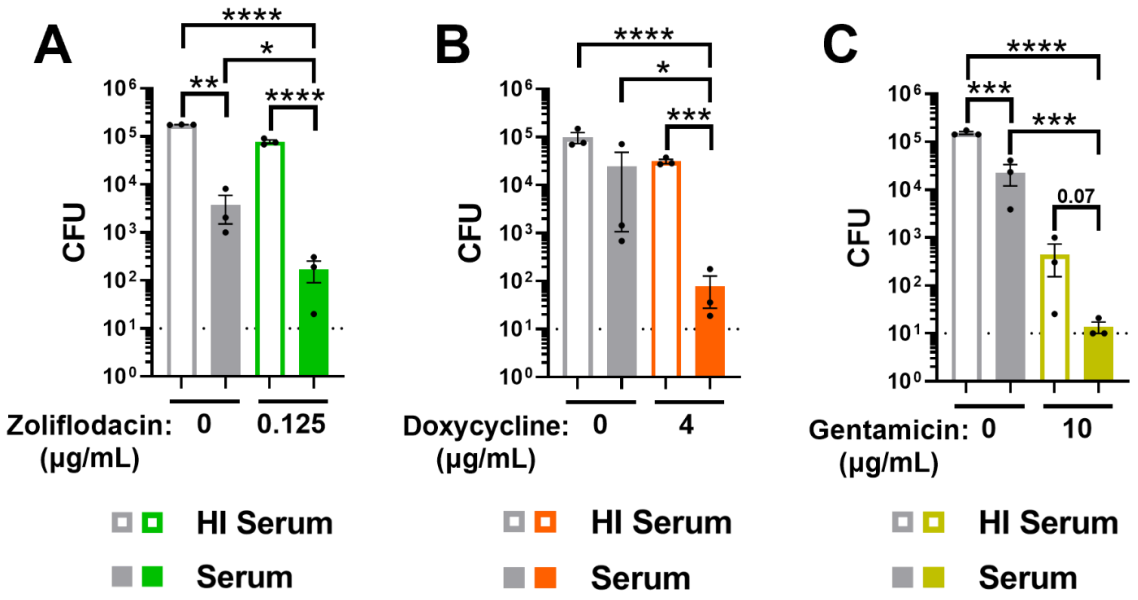

Figure 17. The MAC enhances anti-gonococcal activity of new antibiotic regimens

H041 Gc was pre-incubated with anti-Gc IgM followed by incubation with 2% IgG/M-depleted human serum with or without heat-inactivation (HI). Gc was then incubated with zoliflodacin (A), doxycycline (B), or gentamicin (C), followed by CFU enumeration. Error bars are standard error of the mean. Significance was determined by 1-way ANOVA with Tukey's multiple comparisons on Log_{10}-transformed data. *=p<0.05, **=p<0.01, ***=p<0.001, ****=p<0.0001. Dotted line represents minimum reportable CFUs.

2.2.5 C5b-C8 complement complexes promote measurable bactericidal activity and damage the gonococcal outer and inner membranes.

C5b-C8 complexes have been reported to form ~2-4nm diameter pores in liposomes and eukaryotic membranes.[154,189,324] Without C9, these smaller complexes are expected to interact differently with target membranes due to fewer transmembrane domains and their smaller size.[154,161,183] In *E. coli*, serum depleted of C9 results in diminished outer membrane damage and little to no measurable bactericidal activity or inner membrane damage, compared to C9-replete serum.[183,188] In contrast, the viability of H041 Gc exposed to anti-lipooligosaccharide IgM and 25% C9-depleted active serum was decreased by 1.2 logs; the effect was lost when this serum was heat inactivated (Fig. 18A). Although serum reconstitution with C9 to native levels (60µg/mL) further enhanced bactericidal activity (4.1 log decrease in viability; Fig. 18A)[190], these results demonstrate that serum without C9 retains direct anti-gonococcal activity.

To uncover how C5b-C8 complexes affect Gc outer and inner membranes, we measured NPN and Sytox Green fluorescence, respectively, as in Figure 2.[161,310,313,316] IgM-bound Gc incubated with 50% C9-depleted or C9-reconstituted serum were indistinguishable in NPN fluorescence, and both were significantly greater than Gc in HI serum or buffer (Fig. 18B). Sytox Green fluorescence increased over 2 hours following incubation with 2% C9-depleted or C9-reconstituted serum (Fig. 18C). Endpoint Sytox Green fluorescence was not significant between C9-depleted and C9-reconstituted sera. However, there was a significant increase in Sytox Green AUC for Gc incubated with C9-reconstituted

serum compared to C9-depleted serum (Fig. 18C,D). Endpoint and AUC intensities were significantly lower for Gc incubated in buffer or with HI C9-reconstituted serum compared to active C9-depleted or C9-reconstituted serum (Fig. 18D).

Using imaging flow cytometry on single bacteria[177], we confirmed that Gc exposed to C9-depleted and C9-reconstituted serum had equivalent amounts of C3b and C7 on their surface, and both were significantly greater than buffer or HI serum controls (Fig. 19). As expected, the C9 signal on Gc exposed to active C9-reconstituted serum was significantly higher than bacteria exposed to C9-depleted serum, HI C9-reconstituted serum, or buffer, all of which were at background levels (Fig. 19). Thus C9-depleted serum is equivalent to C9-reconstituted serum for deposition of early (C3b) and precursor terminal (C7) complement components, and reconstitution with purified C9 allows C9 deposition into the Gc outer membrane.

Taken together, these results indicate that C5b-C8 complement complexes are sufficient to disrupt the gonococcal cell envelope and promote bactericidal activity, but C9 incorporation enhances inner membrane disruption and consequent Gc killing.

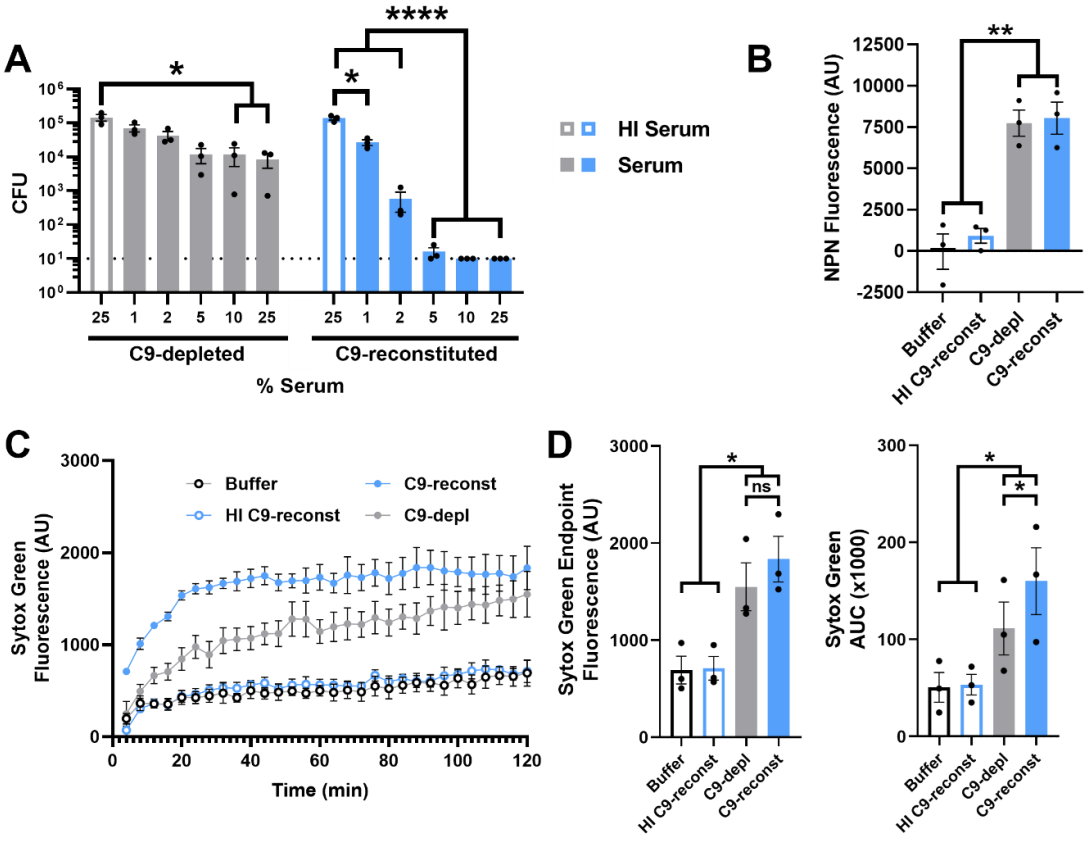
A
CFU
HI Serum
Serum
C9-depleted
C9-reconstituted
% Serum
B
NPN Fluorescence (AU)
Buffer
HI C9-reconst
C9-depl
C9-reconst
C
Sytox Green Fluorescence (AU)
Buffer
HI C9-reconst
C9-reconst
C9-depl
Time (min)
D
Sytox Green Endpoint Fluorescence (AU)
Sytox Green AUC (x1000)
ns

Figure 18. Complement C5b-C8 complexes promote measurable anti-gonococcal activity and damage the Gc outer and inner membranes

(A) H041 Gc was preincubated with anti-Gc IgM, followed by incubation with the indicated concentration of C9-depleted or C9-reconstituted serum with or without heat-inactivation (HI), and CFU were enumerated. Dotted line represents minimum reportable CFUs. (B,C) Gc was pre-incubated with IgM followed by incubation with buffer, C9-depleted human serum, or C9-reconstituted human serum with or without heat-inactivation. NPN (B) or Sytox Green (C) fluorescence was measured as in Figure 12. NPN experiments used 1-81-S2/S-23 Gc, while Sytox experiments used H041. (D) Sytox green data from (C), displayed as fluorescence value at the end of the 2-hour incubation and as area under the curve (AUC) over the time course. Error bars are the standard error of the mean. Significance was determined by 1-way ANOVA with Tukey's multiple comparisons on Log_{10}-transformed data (A,D) or as 1-way ANOVA with Tukey's multiple comparisons (B). *=p<0.05, **=p<0.01, ****=p<0.0001, ns = not significant.

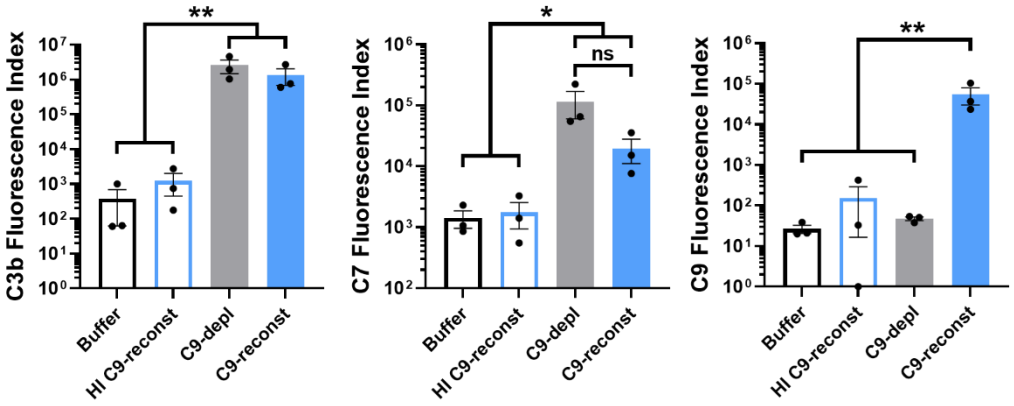

Figure 19. C9-depleted and C9-reconstituted sera produce similar terminal complement deposition

H041 Gc was treated with IgM for 30min, then incubated with 2% (for C3b) or 50% (for C7 and C9) IgG/M-depleted human serum for 2hr. Imaging flow cytometry for the indicated complement component was conducted as above. Data are presented as Fluorescence Index (median fluorescence intensity * percent positive). Error bars are the standard error of the mean. Significance was determined by 1-way ANOVA with Tukey's multiple comparisons on Log_{10}-transformed data. *=$p<0.05$, **=$p<0.01$, ns = not significant.

2.2.6 Complement C5b-C8 complexes and full C5b-C9 MACs differentially potentiate antimicrobial activities.

Given that C5b-C8 and C5b-C9 complexes both displayed anti-gonococcal activity, we evaluated how the presence or absence of C9 potentiated the activity of antimicrobials. Using the SBA protocol from Figure 4, H041 Gc was challenged with 1% C9-reconstituted or C9-depleted active serum or HI serum controls, followed by 4μg/mL azithromycin or vehicle. Azithromycin is a 749Da antibiotic with an estimated diameter of <2nm.[325] Both C9-depleted and C9-reconstituted sera potentiated azithromycin activity against H041 Gc, with potentiation indexes of 535.1 and 120.7, respectively (Fig. 20A, Table 1). C9-depleted and -reconstituted sera also potentiated the <2nm antibiotic ceftriaxone (potentiation indexes 8.0 and 9.3, respectively) (Fig 20B, Table 1).

The peptidoglycan-degrading enzyme lysozyme has potent activity against Gram-positive bacteria with exposed cell walls, but low activity against Gram-negatives due to the outer membrane barrier.[192,194,196,228,250,307] Human lysozyme has a molecular weight of 14,300Da and a maximum diameter of ~9nm by X-ray crystallography.[326,327] 2% active serum natively containing C9 enhanced the activity of 1000μg/mL lysozyme against FA1090 Gc with a potentiation index of 3.8; OMCI treatment abrogated the potentiation, indicating MAC dependence (Fig. 20C, Table 1). H041 Gc was resistant to killing by 1000μg/mL lysozyme when HI serum was used (Fig. 20D). Adding 1% C9-reconstituted human serum reduced Gc viability 29.7-fold, with a potentiation index of 9.3 (Fig. 20D, Table 1). In contrast, C9-depleted serum showed no potentiation of lysozyme (index of

0.95) (Fig. 20D, Table 1). Similarly, nisin (~6.7nm) was potentiated by C9-reconstituted but not C9-depleted serum (Fig. 20E, Table 1). We conclude that C5b-C8 and C5b-C9 complement complexes can permit small molecules, including some antibiotics, to bypass the Gc outer membrane, but larger molecules or antimicrobial enzymes require full C9-containing MAC pores for intracellular access.

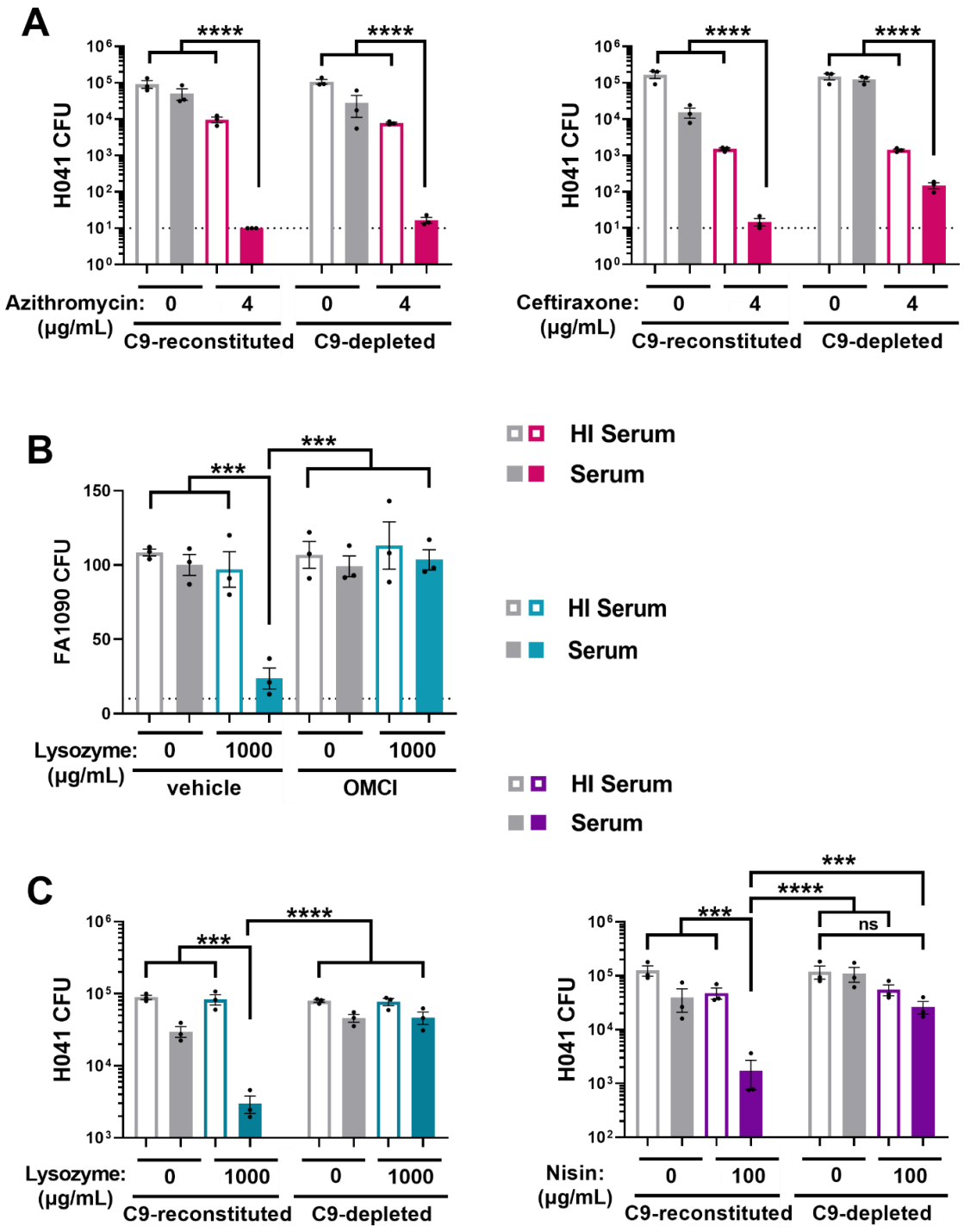
A
H041 CFU
****
****
Azithromycin: 0 4 0 4
(µg/mL)
C9-reconstituted
C9-depleted
Ceftiraxone: 0 4 0 4
(µg/mL)
C9-reconstituted
C9-depleted
B
FA1090 CFU
***
***
Lysozyme: 0 1000 0 1000
(µg/mL)
vehicle
OMCI
HI Serum
Serum
HI Serum
Serum
HI Serum
Serum
C
H041 CFU
***
****
Lysozyme: 0 1000 0 1000
(µg/mL)
C9-reconstituted
C9-depleted
***
****
ns
Nisin: 0 100 0 100
(µg/mL)
C9-reconstituted
C9-depleted

Figure 20. Complement C5b-C8 complexes and full C5b-C9 MAC differentially potentiate the activities of antimicrobials against Gc

H041 (A,C) or FA1090 (B) Gc was preincubated with anti-Gc IgM followed by incubation with 1% (A,C) or 2% (B) C9-depleted or C9-reconstituted human serum with or without heat-inactivation (HI). Gc was then incubated with azithromycin (A) or human lysozyme (B,C) and then plated for CFU enumeration. Where indicated serum was first incubated with the C5 inhibitor OMCI (20µg/mL) or vehicle. Error bars are standard error of the mean. Significance was determined by 1-way ANOVA with Tukey's multiple comparisons on Log_{10}-transformed data. ***=$p<0.001$, ****=$p<0.0001$. Dotted line represents minimum reportable CFU.

2.3 Chapter Discussion

Deficiencies in terminal complement components which comprise the MAC are highly predisposing to serious infections by Gc and *N. meningitidis*.[21,206] The capacity for MAC to damage Neisserial membranes and enhance antimicrobial activity represents a promising avenue for combating these pathogens. Here, using laboratory and multidrug-resistant strains of Gc, we found the MAC disrupted both outer and inner membrane integrity. Beyond direct bactericidal activity, MAC enhanced the anti-gonococcal activity of antibiotics and rendered multidrug-resistant Gc susceptible to frontline and new antibiotic programs. Intriguingly, C5b-C8 complexes also disrupted Gc outer and inner membranes and exerted bactericidal activity. C5b-C8 complexes potentiated the activity of azithromycin, but C9 addition was necessary to potentiate lysozyme. We conclude that terminal complement components, both MAC and C5b-C8 complexes, are both directly bactericidal for Gc and also potentiate the activity of diverse antimicrobials.

As a mucosal pathogen, Gc encounters complement via serum transudate and local production by resident epithelial cells, fibroblasts, and immune cells.[1,48,149,295] Here, we showed that serum exposure enhances killing of Gc by antimicrobials targeting the periplasm (vancomycin, ceftriaxone, lysozyme), inner membrane (nisin), and cytoplasm (linezolid, azithromycin, zoliflodacin, doxycycline, gentamicin), which is abrogated by heat inactivation or OMCI. Thus, antimicrobial potentiation is MAC-dependent and broadly applicable to different treatment options. As C5b-C8/C9 complexes disrupt both outer and inner

membranes, we conclude that terminal complement perturbs the Gc envelope to enhance antimicrobial penetration. MAC-mediated potentiation underscores the promise of membrane-disrupting therapies as adjuvants to enhance antibiotic efficacy against multidrug-resistant bacteria like Gc.

Although the MAC cannot extend past the outer membrane, inner membrane disruption is required for MAC to kill Gram-negative bacteria.[161,182,183,193] The exact mechanism of MAC killing remains undefined but could include generalized osmotic instability, leakage of vital intracellular factors, influx of toxic factors, homeostatic disturbance (diminished PMF), and triggering of stress responses leading to bacterial death.[161,328] Several non-exclusive hypotheses can explain how MAC potentiates antimicrobial activity in Gc. First, outer membrane disruption increases the periplasmic concentration of antibiotics, which then access the cytoplasm. This possibility is supported by MAC restoring antibiotic sensitivity to multidrug-resistant Gc like H041 with more restrictive porin.[110,111] Relatedly, inner membrane disruption via MAC would also enhance cytoplasmic access of antimicrobials. Finally, inner membrane perturbation would inhibit efflux pumps that directly or indirectly require the PMF.[15] Although efflux pumps are frequently upregulated in multidrug-resistant Gc, terminal complement activity would overcome their activity. Future studies can test among these hypotheses by tracking antimicrobial access to subcellular compartments.

We found that serum containing C9 was bactericidal for Gc and that C9-containing MAC disrupted Gc outer and inner membranes. Notably, C5b-C8 complexes also promoted anti-gonococcal activity, though less robustly. The Gc

outer membrane was damaged similarly by C9-depleted and C9-reconstituted serum, while inner membrane damage by C9-depleted serum was delayed but reached the same endpoint as with C9. These findings contrast with results from *E. coli,* where C5b-C8 complexes minimally affected inner membrane integrity compared to MAC.[183,188] The uniqueness of *Neisseria* cell wall composition and integrity versus other Gram-negative bacteria may underlie these C9-dependent differences. The outer leaflet of the Neisserial outer membrane is composed of lipooligosaccharide, not lipopolysaccharide.[329,330] Unlike other Gram-negative bacteria, Gc lipid membranes contain significant levels of phosphatidylcholine and differ in other phospholipid species composition.[331-333] Gc lacks Braun's lipoprotein[334] or full-length OmpA or Pal homologues, which link the outer membrane to the cell wall.[18,57] The Rcs system that senses outer membrane stress is also absent in Gc.[335-337] Because Gc subverts both human cellular and humoral immunity, including resistance to neutrophils[12,146,228,338], prevention of protective T_H1 responses[27,339], induction of B cell death and impaired antibody production[285], and phase and antigenic variation to evade antibody recognition[35,340], complement may be the most effective arm of immunity to control Gc, and its absence greatly increases susceptibility to infection. Our findings with C9 align with epidemiologic evidence that C9 deficiencies more modestly predispose individuals to *Neisseria* compared to other terminal complement deficiencies.[21,190,198] Beyond genetic C9 deficiencies, reduced C9 on the Gc surface could occur by bacterial recruitment of the C9 inhibitor vitronectin.[21,52,191,301,341]

If terminal complement pores directly enable intracellular access to bacteria, then 10-11nm MAC pores would allow access of some antimicrobials that would be excluded by 2-4nm C5b-C8 complexes based on the antimicrobials' diameter. We found that lysozyme and nisin were only potentiated by C9-reconstituted serum, but azithromycin and ceftriaxone were potentiated in a C9-independent manner. Thus, our results support a model in which potentiation in Gc occurs through direct transit, and that C5b-C8 complexes and MAC differentially potentiate antimicrobials in a size-dependent manner (Fig. 21). However, the possibility remains that generalized outer membrane perturbation or 'fracturing' allows compounds to gain intracellular access without transiting directly through pores formed by terminal complement.[314]

Our results emphasize how complement envelope perturbation could enhance anti-Gc therapeutics, including vaccines. This study used an anti-lipooligosaccharide IgM as proof of concept to drive classical complement activation on Gc.[177,295,342] Antibody-eliciting vaccines and passive immunization with monoclonal antibodies have shown preclinical promise in preventing Gc infection in animal models and epidemiological studies.[156,290,293,294,343] However, antibodies as immune correlates for protection have not yet been established.[156,177,180] Even if antibodies do not drive strong bactericidal activity, our findings show that sublethal terminal complement deposition potentiates antibiotic activity. Aligning with our results, a chimeric IgM-C4b binding protein fusion increases direct killing of Gc and enhances killing by azithromycin and ciprofloxacin.[155,310] These observations are relevant to treatment of antibiotic-

resistant Gc, where prolonged and increased dosing of ceftriaxone ultimately overcomes resistance determinants to clear infection.[110,111] Beyond antibiotics, the finding that MAC renders Gc susceptible to killing by human lysozyme suggests that enhancing terminal complement deposition on Gc in immunocompetent individuals would enhance killing of Gc at mucosal surfaces and within immune cell phagosomes where these antimicrobials are found. Although C9-deficient individuals have increased susceptibility to *Neisseria* infections, our evidence indicates that C5b-C8 complexes could still augment antibiotic therapy in them against antibiotic-resistant Gc. In all cases, antibodies and complement would work together against Gc in three ways: direct lysis, opsonophagocytic killing, and potentiating antimicrobial sensitivity within and outside cells.[226]

This study emphasizes that complement-mediated control of Gc can be accomplished through both MAC and C5b-C8 complexes that potentiate existing and novel antibiotic regimens and enhance host-derived antimicrobial activity. New therapeutic approaches that exploit terminal complement are promising countermeasures to combat antibiotic-resistant gonorrhea.

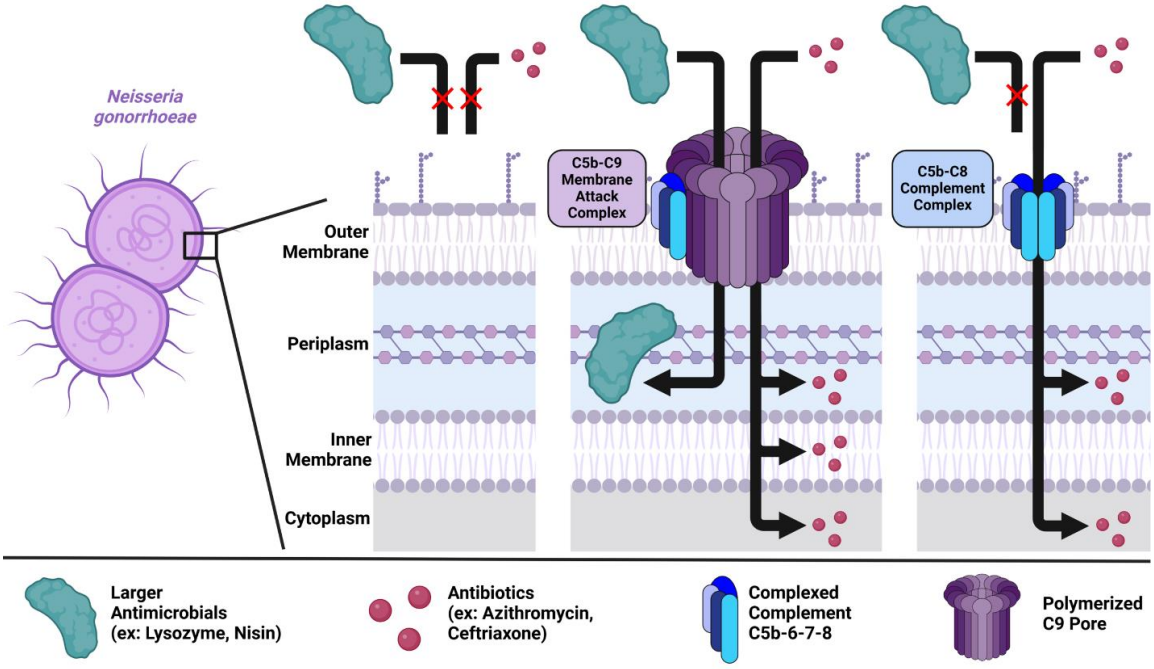

Figure 21. Proposed model of antimicrobial potentiation by terminal complement complexes against *N. gonorrhoeae*

In the absence of complement, antimicrobials may have limited ability to cross the outer membrane and reach their targets (left). When the C5b-C9 membrane attack complex (MAC; pore size 10-11nm) penetrates the gonococcal outer membrane, antibiotics and host-derived antimicrobials can bypass the outer membrane barrier to access their targets within the periplasm, inner membrane, or cytoplasm (middle). In the absence of C9, C5b-C8 complexes can enhance access of antimicrobials that are predicted to be smaller than the 2-4nm pore size of these complexes (right).

2.4 Materials & Methods

2.4.1 Sex as a biological variable.

Human serum was pooled from both sexes.

2.4.2 *Neisseria gonorrhoeae.*

The following Gc strains were used for this study[177]: FA1090 (1-81-S2, and 1-81-S2/S-23)[289], H041 (WHO X)[110,111], MS11[344], and FA19.[135] The 1-81-S2 strain of Gc is an FA1090 derivative with a defined pilin antigen[79,345,346]; S-23 is a 1-81-S2 derivative where all *opa* genes were deleted and containing a loop 6 *porB* mutation that abrogates binding of C4b-binding protein to enhance serum sensitivity.[38,48,347] Gc was routinely streaked on gonococcal base medium (BD Difco) plus Kellogg's supplement I and 1.25μM $Fe(NO_3)_3$ (gonococcal base, GCB) plates for single colonies for 14-16 h at 37°C, 5% CO_2.[45,177] When indicated, Gc was inoculated into GCB liquid media (GCBL) or Hanks' Balanced Salt solution with 2% bovine serum albumin (HBSS + 2% BSA).

2.4.3 Human serum complement sources

IgG/IgM-depleted pooled human serum (IgG/M-depleted serum, Pel-Freez, Catalog #34010, Lot #28341) was used as the complement source for SBA assays with native C9, flow cytometry assays, and MIC assays. IgG/M-depleted serum from lots #28341 and #15443 were used for membrane integrity assays. Use of IgG/M-depleted serum removes the potential for variable bactericidal activity conferred by different individuals' serum.[147,348] SBA assays evaluating C9 used C9-depleted human serum (no immunoglobulin depletion; Complement Technology, Catalog #A326, Lot #10a), reconstituted to

physiological concentration with 60µg/mL C9 protein (Complement Technology, Catalog # A126, Lot #13).[349] Sera were stored at -80°C until thawed on the day of use, then diluted in HBSS + 2% BSA. Sera were heat-inactivated by incubation at 56°C for 30min.[181]

2.4.4 Antibodies and antimicrobials.

See Table 2. Antimicrobial concentrations were determined experimentally, contextualized by *in vivo* concentrations or as antibiotic breakpoints where applicable.[350-356]

Table 2: Antibodies and Antimicrobials						
Antibody (target)	Source	Clone	Conjugate	Catalog Number	Lot	Stock Concentration
LOS	Sanjay Ram	6B4[a]	-	-	-	330µg/mL
(i)C3b	BioLegend	3E7/C3b	PE	846103	B362314	100µg/mL
C7	Invitrogen	15D1	-	MA5-34943	ZF4349897A	2mg/mL
C9	Novus	22	FITC	NBP-21612F	D162593	1.35mg/mL
mouse IgG_{1-3}	Jackson ImmunoResearch	polyclonal	AF488	115-545-164	152191	700µg/mL
Antimicrobial	Source	Catalog Number				
Vancomycin	Caisson	V007-1GM				
Nisin	Cayman	16532				
Linezolid	Cayman	15012				
Ceftriaxone	Cayman	18866				
Azithromycin	Cayman	15004				
Gentamicin	Sigma Aldrich	G3632-250MG				
Zoliflodacin	TargetMol	1620458-09-4				
Doxycycline	Sigma Aldrich	D9891-1G				
Human Lysozyme	Sigma Aldrich	L1667-1G				

Table 2. Antibodies and antimicrobials for MAC potentiation studies

[a] 6B4 was generated from murine hybridoma and purified by thiophilic chromatography; RRID: AB_2617193. LOS = lipooligosaccharide.

2.4.5 SBAs and antimicrobial potentiation assays.

Single Gc colonies were swabbed from GCB plates into GCBL, diluted to OD_{550} nm of 0.07, then diluted 2.5-fold into HBSS + 2% BSA (buffer, ~1.8e7 CFU/mL). Bacteria (20µL) were added to 20µL of 410ng/mL 6B4 IgM in buffer in a V-bottom 96-well plate and incubated at 37°C, 5% CO_2 for 15min. Gc-antibody mixtures were then incubated with 40µL of buffer or indicated final percentages of serum for 45min. For SBA assays without antimicrobial challenge, bacteria were mixed with 80µL of PBS for indicated times. For potentiation SBA assays, Gc-antibody-serum mixtures were incubated with 80µL of the indicated final antimicrobial concentrations (in PBS for antibiotics or sterile water for lysozyme), and incubated at 37°C, 5% CO_2 for 2 hr. Samples were then serially diluted and plated on GCB agar for CFU enumeration after overnight culture at 37°C, 5% CO_2. Where indicated, OMCI (20µg/mL final concentration) or equal volume of TBS buffer was incubated with serum for 30min at 4°C prior to adding Gc.

2.4.6 Potentiation indexes.

For each antimicrobial concentration and serum percentage, CFU enumerated from serum alone was divided by the CFU from serum with the antimicrobial. Similarly, CFU enumerated from HI serum alone was divided by CFU from HI serum with the antimicrobial. The potentiation index is the ratio of the effect of antibiotic on active serum vs. HI serum:

$$\frac{(\text{Serum without antibiotic} \div \text{Serum with antibiotic})}{(\text{HI serum without antibiotic} \div \text{HI serum with antibiotic})}$$

A potentiation index >1.0 indicates a greater-than-additive effect of combining active serum and antimicrobial, while a potentiation index ≤1.0 indicates no enhanced effect.

2.4.7 Complement deposition by imaging flow cytometry.

Bacteria from GCB plates were inoculated into HBSS-BSA to an OD_{550} nm of 0.25 and mixed 1:1 with IgM for 30min at 37°C, 5% CO_2. Buffer or serum were then added (final serum concentration of 2% for C3, or 50% for C7 and C9) and incubated for 2hr more. Bacteria were washed three times with PBS (for C3 and C9) or HBSS-BSA (for C7). For C7, AlexaFluor 488-conjugated (AF488) anti-IgG was then added for 30min at 4°C in the dark, then washed into PBS. Bacteria were counterstained with Tag-it Violet (TIV; BioLegend) for 15min at 37°C with 5% CO_2, washed into buffer, and fixed with 1% paraformaldehyde overnight. Samples were assayed using the Imagestream^X Mk II with INSPIRE software (Luminex) within 72hr. FITC and AF488 were detected with excitation at 488nm and 480–560nm emission; PE with 561-nm laser excitation and 560–561nm emission; and TIV with excitation at 405 nm and 420–505nm emission. Single-color fluorescence samples were collected without brightfield or scatter to create compensation matrices for each experiment and aid in gate-setting. All events (10,000 per sample) were collected on focused singlet cell events and micrographically verified as described.[177] Results are presented as the fluorescence index, defined as the median fluorescence intensity multiplied by the percentage of positive-gated bacteria.

2.4.8 Fluorometric measurements of bacterial membrane integrity.

Gc was inoculated from plates into HBSS-BSA to an OD_{550} nm of 0.1. IgM (90µL) was added to 90µL of Gc for 30min at 37°C, 5% CO_2. For NPN, Gc was then incubated with 50% final concentration IgG/M-depleted serum for 15min (lot #15443); for SYTOX Green, Gc was incubated with 2% IgG/M-depleted serum for 30min (lot #28341). Bacteria were washed three times with buffer and resuspended in 30µM NPN (Sigma-Aldrich, Cat. #104043)[313,316] or 10µM SYTOX Green nucleic acid stain (Sytox Green; Invitrogen, Cat. #S7020)[183,310], respectively. Bacteria were resuspended, transferred to black flat-bottom 96-well plates in 100µL technical duplicates, and assayed immediately. NPN measurements were collected on a BioTek Synergy2 plate reader with Gen5 software using 360nm excitation and 420-480nm emission. Sytox Green was measured every 2-4 min over 120 min at 37°C on a PerkinElmer Victor^3 1420 Multilabel Counter with associated software, using 490nm excitation and 535nm emission filters. Each experiment included buffer-alone and NPN/Sytox Green without bacteria controls (i.e. blanks), the values of which were subtracted from experimental conditions.

2.4.9 Minimum inhibitory concentrations (MICs).

100µL of IgG/M-depleted human serum, diluted to 10% in GCBL with Kellogg's supplement I[45] and 1.25µM $Fe(NO_3)_3$ (GCBL+Supp), was added to each well in one row of a round-bottom 96-well plate. Wells in the next row were filled with 100µL GCBL+Supp (0% serum). 100µL of antimicrobials (4x final concentration) were added to the second column of each row, leaving the first

column as no-antimicrobial control. Antimicrobials were then serially diluted 2-fold across the remaining wells in each row. To the no-antimicrobial wells, 100µL of GCBL+Supp was added and mixed thoroughly, and 100µL was removed and discarded. Gc was inoculated into GCBL+Supp to a final OD_{550} nm of 0.07, diluted 10-fold (~5e6 CFU/mL), and 100µL added to each well and mixed thoroughly. After incubation for 16hr at 37°C, 5% CO_2. wells were gently resuspended and assessed visually for gonococcal growth, from which MICs were determined.[357]

2.4.10 Statistics, analyses, and data availability,

Results are depicted as mean ± standard error for ≥3 independent replicates. Statistics were calculated and data were graphed using GraphPad Prism. Data were assumed to be parametric, and statistical tests were 2-sided where applicable. Data and statistics for flow cytometry were obtained using IDEAS 6.2 software (Amnis).

3 High-dimensional spectral flow cytometry of activation and phagocytosis by peripheral human polymorphonuclear leukocytes

This chapter is a modified version of the previously published article: Lamb ER, et al. High-dimensional spectral flow cytometry of activation and phagocytosis by peripheral human polymorphonuclear leukocytes. (2025). Journal of Leukocyte Biology. Unpublished data is presented in Figure 32 and Figure 33.

Contributors:

Evan Lamb – Conceptualization, Methodology, Analysis, Investigation, Authorship, Validation, Visualization, Funding Acquisition.

Ian Glomski – Analysis, Investigation, Authorship, Validation, Visualization.

Taylor Harper – Methodology, Analysis, Investigation, Authorship.

Michael Solga – Methodology, Analysis, Authorship, Funding Acquisition.

Alison Criss – Conceptualization, Methodology, Analysis, Authorship, Funding Acquisition, Project Administration.

3.1 Introduction

Polymorphonuclear leukocytes (PMNs) are principal cellular responders to infection and inflammation in vertebrates. The granulocytic PMN population is predominantly composed of neutrophils, professional phagocytes with many specialized antimicrobial properties. Among these antimicrobial mechanisms are phagocytosis with subsequent phagolysosome maturation, active chemotactic migration toward pathogens, coordinated exocytosis of antimicrobial-containing granule subsets, and reactive oxygen species (ROS) generation.[209-212] PMNs sense a variety of host- and pathogen-derived stimuli from the inflammatory milieu and integrate the resulting signals to coordinate their activation states and responses.[167,214,215] Activation includes mobilization of surface proteins required for transmigration from the circulation to the site of infection/inflammation, downregulation of other surface proteins throughout this process through endocytosis or ectodomain shedding, and coordinated upregulation of proteins representative of primed antimicrobial activity.[224,238-241,257,358] The breadth of stimuli and potential PMN reactions imply that PMNs have heterogenous responses to infection and injury. Approaches to measure the heterogeneity of PMN activation and responses on both single cell and population levels can elucidate how PMNs respond in a variety of conditions.[229-233]

Flow cytometry is a time-tested methodology to characterize and quantify leukocyte activation in response to diverse stimuli. Its advantages include its general availability, high throughput nature, relatively small cell numbers needed, differentiation of surface versus intracellular expression, and ability to identify and

analyze subpopulations.[234,235,359,360] However, conventional flow cytometry is constrained by the number of markers that can be analyzed at a given time due to overlapping emission profiles collected by an instrument's detector array which are not always able to be separated by fluorochrome compensation. Due in part to such limitations, PMN flow cytometry generally analyzes one or a few parameters related to granulocyte development/ontogeny[361-363], migration/chemotaxis, phagocytosis, ROS generation, NETosis, or antimicrobial release in isolation.[257,364-368] To surmount limitations of conventional flow cytometry, technologies that increase the number of parameters have been developed. One such high-dimensional method is cytometry by time of flight (CyTOF) which uses heavy metal-conjugated antibodies to label cells of interest and measure target positivity and expression levels. This technology enables analysis of numerous markers in a single sample, including on PMNs.[369,370] However, CyTOF is expensive in equipment and reagent costs, and requires sample destruction for data generation.[371,372]

Spectral flow cytometry is an advanced methodology in which the full fluorescence spectrum of individual antibody-conjugated fluorochromes is collected from each excitation laser in a cytometer's configuration, allowing for a full 'spectral fingerprint' to be identified. Spectral flow cytometry permits many more fluorochrome combinations, and thereby more cell parameters, to be examined per experimental condition than conventional flow cytometry.[373,374] Spectral flow cytometry has been effectively deployed to analyze PMN activation and identify subsets in healthy and diseased states for up to 15 surface markers

simultaneously.[234,237,375-377] Recent advances in spectral flow cytometry technology, including spectral cell sorting and dimensionality-reducing analytical software, enable analysis of high-dimensional datasets.[378,379]

The principal goal of this study was to design a flow cytometry panel that 1) analyzes mature human PMNs, 2) does so in a high-dimensional manner, 3) does so without sample destruction to allow for downstream sorting/analysis, 4) focuses on both PMN functionality and activation, and 5) is adaptable to diverse research questions in the field. Such a methodology could advance the understanding of PMN activation and diversity as well as the contribution that such diversity provides to outcomes in inflammation, infection, and injury.

To this end, we present a 22-color spectral flow cytometry panel that profiles the activation of mature human PMNs in response to diverse stimuli. The panel described here was designed with particular emphasis on PMN (opsono)phagocytic receptors, degranulation markers, migratory proteins, chemokine receptors, and the option to fluorescently-label cargo, such as microbes. We describe best practices for using the panel in different laboratories and detail options for customization as common fluorochromes/channels left available for incorporation of other markers of interest, enabling its adaptation to many research endeavors. We demonstrate that the panel can identify PMNs in a population that respond to phorbol ester stimulation and infection by the bacterial pathogen *Neisseria gonorrhoeae* (the gonococcus, Gc). Moreover, we show the multidimensional utility of this panel by identifying subpopulations of Gc-infected PMNs with varying degrees of activation and bacterial burdens. Gc

expressing or deleted for surface adhesins which enhance Gc-PMN association are examined

3.2 Results

3.2.1 Spectral flow cytometry panel design for PMN function and activation.

We designed the following spectral flow cytometry panel for mature human PMN functions (Fig. 22). Analyses were performed on human peripheral blood PMNs, which were freshly isolated on the day of each experiment from healthy subjects as described in Materials and Methods.[43]

Cell viability and exclusion of non-PMNs: This panel was designed with an amine-reactive live-dead stain to exclude non-viable cells (Zombie Near-Infrared, ZNIR). The major co-purifying cell type in the PMN preparations are $CD14^{High}$ monocytes; therefore, an anti-CD14 antibody was added to exclude $CD14^{High}$ cells from downstream analysis.[235]

PMN phagocytosis: The panel contains antibodies against CD64 (FcγRI), CD32 (FcγRII), and CD16 (FcγRIII), which mediate phagocytosis of IgG-opsonized cargo[168], and antibodies against CD35 (complement receptor 1, CR1) and CD11b and CD18 (complement receptor 3, CR3) for complement C3b-, iC3b-, and C3d(g)-mediated opsonophagocytosis.[370] CD11b undergoes activation-dependent conformational changes; thus antibodies against total and active forms of CD11b were included.[170] We also included an antibody against human carcinoembryonic antigen-related cell adhesion molecules (CCMs), which

serve as non-opsonic phagocytic receptors for many pathogens including *N. gonorrhoeae*.[39,46] Of the CCM family members, the antibody used in this study recognizes the granulocyte-expressed CCMs 1, 3, and 6 (but not CCM 8/CD66b; Table 3).

PMN degranulation: The panel contains antibodies against the primary/azurophilic granule protein CD63 and the secondary/specific granule protein CD66b. Both are well described markers for individual granule subsets that are sequentially exocytosed from PMNs upon activation.[358]

PMN migration and chemotaxis: The panel includes antibodies against CD62L (L-selectin) which is shed as PMNs migrate to target sites[238,239], CD54 (ICAM-1), CD172 (signal-regulatory protein, SIRP), CD44, and CD47 (integrin associated protein, IAP) which is also a ligand for CD172. These receptors enable nuanced, context- and location-specific migratory responses of immune cells in infection and inflammation.[220,380] The panel also contains antibodies against chemotactic receptors that are known to promote directional migration and PMN activation: CXCR1 for IL-8, BLT1 for leukotriene-B4 (LTB_4), fPR1 for formylated peptides, and C5aR1 for the anaphylatoxin C5a of the complement cascade.[174]

The selected markers serve as broad examples of PMN activation/stimulation and phenotypic functional groups. They also reflect underlying PMN biology of granule mobilization to the plasma membrane (ex: CD63, CD66b, CD11b, CD18)[358], endocytic downregulation of surface markers to

ablate signal reception (ex: fPR1, C5aR1)[241], and ectodomain shedding (CD16, CD62L).[238-240]

Viability	**Live-Dead ZNIR**				
Dump / Exclusion	**CD14**				
Phagocytic Receptors	**CD11b-total (α_M Integrin)**	**CD11b-active (α_M Integrin)**	**CD16 (FcγRIII)**	**CD18 (β_2 Integrin)**	
	CD32 (FcγRII)	**CD35 (CR1)**	**CD64 (FcγRI)**	**CCM 1, 3, 6**	
Degranulation	**CD63**	**CD66b (CCM8)**			
Adhesion / Migration	**CD44**	**CD47 (IAP)**	**CD54 (ICAM-1)**	**CD62L (L-selectin)**	**CD172 (SIRP)**
Chemokine Receptors	**BLT1**	**C5aR1**	**CXCR1**	**fPR1**	

Figure 22. PMN spectral flow cytometry panel surface markers/parameters grouped by functional category

Schematic of the selected parameters in the PMN spectral flow cytometry panel, organized by function/purpose. Where applicable, cluster of differentiation (CD) label is listed with other common names in parentheses. Zombie Near-infrared (ZNIR); Fcγ Receptor (FcγR); Complement Receptor (CR); Carcinoembryonic Antigen-related Cell Adhesion Molecules (CCM); Integrin Associated Protein (IAP); Intercellular Adhesion Molecule 1 (ICAM-1); Signal-regulatory Protein (SIRP).

Table 3: Spectral Flow Antibodies and Reagents								
Marker	Other Name(s)	Fluorochrome	Vendor	Clone	Cat. No.	Stock Conc.	µL per test	Conc. per test
Viability	Live-Dead	Zombie NIR	BioLegend	-	423105	1,000x	1	-
N. gonorrhoeae (or cargo of interest)	Gonococcus	CellTrace Blue	Thermo	-	C34568	5mM	1	5µM
CCM (1,3,6)	CD66a,d,c	NFYellow 700	Santa Cruz	YTH71.3	sc-59898	225µg/mL	2.5	562.5ng/mL
CD64	FcγRI	BV 605	BioLegend	10.1	305033	100µg/mL	2.5	250ng/mL
CD32	FcγRIII	BUV 496	BD	3D3	750498	200µg/mL	0.625	125ng/mL
CD16	FcγRIII	BUV 737	Thermo	CB16	367-0168-42	25µg/mL	2.5	62.5ng/mL
CD63		BV 711	BioLegend	H5C6	353041	100µg/mL	5	500ng/mL
CD66b	CCM8	BV 421	BioLegend	6/40c	392915	50µg/mL	2.5	125ng/mL
CD35	CR1	BV 750	BD	E11	747132	200µg/mL	1.25	250ng/mL
CD11b-total	Mac1, Complement Receptor 3, CR3, $\alpha_M\beta_2$ integrin	eFluor 506	Thermo	ICRF44	69-0118-42	25µg/mL	5	125ng/mL
CD11b-activated		AF 700	Thermo	CBRM1/5	56-0113-42	100µg/mL	2.5	250ng/mL
CD18		BUV 805	BD	6.7	749381	200µg/mL	5	1000ng/mL
CD62L	L-Selectin	APC-Fire810	BioLegend	DREG-56	304865	100µg/mL	2.5	250ng/mL
CD54	ICAM-1	BUV 563	BD	LB-2	741442	200µg/mL	1.25	250ng/mL
CD172	SIRP	BV 650	BD	SE5A5	743565	200µg/mL	2.5	500ng/mL
CD44		PerCP-Cy5.5	Thermo	IM7	45-0441-82	200µg/mL	2.5	500ng/mL
CD47	integrin associated protein (IAP)	PE-Cy7	BioLegend	CC2C6	323113	200µg/mL	2.5	500ng/mL
CXCR1	IL8R, CD181	PE	BioLegend	8F1/CXCR1	320608	100µg/mL	1.25	125ng/mL
BLT1		BV 786	BD	203/14F11	744669	200µg/mL	1.25	250ng/mL
fPR1		AF 647	BD	5F1	565623	200µg/mL	2.5	500ng/mL
C5aR1	CD88	PE-Dazzle 594	BioLegend	S5/1	344317	200µg/mL	2.5	500ng/mL
CD14		eFluor 450	Thermo	61D3	48-0149-42	100µg/mL	1.25	125ng/mL
CD14		BV 711	BD	MφP9	563373	200µg/mL	2.5	500ng/mL
CD49d		PE-Cy7	BioLegend	9F10	304313	200µg/mL	2.5	500ng/mL

Table 3. Spectral flow antibodies and reagents

3.2.2 Fluorochrome selection and panel similarity and complexity.

Cognate fluorochromes for each marker were selected to optimize functionality of the spectral flow cytometry panel while maximizing the number of parameters to include (Fig. 23A). Considerations incorporated into panel design included cytometer laser and detector array configuration, spectral overlap between fluorochromes, epitope densities, and brightness indexes of the fluorochromes. However, given the intrinsic variability of human PMNs and the range of activation-dependent surface expression, selecting appropriate fluorochrome-marker pairings required testing and validation within the context of the broader panel. Where possible, markers known to be in the same subcellular (granule) location were paired with fluorochromes with distinct spectra to minimize spectral overlap increasing the overall resolution of the panel.[224,381] While most fluorescent antibodies used here are commercially available, the anti-CCM antibody was conjugated in-house to NovaFluor Yellow 700. The final PMN panel pairings yielded similarity and complexity values which were calculated using Cytek's Full Spectrum Viewer, with lower overall complexity score being optimal (Fig. 23B).[381]

To maximize panel adaptability to different research questions, the 355nm excitation/420nm peak emission (BUV395, CellTrace Blue; UV2 detector) and 488nm excitation/520nm peak emission (FITC, Alexa Fluor 488; B2 detector) channels were left available. Here, we used the BUV395 channel to pre-label *N. gonorrhoeae* with the amine-reactive dye CellTrace Blue. The FITC/Alexa Fluor 488 (AF 488) channel is a popular choice for many antibody conjugations and

functional dyes and was left unused. Addition of AF488 to the panel did not appreciably alter the calculated similarity matrix or complexity index (Fig. 23C).

A PMN Spectral Flow Cytometry Panel on Cytek Aurora 5-laser Cytometer

Approx. Peak Emission Wavelength (nm)	UV Laser (355nm)			Violet Laser (405nm)			Blue Laser (488nm)			Yellow Green Laser (561nm)			Red Laser (640nm)		
	Detector	Marker	Fluorochrome	Detector	Marker	Fluorochrome	Detector	Marker	Fluorochrome	Detector	Marker	Fluorochrome	Detector	Marker	Fluorochrome
395	UV1														
420	UV2	Available	CellTrace Blue / BUV395	V1	CD66b (CCM 8)	BV421									
440	UV3			V2											
450	UV4			V3	CD14	eFluor 450									
480	UV5			V4											
500	UV6	CD32 (FcγRII)	BUV496	V5	CD11b-total (αM integrin)	eFluor 506	B1								
520	UV7			V6			B2	Available	FITC / AF488						
550	UV8			V7			B3								
570	UV9	CD54 (ICAM-1)	BUV563	V8			B4			YG1	CXCR1 (CD181)	PE			
580				V9			B5			YG2					
600	UV10			V10	CD64 (FcγRI)	BV605	B6			YG3	C5aR1 (CD88)	PE-Dazzle594			
660	UV11			V11	CD172 (SIRP)	BV650	B7			YG4			R1		
680							B8			YG5			R2	fPR1	AF647
690	UV12			V12	CD63	BV711	B9	CD44	PerCP-Cy5.5	YG6			R3		
700							B10			YG7	CCM	NFY700	R4	CD11b-active (αM intergrin)	AF700
730	UV13	CD16 (FcγRIII)	BUV737	V13			B11						R5		
750	UV14			V14	CD35 (CR1)	BV750	B12			YG8			R6		
780	UV15			V15	BLT1	BV786	B13			YG9	CD47 (IAP)	PE-Cy7	R7	Live-Dead Viability	Zombie NIR
800	UV16	CD18 (β2 integrin)	BUV805	V16			B14			YG10			R8	CD62L (L-selectin)	APC-Fire810

B PMN Panel Similarity

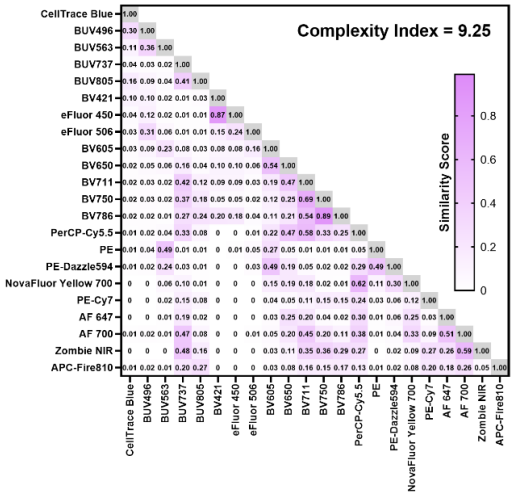

C PMN Panel + AF488

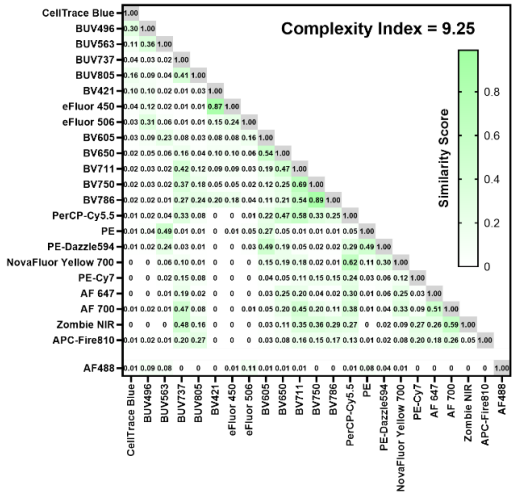

Figure 23. PMN spectral flow cytometry panel surface marker fluorochrome pairings, similarity, and complexity

(A) Representation of the Cytek Aurora 5-laser spectral flow cytometer detector array with 355, 405, 488, 561, and 640 nm laser configuration. Approximate peak emission wavelengths are listed top to bottom for each laser with corresponding detector array. Fluorochromes are listed in their peak detector slot with their cognate surface marker/parameter. The UV2 and B2 detector channels have been left available for customization. (B) The similarity of each of the 22 tested fluorochromes' predicted spectral fingerprints compared to each other was calculated using Cytek's Full Spectrum Viewer. Calculated similarity is shown in each cell with a value of 0.0 indicating no similarity and 1.0 indicating exact similarity. The overall complexity index is shown at the top right. (C) The similarity and complexity are shown as in panel (B) but with the AlexaFluor 488 (AF488) fluorochrome included.

3.2.3 Panel gating strategy.

Purified cells were first gated on events which passed FlowAI cleaning within OMIQ. These events were then gated into the PMN/granulocyte population based on characteristic forward and side scatter profiles (FSC-A, SSC-A; Fig. 24A i) followed by selection of single cell events (Fig. 24A ii). Singlets were then sub-gated on $CD14^{Low}$ events to exclude contaminating monocytes (Fig. 24A iii). The CD14 gate was set using a mixture of the PMN preparation and the Ficoll-PBS interface (collected and saved on ice during the preparation process) which is enriched in $CD14^{High}$ monocytes (Fig. 24B). Finally, $CD14^{Low}$ singlets were gated on live cells for subsequent analyses (Fig. 24A iv). The live-dead gate was set using a 1:1 mixture of cells that were killed by heating at 65°C for 5min and cells that were kept on ice before Zombie NIR staining (Fig. 24C).

While most PMNs in circulation are neutrophils, eosinophils also co-purify in the granulocyte preparations. Separate experiments were conducted in which live singlet PMNs were further gated on CD49d to discriminate eosinophils (CD49d+) from neutrophils (CD49d-; Fig. 24D).[202,362,382] PMN preparations were further evaluated for CD16, CD66b, and CD11b positivity to verify neutrophil predominance (Fig. 25).[237] PMN preparations from healthy subjects used here contain less than 1% eosinophils.[202]

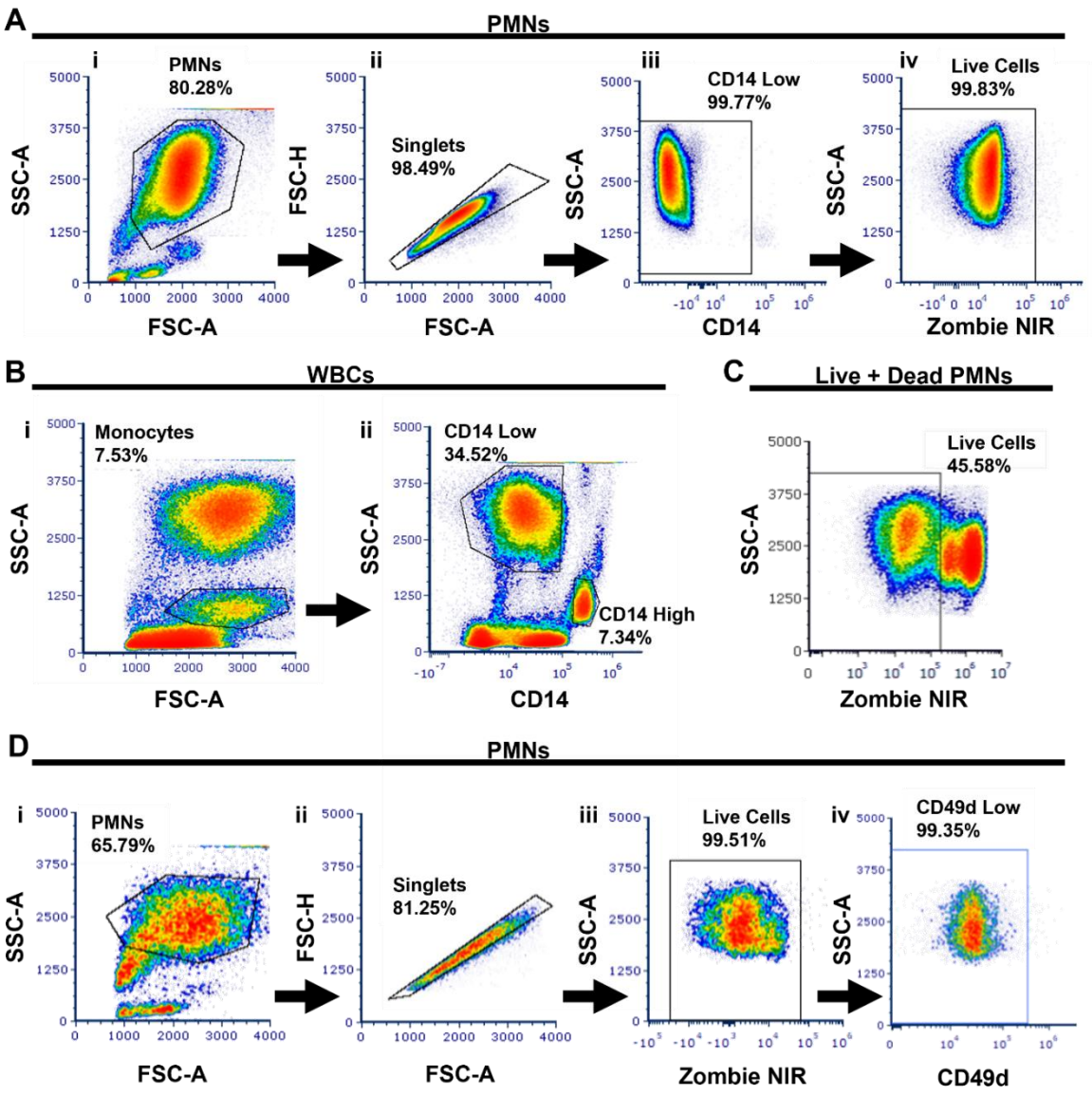
A
PMNs
i
PMNs
80.28%
SSC-A
FSC-A
ii
Singlets
98.49%
FSC-H
FSC-A
iii
CD14 Low
99.77%
SSC-A
CD14
iv
Live Cells
99.83%
SSC-A
Zombie NIR
B
WBCs
i
Monocytes
7.53%
SSC-A
FSC-A
ii
CD14 Low
34.52%
CD14 High
7.34%
SSC-A
CD14
C
Live + Dead PMNs
Live Cells
45.58%
SSC-A
Zombie NIR
D
PMNs
i
PMNs
65.79%
SSC-A
FSC-A
ii
Singlets
81.25%
FSC-H
FSC-A
iii
Live Cells
99.51%
SSC-A
Zombie NIR
iv
CD49d Low
99.35%
SSC-A
CD49d

Figure 24. Gating strategy for live primary human PMNs

The PMN/granulocyte population was gated from Ficoll-purified cells (see Materials & Methods based on characteristic forward and side scatter profiles (I; FSC-A, SSC-A), followed by fating on single cells (ii), CD14 Low events (iii), and live cells (iv; Zombie Near-infrared (Zombie NIR) exclusion). (B) the CD14 gate was set using a mixture of purified PMNs and cells collected from the Ficoll-PBS interface during PMN preparation which is enriched in CD14 High monocytes. The monocytes gate was set on the characteristic FSC-A and SSC-A profiles (i) with this gate being used to delineate CD14 High from CD14 Low populations (ii). (C) The viability (Zombie NIR) gate was set using a 1:1 mixture of viable and heat-killed PMNs. (D) The PMN/granulocyte population was gated on characteristic FSC-A and SSC-A profiles (i) followed by singlet cells (ii) and live cell events (iii) as described above. Live cells were gated into the CD49d Low population (iv) which was determined by labeling UltraComp Beads (Invitrogen) to determine neutrophil and eosinophil representation within the PMN gate.

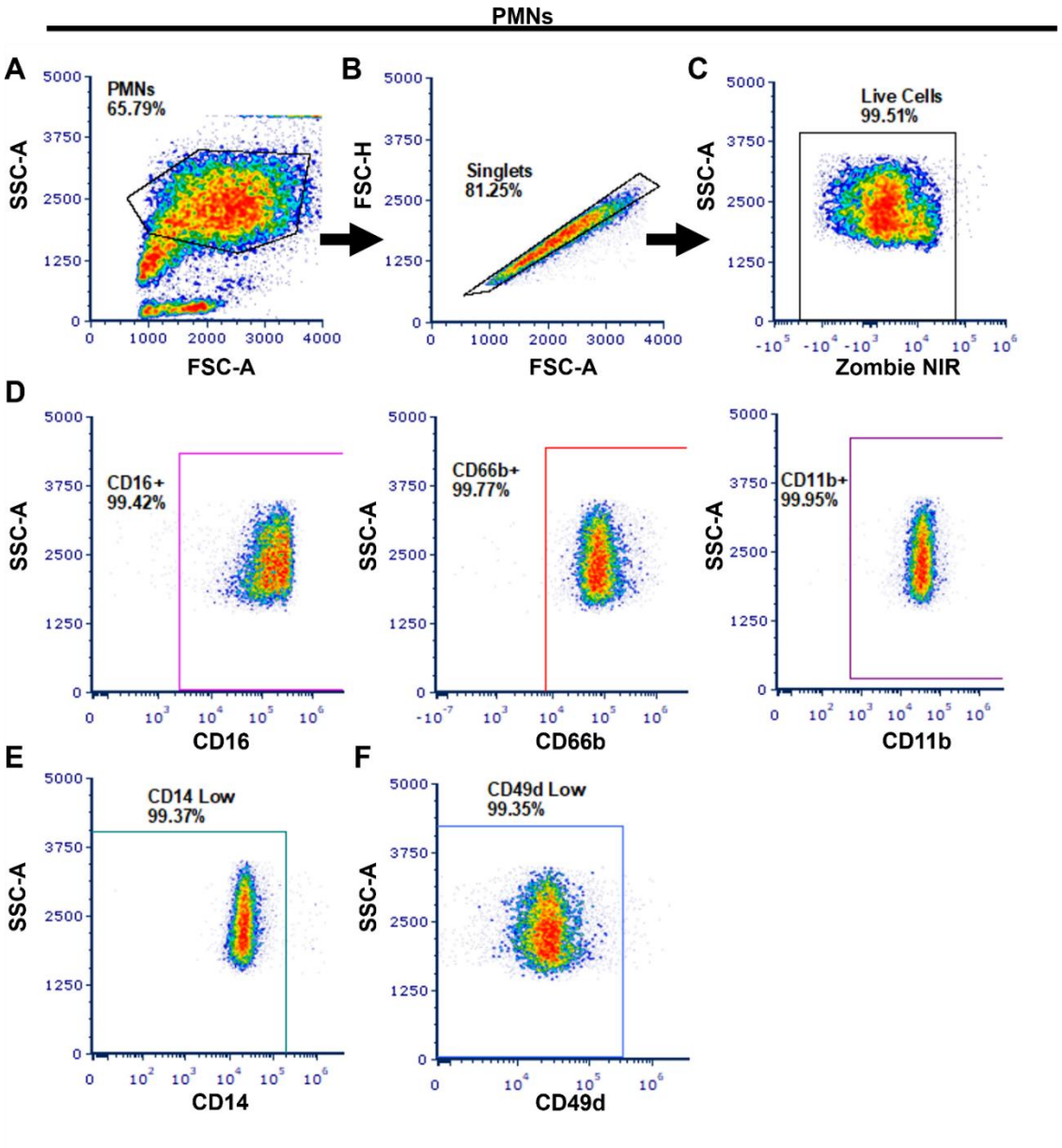
PMNs
A
PMNs
65.79%
SSC-A
FSC-A
B
Singlets
81.25%
FSC-H
FSC-A
C
Live Cells
99.51%
SSC-A
Zombie NIR
D
CD16+
99.42%
SSC-A
CD16
CD66b+
99.77%
SSC-A
CD66b
CD11b+
99.95%
SSC-A
CD11b
E
CD14 Low
99.37%
SSC-A
CD14
F
CD49d Low
99.35%
SSC-A
CD49d

Figure 25. Purity of PMN preparations.

Ficoll-purified cells were adhered and stained (see Materials & Methods) for markers enriched in different leukocyte populations (A) Cells were gated into PMNs based on the characteristic forward and side scatter profiles (FSC-A, SSC-A), single cell events, and live cells by Zombie Near-infrared (Zombie NIR) exclusion. (B) Cells were gated by positivity for canonical neutrophilic markers CD16, CD66b, and CD11b. Cells were further assessed for their low expression of the monocyte surface marker CD14 (C) or eosinophil marker CD49d (D).

3.2.4 Intra- and inter-subject PMN responses to phorbol ester treatment.

The panel was applied to adherent, IL-8 treated primary human PMNs[43] under three conditions to model different types of stimulation: 1) PMNs with no further stimulus as a baseline, 2) PMNs that were also treated with phorbol myristate acetate (PMA), a potent protein kinase C agonist with known neutrophil-activating properties[383], and 3) PMNs that were also infected with CellTrace Blue-labeled *N. gonorrhoeae*. The PMA concentration was selected to maximized the PMN response across different subjects, and the bacteria:PMN ratio was varied to obtain PMNs that ranged in degree of association with *N. gonorrhoeae*. The spectral flow cytometry panel was applied to measure variability in PMN responsiveness over time (>1 month between experiments), and to measure inter-subject variability for PMNs from three unrelated individuals. For inter-donor variability, replicate #1 from Subject #1 was analyzed against single replicates for two more subjects. Results with each parameter are grouped by trend. Since each parameter's intensity is assumed to be normally distributed, statistical significance was determined by paired Student's *t*-test ($p<0.05$ considered significant).

For PMNs from the same subject, 10 of the 19 parameters increased in surface expression with PMA stimulation (Fig. 26A). CCM, CD64, CD63, CD66b, CD18, CD11b-total, CD11b-active, and fPR1 were statistically significantly increased; CD47 and BLT1 were not. 5 parameters decreased in surface expression on PMA-treated PMNs (CD16 and CD35 were statistically significant; CD172, C5aR1, and CD62L were not; Fig. 26B). The remaining 4 markers

showed no consistent trends between replicates (CD32, CD54, CD44, CXCR1; Fig. 26C).

For inter-subject responses, PMNs from three unrelated subjects showed consistently increased surface expression for 9 markers upon PMA stimulation (CCM, CD64, CD63, CD11b-active, and fPR1 were statistically significant; CD32, CD18, CD47, and BLT1 were not; Fig. 27A). PMA stimulation increased CD66b and CD11b-total surface expression on PMNs from Subject #1 and #3 but not Subject #2 (Fig. 27B). Six markers decreased in all three subjects' PMNs after PMA treatment (CD16, CD62L, CD44, and C5aR1 were statistically significant; CD35 and CD172 were not; Fig. 27C). As seen for the replicates from Subject #1 (Fig. 26), the three unique subjects' PMNs did not have consistent responses to PMA treatment in surface expression of CD54 or CXCR1, (Fig. 27C,D).

To highlight the high-dimensional and single cell power of spectral flow cytometry we analyzed the adhered and PMA-stimulated PMN data via uniform manifold approximation and projection (UMAP) dimensional reduction (Fig. 28).[378] Cells from the spectral flow data sets were grouped by the UMAP algorithm based on the similarity of their full surface marker repertoires. PMA-treated PMNs are plotted by individual surface marker intensity, from which surface marker expression patterns and overlap can be qualitatively identified.

Taken together, these results demonstrate that trends in PMN responses to a known activating stimulus can be identified using this multiparametric panel and that multidimensional analysis can be deployed to identify unique populations for subsequent interrogation.

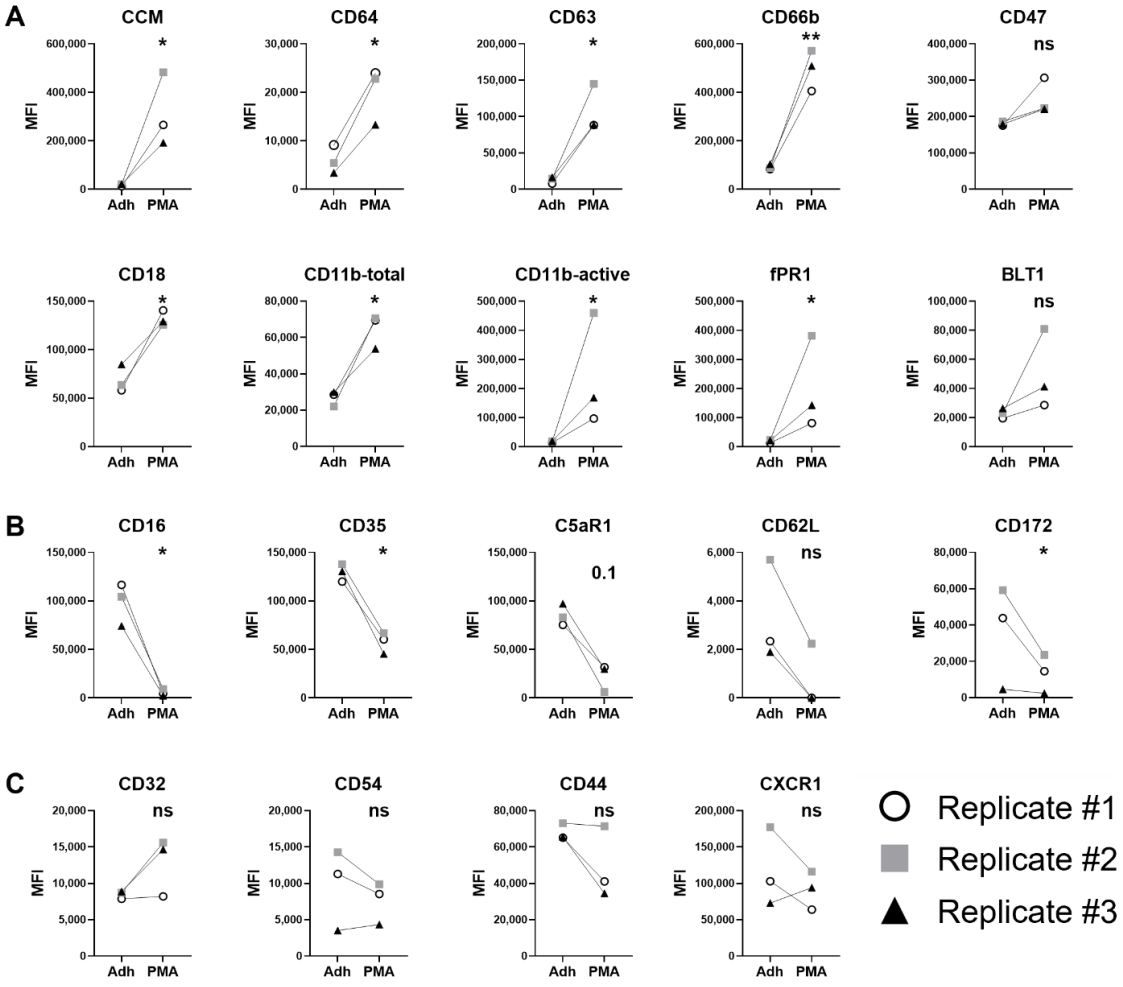
A
CCM
*
CD64
*
CD63
*
CD66b
**
CD47
ns
CD18
*
CD11b-total
*
CD11b-active
*
fPR1
*
BLT1
ns
B
CD16
*
CD35
*
C5aR1
0.1
CD62L
ns
CD172
*
C
CD32
ns
CD54
ns
CD44
ns
CXCR1
ns
MFI
Adh
PMA
Replicate #1
Replicate #2
Replicate #3

Figure 26. Assessing PMN activation by phorbol ester (PMA) and intra-subject variability using high-dimensional spectral flow cytometry

PMNs were purified from a single individual (Subject #1) on three separate days (Replicates #1-3), represented by different colors/shapes. The MFI was calculated for each parameter of the spectral flow cytometry panel. (A) Proteins with greater surface expression following PMA treatment compared to adherence alone (Adh) in each replicate. (B) Proteins with reduced surface expression following PMA treatment compared to adherence alone in all replicates. (C) Proteins with no consistent change in surface MFI between replicates. Statistical analyses were performed on paired Log_{10}-transformed data, Student's paired *t*-test. *=p<0.05, **=p<0.01, ns = not significant, p-value indicated if >0.05. Negative MFI values at the population level were set to a value of 1.0 for graphing, log transformation, and subsequent statistical analyses.

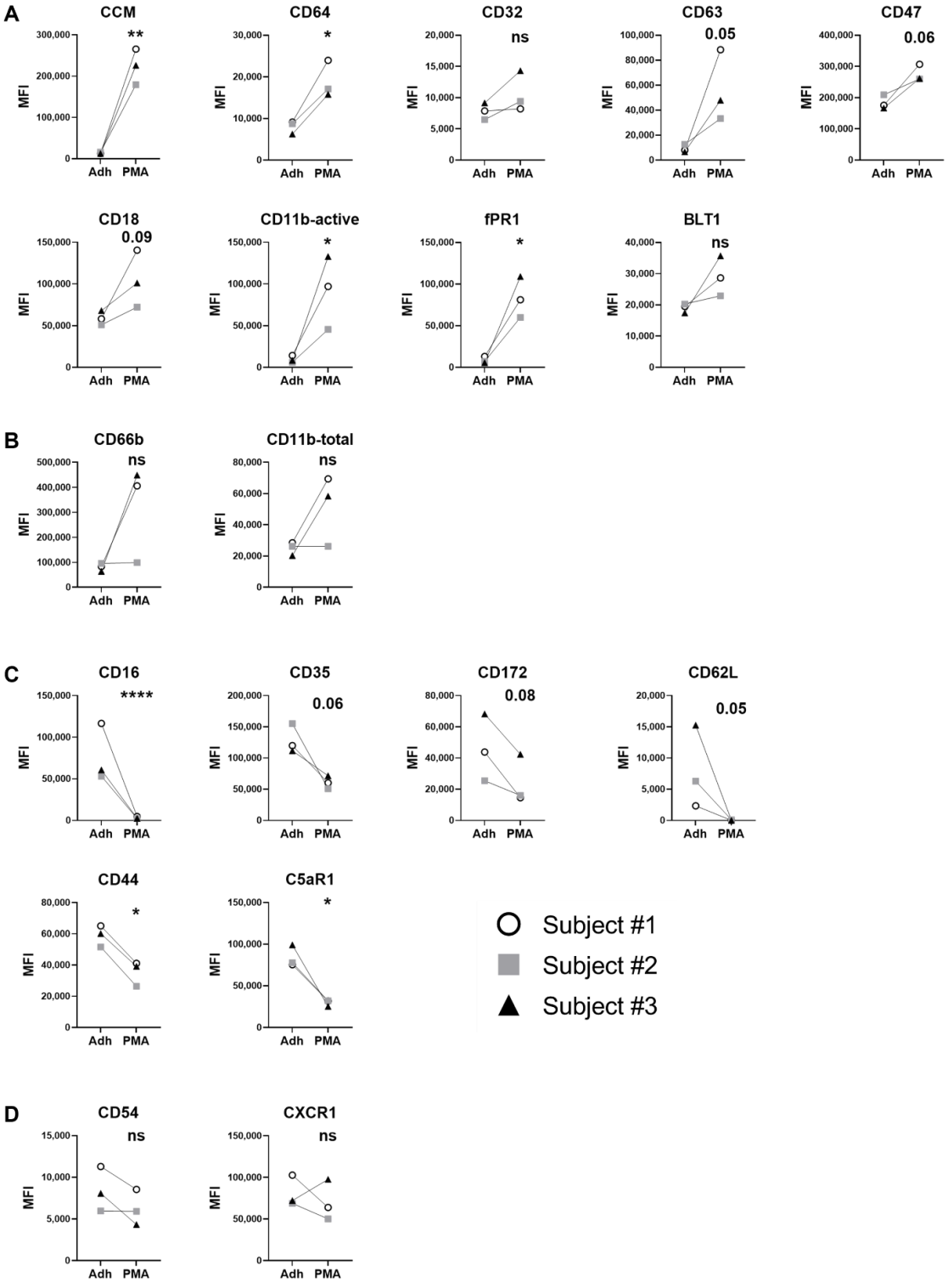
A
CCM
**
CD64
*
CD32
ns
CD63
0.05
CD47
0.06
CD18
0.09
CD11b-active
*
fPR1
*
BLT1
ns
B
CD66b
ns
CD11b-total
ns
C
CD16
****
CD35
0.06
CD172
0.08
CD62L
0.05
CD44
*
C5aR1
*
D
CD54
ns
CXCR1
ns
MFI
Adh
PMA
Subject #1
Subject #2
Subject #3

Figure 27. Assessment of inter-subject variability of PMN activation with high-dimensional spectral flow cytometry

Three individual subjects were assayed on separate days. Replicate #1 (see Figure 26) was used for Subject #1. Surface markers were analyzed via MFI for those that were (A) consistently upregulated with PMA compared to adherence alone (Adh) for each subject, (B) upregulated in two out of three subjects, (C) downregulated in each of the three subjects, or (D) showed no consistent trend between the three subjects with PMA stimulation. Statistical analyses were performed on paired Log_{10}-transformed data, Student's *t*-test. *=p<0.05, **=p<0.01, ****=p<0.0001, ns = not significant, p-value indicated if >0.05. Negative MFI values at the population level were set to a value of 1.0 for graphing, log transformation, and subsequent statistical analyses.

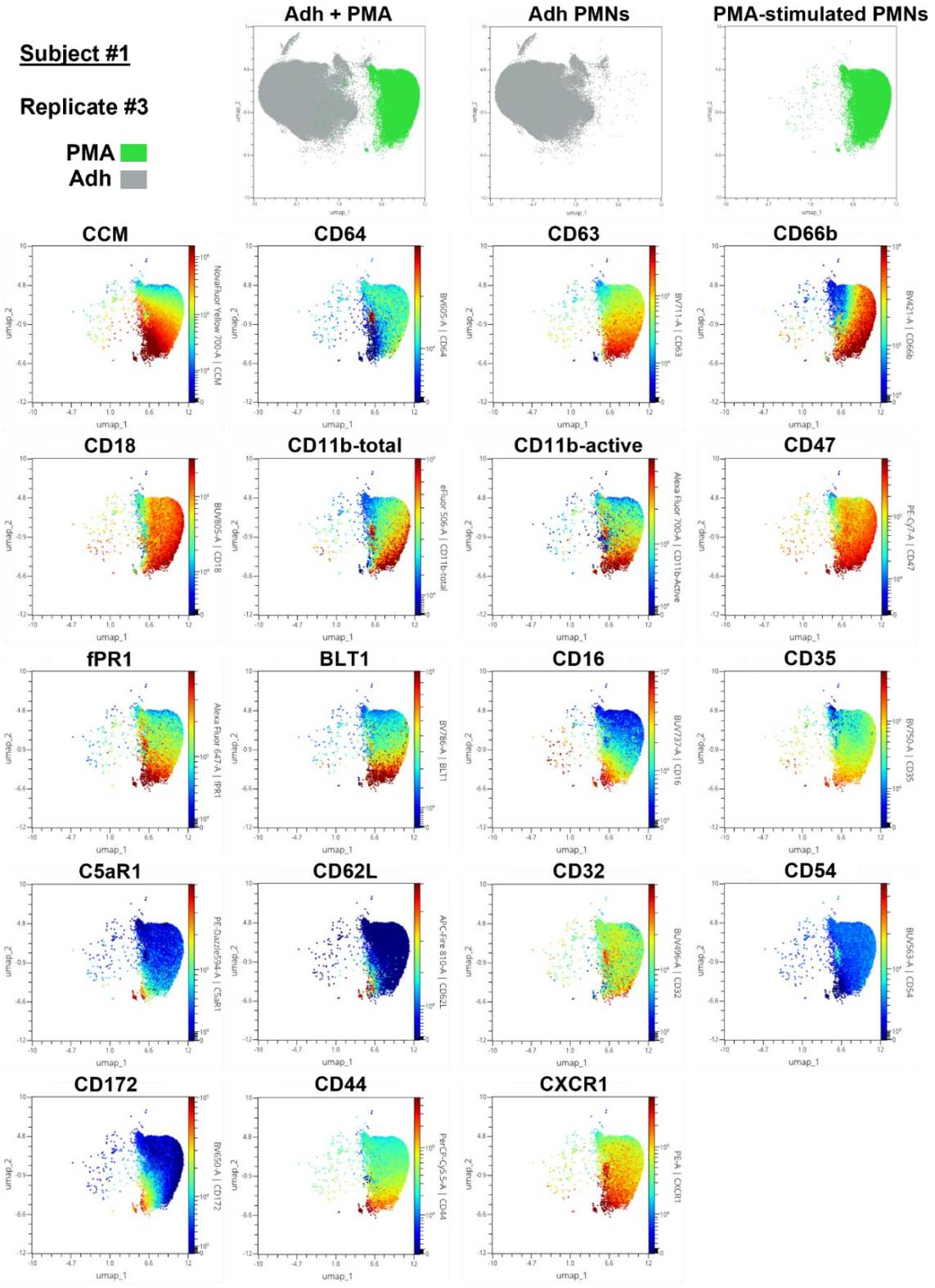
Subject #1
Replicate #3
PMA
Adh
Adh + PMA
Adh PMNs
PMA-stimulated PMNs
CCM
CD64
CD63
CD66b
CD18
CD11b-total
CD11b-active
CD47
fPR1
BLT1
CD16
CD35
C5aR1
CD62L
CD32
CD54
CD172
CD44
CXCR1
umap_1
umap_2

Figure 28. PMA-stimulated PMN phenotypic subsets following UMAP dimensional reduction

Replicate #1 from Subject #1's PMA-stimulated PMNs, stained with the full spectral flow cytometry panel, were processed and analyzed via uniform manifold approximation and projection (UMAP) dimensional reduction using OMIQ flow cytometry software. Top row: adherent alone (Adh, gray) and PMA-stimulated (PMA, green) PMN events arrayed by the two principal UMAP components (umap_1 and umap_2). Each of the 19 markers analyzed on live PMNs is displayed by the two principal UMAP components and by color intensity (red = highest surface expression, blue = lowest surface expression).

3.2.5 PMN responsiveness to the bacterial pathogen *Neisseria gonorrhoeae*.

To demonstrate the utility of this panel to interrogate PMN interactions with phagocytic cargo including pathogens, CellTrace Blue-labeled Gc was introduced to adherent PMNs at multiplicity of infection (MOI) of either 1 or 10 bacteria per PMN for 1hr. Gc used for infection either constitutively expressed a single opacity-associated protein adhesin (OpaD), which binds CCM-1 and CCM-3 on PMNs, or were deleted for all opacity-associated protein adhesins (Opaless). Subject #1's PMNs were challenged on three different days with fluorescent bacteria, unlabeled control bacteria, or adherent-alone PMNs with no bacteria exposure.

Eight PMN markers showed consistently increased trends in surface expression with Gc challenge, which increased with the MOI of OpaD Gc (CCM, CD64, CD63, CD66b, fPR1, CD18, CD11b-active, and BLT1; Fig. 29A). Three other markers, CD11b-total, CD35, and CD47, had increased surface expression with infection at an MOI of 1 but a decrease at an MOI of 10 with the MFI of CD35 lower at the MOI of 10 than in the uninfected population (Fig. 29B). Five markers (CD16, CD172, CD62L, C5aR1, and CD44) consistently decreased in surface expression after infection with Gc (Fig. 29C). CD32, CD54, and CXCR1 had no consistent trends among the three experimental replicates (Fig. 29D).

We next examined CellTrace Blue fluorescence to indicate PMN bacterial burden. PMNs were gated into CellTrace Blue-positive and -negative populations. PMNs infected at an MOI of 1 exhibited 8.2-62.7% CellTrace Blue

positivity, leaving a considerable portion of the population CellTrace-negative in each replicate (Fig. 29E). In comparison, PMNs at an MOI of 10 were greater than 97% positive in all biological replicates (Fig. 29E). The measured MFI for PMNs infected at an MOI of 10 was more than a $\log_{10}$-fold greater than those in the MOI of 1, and the population distribution of fluorescence intensity was more homogenous (coefficient of variance 49.4 versus 104.9; Fig. 29F,G). The observed CellTrace Blue heterogeneity in the MOI of 1 infection dosage prompted more nuanced investigation into how PMN surface markers varied with bacterial burdens.

To verify that CellTrace intensity corresponded with bacterial burden, PMNs exposed to OpaD Gc at an MOI of 1 were examined using imaging flow cytometry in which single, focused cells were gated by CellTrace MFI into CellTrace-negative PMNs with ‘No Gc’, the lowest quartile of CellTrace-positive PMNs as the ‘Low Gc’ population, and the highest quartile of CellTrace-positive PMNs as the ‘High Gc’ population (Fig. 30A). The No Gc gate represented 20-50% of the total population (Fig. 30B). The High Gc population’s MFI was 19.2-fold greater than the Low population’s MFI; there was negligible fluorescence in the No Gc population (Fig. 30B). Bacterial burden was verified by imaging flow cytometry as CellTrace intensity corresponded with the numbers of bacteria directly associated with individual PMNs which also showed that PMNs in the High Gc gate frequently contained 10 or more bacteria (Fig. 30C).

Using spectral flow cytometry, MOI of 1 PMNs (see Fig. 29) were subgated into No, Low, and High Gc populations as above; also included were

adherent-alone PMNs which had not been exposed to bacteria (Fig. 31A). The CellTrace Blue MFI for the uninfected and No Gc populations were undetectable, whereas the High Gc population had a 9.8-fold greater MFI on average than the Low Gc population (Fig. 31A,B). Taken together, the imaging and spectral flow cytometry demonstrate that the MOI of 1 experimental condition yields a population of PMNs that exhibit a range of interactions with bacteria, despite exposure to the same inoculum of infectious particles.

The No, Low, and High Gc populations were examined for surface markers expression using the spectral flow cytometry panel and compared with the uninfected control PMNs. The MFIs of CCM, CD64, CD63, CD11b-active, and fPR1 all increased in a bacterial burden-dependent manner (Fig. 31C). Interestingly, CCM, CD64, and CD63 surface expressions were greater in the No Gc population from Gc-exposed PMNs than in the uninfected controls (Fig. 31C). Conversely, CD16 and CD44 decreased consistently in a bacterial burden-dependent manner, and the uninfected control had a higher MFI than the No Gc population from the bacteria exposed PMNs (Fig. 31D).

Other markers changed in surface expression levels with Gc infection compared to the uninfected control, but did not vary with MOI across the No, Low, and High Gc populations: CD66b, CD18, CD11b-total, CD47, and BLT1 all increased in the presence of Gc (Fig. 31E), whereas CD172, CD62L, CXCR1, and C5aR1 all decreased (Fig. 31F). CD32, CD35, and CD54 did not consistently respond to infection across replicates or showed no change regardless of bacterial burden (Fig. 31G).

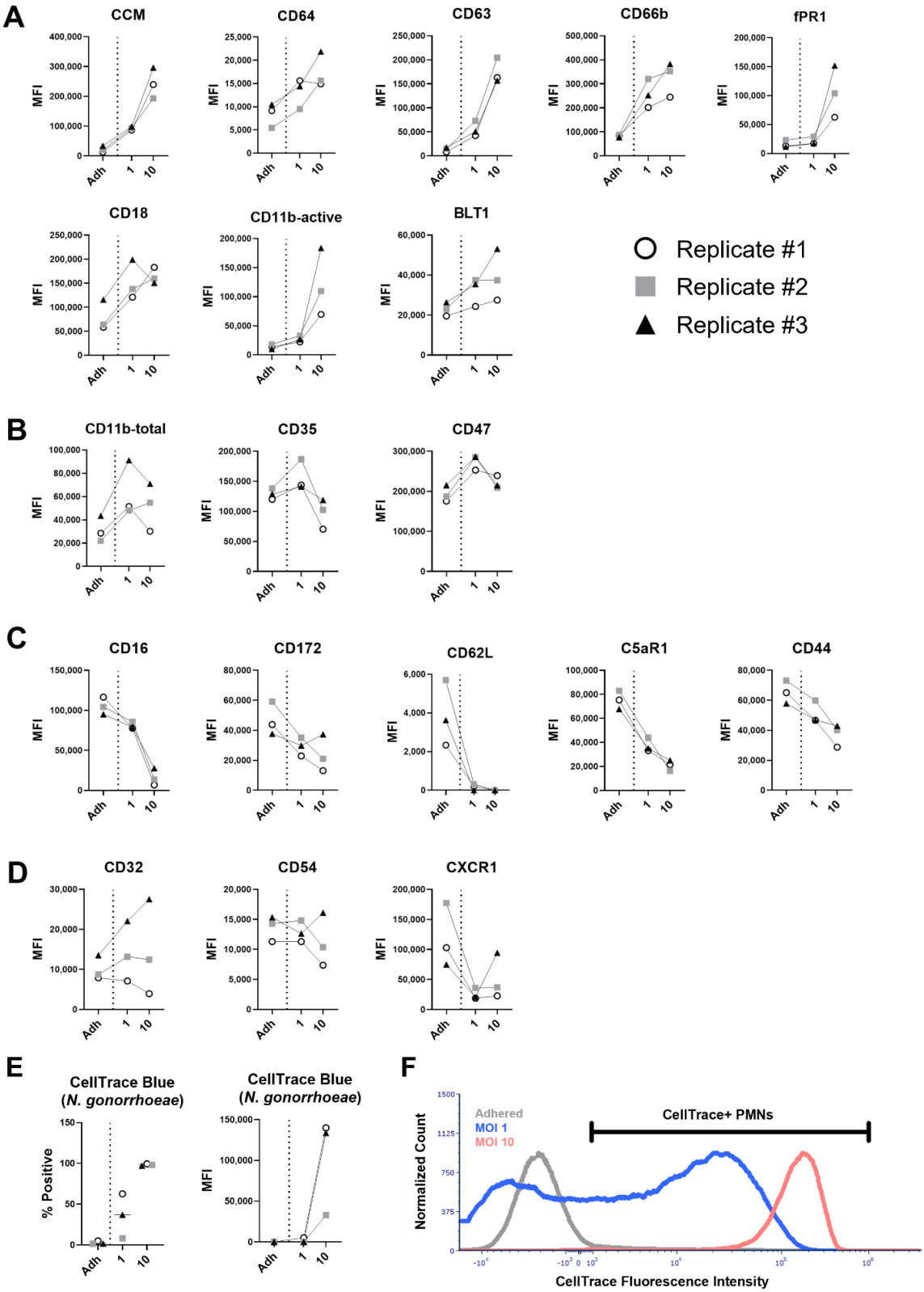
A
CCM
CD64
CD63
CD66b
fPR1
CD18
CD11b-active
BLT1
MFI
Adh
1
10
Replicate #1
Replicate #2
Replicate #3
B
CD11b-total
CD35
CD47
C
CD16
CD172
CD62L
C5aR1
CD44
D
CD32
CD54
CXCR1
E
CellTrace Blue
(N. gonorrhoeae)
% Positive
F
Adhered
MOI 1
MOI 10
CellTrace+ PMNs
Normalized Count
CellTrace Fluorescence Intensity

Figure 29. Fluorescently-labeled bacteria alter PMN surface protein expression in an infectious dose-dependent manner

Adherent primary human PMNs were challenged with CellTrace Blue-labeled *N. gonorrhoeae* at a multiplicity of infection (MOI) of 1 or 10 bacteria per PMN or left uninfected, and analyzed via spectral flow cytometry. (A) Surface proteins which were consistently elevated upon *Neisseria* infection compared to adherent alone (Adh) conditions and trended upwards in a dose-dependent manner (MOI 1 versus 10). (B) PMN markers which increased with an infection of 1 bacterium per PMN over adherent alone PMNs but decreased in the MOI of 10 condition versus MOI of 1. (C) Surface markers which consistently decreased with bacterial infection in ach replicate in an infectious dose-dependent manner. (D) Surface markers which showed no consistent trends between replicates of bacterial infection. (E) Percent positivity and CellTrace Blue MFI of PMNs in each condition as a representation of direct association with fluorescently-labeled bacteria. (F) Representative distribution of CellTrace Blue intensity in the adherent alone, MOI 1, and MOI 10 conditions. Marker denotes gating limits of positive CellTrace Blue signal. Dotted lines (A-E) separate bacteria-exposed from adherent alone PMNs.

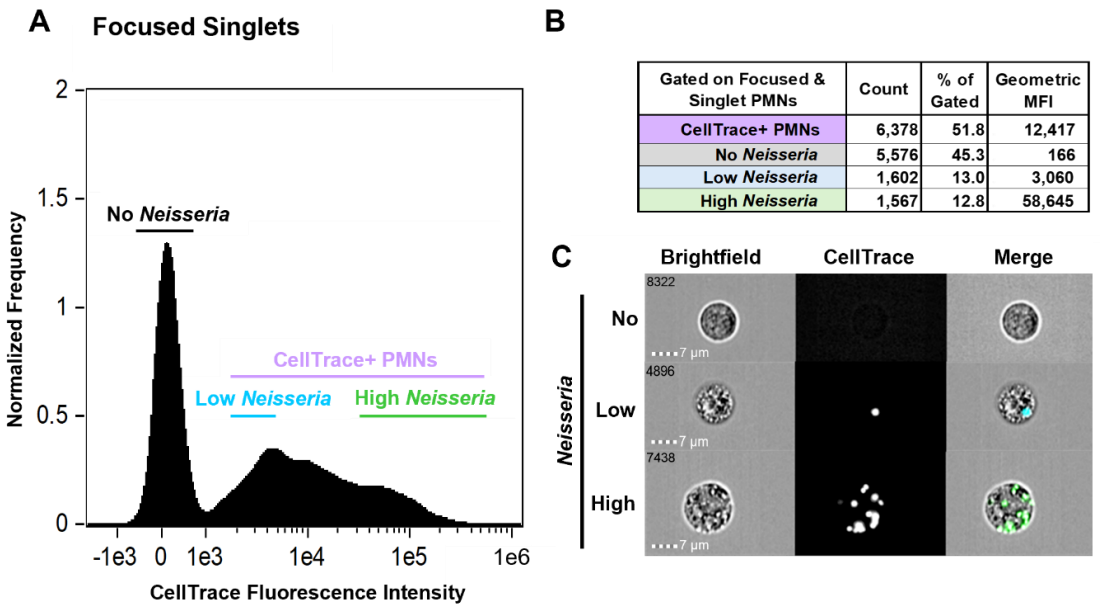

Figure 30. Imaging flow cytometry of bacterial burden per PMN

Primary human PMNs were isolated and adhered as described and infected with CellTrace Blue-labeled *N. gonorrhoeae* at a ratio of 1 bacterium per PMN for 1 hour and assayed via imaging flow cytometry. (A) Focused, single cell events were gated based on CellTrace MFI. CellTrace-negative events were classified as having No *N. gonorrhoeae*, whereas CellTrace-positive PMNs were classified as being associated with *N. gonorrhoeae*. CellTrace-positive PMNs were further subdivided into *N. gonorrhoeae* Low and *N. gonorrhoeae* High populations by quartile. (B) Statistics from panel (A) are shown with number of events, percentages, and geometric MFIs in each gate. (C) Representative micrographs from each gate of panel (A) showing the brightfield channel, CellTrace/bacteria channel, and a merged channel demonstrating bacterial burden on a single PMN basis. Numbers in the top lefthand corner of each image series represent the event number acquired out of 10,000 individual focused singlet events.

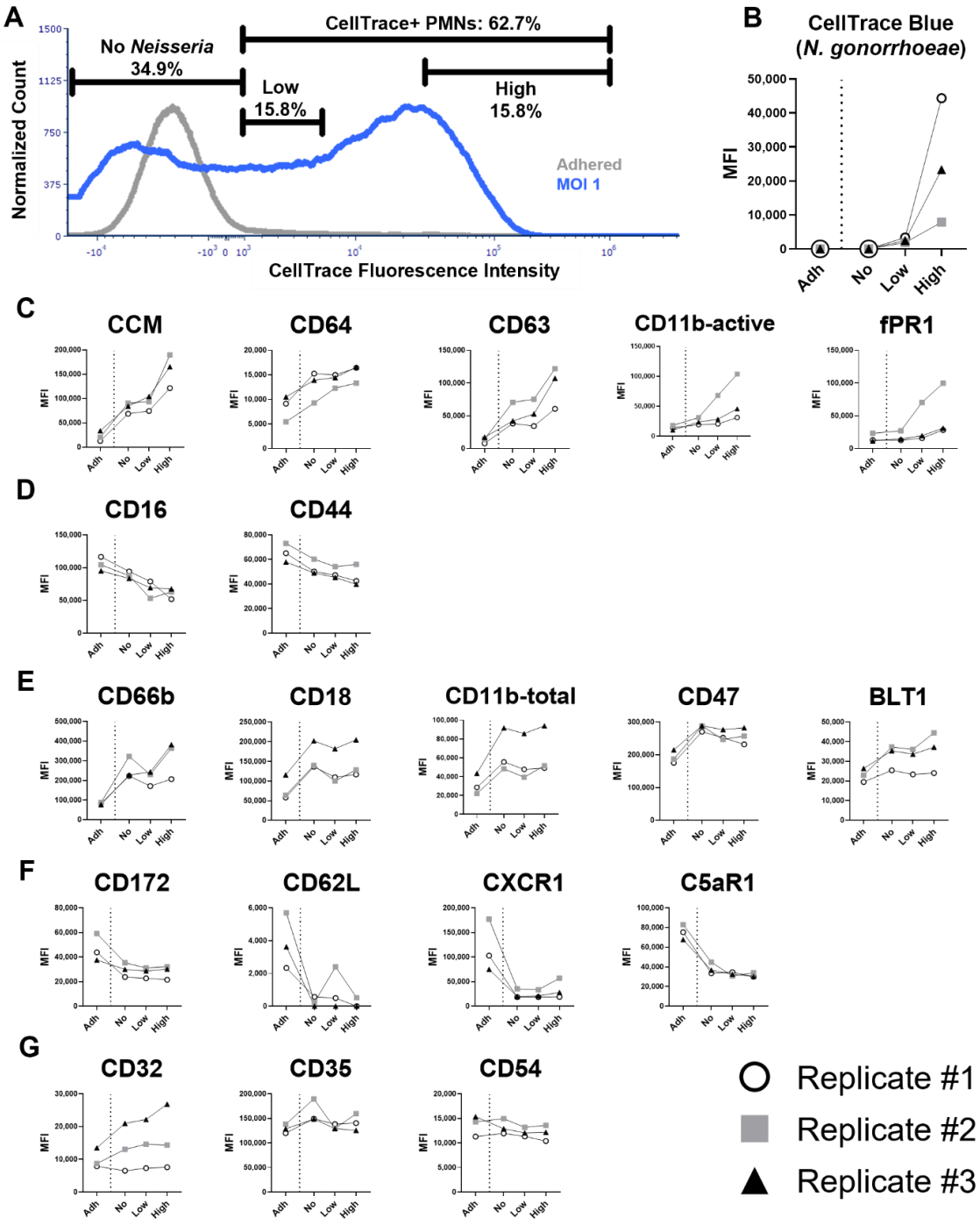
A
Normalized Count
No Neisseria
34.9%
Low
15.8%
CellTrace+ PMNs: 62.7%
High
15.8%
Adhered
MOI 1
CellTrace Fluorescence Intensity
B
CellTrace Blue
(N. gonorrhoeae)
MFI
Adh
No
Low
High
C
CCM
CD64
CD63
CD11b-active
fPR1
D
CD16
CD44
E
CD66b
CD18
CD11b-total
CD47
BLT1
F
CD172
CD62L
CXCR1
C5aR1
G
CD32
CD35
CD54
Replicate #1
Replicate #2
Replicate #3

Figure 31. Differential surface marker expression patterns based on bacterial exposure and burden

PMNs were challenged with CellTrace Blue-labeled *N. gonorrhoeae* at a multiplicity of infection (MOI) of 1 bacterium per PMN or adherent alone without bacterial exposure (Adh). PMNs in the infected condition were subgated by CellTrace Blue intensity into a No *Neisseria* population and populations with Low and High bacterial burdens, based on fluorescence quartiles. (B) CellTrace Blue MFI from three independent experiments separated by bacterial burden subgate. Adherent alone PMNs to the left of the dotted line displayed as a control. (C) PMN markers which consistently increased with infection over adherent alone conditions and in a bacterial burden-dependent manner, i.e. High *Neisseria* over Low *Neisseria*. (D) Surface markers which consistently decreased in a bacterial burden-dependent manner and compared to adherent alone. (E) Surface markers which consistently increased with infection compared to adherent alone PMNs, but with no bacteria burden-dependent variation in surface protein expression. (F) Surface markers which consistently decreased with infection compared to adherent alone PMNs but with no bacterial burden-dependent variation in surface protein expression. (G) PMN surface markers which showed either no change in expression or no consistent trends in variation between replicates. Dotted lines (B-G) separate bacteria-exposed from adherent alone PMNs.

To identify heterogeneity within the PMN population, PMNs were infected with OpaD Gc at an MOI of 1 and 10 (data from replicate #1 of Fig. 29) then analyzed via UMAP and clustered according to spectral panel phenotype (Fig. 32A). Differential clustering was driven to a considerable extent by bacterial burden with overlapping yet distinct profiles (Fig. 32B,C). PMNs with the greatest Gc burden were in clusters 1 and 2 and to a lesser extent in clusters 4 and 6 (Fig. 32C). The significant Gc burden in clusters 1 and 2 was accompanied by markers of PMN activation including elevated CCM, CD63, CD11b-active, and fPR1 and decreased CD16 (Fig. 32D,E). Despite a relatively low Gc burden, cluster 3 also showed signs of PMN activation including elevated CCM, CD63, and CD11b-active and was the subpopulation with the greatest CD66b expression (Fig. 32D,E). Cluster 5 was unique in its lack of CD11b-active and fPR1 expression, although it had a bacterial burden similar to the population as a whole. Cluster 9 was the only cluster with appreciable CD62L expression after infection. Clusters 7 and 10 were unique with low CD47 levels (Fig. 32E). The two clusters with the lowest CellTrace Blue signal, numbers 7 and 9, had some canonical signs of activation (low CD16, elevated CD66b in cluster 9, etc.) but their spectral profiles suggest their activation states are different from that of PMNs with high bacterial burdens (Fig. 32E).

Finally, adhered PMNs were infected at an MOI of 1 or 10 with either OpaD or Opaless Gc.[38] Opacity-associated proteins bind CCMs on PMNs thereby increasing Gc association, internalization, and subsequent death compared to Gc which lack these adhesins.[39] Gc-PMN association was

enhanced with OpaD expression based on CellTrace Blue intensity in the spectral flow panel (Fig. 33A). Infecting at an MOI of 10 with OpaD resulted in a PMN population in which more than 99% of the PMNs were associated with Gc. In comparison, infected with the lower MOI of OpaD or at the MOI of 10 with Opaless Gc yielded 63.0% and 73.3% positivity, respectively (Fig. 11A). These latter conditions also yielded MFIs approximately one $\log_{10}$ lower than infection with OpaD at an MOI of 10 with wider population distributions similar to those seen in Figure 29. Infection with Opaless Gc at an MOI of 1 yielded only 16.4% positivity (Fig. 33A). To examine the impact of opacity-associated protein signaling through PMNs, we performed UMAP dimensional reduction on spectral data from OpaD and Opaless infected PMNs at MOIs of 1 and 10, respectively (Fig. 33B). These experimental conditions were chosen due to their similar CellTrace Blue population distributions to account for differences in Gc association due to OpaD expression. PMNs infected with either Gc strain showed significant overlap in their population structures (Fig. 33B,C) and strikingly similar spectral profiles (Fig. 33D).

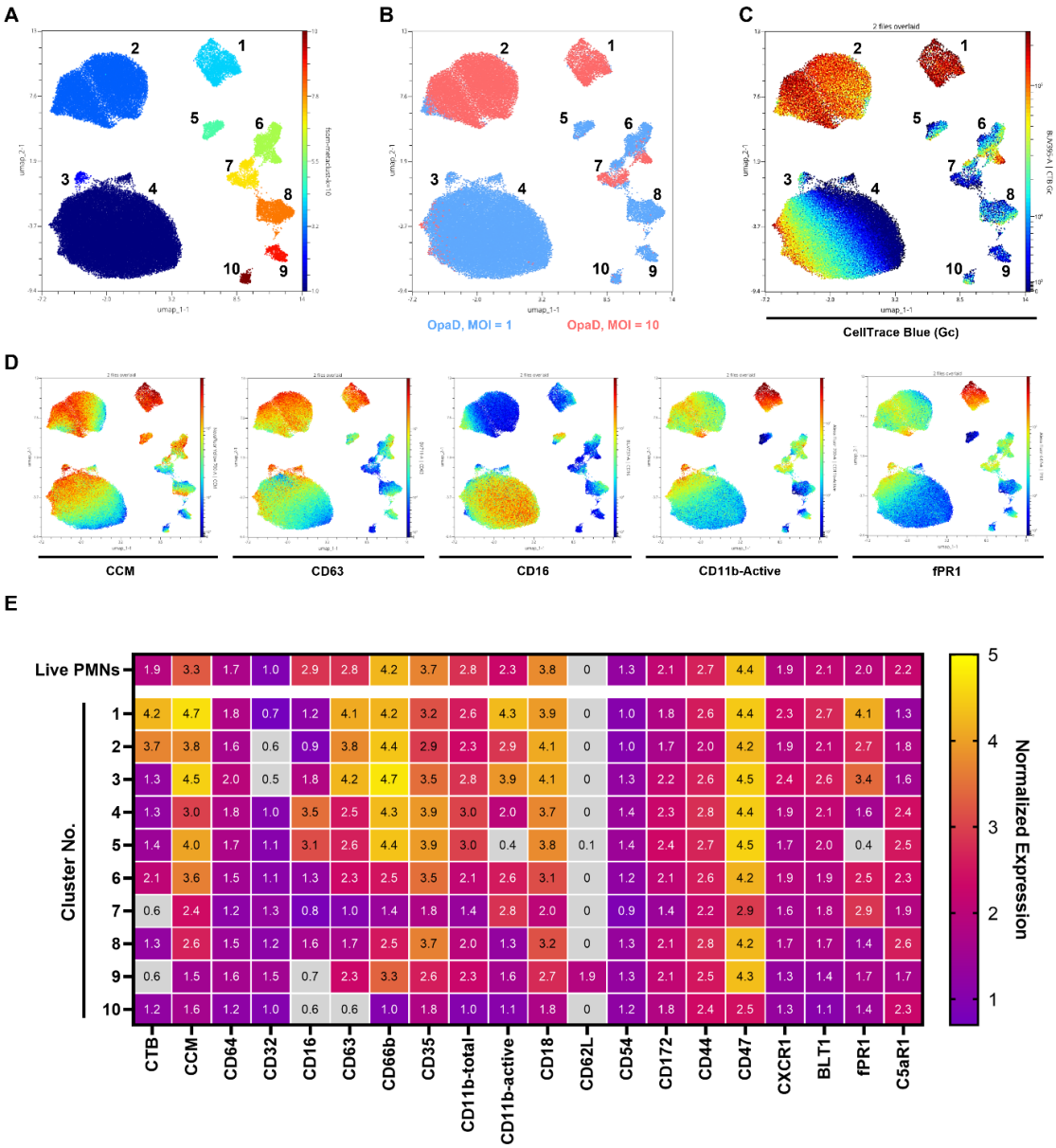
A
B
C
OpaD, MOI = 1
OpaD, MOI = 10
CellTrace Blue (Gc)
D
CCM
CD63
CD16
CD11b-Active
fPR1
E
Live PMNs
Cluster No.
CTB
CCM
CD64
CD32
CD16
CD63
CD66b
CD35
CD11b-total
CD11b-active
CD18
CD62L
CD54
CD172
CD44
CD47
CXCR1
BLT1
fPR1
C5aR1
Normalized Expression

Figure 32. Differential clustering of PMN subsets following infection with fluorescently-labeled *N. gonorrhoeae*

Purified primary human PMNs were adhered and infected with CellTrace Blue-labeled *N. gonorrhoeae* at a multiplicity of infection (MOI) of either 1 or 10 bacteria per PMN. Bacteria were of the FA1090 strain background in which only one opacity-associated protein (OpaD) was constitutively expressed. PMNs were stained with the full spectral flow cytometry panel, analyzed via uniform manifold approximation and projection (UMAP) dimensional reduction, and displayed according to the two principal UMAP dimensions (umap_1-1 and umap_2-1). (A) 10 distinct clusters were identified via FlowSOM clustering in OMIQ cloud software with each cluster in a different color. (B) UMAP projection of the MOI 1 and MOI 10 datasets overlayed. (C) CellTrace Blue fluorescence displayed by the two principal UMAP components and by color intensity (red = highest CellTrace signal, blue = lowest CellTrace signal). (D) Examples of surface marker expression patterns across UMAP clusters. Carcinoembryonic Antigen-related Cell Adhesion Molecule (CCM), formylated Peptide Receptor 1 (fPR1). (E) Heat map of normalized surface marker/parameter expression by distinct FlowSOM-identified cluster. Top row: bulk expression of all Live PMNs used in analysis without cluster separation. Values falling below 0.7 displayed in gray as being unexpressed in that cluster. Negative values at the cluster level for CD62L were set to a 0.0 value.

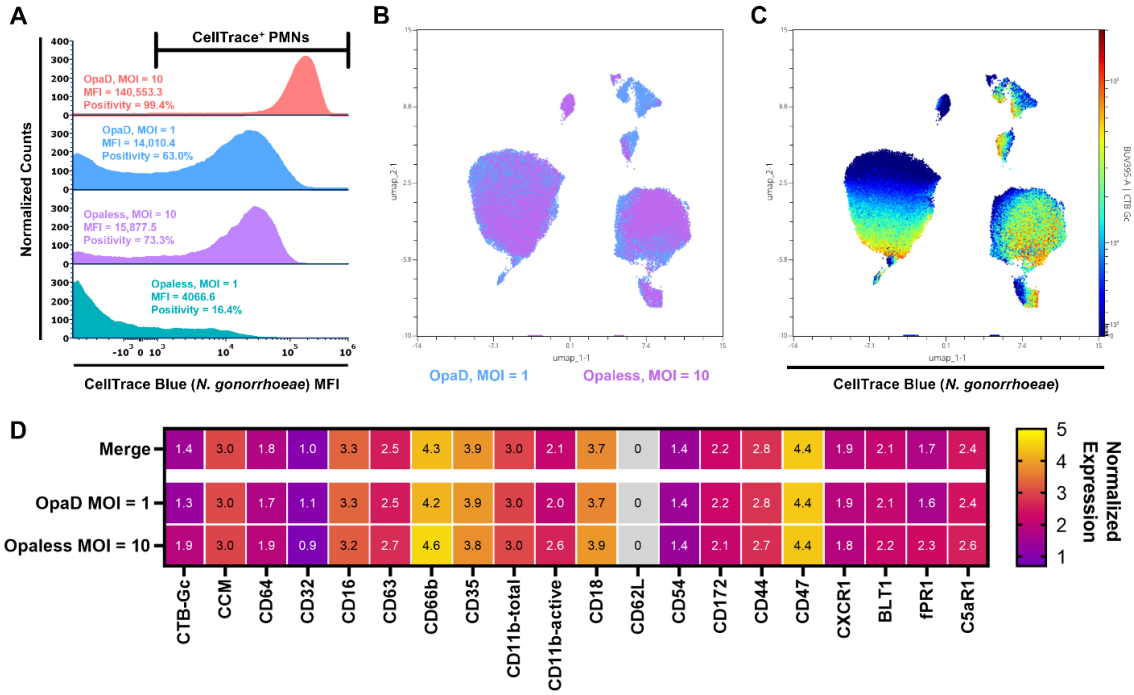
A
CellTrace+ PMNs
OpaD, MOI = 10
MFI = 140,553.3
Positivity = 99.4%
OpaD, MOI = 1
MFI = 14,010.4
Positivity = 63.0%
Opaless, MOI = 10
MFI = 15,877.5
Positivity = 73.3%
Opaless, MOI = 1
MFI = 4066.6
Positivity = 16.4%
Normalized Counts
CellTrace Blue (N. gonorrhoeae) MFI
B
OpaD, MOI = 1
Opaless, MOI = 10
C
CellTrace Blue (N. gonorrhoeae)

D
Merge 1.4 3.0 1.8 1.0 3.3 2.5 4.3 3.9 3.0 2.1 3.7 0 1.4 2.2 2.8 4.4 1.9 2.1 1.7 2.4
OpaD MOI = 1 1.3 3.0 1.7 1.1 3.3 2.5 4.2 3.9 3.0 2.0 3.7 0 1.4 2.2 2.8 4.4 1.9 2.1 1.6 2.4
Opaless MOI = 10 1.9 3.0 1.9 0.9 3.2 2.7 4.6 3.8 3.0 2.6 3.9 0 1.4 2.1 2.7 4.4 1.8 2.2 2.3 2.6
CTB-Gc
CCM
CD64
CD32
CD16
CD63
CD66b
CD35
CD11b-total
CD11b-active
CD18
CD62L
CD54
CD172
CD44
CD47
CXCR1
BLT1
fPR1
C5aR1
Normalized Expression
5
4
3
2
1

Figure 33. PMN surface marker variation in response to Opa-expressing and Opaless *N. gonorrhoeae*

Purified primary human PMNs were adhered and infected with CellTrace Blue-labeled *N. gonorrhoeae* at a multiplicity of infection (MOI) of either 1 or 10 bacteria per PMN. Bacteria were of the FA1090 strain background in which only one opacity-associated protein (OpaD) was constitutively expressed, or in which all opacity-associated genes were deleted (Opaless). PMNs were stained with the full spectral flow cytometry panel, analyzed for median fluorescence intensity and via uniform manifold approximation and projection (UMAP) dimensional reduction, and displayed according to the two principal UMAP dimensions (umap_1-1 and umap_2-1). (A) population level distribution of CellTrace Blue intensities after infection with OpaD or Opaless bacteria at an MOI of either 1 or 10. Marker denotes gating limits of positive CellTrace Blue signal. (B) UMAP projection of the OpaD MOI 1 and Opaless MOI 10 datasets overlayed. (C) CellTrace Blue fluorescence displayed by the two principal UMAP components and by color intensity (red = highest CellTrace signal, blue = lowest CellTrace signal). (D) Heat map of normalized surface marker/parameter expression by infection condition. Top row: bulk expression of all Live PMNs used in analysis without strain/MOI separation. Values falling below 0.7 displayed in gray as being unexpressed in that cluster. Negative values at the cluster level for CD62L were set to a 0.0 value.

3.3 Chapter Discussion

PMNs have major roles in infection, sterile inflammation, and tissue injury and repair. Here we describe the development, validation, and application of a high-dimensional spectral flow cytometry panel for profiling PMNs isolated from human subjects. It was designed to interrogate PMN activation and surface expression of markers for cellular functionality including phagocytosis, degranulation, migration, and chemotaxis. In support of our findings with this panel, PMN responses to PMA and Gc aligned with previous reports using conventional flow cytometry.[202,383-388] This spectral flow cytometry panel enables rapid, high throughput, multiparametric analysis, and sample preservation with broad applicability to PMN biology.

Care was taken to allow adaptability of this panel for different research groups' needs. For example, in place of CCMs as surface receptors that bind and phagocytose Gc in the NFY700 channel, a research team could substitute a parameter of their interest such as markers of PMN maturation/senescence or differentiation to immunomodulatory subtypes.[389-391] In the CTB/BUV395 channel, another surface marker or labeled cargo could be interrogated including a vast diversity of pathogens, beads, cellular debris, immune complexes, etc. Additional PMN functions that could be incorporated into the panel include ROS generation, NET release, death modalities (e.g. apoptosis, pyroptosis, etc.), maturation and differentiation, intracellular signaling, and cytokine production.

As highly differentiated, terminal cells, PMNs present unique challenges for building and applying a flow cytometric panel. Measuring PMN activation

between a baseline and stimulated state is inherently challenging due PMNs' sensitivity to activation including during the isolation procedure. Here, PMNs were isolated by Ficoll gradient and hypotonic erythrocyte lysis, which differ in basal activation state from PMNs in anticoagulated whole blood, purified by immunomagnetic negative selection, or in tissues.[258] The surface epitope density of a selected marker can vary dramatically across a continuum of resting, primed, and activated states. Furthermore, some surface markers are shed or internalized by activated PMNs. For these reasons, the selection of marker-fluorochrome pairings, which is based on epitope density and brightness index, must be experimentally determined through antibody titrations in single-stained samples at low and high epitope density conditions as well as in the context of the full stained panel. As each marker uses a different antibody-fluorochrome pairing, direct comparisons between markers of absolute or relative changes should be cautioned against. Fluorescence-minus-one (FMO) controls should also be employed where necessary to discriminate between positive and negative populations for accurate gate setting.[392,393] Isotype controls may be used to account for non-specific binding, however, their reliability is controversial.[392] Given PMN surface marker variability basally and upon stimulation between subjects, as well as on different days for the same subject (Fig. 25 and 26), it may be prudent to assess subjects multiple times. Future studies are needed to define the number of individuals or experiments on a single subject needed for statistical power while considering the time and cost of

these experiments (approximately $500/experiment with 4 full-stain samples and single stain controls).

PMNs play a preeminent role in controlling pathogenic organisms. However, some pathogens have evolved to counteract the antimicrobial mechanisms of PMNs. Among these is the Gram-negative bacterium Gc which infects mucosal surfaces of its obligate human host and stimulates a PMN-driven inflammatory response.[1,4] Here, Gc was chosen as a model infectious organism and phagocytic cargo for its capacity to survive within phagosomes of human neutrophils.[228] By engaging neutrophil surface receptors Gc can block neutrophil phagosome maturation and suppress neutrophil activation, such that viable bacteria are isolated from the PMN-rich exudates of infected individuals.[394-396] Intriguingly, PMNs in urethral gonorrheal exudates have a heterogenous distribution of associated Gc resembling that of Figure 30 in which many PMNs have no bacteria, some having single-digit numbers of bacteria, and others having tens of bacteria.[12,394] These observations inspired the application of the spectral flow panel to understand differences in PMN responsiveness to Gc *ex vivo*, which we ultimately intend to examine in primary human specimens. During infection, PMNs interact directly with in-tact microbes as well as the soluble factors they release such as cell wall fragments, formylated peptides, and lipo-poly/oligo-saccharides, alone or in outer membrane vesicles. Intriguingly, we observed differences in surface marker expression between PMNs not exposed to Gc and those in the infection milieu that did not contain associated or phagocytosed bacteria (Fig. 30, 31, 32). This observation implies that soluble

factors within the infectious milieu are sufficient to initiate PMN activation, which is enhanced with bacterial association (i.e. in the Low/High Gc conditions) and a heterogenous PMN population is produced (Fig. 32). Additionally, paracrine signaling among PMNs during infection, such as release of leukotriene-B_4 could contribute to the observed changes in some surface markers.[397] Moreover, PMN responses to PMA and infection with Gc were similar, indicating a largely conserved response to these different stimuli. Our findings prompt further investigation with purified soluble factors and/or outer membrane vesicles and Gc mutants that produce or release different quantities of these factors.

PMNs sense many stimuli in the context of infection, tissue damage, or inflammation and integrate these signals to respond. The field now appreciates that PMNs vary within a population resulting from factors such as their age and prior experience (“trained innate immunity”)[398], yet the contribution of this diversity in host response is incompletely understood. We developed this high-dimensional spectral flow cytometry panel to profile the diversity of PMN responses, identify subsets of PMNs with phenotypes of interest to the investigator, and generate new hypotheses about human PMN functionality. Dimensionality reduction approaches and differential clustering (Fig. 28, 32) can then be applied to generate hypotheses and reveal underlying biology from the vast amounts of data generated from this panel. We observed PMN subpopulations with unique marker expression profiles and degrees of bacterial association (Fig. 32) and look forward to dissecting the source and implications of this diversity.

Going forward, this panel can be directly transferred to spectral cell sorting instruments with appropriate laser and detector configurations to isolate PMN populations of interest. This panel and protocol are also suitable for collection of viable PMNs containing Gc which can be used for downstream applications such as single cell RNA-sequencing (Fig. 34).[399,400] As spectral flow cytometers and related technologies continue to advance, it is our hope the human PMN functional panel presented here will be used and expanded by many investigators to understand the breadth of responses of PMNs, uncovering the contribution of these biologically meaningful cells to diverse fields of biology and medicine.

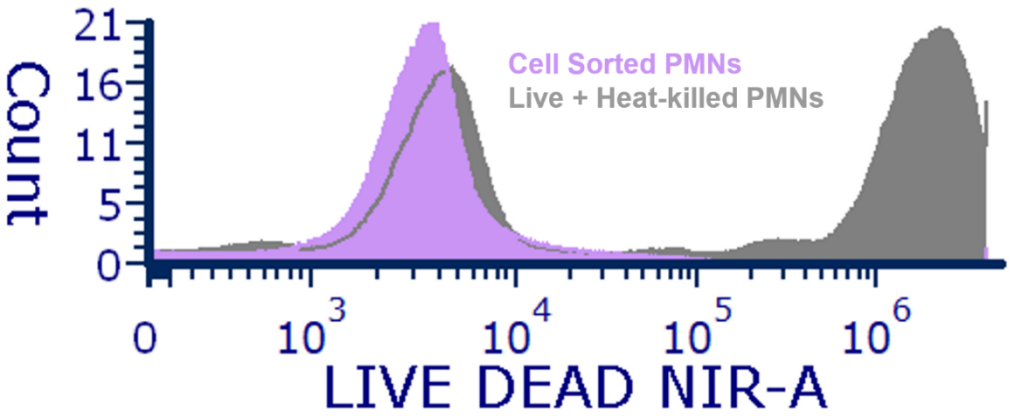

Figure 34. Viability of PMNs after staining with full spectral flow cytometry panel and spectral cell sorting

Primary human PMNs were adhered and infected with *N. gonorrhoeae* as described (see Materials & Methods). PMNs were run on a Cytek CS Spectral Cell Sorter and sorted in populations based on bacterial burden. Combined post-sorting PMNs (purple) were then assayed on a Cytek Aurora spectral flow cytometer to assess for viability after sorting. Data displayed as normalized counts and Zombie NIR fluorescence intensity. A 1:1 mixture of viable and heat-killed PMNs (gray) was used as a viability staining control.

3.4 Materials & Methods

3.4.1 PMN isolation from human subjects.

Human subjects research was conducted in accordance with the University of Virginia Institutional Review Board for Health Sciences Research under protocol #13909. Informed written consent was obtained from each human subject. All subjects were 18-65 years of age, with no reported comorbidities, and healthy at the time of blood collection. Primary human PMNs were collected via venipuncture as previously described.[43] Briefly, venous blood was collected into heparin-coated Vacutainer® tubes (BD) and fractionated by dextran sedimentation to enrich for leukocytes. Granulocytes were purified by Ficoll-Paque™ density centrifugation with DPBS (Gibco) + 0.1% (v/v) glucose (DPBSG; Ricca Chemical). The Ficoll-PBS interface enriched for monocytes and depleted of granulocytes was collected for CD14 gate setting. The granulocyte pellet was then resuspended, lysed with endotoxin-free water to remove remaining erythrocytes, and resuspended in DPBSG on ice and enumerated using a hemacytometer.

3.4.2 *Neisseria gonorrhoeae* growth and labeling.

A derivative of strain FA1090[289] *N. gonorrhoeae* in which all opacity-associated proteins had been deleted (Opaless) or which constitutively expresses the PMN-binding surface protein OpaD and no other opacity-associated proteins (OpaD)[38] were streaked on gonococcal base media agar plates and incubated at 37°C with 5% supplemental CO_2 for 16 hours.[45,177] Single colonies were then swabbed into Hank's balanced salt solution (HBSS, with

1.2mM calcium and 1mM magnesium, Gibco) with 10mM HEPES (Sigma-Aldrich) pH 7.4 and 5mM sodium bicarbonate to a concentration of 1.5e8 bacteria per mL and labeled with CellTrace Blue (ThermoFisher) for 20min at 37°C. Bacteria were then pelleted and resuspended in HBSS + 2% bovine serum albumin (BSA) to quench remaining CellTrace Blue dye. Un-labeled bacteria were used as non-fluorescent controls.

3.4.3 PMN adherence and stimulation.

To simulate post-migration status of innate immune cells at inflamed mucosa, isolated primary human PMNs were primed with 10nM recombinant human interleukin-8 (IL-8, R&D Systems) in Roswell Park Memorial Institute Medium (RPMI, Gibco) + 10% (v/v) heat-inactivated fetal bovine serum (RPMI + 10% FBS, Hyclone) as in Ragland and Criss.[43] PMNs were then allowed to settle and adhere onto 25mm plastic cover slips (Starstedt) in 6-well tissue culture plates in 1mL medium at 37°C, 5% CO_2 for 30-60min. Following adherence, PMNs were either left untreated, stimulated with 10ng/mL phorbol 12-myristate 13-acetate (PMA, Sigma-Alrich), or infected with *N. gonorrhoeae* at a multiplicity of infection of either one or ten bacteria per PMN for 60min at 37°C, 5% CO_2. Controls included unstained, untreated, and single fluorochrome samples. Each condition consisted of two wells in a 6-well plate with 2e6 PMNs per well which were pooled following stimulation.

3.4.4 PMN washing and labeling.

After 60min of stimulation/infection, EDTA (Sigma-Aldrich) was added to adhered PMNs to a final concentration of 0.5mM. PMNs were gently

resuspended using a cell scraper (Falcon). Cells from two wells per condition were pooled into a 15mL conical tube and centrifuged at 860 x g for 7min at 4°C. Medium was removed via aspiration to approximately 50µL. PMNs were gently resuspended in 2mL ice cold HBSS+ and washed likewise twice more. PMNs were then resuspended in 200µL ice cold HBSS+ and transferred to a V-bottom 96-well plate on ice. Additional samples added to the 96-well plate included: PMNs which had been untreated and left in suspension to be used both for full antibody staining and for unstained controls; suspension PMNs on ice mixed 1:1 with suspension PMNs that were heat-killed (65°C for 5min) for viability gate setting; and granulocyte-depleted DPBSG-Ficoll interface 'buffy-coat' enriched with monocytes for CD14 dump gate setting. The plate was centrifuged at 600 x g for 7min at 4°C, 100µL were removed from each well via multichannel pipet, and a 1:1000 dilution of Zombie Near-Infrared (Zombie NIR, ZNIR) live-dead dye (BioLegend) was added to the full-stain and single/gate-setting stain wells per manufacturer's directions (15min at room temperature in the dark) and pellets gently resuspended. One hundred µL of Flow Staining Buffer (eBiosciences) was then added to each well to quench ZNIR dyes. The plate was centrifuged as above, 150µL were removed from each well via multichannel pipet, and 150µL Flow Staining Buffer was added. 150µL was removed from each well via multichannel pipet so that each well contained 50µL of Flow Staining Buffer and pelleted cells. Flow Staining Buffer was added to wells followed by individual antibodies as indicated in Table 3 to a total of 100µL per well. Cells were gently resuspended with staining buffer/antibody mixtures and incubated at 4°C for

30min in the dark. The plate was then centrifuged as above, 50µL was removed from each well, and pellets were gently washed three times in sterile PBS. The final wash was into a final volume of 100µL of PBS + 1% (v/v) paraformaldehyde (Electron Microscopy Sciences). The plate with fixed samples was stored at 4°C in the dark wrapped in aluminum foil for no more than three days before analysis on the spectral flow cytometer.

3.4.5 Spectral flow cytometry acquisition.

Samples were run on a Cytek Aurora spectral flow cytometer with a 20mW 355nm, 50mW 488nm, 100mW 405nm, 50mW 561nm, and 80mW 640nm 5-laser configuration. Samples were run using the 96-well plate autosampler apparatus within three days after fixation. Unmixing and spillover correction was performed in SpectroFlo (Cytek) software.

3.4.6 Antibody-fluorochrome conjugation and titration.

All fluorescently labelled antibodies were obtained from commercial suppliers (Table 3), except for the anti-CCM 1,3,6 antibody which was conjugated in-house with NovaFluor Yellow 700 (NFYellow 700, NFY700) using the NovaFluor Antibody Conjugation Kit (ThermoFisher) per manufacturer's protocols. Each antibody was titrated to establish the lowest concentration that maximized the fluorescence intensity differential between labelled and unlabeled cells.

3.4.7 Imaging flow cytometry analysis of *N. gonorrhoeae* infected PMNs.

Primary human PMNs were infected as described above with *N. gonorrhoeae,* which was labeled with both CellTrace Blue and CellTrace Yellow

(ThermoFisher) per manufacturer's protocols for detection on both the Cytek Aurora spectral flow cytometer (both fluorochromes) and the Cytek ImageStream^X MkII imaging flow cytometer (CellTrace Yellow). Single-stained and unstained bacteria were included as controls. Infected cells were collected and fixed as above, and data collected on each cytometer with appropriate single stained controls. Imaging flow cytometry was performed at 60x magnification using brightfield to collect micrographs of individual cells, side scatter channels, and the 561nm (100mW) excitation laser to collect CellTrace Yellow-Gc MFI. Ten-thousand individual, focused singlet PMN events were collected for each sample, and data were analyzed using the IDEAS 6.2® software package.[171,177]

3.4.8 PMN cell sorting.

PMNs were infected with CellTrace Yellow and CellTrace Blue dual-labeled *N. gonorrhoeae* and stained with Zombie NIR, and run on a Cytek CS Spectral Cell Sorter. Live unmixing was performed, and PMNs were sorted into CellTrace Blue negative, low, and high subgated populations, as well as a non-gated group, into 1.5mL Eppendorf tubes. PMNs were subsequently run on a Cytek Aurora spectral flow cytometer to assess post-sorting viability via Zombie NIR exclusion using a 1:1 mixture of viable and heat-killed PMNs as a reference.

3.4.9 Statistics, analyses, and data availability.

Analyses were performed as indicated. MFI were assumed to be parametric. Data were analyzed using SpectroFlo (Cytek), FCS Express (De Novo), IDEAS (Amnis), and GraphPad Prism software. Data were unmixed in SpectroFlo software and uploaded into OMIQ cloud software for uniform manifold

approximation and projection (UMAP) dimensional reduction processing and analysis.[378] Data were cleaned using FlowAI within OMIQ, gated onto viable single PMN events, and UMAP analyses conducted with all fluorescent features except those used for gating. Clustering was performed in OMIQ using FlowSOM. OMIQ's default settings were used. Raw flow cytometry data is available through the MyFlowCyt flow cytometry repository under the Experiment title: PMN Spectral Flow Panel, and Experiment ID: (FR-FCM-Z8EX).

4 Neutrophil transepithelial migration in an endocervical Transwell system

This chapter is comprised of unpublished data collected between January 2019 and December 2021. Dr. Aimee Potter began this project as an extension of Dr. Jacqueline Stevens' thesis work (Neutrophilic inflammation initiated by gonococcal-endocervical cell interactions and amplified by migrating neutrophils. (2018). Journal of Infectious Diseases). Evan Lamb adopted this project upon joining the Criss Lab in April 2021. Data originally published in Dr. Stevens' thesis work were adapted for Figure 36D (*rmp* and *pilQ*).

Contributors:

Evan Lamb – Conceptualization, Methodology, Analysis, Investigation, Authorship, Validation, Visualization, Funding Acquisition.

Aimee Potter – Conceptualization, Methodology, Analysis, Investigation, Validation. Project Administration.

Jacqueline Stevens – Conceptualization, Methodology, Analysis, Investigation, Authorship, Validation.

Alison Criss – Conceptualization, Methodology, Analysis, Authorship, Funding Acquisition, Project Administration.

We thank Drs. Jim Casanova, Holly Torsilieri, Doug DeSimone, and Ryan Mulligan for their assistance with and access to confocal and spinning disk microscopy related to this work. We thank Drs. Hervé Agaisse and Volkan

Köseoğlu for their assistance in generating membrane-YFP expressing epithelial cells via lentiviral infection.

4.1 Introduction

Neisseria gonorrhoeae (the gonococcus, Gc) is a human-specific bacterial pathogen and causative agent of an estimated 80-100 million cases of gonorrhea annually worldwide.[1,3,101,102] Gc adheres to and infects mucosal epithelia of the cervix, urethra, conjunctiva, rectum, and oropharynx through surface factors such as opacity-associated proteins (Opa) and Pili.[1,2] Infection elicits a vigorous innate immune response with neutrophil (polymorphonuclear leukocyte, PMN)-predominant infiltration. Despite the abundance of PMNs at the infected mucosa, Gc infection frequently persists in the absence of appropriate antibiotic therapy. The ability of Gc to persist in its obligate human host owes in part to its many evolved strategies to evade PMN-mediated killing including production of detoxifying enzymes, efflux pump expression, avoidance of phagocytic uptake, and inhibition of phagosome maturation. Sustained infection results in prolonged PMN recruitment and collateral damage to host epithelial tissues which have been linked to complications of gonorrhea including pelvic inflammatory disease, ectopic pregnancies, and infertility.[1,273] Therefore, interrogating the interplay between the bacteria, PMNs, and epithelial cells may hold key insights into the pathogenesis of Gc infection.

To reach the apical epithelial infection site, PMNs must be recruited from systemic circulation and migrate through the endothelium, underlying stroma, and epithelium.[217,220] Soluble factors released locally at the inflamed tissue form chemotactic gradients that recruit and stimulate PMNs. Factors such as interleukin-8 (IL-8; CXCL8) are released basolaterally from infected epithelial

cells to initiate PMN influx. Additional chemotactic gradients are generated to complete PMN migration across the epithelial layer to the apical/luminal aspect in a process referred to here as transmigration or more specifically transepithelial migration.[216,218,220] A major group of compounds that stimulate PMNs and promote transepithelial migration to bacterial pathogens are the arachidonic acid-derived eicosanoids including the hepoxilins, leukotrienes, and prostaglandins.[216,222,401] Gc infection of an endocervical monolayer induces PMN transmigration via a primary chemotactic gradient of hepoxilin-A3 (HXA_3) secreted by the epithelial cells and a secondary amplifying chemotactic gradient of leukotriene-B4 (LTB_4) secreted by PMNs themselves.[216] However, the interactions between Gc and the epithelial cells which initiate synthesis and secretion of chemotactic signals and cytokines have not yet been identified.

PMN recruitment and migratory processes are associated with increased neutrophil activation and enhanced antimicrobial activity due to exposure to stimulatory agents and through adhesion-based signaling (e.g. by integrin-substrate binding).[221-223,401,402] PMN-pathogen interactions may also be influenced at an apical epithelial surface resulting from organelle/nuclear deformation during transmigration, altered PMN metabolic activity, bacterial adherence to the epithelial surface, bacterial adherence to each other in microcolonies or biofilms, etc. Neither the impact of Gc adherence to epithelial cells nor the transmigration process have been previously investigated regarding PMN anti-gonococcal activity.

To address this gap in knowledge, our lab developed a tripartite Transwell system in an endocervical epithelial monolayer is infected with Gc with consequent transepithelial migration of primary human PMNs.[216] We investigate the host-pathogen interactions which induce transepithelial migration and interrogate the capacity of transmigrated PMNs to phagocytose and kill apically adhered Gc. This model is contrasted to one in which PMN activity is assessed in the absence of epithelial cells and transmigration[43] and caveats to comparison between the two models is discussed.

4.2 Results

4.2.1 PMNs migrate in response to Gc infection and interact with bacteria on the apical epithelium in a tripartite Transwell system.

Gc is a human-specific pathogen, complicating applications of *in vivo* infection models with animals and/or human subjects.[1,146,273] Many *in vitro* models of PMN-Gc combat use human cells collected and purified from peripheral blood to challenge bacteria. A model used extensively by our group consists of isolated primary human PMNs adhered to coverslips in a well-plate and pre-treated with IL-8 to mimic PMNs after migrating to the infected apical epithelium with subsequent Gc inoculation (‘Adhered IL-8 primed model’; Fig. 35A).[43] Despite the addition of IL-8 and the adherent nature of PMNs in this model, it lacks the repertoire of signals released by epithelial cells, the transmigratory process, and Gc-epithelium interactions. Therefore, investigating PMN-Gc-epithelium interplay *in vitro* required development of a new system.

To this end, our lab established an inverted Transwell system in which a confluent layer of immortalized endocervical epithelial cells was cultured on a polycarbonate filter support (the Transwell) with 3µm pores.[216] The established epithelium was then infected with Gc on the apical aspect, and isolated primary human PMNs were added to the basolateral chamber to induce transepithelial migration (Fig. 35B-D). PMN transmigration could be quantified using myeloperoxidase (MPO) assays which demonstrated significant recruitment across the epithelium with Gc infection which was reproducible at 2 hours after PMN addition (Fig. 35E).[216,403] Furthermore, PMNs could be observed to interact with apically adhered Gc via scanning electron and fluorescent microscopy (Fig. 35F,G). Live fluorescent imaging demonstrated PMN migration through and across the epithelial cell layer to actively target and phagocytose Gc in microcolonies (Image series Fig. 35G). This system also recapitulated PMN behavior observed in other systems such as PMNs releasing from the epithelial surface to ‘fall’ into the apical chamber representing the luminal space.[219] Released PMNs were allowed to settle onto glass coverslips for subsequent investigations.

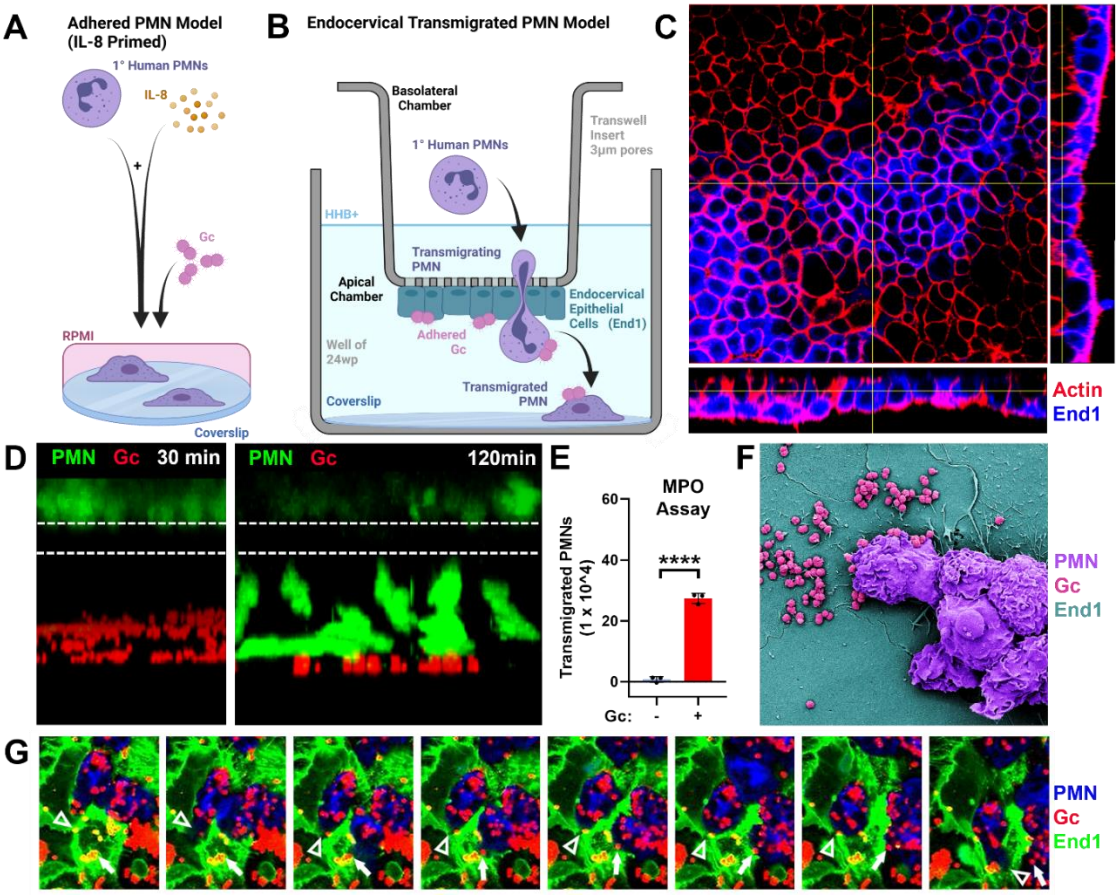
A
Adhered PMN Model
(IL-8 Primed)
1° Human PMNs
IL-8
+
Gc
RPMI
Coverslip
B
Endocervical Transmigrated PMN Model
Basolateral
Chamber
1° Human PMNs
Transwell
Insert
3µm pores
HHB+
Transmigrating
PMN
Apical
Chamber
Endocervical
Epithelial
Cells (End1)
Adhered
Gc
Well of
24wp
Coverslip
Transmigrated
PMN
C
Actin
End1
D
PMN Gc 30 min
PMN Gc 120min
E
MPO
Assay
Transmigrated PMNs
(1 x 10^4)
60
40
20
0
****
Gc: - +
F
PMN
Gc
End1
G
PMN
Gc
End1

Figure 35. Models of PMN-Gc interactions and characterization of tripartite Transwell system

(A) The Adhered IL-8 primed model of PMN-Gc interactions in which primary (1°) human neutrophils are adhered to coverslips in a well-plate with 80ng/mL IL-8 in RMPI media for 30-60 minutes and infected with Gc. (B) The tripartite Transwell system in which immortalized endocervical epithelial cells (End1) are cultured on a Transwell filter insert with 3µm pores for 7-10 days then infected apically with Gc for 2 hours in HHB+ media. Primary human PMNs are then added to the basolateral chamber and allowed to transmigrate across the epithelial layer, interact with Gc, and release onto a coverslip. (C) Fluorescent confocal micrograph of a 10-day-old Transwell End1 epithelial layer stained with CellTrace Far Red (blue) and actin labeled with fluorescent phalloidin (red). (D) Fluorescent confocal micrographs of CFSE-labeled PMNs (green) migrating toward CellTrace Yellow-labeled Gc (red) in the Transwell system at 30 and 120 minutes after PMN addition Dashed lines indicate the Transwell membrane. (E) Quantification of PMN transmigration with and without Gc infection. Measured by myeloperoxidase (MPO) activity compared to a standard curve. Error bars represent the standard error of the mean. Significance determined by unpaired Student's *t*-test. ****=$p<0.0001$. (F) Scanning electron micrograph of post-migration PMNs (purple) interacting with individual gonococci, diplococci, and bacterial clusters (pink) on the apical surface of End1 cells (cyan). (G) Image series from fluorescent live cell imaging of CellTrace Far Red-labeled PMNs (blue) migrating through and across an End1 cell (green, expressing membrane-localized YFP) epithelium to interact with CellTrace Yellow-labeled gonococci

(red) as individual bacteria and microcolonies/clusters. Arrowhead and arrow denote two individual bacteria over the time course of approximately 12 minutes.

4.2.2 Efforts to identify the Gc factor(s) which induce PMN transmigration.

Infection of inverted endocervical cells in the Transwell system with Gc induces PMN transmigration through a synthetic pathway involving epithelial protein kinase C (PKC), phospholipase-A_2 (PLA_2), and an array of lipoxygenases (LOX) to produce HXA_3 and secondary PMN secretion of LTB_4 (Fig. 36A).[216] However, the interaction between Gc and host epithelial cells which initiates this process was not identified. Data implicated a gonococcal proteinaceous surface structure as being a necessary component in this interaction. Trypsin-shaving of Gc significantly decreased PMN transmigration compared to intact bacteria at equivalent multiplicities of infection (MOI; Fig. 36B). Moreover, paraformaldehyde (PFA) fixed Gc also induced no measurable PMN transmigration whereas live, heat-killed, and isopropanol-fixed bacteria induced similar PMN transmigration levels. Endocervical cell treatment with purified Gc lipooligosaccharide, a TLR4 agonist, or TLR2 agonistic agents also did not elicit transmigration.[216]

A ready hypothesis was that the known immunogenic surface structures Opa and Pili could have been responsible for stimulating the epithelial cells. However, using strains deleted genes encoding either all Opa or the major pilin subunit, PilE, did not impact PMN transmigration levels when equivalent numbers of bacteria were adhered to the epithelium. Therefore, trypsin-shaved supernatants were collected for mass spectrometry to identify cleaved protein candidates. Figure 35C documents the proteins identified in greater abundance

in trypsin-shaved supernatants compared to vehicle-treated supernatants. A number of surface-exposed non-PilE subunits of Pili were identified (PilC, PilQ, PilN) as well as the major outer membrane proteins Porin and Rmp (formerly PI and PIII, respectively). Also identified were gonococcal MIP (macrophage infectivity potentiator-like protein)[276], the lysozyme inhibitor encoded by *ngo1981* (sometimes referred to as NgACP or LecA based on homology to factors in other species)[250], and the putative hemolysin encoded by *ngo1985*. Isogenic mutant and wild-type strains were generated or acquired for *rmp*, *pilQ*, *ngo1985*, and *ngo1981*. No mutant strain produced the hypothesized decrease in PMN transmigration compared to its wild-type counterpart (Fig. 36D). Interestingly, the *rmp* and *ngo1985* mutant strains trended toward greater PMN recruitment across the epithelium compared to factor-expressing strains. Mutant strains lacking PilC (encoded by two genes in most Gc strains[73], *pilC1* and *pilC2*), PilN, and MIP were not obtained during the course of these studies, and Porin is an essential outer membrane protein. Therefore, additional studies ought to be pursued to assess these remaining factors singly or in combination.

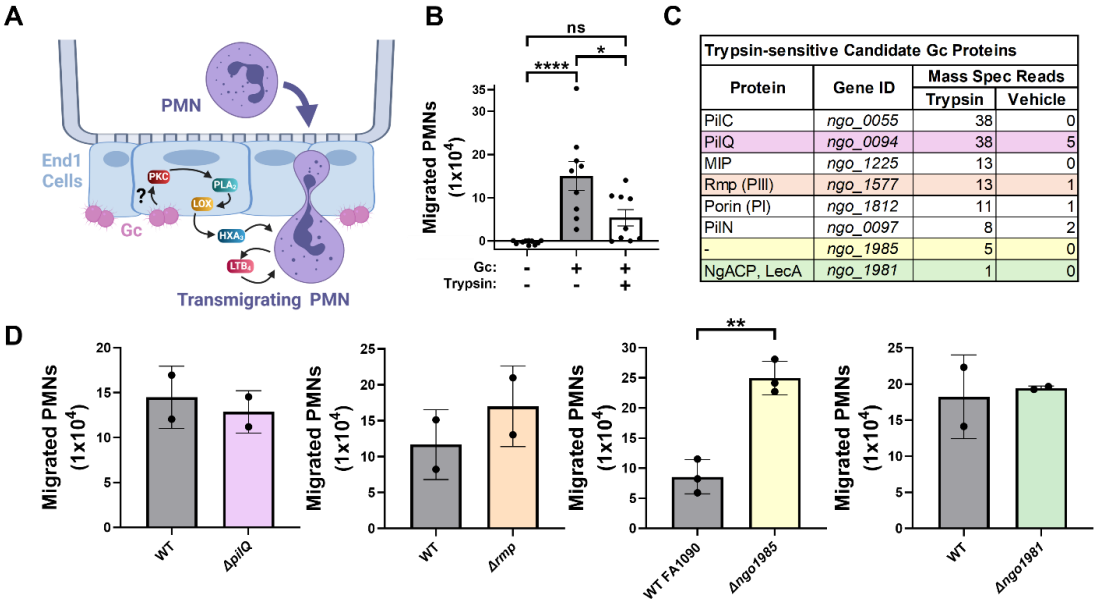

Trypsin-sensitive Candidate Gc Proteins			
Protein	Gene ID	Mass Spec Reads	
		Trypsin	Vehicle
PilC	*ngo_0055*	38	0
PilQ	*ngo_0094*	38	5
MIP	*ngo_1225*	13	0
Rmp (PIII)	*ngo_1577*	13	1
Porin (PI)	*ngo_1812*	11	1
PilN	*ngo_0097*	8	2
-	*ngo_1985*	5	0
NgACP, LecA	*ngo_1981*	1	0

Figure 36. PMN transmigration responses to Gc surface components

(A) Schematic of known PMN transepithelial migration induction in the tripartite Transwell system. Protein kinase C (PKC) in endocervical epithelial cells (End1) is activated by an unidentified mechanism (question mark) which in sequence promotes phospholipase-A_2 (PLA_2) and lipoxygenases (LOX) to synthesize and secrete hepoxilin-A3 (HXA_3) as a primary chemoattractant gradient. Recruited PMNs then generate a secondary and self-amplifying chemoattractant gradient by producing leukotriene-B4 (LTB_4). (B) Quantification of PMN transmigration via myeloperoxidase assay in the absence of Gc infection, with Gc infection with or without trypsin-shaving. Error bars are standard error of the mean. Significance determined by 1-way ANOVA with Tukey's multiple comparisons. *=$p<0.05$, ****=$p<0.0001$, ns = not significant. (C) Table of mass spectrometry reads from supernatants collected from trypsin-shaved and vehicle-treated Gc. Gene ID based on the FA1090 strain Gc genome. (D) PMN transmigration via myeloperoxidase assay to Gc strains mutated for surface factors found in panel (C) compared to isogenic wild-type (WT) strains. Error bars = standard error of the mean. Significance for *ngo1985* determined by unpaired Student's *t*-test. **=$p<0.01$. Data for *rmp* and *pilQ* mutants were adapted from Stevens, 2018.

4.2.3 Transmigration impacts PMN association with and killing of Gc.

Signaling components present during the transmigration process have been reported to enhance PMN activation status and result in greater bactericidal capacity. However, the impact of transmigration on PMN activity against Gc has not yet been directly explored and many *in vitro* PMN-Gc infection models lack epithelial cells altogether. To investigate this question, we sought to compare numbers of Gc associated with PMNs as well as Gc viability between the Transwell and Adhered IL-8 primed models in which transmigration does and does not occur, respectively.

In the Adhered IL-8 primed model, PMNs infected at an MOI of ten bacteria per PMN yielded a heterogenous population in which some PMNs were associated with no Gc, some with single digit numbers of Gc, and some with tens of bacteria (Fig. 37A,B). In this model, the mean number of Gc per PMN was 8.2 and the median was 6. Only 6.0% of PMNs had no associated Gc and 9.5% had 20 or more bacteria. The Transwell model with PMN transmigration (MOI = 10 Gc per PMN) also produced a heterogenous PMN population based on Gc association. In contrast, the mean number of Gc per PMN was 7.1 and the median was 2. PMNs with no associated Gc constituted 27.3% of the population and 14.7% had 20 or more bacteria (Fig. 37B).

The observed differences in PMN-Gc population structures, and the evidence that transmigration influences PMN antimicrobial properties, prompted us to assess the bactericidal activity of PMNs against Gc in both models. To assess Gc viability with single-PMN and single-bacterium resolution we used a

live-dead fluorescence imaging technique coupled with extracellular versus intracellular Gc staining based on dye exclusion.[404] Extracellular bacteria were stained by fluorescently conjugated soybean lectin, whereas intracellular bacteria were not. Bacteria with intact envelopes (classified as live Gc) were stained by the membrane-permeable DNA binding dye Syto-9, whereas those with damaged envelopes (classified as dead Gc) were stained with the membrane-impermeant dye propidium iodide (Fig. 38A). In both infection models, bacteria associated with, but not internalized by, PMNs had greater population viability (Fig. 38B). However, regardless of phagocytic status, Gc interacting with transmigrated (TM) PMNs in the Transwell model had significantly greater viability numbers compared to those in the Adhered IL-8 primed infection model (Fig. 38B). These data were in opposition to our initial hypothesis based on the increased antimicrobial activity reported in the literature.

To further dissect PMN antimicrobial capacity with and without transmigration, we challenged Gc expressing (Opa+) or deleted for (Opa-) Opa proteins, gonococcal surface factors important for association with human epithelial cells and PMNs.[38,39] In the Adhered IL-8 primed model, Opa- Gc displayed greater viability compared to constitutively Opa+ Gc, recapitulating previously published results with this system (Fig. 38C).[38,39,49] However, this survival advantage was reversed in the Transwell model in which Opa+ Gc had significantly greater viability compared to the Opa- Gc (Fig. 38C). Moreover, Opa- Gc viability was not significantly different between the two models, but Opa+ Gc viability was significantly increased in Transwell system (Fig. 38C). A

colony forming unit-based (CFU) survival time course representative of the Adhered IL-8 primed model also demonstrated a survival advantage for Opa- Gc, but only in RPMI media and not in HHB+ media (Fig. 38D,E).[43]

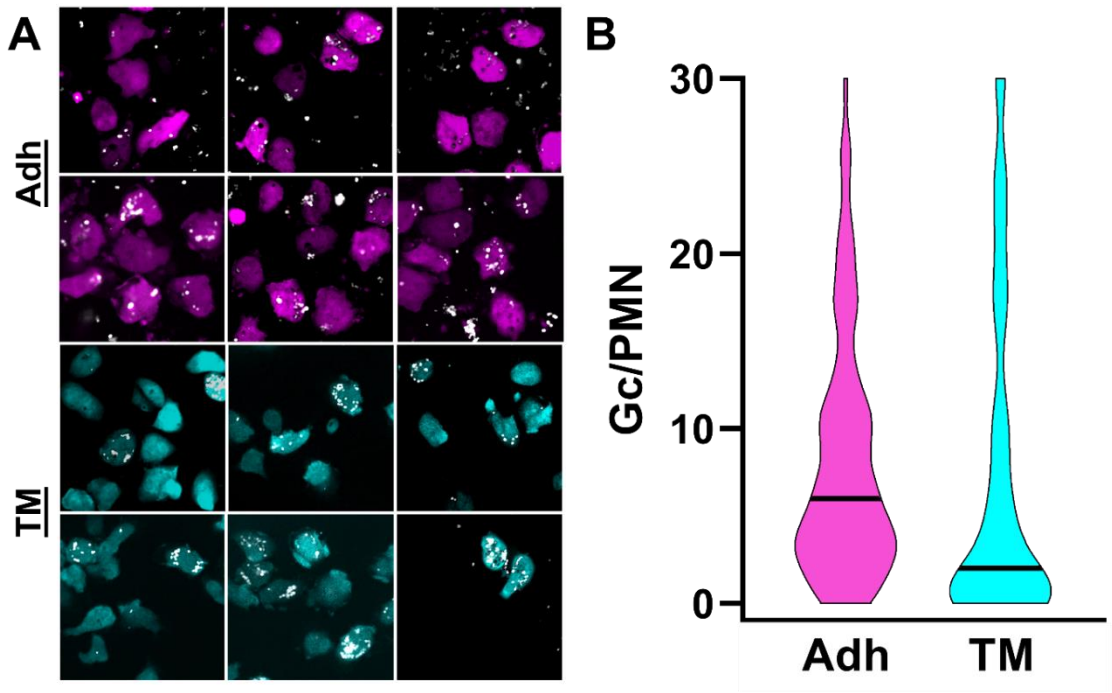

Figure 37. PMN-Gc association differences with and without transepithelial migration

PMNs were challenged in the Adhered IL-8 primed model (Adh) or tripartite Transwell transepithelial migration model (TM) with Gc at an MOI of 10 bacteria per PMN. Adh PMNs were challenged for 1 hour after Gc addition, TM PMNs were challenged for 2 hours after PMN addition to the basolateral chamber to account for the approximate 1 hour needed to observe transmigration. (A) Adh (top, magenta) and TM (bottom, cyan) CFSE-labeled PMNs were imaged and CellTrace Yellow-labeled Gc were enumerated on a per PMN basis. Representative micrographs. (B) Violin plots of Gc association per Adh and TM PMN. N = 84-143 PMNs. Dark bars in plots represent median number of Gc per PMN.

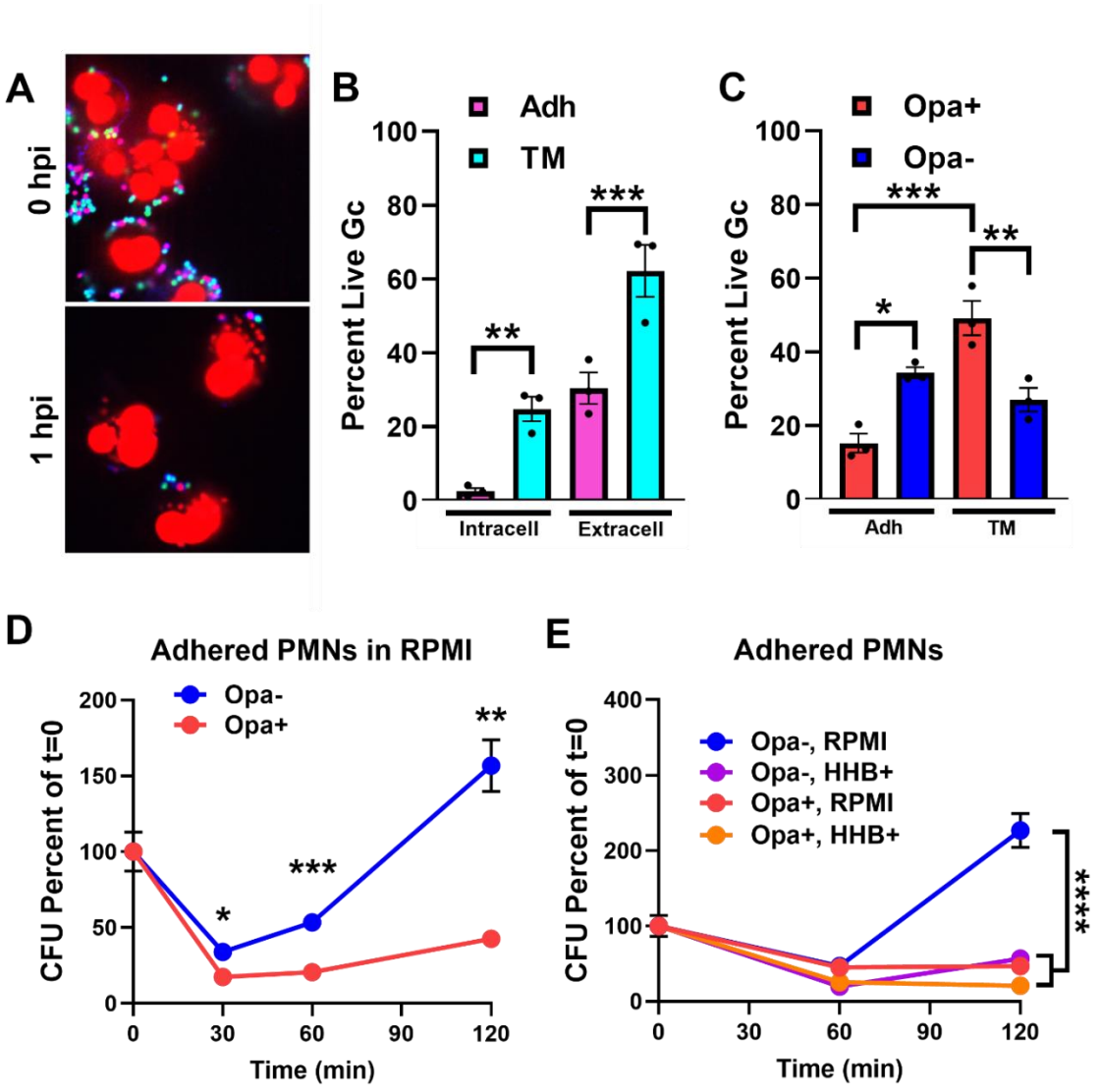
A
0 hpi
1 hpi
B
Adh
TM
Percent Live Gc
100
80
60
40
20
0
**
***
IntraeII
ExtraeII
C
Opa+
Opa-
Percent Live Gc
***
**
*
Adh
TM
D
Adhered PMNs in RPMI
Opa-
Opa+
CFU Percent of t=0
200
150
100
50
0
*
***
**
0
30
60
90
120
Time (min)
E
Adhered PMNs
Opa-, RPMI
Opa-, HHB+
Opa+, RPMI
Opa+, HHB+
CFU Percent of t=0
400
300
200
100
0
****
0
30
60
90
120
Time (min)

Figure 38. Gc viability with PMN challenge depends on infection model and Opa-expression

(A) PMNs with associated Gc on glass coverslips were analyzed via differential live-dead and extracellular versus intracellular staining on a single-PMN and single-bacterium basis. Representative images of PMNs and Gc in the Adhered IL-8 primed model at 0 (top) and 1 (bottom) hours post infection (hpi). Red = dead Gc labeled with propidium iodide. Green = live Gc labeled with Syto 9. Blue = extracellular Gc labeled with fluorescent soybean lectin. (B) Gc viability based on differential staining in the Adhered IL-8 primed (Adh) and Transwell transmigration (TM) models by percentage of live Gc out of all counted Gc. Viability delineated by intracellular, phagocytosed Gc and extracellular, PMN-associated Gc. (C) Gc viability based on differential staining in the Adh and TM infection model. Isogenic Gc constitutively expressing a single opacity-associated protein adhesin (Opa+) or deleted for all Opa proteins (Opa-). (D) Opa- and Opa+ Gc survival over 120 minutes against Adhered, IL-8 primed PMNs in RPMI media. (E) Opa- and Opa+ Gc survival over 120 minutes against Adhered, IL-8 primed PMNs in either RPMI or HHB+ Media. Survival presented as percent of viable Gc at the zero timepoint (t=0; D,E) Error bars are standard error of the mean. Statistical significance determined by 1-way ANOVA with Tukey's multiple comparisons (B,C), Student's *t*-test at each timepoint (D), or 1-way ANOVA with Tukey's multiple comparisons at each timepoint (E). *=$p<0.05$, **=$p<0.01$, ***=$p<0.001$, ****=$p<0.0001$.

4.2.4 Chapter Discussion

PMN recruitment to infected tissues is essential for combatting pathogens, yet the effect of recruitment and transepithelial migration is not well characterized. This is especially true for tissues of the female reproductive tract and against Gc. Here, we used a Transwell system to model PMN transepithelial migration across endocervical epithelial cells and subsequent interaction with apically adhered Gc. Previous work and preliminary data presented here show that PMN transmigration can be quantified in this model, PMN-Gc interactions can be observed via microscopy, and that Gc phagocytosis and killing can be quantified.[216]

The endocervical Transwell system presents a promising development in models of Gc infection in that it incorporates epithelial cells and the transmigratory process unlike other *in vitro* systems. It also incorporates leukocytes in contrast to *ex vivo* systems such as cervical explants.[272,273] With these advantages, this system demonstrated that PMN migration across the endocervical epithelium depends on the PKC-PLA_2-LOX axis to synthesize epithelium-derived HXA_3 with subsequent LTB_4 amplification. These findings may partially explain observations from murine infection models in which BALB/c mice, which synthesize PLA_2, elicit neutrophilic infiltration to Gc infection but C57BL/6 mice which lack PLA_2 synthesis do not.[260,263] The endocervical model also establishes a basis for future refinement or expansion such as incorporating other epithelial cell types (e.g. endometrial, fallopian, urethral, etc.).[273] Lessons learned from this model can also be applied to more expansive systems such as

biomimetic models of the female reproductive tract which can incorporate other components such as ECM, endothelium, microbiota, mucus, fluid flow, etc. Ultimately, no model will fully recapitulate all aspects of natural gonococcal infections in human, but interrogating components in different models can grant important insights.

One aim in this work was to identify the gonococcal factor(s) which induce epithelial cell activation and resultant PMN transepithelial migration. Results using trypsin shaving and PFA fixation suggested that a proteinaceous Gc factor was involved in transmigration elicitation. However, addition of exogenous components or Gc mutated for specific surface candidates did not point to any single factor.[216] Other candidates remain to be tested but it is conceivable that epithelial cell stimulation is multifactorial and will require more comprehensive analysis. Interestingly, Gc singly mutated for *rmp* or *ngo1985* trended toward increased PMN transmigration compared to wildtype parental strains (Fig. 36D). Although no immunosuppressive roles for these factors against epithelial cells have been described, such functions could explain these results with further investigation. Other candidates remain to be tested, including the major outer membrane protein Porin. Mutations in extracellular loops of Porin have been generated although full deletions are lethal.[347] Porin has been reported to translocate into host cell membranes resulting in ion flux which can be stimulatory or apoptosis-inducing.[30] In the case of epithelial cells, calcium ion influx due to porin could result in PKC activation with subsequent HXA_3 secretion. Gc adherence to epithelial cells can also induce calcium flux through

CD46 activation, a multifunctional receptor which has also been proposed to interact with PKC.[405-408] Gonococcal PilC, one of our identified candidates (Fig. 36C), has been proposed to bind CD46.[245] Therefore, efforts should be taken to test Gc mutants lacking both PilC-encoding genes (*pilC1*, *pilC2*).

Investigating Gc viability in the Transwell model, and juxtaposing this to the Adhered IL-8 primed model revealed surprising results with transmigrated PMNs less readily killing Gc than adhered-alone PMNs. However, important differences exist between these two models which make direct comparisons difficult in their current iterations. An advantage of the Adhered IL-8 primed system is that infection is synchronized upon Gc inoculation via centrifugation to force PMN-Gc association. This allows for more controlled uniform study of Gc killing by the PMNs. However, in a native infection, PMNs encounter Gc asynchronously as they are recruited from the vasculature and migrate toward infecting bacteria. In these preliminary studies, 1 hour of infection was used in the Adhered IL-8 primed model and a total of 2 hours in the Transwell transmigration model to account for the approximate 1 hour needed to initiate PMN transepithelial migration.[216] Additionally, media in the Adhered IL-8 primed model was RPMI (4.5g/L D-glucose) compared to HHB+ (1g/L D-glucose) in the Transwell model. PMNs are highly glycolytic and differences in nutrient abundance between these two systems may have significant consequences.[8] To better compare transmigrated and non-transmigrated PMNs, standardizing media between these two models would be required. Another approach would be to induce PMN transmigration in the Transwell model to a known chemoattractant

such as a formylated peptide (e.g. fMLP), collect an equivalent number of PMNs from the apical chamber (transmigrated) and basolateral chamber (not yet transmigrated) and challenge these with Gc.

An additional caveat to data interpretation identified during the course of these studies is that some actively growing gonococci, although still viable and culturable, appeared to allow propidium iodide flux across their envelope. This may be due to Gc's unique envelope structure compared to other Gram-negative bacteria for which the differential live-dead viability staining kit was developed. Therefore, data acquired with this differential live-dead technique ought to be validated through additional means such as CFU assays or methods such as transmission electron microscopy which can identify live and dead Gc at single-PMN and single-bacterium levels based on electron density.[396] However, prior findings were recapitulated such as the intracellular Gc population being less viable than the extracellular Gc population. Assuming the validity and reproducibility of results from Figure 38 with other techniques and more rigorous transmigration vs non-transmigrated models, non-mutually exclusive hypotheses are proposed in the following paragraphs.

The Adhered IL-8 primed and Transwell transmigration model both showed heterogenic PMN-Gc association with the Transwell model enriched for PMNs at the extremes (0 Gc, 20+ Gc) compared to the model without transepithelial migration. Clinical samples of urethral exudate reflect these extremes.[12] PMNs with greater numbers of Gc may be observed more readily in the endocervical Transwell model as Gc microcolonies on epithelial cells (Fig.

35D,F,G) can be targeted by a single approaching PMN. These clusters may be preferentially targeted by PMNs via steeper chemoattractant agents. Therefore, a first-mover PMN may be more likely to encounter greater numbers of Gc/microcolonies than those which transmigrate after. Asynchronous encountering of bacteria may also explain the prevalence of PMNs with no Gc. PMNs have been described to transmigrate at ‘hotspots’ in endothelia and epithelia where adhesins are more abundant and cell-cell junctions are disrupted.[218] PMNs recruited at the later timepoints in the Transwell model may then have fewer bacteria with which to contend than their trailblazing counterparts. Figure 35F depicts a possible instance of this with 1 PMN engaging 10+ visible gonococci with at least 5 PMNs following in close pursuit. PMNs with little to no Gc may also be a result of Gc adherence to epithelial cells making phagocytosis more challenging. Another intriguing possibility is that the transmigration process produces a PMN population heterogenous in activation state with varying levels of phagocytic capacity due to surface receptor expression, cytoskeletal mobilization, etc.[230] Use of protocols such as high-dimensional flow cytometric panels to assess pre- and post-migratory PMNs could shed light on this question.[380,409]

Multiple factors could contribute to decreased PMN lethality in the Transwell transmigration model. PMNs which internalize tens of bacteria may be less efficient killers as bactericidal granule contents would be delivered to multiple phagosomes thereby being less potent. The asynchronous nature of the model may also mean that detached PMNs were incubated with Gc for a shorter

functional time than the full 1-hour challenge in the Adhered IL-8 primed model. A system with standardized transmigration followed by Gc challenge as described above would work toward addressing this discrepancy – as would a system in which migrated PMNs were labeled as they migrate at timepoints throughout the infection. Compared to other systems, endocervical transmigration appears to dampen PMN killing capacity. This may be specific to this cell type or a result endocervical cell stratification which was observed in some Transwells (Fig. 35C). Exploring effects of transmigration through other epithelial types, including stratified squamous ectocervical cells, may be of interest. It is also worth noting that Gc adhered to epithelial cells are more resistant to nutrient-starving mechanisms of PMNs (e.g. zinc sequestration by calprotectin)[410] which may be playing a role in this system.

Experimental gonococcal infections of human volunteers are selective for Opa-expressing Gc.[54] This contrasts with data using the Adhered IL-8 primed model in which Opa+ Gc have a survival disadvantage against primary human PMNs (Fig. 38D).[38,49,52,261] It has been proposed that epithelial adherence via Opa surface adhesins explains this phenomenon. Our findings with the Transwell model reflect the Opa+ Gc selective advantage (Fig. 38C). It is interesting that the Transwell model more closely recapitulates findings from human infections compared to the Adhered IL-8 primed *in vitro* model. The underlying basis for this, whether it be due to Gc or PMN differences or their interaction with the epithelium remains to be explored.

4.3 Materials & Methods

4.3.1 *Neisseria gonorrhoeae* strains and culturing.

The following Gc strains were used in this study: a derivative strain of piliated FA1090 Gc with an antigenically locked major pilin subunit (PilE) in which all Opa genes had been deleted (Opa-) or which constitutively expresses only one Opa (OpaD, Opa+)[38]; an Opa- and pilus-variable FA1090 Gc and isogenic *ngo1985*::kanamycin resistance cassette insertional mutant; and an MS11 strain of Gc with an isogenic *ngo1981*::kanamycin resistance cassette insertional mutation. Data adapted from Stevens 2018 included isogenic Opa+ parent and *rmp*::erythromycin resistance cassette insertional mutant as well as an Opa- parent and *pilQ*-null mutant.

Gc was routinely cultured as described previously.[43] Briefly, Gc was streaked on gonococcal base medium (BD Difco) plus Kellogg's supplement I and 1.25μM $Fe(NO_3)_3$ (gonococcal base, GCB) agar plates for 14-16 hours at 37°C, 5% CO_2. Single colonies were lightly swabbed onto fresh, pre-warmed agar plates to grow bacterial lawns for approximately 8 hours, swabbed into GCB liquid media and grown overnight at 30°C with rotation. On the morning of each experiment, Gc were back-diluted twice in fresh GCB liquid media and grown at 37°C to reach the mid-exponential growth phase.

4.3.2 PMN isolation from human subjects.

Human subjects research was conducted in accordance with the University of Virginia Institutional Review Board for Health Sciences Research under protocol #13909. Informed written consent was obtained from each

subject. All subjects were 18-65 years of age, with no reported comorbidities, and healthy at the time of blood collection. Primary human PMNs were collected via venipuncture as previously described.[43] Briefly, venous blood was collected into heparin-coated Vacutainer® tubes (BD) and fractionated by dextran sedimentation to enrich for leukocytes. Granulocytes were purified by Ficoll-Paque™ (Ficoll) density centrifugation with DPBS (Gibco) + 0.1% glucose (DPBSG; Ricca Chemical). The granulocyte-enriched pellet was then resuspended, lysed with endotoxin-free water to remove remaining erythrocytes, and resuspended in DPBSG on ice and enumerated using a hemacytometer.

4.3.3 Adherent, IL-8 primed model.

Purified PMNs were pre-treated with IL-8 and adhered then infected with Gc as previously described with slight alterations.[43] Briefly, $1x10^6$ Ficoll-purified PMNs were added onto 13mm plastic (Sarstedt) or glass (Fisher) coverslips in a 24-well plate in 400µL of Roswell Park Memorial Institute medium (RPMI) supplemented with 10% fetal bovine serum (FBS) and 80ng/mL recombinant human IL-8 (R&D Systems). Figure 38E used HHB+ media (Hank's balanced salt solution with 1.2mM calcium and 1mM magnesium [Gibco] with 10mM HEPES [Sigma-Aldrich] and 5mM sodium bicarbonate at pH 7.4) in place of RPMI. Triplicate wells were used in all experiments. PMNs were allowed to settle and adhere for 30-60 minutes at 37°C with 5% CO_2. PMNs were then challenged with indicated strain of mid-exponential phase Gc at an MOI of 10 ($1x10^7$ Gc per well) by centrifugation at 600 x g for 4 minutes at 12°C. Gc inoculum was serially diluted and plated for CFU enumeration each day to verify MOI. PMNs were then

either prepared for imaging at 1 hour post-infection. Alternatively, Gc CFU were enumerated at 0, 30, 60, and 120 minutes post-infection by aspirating off media with unassociated bacteria, specifically lysing PMNs with 1% saponin (Fluka Analytical), and serial dilution and plating of bacteria

4.3.4 Transwell endocervical transmigration model.

Mycoplasma-free human End1/E6E7 (End1)[411] endocervical epithelial cells (ATCC, CRL-2615TM) were maintained at 37°C and 5% CO_2 in keratinocyte serum-free medium (KSFM, Life Technologies) with 0.4mM $CaCl_2$ supplemented with 50µg/mL bovine pituitary extract and 0.1ng/mL recombinant human epidermal growth factor. End1 cultures in flasks and on Transwell inserts were cultured with 1X Antibiotic-Antimycotic (Gibco; penicillin, streptomycin, amphotericin) and washed into antimicrobial-free media 24 hours before infection. End1 cells were seeded on inverted 6.5mm Transwell filter inserts with 3µm pores (Corning) coated with 5µg/cm^2 human type IV collagen (Sigma). End1 cells ($7x10^4$ per Transwell) were allowed to adhere for 4-5 hours then reverted into a 24-well tissue culture plate with KSFM in both chambers and incubated at 37°C and 5% CO_2 for 7-10 days. End1 layer barrier function was previously verified by transepithelial electrical resistance measurement and 10kDa FITC-conjugated dextran flux assay.[216]

On the day of infection, established End1 Transwell systems were washed with 37°C HHB+ media, inverted, and infected with $1x10^7$ Gc in 30µL HHB+ for 2 hours at 37°C and 5% CO_2. Infected inserts were then gently dunked into fresh HHB+ media to remove non-adhered gonococci and reverted into a fresh 24-well

plate with 1mL HHB+ in the lower/apical chamber. Ficoll-purified PMNs ($1x10^6$) were then added to the upper/basolateral chamber in 200µL HHB+ and incubated for 2 hours or indicated duration at 37°C and 5% CO_2. Previous studies showed that transmigration begins around 1-hour post-infection.

4.3.5 Fluorescent microscopy.

Epithelial cells, PMNs, and Gc were pre-labeled with CFSE or CellTrace series amine-reactive dyes according to manufacturer's protocols prior to addition of other components into infection models as indicated in HHB+ media (protein free). Epithelial cell actin was labeled with 66nM AlexFluor Plus 555-conjugated phalloidin (Invitrogen) following 4% paraformaldehyde fixation and 0.1% Triton X-100 permeabilization.

Live-cell, Gc-PMN association (Fig. 37A), and differential live-dead (Fig. 38A) imaging were performed on a Nikon Eclipse TE2000-E spinning disk confocal microscope with an EXFO X-Cite 120Q Lamp, and Nikon T-PFC Perfect Focus System. Confocal microscopy (Fig. 35C,D) and live-cell imaging (Fig. 35G) were performed using a Nikon C1 confocal microscope at 0.5µm intervals.

4.3.6 Scanning electron microscopy (SEM).

Transwell systems were infected and loaded with PMNs as described above. At 2 hours after PMN addition, media in both chambers was replaced with fixative (4% PFA/2%glutaraldehyde in 0.1M sodium cacodylate buffer at pH 7.4) overnight at 4°C. Samples were secondarily fixed with 1% osmium tetroxide and serially dehydrated with 100% ethanol. Samples were then gold-platinum sputter coated and imaged on a Zeiss SIGMA VP-FESEM in the Advanced Microscopy

Facility at the University of Virginia. Images were false colored in Adobe Photoshop.

4.3.7 Membrane-YFP End1 cell generation.

A yellow fluorescent protein (YFP) construct with palmitoylation signal was previously generated to target YFP to cell membranes (m-YFP).[412] HEK-293T cells in DMEM with 10% FBS in 24-well plates were transfected at approximately 20% confluence with 500ng m-YFP plasmid, 400ng packaging plasmid (Moloney murine leukemia virus, MMLV), and 100ng envelope plasmid (vesicular stomatitis virus envelope glycoprotein, VSV-G) in serum-free DMEM media for 48 hours. Transfection supernatant was collected, buffered with 10mM HEPES, filtered through 0.45µm mixed cellulose ester filters (MilliporeSigma), and stored at -80°C as 500µL aliquots until use.

Low-passage End1 endocervical epithelial cells were seeded into a 24-well plate ($1x10^5$ per well) with KSFM media. At 16 hours, adhered and proliferating End1 cells were infected with 500µL m-YFP lentivirus at 37°C and 5% CO_2 for 12 hours at which point media was replace with virus-free KSFM for 24 hours. Lentivirus-infected cells were then selected for with 5µg/mL puromycin for 3 days, verified for m-YFP expression, and moved to 6-well plates for culturing and long-term liquid nitrogen storage.

4.3.8 Myeloperoxidase (MPO) transmigration assays.

Endocervical Transwell systems were infected as above. At 2 hours post-infection, PMN transmigration was quantified using colorimetric myeloperoxidase assays as previously described. Briefly, Transwells were removed from their

wells with gentle agitation to release loosely adhered PMNs. PMNs were lysed with 0.5% Triton X-100 for 20 minutes at 4°C with rocking. A fresh H_2O_2-ABTS chromophore diammonium salt (EMD Millipore) with was prepared as previously described to detect MPO activity. To a transparent, flat-bottom 96-well plate, 100µL sample, 50µL 1M citrate-citric acid buffer (pH 4.2), and 50µL H_2O_2-ABTS Solution were added. The plate was developed in the dark at 37°C for 10-20 minutes then read on a Wallac Victor-2 1420 plate reader (Perkin-Elmer) at 405nm with 1 second integration. The 96 well plate also included a standard curve of 2-fold PMN dilutions treated as described above ranging from $1x10^6$ to ~$2x10^3$ PMNs. All standards and samples were run in duplicate. Negative controls were of Transwells in HHB+ media alone without Gc infection; positive controls included 1µM fMLP (formylated tripeptide Met-Leu-Phe), a potent chemotactic agent.

4.3.9 Bacterial trypsin shaving and mass spectrometry.

Piliated Opa+ Gc were swabbed into GCB liquid media after 18 hours lawn growth on GCB agar plates and $5x10^8$ Gc were treated with 40µg/mL sequencing-grade trypsin (Promega) or vehicle (trypsin resuspension buffer, Promega) for 1 hour at 37°C on a rotating drum. Supernatants were collected and prepared for analysis by passing over a Sulpeco Discovery DSC-18 SPE column (Sigma). The column was sequentially flushed with 50% acetonitrile and 1% acetic acid, flushed with 1% acetic acid, loaded with sample, washed with 1% acetic acid, and eluted with 80% acetonitrile, 1% acetic acid. Samples were analyzed via mass spectrometry at the W.M. Keck Biomedical Mass

Spectrometry Laboratory at the University of Virginia. The following is adapted from the report number 2135 from the W.M. Keck Biomedical Mass Spectrometry Laboratory: Samples were reduced with 10mM DTT in 0.1M ammonium bicarbonate at room temperature for 30 minutes then alkylated with 50mM iodoacetamide in 0.1M ammonium bicarbonate at room temperature for 30 minutes. Samples were digested overnight at 37°C with 1µg trypsin in 50mM ammonium bicarbonate. Samples were then acidified with acetic acid and dried to 15µL for analysis. The LC-MS system consisted of a Thermo Electron Velos Orbitrap ETD mass spectrometer system with an Easy Spray ion source connected to a Thermo 3µm C18 137 Easy Spray column. 7µL extract was injected and peptides eluted by an acetonitrile/0.1M acetic acid gradient at a flow rate of 0.25µL/minute. The nanospray ion source was operated at 2.3kV. The digest was analyzed using the rapid switching capability of the instrument acquiring a full scan mass spectrum to determine peptide molecular weights followed by product ion spectra to determine amino acid sequence in sequential scans. This mode of analysis produces approximately 50,000 MS/MS spectra of ions ranging in abundance over several orders of magnitude. Not all MS/MS spectra are derived from peptides. The data were analyzed by database searching using the Sequest search algorithm against Uniprot *N. gonorrhoeae* and Uniprot SwissProt

4.3.10 Differential Live-Dead and extracellular versus intracellular staining.

Gc were inoculated into the Adhered, IL-8 primed or Transwell transmigration as described. PMNs settled onto acid-washed glass coverslips. At

the indicated timepoints, media was removed. Coverslips with PMNs and Gc were gently rinsed in the well-plate with fresh 0.1M 3-(N-morpholino)propanesulfonic acid (MOPS) media at pH 7.2 with 1mM $MgCl_2$ (MOPS buffer) and stained with AlexaFluor 647-conjugated soybean lectin (5µg/mL) for 10 minutes at room temperature in the dark. Coverslips were rinsed with MOPS buffer and incubated for 15 minutes at room temperature in the dark with the LIVE/DEAD® BacLight bacterial viability kit (Life Technologies) containing 5µM Syto 9, 30µM propidium iodide, and 0.1% saponin. Coverslips were then rinsed into PBS and immediately imaged via spinning disk fluorescent microscopy.[404]

4.3.11 Statistics, analyses, and data availability.

Statistical analyses were performed as indicated in figure legends. Data were assumed to be parametric, and statistical tests were 2-sided where applicable. Data were analyzed using GraphPad Prism, Adobe Photoshop for false coloring SEM, Fiji, and Nikon Elements software. Schematics were generated with BioRender.

5 CONCLUDING REMARKS AND FUTURE DIRECTIONS

This chapter includes unpublished data collected between January 2022 and September 2023. Data that formed a significant basis for work present in Figure 41 was published in: Gray MC* and Thomas KS*, Lamb ER, Werner LM, Connolly KL, Jerse AE, Criss AK. Evaluating vaccine-elicited antibody activities against *Neisseria gonorrhoeae*: cross-protective responses elicited by the 4CMen-B meningococcal vaccine. (2023). Infection and Immunity. 91(12):e0030923.

* indicates co-first authorship

Contributors:

Evan Lamb – Conceptualization, Methodology, Analysis, Investigation, Authorship, Validation, Visualization, Funding Acquisition.

Mary Wakim Broden – Conceptualization, Methodology, Analysis, Investigation, Validation. (Fig. 39,40).

Tinaya Eason – Investigation. (Fig. 39,40).

Lacie Werner – Methodology, Analysis, Investigation. (Fig. 40A).

Alison Criss – Conceptualization, Methodology, Analysis, Authorship, Funding Acquisition, Project Administration.

5.1 Summary

In this work I investigated principal innate immune responses to Gc. In Chapter 2, terminal complement complexes of C5b-C9 MACs and C5b-C8 were investigated for their capacity to directly kill Gc and potentiate activities of a broad panel of antimicrobials. The MAC was found to kill gonococci and disrupt both the outer and inner membranes. These 10-11nm pores enhanced anti-gonococcal activity of antimicrobials that acted at all layers of the Gram-negative cell, allowed otherwise impermeant antimicrobials to access their targets, and re-sensitized multidrug-resistant Gc to clinically relevant antibiotics. 2-4nm C5b-C8 complexes lacking polymerized C9 also killed gonococci, albeit less effectively, and also disrupted both bacterial membranes. These complexes were restricted in the antimicrobials they could accommodate based on size. In Chapter 3, a multi-parametric spectral flow cytometry panel was developed to interrogate primary human neutrophil activation in response to soluble stimulatory agents and Gc infection. Conserved responses were found among surface markers for phagocytosis, degranulation, migration, and chemotaxis. Variability was also appreciated among neutrophils from the same and different donors. Neutrophil populations were heterogenic regarding the numbers of associated Gc and in their activation states. Heterogenic neutrophil interactions with gonococci were also observed in Chapter 3 in which neutrophil-Gc interaction models were compared with and without neutrophil transmigration across and endocervical cell layer. Apical infection of the epithelia induces neutrophil transmigration (through a still unclear mechanism) with subsequent neutrophil phagocytosis of

the gonococci. Transmigrated neutrophils were more likely to have no bacteria or tens of bacteria than their non-transmigrated counterparts. They also appeared less effective at killing the gonococci than the non-transmigrated PMNs.

Together, these findings expand our understanding of how these innate immune effectors complement one another to combat Gc and shed light on how they accomplish this mission. This work serves as a basis for future research to answer lingering questions. For example, does MAC-mediated potentiation of antimicrobials occur *in vivo* in which complement, complement inhibitors, phagocytes, secreted antimicrobials, and antibiotics co-occur? Do novel complement-fixing therapeutics or vaccine-elicited antibodies also promote MAC-mediated antimicrobial potentiation? What is the nature (structure, localization, abundance, etc.) of C5b-C8 complexes within a Gram-negative outer membrane? What is the functional importance of neutrophil heterogeneity and different subpopulations on anti-gonococcal capacity?

5.2 Future Directions

5.2.1 MAC-mediated antimicrobial potentiation in broader contexts.

Studies presented here demonstrating antimicrobial potentiation by the MAC were conducted *in vitro* using tailored serum bactericidal assays. These were optimized to show antimicrobial potentiation using sublethal serum concentrations reflective of what may occur *in vivo* regarding infection by complement-resistant Gc isolates. Likewise, antimicrobial concentrations were selected both experimentally and based upon physiologic concentrations (e.g.

1,000µg/mL lysozyme at mucosal secretions)[413] or on concentrations representative of resistance values (e.g. 4µg/mL MIC of H041 Gc to ceftriaxone).[110,111] However, *in vivo* concentrations of antimicrobials and complement components vary widely depending on the site that Gc may occupy.

One such circumstance is within the neutrophil phagosome in which antimicrobials can reach high concentrations.[226] Here, I tested the neutrophil- and serum-derived antimicrobial lysozyme and found that C5b-C9 MAC pores potentiated its activity. Additional neutrophil-derived compounds such as secretory phospholipase-A2 also show enhanced activity against Gram-negative bacteria treated with terminal complement.[196] Neutrophils express a broad repertoire of antibacterial compounds (see section 1.3.2.2) and it will be interesting to identify if MAC can synergize with neutrophilic antibacterial functions either with neutrophils themselves or degranulated components. In a whole cell context, complement could support phagocytic uptake through opsonization and leukocyte stimulation through anaphylatoxin production. Interestingly, neutrophils can also accumulate antibiotics such as azithromycin which can enhance their bactericidal capacity against other bacteria.[414]

Terminal complement has been shown to contribute to Gc control in experimental murine infection models[156] and data from human subjects with complement deficiencies suggest this is also true in human patients (see section 1.3.1.9). Complement deposition on Gc could be induced with pre-clinical therapeutic candidates or monoclonal antibodies in murine genital tract infections alongside antibiotic therapy to identify is potentiation occurs *in vivo*.

The serum environment provides not only complement components but also many complement inhibitors which protect host cells and are exploited by Gc (Fig. 5,8). In these studies, Gc strains with a range of serum sensitivities were used. C4BP binding by otherwise serum-resistant strains was able to be overcome by addition of anti-LOS IgM, demonstrating the importance of complement-activating initiators in killing Gc via serum bactericidal activity. Gc can also bind the complement inhibitor vitronectin (Vn) from human serum.[21,52] Vn exerts its activity by blocking C5b-C7 formation and by blocking C9 incorporation into the nascent MAC.[21,191] I hypothesize that the C5b-C8 complexes discussed in Chapter 2 may therefore result *in vivo* as a result of Vn exploitation by Gc. However, efforts to directly image these complexes (e.g. atomic force microscopy, scanning electron microscopy, cryo-electron tomography) have yet to be conducted in Gc or other bacteria.

During experiments with Gc strain MS11 with phase-variable Opa proteins, I noticed a striking selection for Opa+ bacterial colonies after treatment with active serum but not with buffer or HI serum (Fig. 39A,B). A similar observation was made for an Opa-variable FA1090 Gc strain (Fig. 39C). The Opa homologue in *N. meningitidis*, Opc, was shown to bind vitronectin from human serum suggesting Opa proteins from Gc may also display this capacity, although the exact mechanism was undefined.[21,52,53]

We therefore followed up on these observations and found that Opa+ MS11 Gc survived in serum bactericidal assays (see Chapter 2) compared to their Opa- counterparts (Fig. 39D). Using our FA1090 strain Gc constitutively

expressing only one of the many Opa proteins, we found that Opa expression trended toward a survival advantage in active serum with OpaI-expressing bacteria surviving significantly more than Opa- (Fig. 39E). We hypothesized the serum survival with Opa expression was linked to vitronectin and found that Opa+ but not Opa- Gc bound recombinant and serum Vn via Western blot (Fig. 40A). Vn binding by Opa+ bacteria was confirmed via imaging flow cytometry in which OpaD-, OpaA-, OpaI-, and Opa50-expressing strains had significantly greater Vn signals than Opa- Gc. An Opa-variable wild-type FA1090 strain which was predominantly Opa+ via stereomicroscope showed a near-significant increase in Vn signal as did predominantly Opa+ multidrug-resistant H041 (Fig. 40B,C). However, Vn-binding by Gc strains expressing different Opa is not synonymous with increased survival (e.g. Opa50; Fig. 39E,40B) which suggests Opa-specific interactions with Vn influence serum resistance.

Vitronectin's major role is in blocking C9 incorporation into nascent MAC.[191] We therefore tested the necessity of C9 in the observed Opa-selection phenotype and found that C9-reconstituted sera selected for Opa-expressing colonies whereas C9-depleted or HI sera did not (Fig. 40D). Further studies on additional Opa-expressing strains and with vitronectin depleted sera are underway.

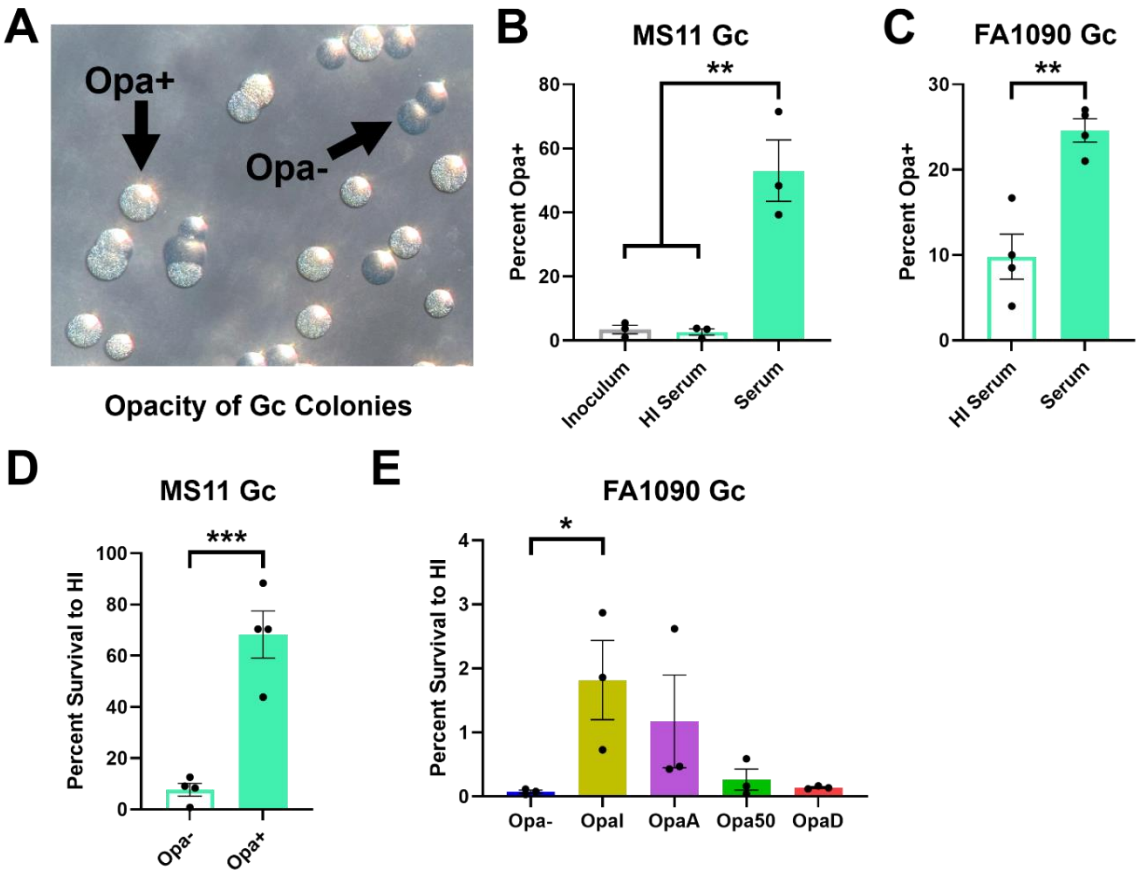

Figure 39. Complement-active serum selects for Opa-expressing Gc

(A) Micrograph on stereomicroscope demonstrating visual differences in Opa-expressing (Opa+) and Opaless (Opa-) Gc colonies. MS11 and FA1090 Gc were challenged via serum bactericidal assay with 1-hour 2% serum exposure and assessed for percent Opa+ colonies (B,C) and percent survival to heat-inactivated (HI) serum (D). (E) FA1090 Gc with all *opa* genes deleted (Opa-) or constitutively expressing a single Opa protein were assessed as above for survival compared to HI serum. Error bars = SEM. 1-way ANOVA with Tukey's multiple comparisons (A), or Student's *t*-test between groups (C,D) or compared to Opa- control (E).

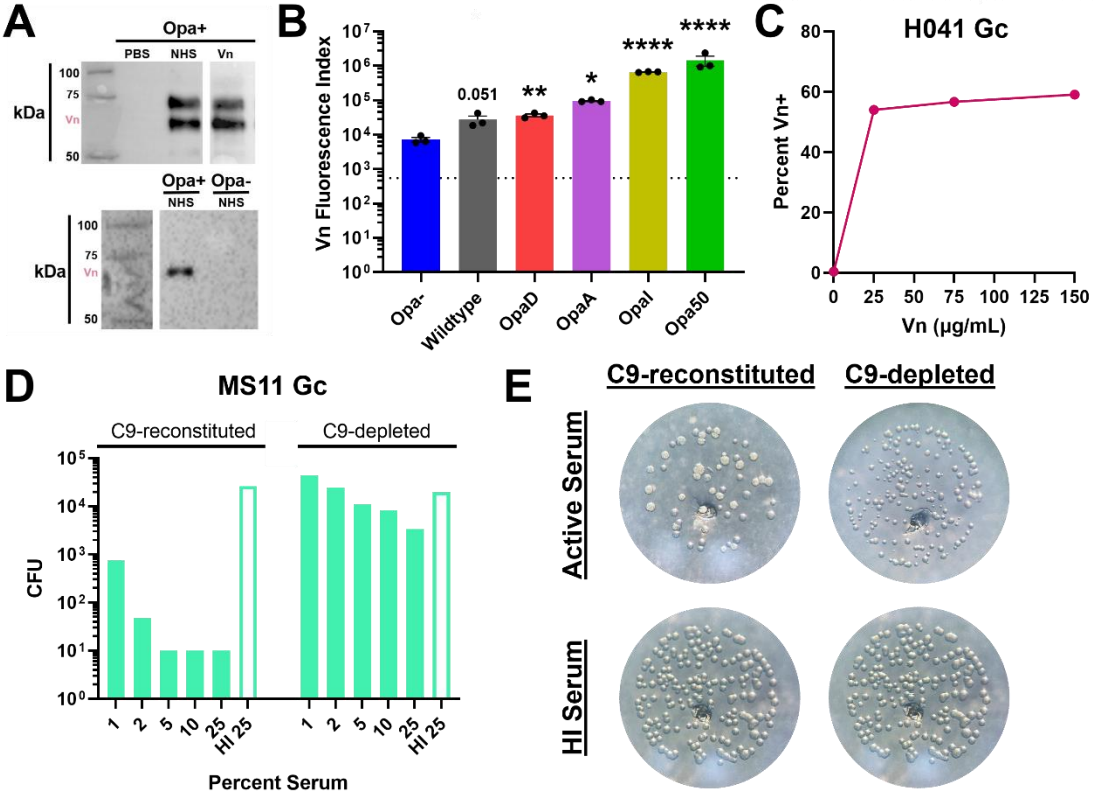
A
Opa+
PBS
NHS
Vn
kDa
100
75
Vn
50
Opa+ Opa-
NHS NHS
kDa
100
75
Vn
50
B
Vn Fluorescence Index
0.051
**
*
****
****
Opa-
Wildtype
OpaD
OpaA
OpaI
Opa50
C
H041 Gc
Percent Vn+
Vn (µg/mL)
D
MS11 Gc
C9-reconstituted
C9-depleted
CFU
1 2 5 10 25 HI 25
Percent Serum
E
C9-reconstituted
C9-depleted
Active Serum
HI Serum

Figure 40. Opa expression increases Vn binding and is selected for in a C9-dependent manner

(A) Western blots (performed by Lacie Werner PhD) with Gc deleted for all *opa* genes (Opa-) or constitutively expressing a single Opa (Opa+, OpaD) incubated in PBS, 50% normal human serum (NHS) or with 50µg/mL recombinant human vitronectin (Vn).Standard kDa ladders at left. (B,C) Single focused Gc were analyzed for Vn binding via imaging flow cytometry in an adapted protocol from Figure 11. Wildtype FA1090 Gc was phase-variable for Opa. Data expressed as Fluorescence Index (median fluorescence intensity * percent positive; B) or as percent of Gc positive for Vn staining (C). (D) MS11 Gc were challenged against increasing concentrations of C9-reconstituted or C9-depleted human serum with or without heat-inactivation (HI) in a serum bactericidal assay (SBA) and enumerated for CFU. N=1. (E) Micrographs from the SBA CFU enumerations showing colony opacity. Active serum: C9-reconstitued at 2%, C9-depleted at 25%. HI Serum: Both sera at 25%.

5.2.2 Implications for therapeutic development.

Chapter 2 demonstrates that outer membrane-embedded MAC can enhance activities of diverse antimicrobials demonstrating the potential for synergistic complement and antibiotic therapies. Therapies that enhance complement fixation specifically on the Gc surface are currently in pre-clinical development. Among these are monoclonal antibodies to be used as therapeutic passive immunization. Effective complement-mediated Gc clearance from murine genital infections was observed with administration of a murine anti-LOS monoclonal and an engineered humanized version with Fc region mutations to enhance IgG1 hexamerization and complement deposition.[156] A C4BP-IgM fusion construct also showed efficacy in Gc clearance from murine infection as well as *in vitro* potentiation of select antibiotics in a terminal complement-dependent manner.[155,310]

Specific complement activation on the Gc surface can also be achieved by vaccine-elicited antibodies.[177,180] Evidence that the 4CMenB meningococcal vaccination in mice and humans induces antibodies that cross react with Gc which exert *in vitro* serum bactericidal activity is promising in efforts to develop preventative measures.[292-294] However, whether 4CMenB elicited antibodies contribute to the reduction in Gc infections is as of yet unknown.[177] Although complement activation occurs in response to these antibodies, their necessity in conferring immunity is unclear.

To this end, I began interrogating antibody-elicited bactericidal capacity using a whole blood infection model which incorporates cellular and soluble

immune factors and is representative of gonococcal bloodstream dissemination.[415,416] This model demonstrated that complement-resistant Gc (FA1090 strain which binds human C4BP) survived in human whole blood but that a complement-sensitive derivative deficient in C4BP binding was readily killed. Addition of the C5 inhibitor OMCI rescued Gc survival indicating a complement-mediated effect (Fig. 41A). Addition of polyclonal anti-Gc antibodies from rabbit immunization produced a 173-fold decrease in complement-resistant Gc viability which was in a complement-dependent manner (Fig. 41B,C). This shows that antibody-induced complement activation is capable of killing Gc in whole blood. However, in this model, C5 inhibition blocks both downstream MAC formation (C5b-C9) as well as leukocyte activation by reduced C5a anaphylatoxin release. Therefore, identifying if vaccine-elicited complement killing is due to serum bactericidal activity, enhanced opsonophagocytic uptake, or both remains to be confirmed. Efforts between our group and those in Anne Jerse's Lab at the Uniformed Services University have shown that 4CMenB-immunized mice elicit antibodies which exert both serum bactericidal activity in human serum and opsonophagocytic uptake by human neutrophils.[177] Antibodies against human terminal complement components (e.g. C7) or opsonophagocytic receptors (e.g. CR3) have shown block terminal complement deposition and complement receptor binding, respectively, in *ex vivo*/*in vitro* systems.[171,417] A C5aR blockade with the inhibitor Avacopan would also be useful in dissecting the role of different complement effector functions in models which integrate complement and cellular effectors.[416]

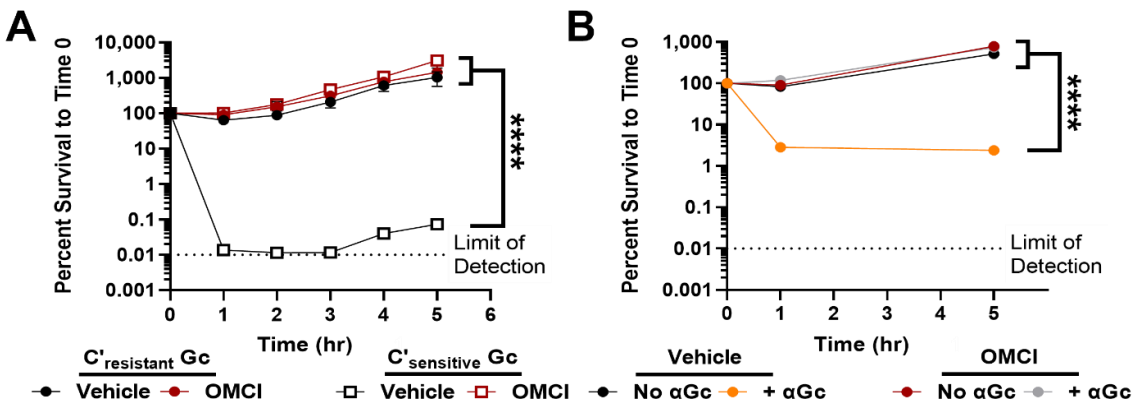

Figure 41. Complement, antibody, and cellular anti-gonococcal effectors in whole blood

Gc were inoculated into freshly collected hirudin-anticoagulated whole blood at 3e6 bacteria per mL. (A) Opa- FA1090 Gc ($C'_{resistant}$) and FA1090 Gc with a loop 6 porin mutation lacking C4BP binding potential ($C'_{sensitive}$) were inoculated into whole blood for hourly CFU enumeration with vehicle or addition of the C5 inhibitor OMCI (20μg/mL). (B) $C'_{resistant}$ Gc were inoculated into whole blood with addition of 45μg/mL polyclonal anti-Gc antibody (αGc) from rabbits immunized with heat-killed bacteria ± OMCI.

5.2.3 Neutrophil heterogeneity in response to diverse stimuli.

As principal responders of the innate immune system, neutrophils are equipped with receptors to sense signals from a broad repertoire of host- and pathogen-derived sources. These signals are integrated to control neutrophil activation state and effector functions.[214] The spectral flow cytometry panel presented in Chapter 3 will enable our lab and other research groups to dissect the neutrophil response to these stimuli by assessing surface markers that both sense pathogens and seek to combat the threat. It will also allow investigation into the recently appreciated diversity of neutrophil populations in their activation states and ability to contend with pathogens.[229,230]

Challenging primary human neutrophils with Opa-expressing Gc yielded distinguishable subpopulations via dimensional reduction and clustering analyses (Fig. 32). The clusters with the greatest bacterial burden (clusters 1 & 2) were comprised predominantly of neutrophils infected at an MOI of 10 and represented a more canonical profile of highly activated neutrophils. However, highly activated neutrophils could also be found with low Gc burden (cluster 3). Some neutrophils had moderate Gc burden but unlike others had negligible markers of strong activation (e.g. cluster 5). Further efforts to identify what these different neutrophil subpopulations are should be conducted, as well as assessing the functional implications of this diversity. To this end, inclusion of other markers such as those of neutrophil senescence may be useful.

Diversity within the pathogen population may also influence neutrophil responses. Gc possesses many phase and antigenically variable surface

proteins, such as opacity-associated proteins, which influence their interactions with host cells including neutrophils.[35,39] Using CellTrace Blue-labeled Gc, we verified that OpaD expression enhanced Gc association with neutrophils (Fig. 33A). However, after accounting for overall bacterial burden, both Opa-expressing and Opa-deleted Gc strains induced similar responses in adherent, IL-8 primed neutrophils (Fig. 33D). Diverse opacity-associated proteins differentially bind neutrophil CCM-1 and CCM-3 receptors with inhibitory and activating motifs, respectively, with OpaD binding both CCM-1 and CCM-3.[39,48,305] Gc which constitutively express only CCM-1 binding opacity-associated proteins (e.g. Opa50, OpaF) may not induce as strong a neutrophil response or possibly suppress stimulation through CCM-1 ITIM signaling.[39,305]

Applying and adapting this panel to other contexts may also yield information on how neutrophils respond to the different stimuli they encounter. In Chapter 3 neutrophils were stimulated with the potent activator PMA. Neutrophils stimulated with other agents found in the infectious milieu from the host (e.g. anaphylatoxins, eicosanoids) or pathogens (formylated peptides, peptidoglycan fragments, LOS, or Gc-conditioned media) could be analyzed using the flow cytometry panel to further dissect neutrophil biology as well as to compare and contrast responses to relevant stimuli in the infectious milieu. The panel can also be applied to neutrophils in different infection models such as the Transwell transmigration model presented in Chapter 4. Many of the markers selected for this panel pertain to migration and chemotaxis, as well as receptors for the many stimuli encountered en route to pathogens. Analyzing pre- and post-

transmigration PMNs from the Transwell model could shed light on the neutrophil heterogeneity and decreased bactericidal capacity found in this system (Fig. 38).

5.3 Overall Conclusions

This dissertation describes interactions between soluble and cellular innate immune effectors and Gc. This work expands upon MAC biology and bactericidal activity and its potential to enhance other arms of the immune system and antibiotic regimens. The development of a new spectral flow cytometry panel to interrogate leukocyte surface markers with an eye toward neutrophil-pathogen interactions is reported. Additional data presented herein describe effects of transepithelial migration on neutrophil anti-gonococcal capacity, Gc recruitment of Vn in a possible Opa-dependent manner, and complement-dependent killing in an integrated whole blood model with enhancement by anti-gonococcal antibodies. Together, these data contribute to foundational biology with possible therapeutic and vaccine implications against a pathogen of pressing public health concern.

REFERENCES

1. Stevens, J. S. and Criss, A. K. Pathogenesis of *Neisseria gonorrhoeae* in the female reproductive tract: neutrophilic host response, sustained infection, and clinical sequelae. *Current Opinion in Hematology* (2018) 25, 13-21.
2. Edwards, J. L. and Butler, E. K. The Pathobiology of *Neisseria gonorrhoeae* Lower Female Genital Tract Infection. *Frontiers in Microbiology* (2011) 2, 102.
3. Rowley, J., van der Hoorn, S., Korenromp, E., Low, N., Unemo, M., Abu-Raddad, L. J., Chico, R. M., Smolak, A., Newman, L., Gottlieb, S., Thwin, S. S., Broutet, N., Taylor, M. M. Chlamydia, gonorrhea, trichomoniasis and syphilis: global prevalence and incidence estimates, 2016. *Bulletin of the World Health Organization* (2019) 1, 548-562.
4. Quillin, S. J. and Seifert, H. S. *Neisseria gonorrhoeae* host adaptation and pathogenesis. *Nature Reviews Microbiology* (2018) 16, 226-240.
5. Lovett, A. and Duncan, J. A. Human Immune Responses and the Natural History of *Neisseria gonorrhoeae* Infection. *Frontiers in Immunology* (2019) 19:9, 3187.
6. Centers for Disease Control and Prevention (2024) Sexually Transmitted Infections Surveillance, 2023.
7. Unemo, M., Bradshaw, C. S., Hocking, J. S., De Vries, H. J. C., Francis, S. C., Mabey, D., Marrazzo, J. M., Sonder, G. J. B., Schwebke, J. R., Hoornenborg, E., Peeling, R. W., Philip, S. S., Low, N., Fairley, C. K. Sexually transmitted infections: challenges ahead. *The Lancet Infectious Diseases* (2017) 17, e235-e279.
8. Potter, A. D. and Criss, A. K. Dinner date: *Neisseria gonorrhoeae* central carbon metabolism and pathogenesis. *Emerg Top Life Sci* (2024) 8, 15-28.
9. Wind, C. M., De Vries, H. J. C., Schim Van Der Loeff, M. F., Unemo, M., Van Dam, A. P. Successful Combination of Nucleic Acid Amplification Test Diagnostics and Targeted Deferred *Neisseria gonorrhoeae* Culture. *Journal of Clinical Microbiology* (2015) 53, 1884-1890.
10. Evans, G. L., Kopyta, D. L., Crouse, K. New selective medium for the isolation of *Neisseria gonorrhoeae*. *Journal of Clinical Microbiology* (1989) 27, 2471-2474.
11. Granato, P. A., Paepke, J. L., Weiner, L. B. Comparison of modified New York City medium with Martin-Lewis Medium for recovery of *Neisseria gonorrhoeae* from clinical specimens. *Journal of Clinical Microbiology* (1980) 12, 748-752.
12. Johnson, M. B. and Criss, A. K. Resistance of *Neisseria Gonorrhoeae* to Neutrophils. *Frontiers in Microbiology* (2011) 13:2, 77.
13. Wolf-Watz, H., Elmros, T., Normark, S., Bloom, G. D. Cell Envelope of *Neisseria gonorrhoeae*: Outer Membrane and Peptidoglycan Composition of Penicillin-Sensitive and -Resistant Strains. *Infection and Immunity* (1975) 11, 1332-1341.

14. Kurre, R., Kouzel, N., Ramakrishnan, K., Oldewurtel, E. R., Maier, B. Speed Switching of Gonococcal Surface Motility Correlates with Proton Motive Force. *PLoS ONE* (2013) 8, e67718.
15. Li, X.-Z., Elkins, C. A., Zgurskaya, H. I., SpringerLink (2016) Efflux-Mediated Antimicrobial Resistance in Bacteria : Mechanisms, Regulation and Clinical Implications. Springer International Publishing.
16. Antignac, A., Rousselle, J.-C., Namane, A., Labigne, A., Taha, M.-K., Boneca, I. G. Detailed Structural Analysis of the Peptidoglycan of the Human Pathogen *Neisseria meningitidis*. *Journal of Biological Chemistry* (2003) 278, 31521-31528.
17. Blake, M. S. and Gotschlich, E. C. Purification and partial characterization of the major outer membrane protein of *Neisseria gonorrhoeae*. *Infection and Immunity* (1982) 36, 277-283.
18. Gotschlich, E. C., Seiff, M., Blake, M. S. The DNA sequence of the structural gene of gonococcal protein III and the flanking region containing a repetitive sequence. Homology of protein III with enterobacterial OmpA proteins. *J Exp Med* (1987) 165, 471-82.
19. Van Der Ley, P., Heckels, J. E., Virji, M., Hoogerhout, P., Poolman, J. T. Topology of outer membrane porins in pathogenic *Neisseria spp*. *Infection and Immunity* (1991) 59, 2963-2971.
20. Matsuka, Y. V., Dilts, D. A., Hoiseth, S., Arumugham, R. Characterization of a subunit structure and stability of the recombinant porin from *Neisseria gonorrhoeae*. *Journal of Protein Chemistry* (1998) 17, 719-728.
21. Lewis, L. A. and Ram, S. Complement interactions with the pathogenic *Neisseriae*: clinical features, deficiency states, and evasion mechanisms. *FEBS Letters* (2020) 594, 2670-2694.
22. Lorenzen, D. R., Günther, D., Pandit, J., Rudel, T., Brandt, E., Meyer, T. F. *Neisseria gonorrhoeae* Porin Modifies the Oxidative Burst of Human Professional Phagocytes. *Infection and Immunity* (2000) 68, 6215-6222.
23. Bjerknes, R., Guttormsen, H. K., Solberg, C. O., Wetzler, L. M. Neisserial porins inhibit human neutrophil actin polymerization, degranulation, opsonin receptor expression, and phagocytosis but prime the neutrophils to increase their oxidative burst. *Infection and Immunity* (1995) 63, 160-167.
24. Mosleh, I. M., Huber, L. A., Steinlein, P., Pasquali, C., Günther, D., Meyer, T. F. *Neisseria gonorrhoeae* Porin Modulates Phagosome Maturation. *Journal of Biological Chemistry* (1998) 273, 35332-35338.
25. Zhu, W., Tomberg, J., Knilans, K. J., Anderson, J. E., McKinnon, K. P., Sempowski, G. D., Nicholas, R. A., Duncan, J. A. Properly folded and functional PorB from *Neisseria gonorrhoeae* inhibits dendritic cell stimulation of CD4(+) T cell proliferation. *J Biol Chem* (2018) 293, 11218-11229.
26. Jones, R. A., Jerse, A. E., Tang, C. M. Gonococcal PorB: a multifaceted modulator of host immune responses. *Trends in Microbiology* (2024) 32, 355-364.

27. Zhu, W., Ventevogel, M. S., Knilans, K. J., Anderson, J. E., Oldach, L. M., McKinnon, K. P., Hobbs, M. M., Sempowski, G. D., Duncan, J. A. *Neisseria gonorrhoeae* Suppresses Dendritic Cell-Induced, Antigen-Dependent CD4 T Cell Proliferation. *PLoS ONE* (2012) 7, e41260.
28. Massari, P., Ho, Y., Wetzler, L. M. *Neisseria meningitidis* porin PorB interacts with mitochondria and protects cells from apoptosis. *Proceedings of the National Academy of Sciences* (2000) 97, 9070-9075.
29. Deo, P., Chow, S. H., Hay, I. D., Kleifeld, O., Costin, A., Elgass, K. D., Jiang, J.-H., Ramm, G., Gabriel, K., Dougan, G., Lithgow, T., Heinz, E., Naderer, T. Outer membrane vesicles from *Neisseria gonorrhoeae* target PorB to mitochondria and induce apoptosis. *PLOS Pathogens* (2018) 14, e1006945.
30. Kozjak-Pavlovic, V., Dian-Lothrop, E. A., Meinecke, M., Kepp, O., Ross, K., Rajalingam, K., Harsman, A., Hauf, E., Brinkmann, V., Günther, D., Herrmann, I., Hurwitz, R., Rassow, J., Wagner, R., Rudel, T. Bacterial Porin Disrupts Mitochondrial Membrane Potential and Sensitizes Host Cells to Apoptosis. *PLoS Pathogens* (2009) 5, e1000629.
31. Massari, P., Gunawardana, J., Liu, X., Wetzler, L. M. Meningococcal Porin PorB Prevents Cellular Apoptosis in a Toll-Like Receptor 2- and NF-κB-Independent Manner. *Infection and Immunity* (2010) 78, 994-1003.
32. Reiser, M. L., Mosaheb, M. M., Lisk, C., Platt, A., Wetzler, L. M. The TLR2 Binding Neisserial Porin PorB Enhances Antigen Presenting Cell Trafficking and Cross-presentation. *Scientific Reports* (2017) 7:1, 736.
33. Singleton, T. E., Massari, P., Wetzler, L. M. Neisserial Porin-Induced Dendritic Cell Activation Is MyD88 and TLR2 Dependent. *The Journal of Immunology* (2005) 174, 3545-3550.
34. Fox, D. A., Larsson, P., Lo, R. H., Kroncke, B. M., Kasson, P. M., Columbus, L. Structure of the Neisserial outer membrane protein Opa60: loop flexibility essential to receptor recognition and bacterial engulfment. *J Am Chem Soc* (2014) 136, 9938-46.
35. Kurzyp, K. and Harrison, O. B. Bacterium of one thousand and one variants: genetic diversity of *Neisseria gonorrhoeae* pathogenicity. *Microb Genom* (2023) 9:6, mgen001040.
36. Malorny, B., Morelli, G., Kusecek, B., Kolberg, J., Achtman, M. Sequence Diversity, Predicted Two-Dimensional Protein Structure, and Epitope Mapping of Neisserial Opa Proteins. *Journal of Bacteriology* (1998) 180, 1323-1330.
37. Bhat, K. S., Gibbs, C. P., Barrera, O., Morrison, S. G., Jahnig, F., Stern, A., Kupsch, E. M., Meyer, T. F., Swanson, J. The opacity proteins of *Neisseria gonorrhoeae* strain MS11 are encoded by a family of 11 complete genes. *Mol Microbiol* (1992) 6, 1073-6.
38. Ball, L. M. and Criss, A. K. Constitutively Opa-Expressing and Opa-Deficient *Neisseria gonorrhoeae* Strains Differentially Stimulate and Survive Exposure to Human Neutrophils. *Journal of Bacteriology* (2013) 195, 2982-2990.

39. Alcott, A. M., Werner, L. M., Baiocco, C. M., Belcher Dufrisne, M., Columbus, L., Criss, A. K. Variable Expression of Opa Proteins by *Neisseria gonorrhoeae* Influences Bacterial Association and Phagocytic Killing by Human Neutrophils. *Journal of Bacteriology* (2022) 204:4, e0003522.
40. Stern, A., Brown, M., Nickel, P., Meyer, T. F. Opacity genes in *Neisseria gonorrhoeae*: control of phase and antigenic variation. *Cell* (1986) 47, 61-71.
41. Murphy, G. L., Connell, T. D., Barritt, D. S., Koomey, M., Cannon, J. G. Phase variation of gonococcal protein II: Regulation of gene expression by slipped-strand mispairing of a repetitive DNA sequence. *Cell* (1989) 56, 539-547.
42. Simon, D. and Rest, R. F. *Escherichia coli* expressing a *Neisseria gonorrhoeae* opacity-associated outer membrane protein invade human cervical and endometrial epithelial cell lines. *Proceedings of the National Academy of Sciences* (1992) 89, 5512-5516.
43. Ragland, S. A. and Criss, A. K. (2019) Protocols to Interrogate the Interactions Between *Neisseria gonorrhoeae* and Primary Human Neutrophils. Springer New York. 319-345.
44. Swanson, J. Studies on gonococcus infection. XIV. Cell wall protein differences among color/opacity colony variants of *Neisseria gonorrhoeae*. *Infection and Immunity* (1978) 21, 292-302.
45. Kellogg, D. S., Peacock, W. L., Deacon, W. E., Brown, L., Pirkle, C. I. NEISSERIA GONORRHOEAE I. *Journal of Bacteriology* (1963) 85, 1274-1279.
46. Sadarangani, M., Pollard, A. J., Gray-Owen, S. D. Opa proteins and CEACAMs: pathways of immune engagement for pathogenic *Neisseria*. *FEMS Microbiology Reviews* (2011) 35, 498-514.
47. Martin, J. N., Ball, L. M., Solomon, T. L., Dewald, A. H., Criss, A. K., Columbus, L. Neisserial Opa Protein-CEACAM Interactions: Competition for Receptors as a Means of Bacterial Invasion and Pathogenesis. *Biochemistry* (2016) 55, 4286-94.
48. Werner, L. M., Alcott, A., Mohlin, F., Ray, J. C., Belcher Dufrisne, M., Smirnov, A., Columbus, L., Blom, A. M., Criss, A. K. *Neisseria gonorrhoeae* co-opts C4b-binding protein to enhance complement-independent survival from neutrophils. *PLOS Pathogens* (2023) 19, e1011055.
49. Johnson, M. B., Ball, L. M., Daily, K. P., Martin, J. N., Columbus, L., Criss, A. K. Opa+ *Neisseria gonorrhoeae* exhibits reduced survival in human neutrophils via Src family kinase-mediated bacterial trafficking into mature phagolysosomes. *Cellular Microbiology* (2015) 17, 648-665.
50. McCaw, S. E., Schneider, J., Liao, E. H., Zimmermann, W., Gray-Owen, S. D. Immunoreceptor tyrosine-based activation motif phosphorylation during engulfment of *Neisseria gonorrhoeae* by the neutrophil-restricted CEACAM3 (CD66d) receptor. *Molecular Microbiology* (2003) 49, 623-637.

51. Boulton, I. C. and Gray-Owen, S. D. Neisserial binding to CEACAM1 arrests the activation and proliferation of CD4+ T lymphocytes. *Nature Immunology* (2002) 3, 229-236.
52. Cole, J. G., Fulcher, N. B., Jerse, A. E. Opacity Proteins Increase *Neisseria gonorrhoeae* Fitness in the Female Genital Tract Due to a Factor under Ovarian Control. *Infection and Immunity* (2010) 78, 1629-1641.
53. Bos, M. P., Hogan, D., Belland, R. J. Selection of Opa+ *Neisseria gonorrhoeae* by limited availability of normal human serum. *Infection and Immunity* (1997) 65, 645-650.
54. Sintsova, A., Wong, H., Macdonald, K. S., Kaul, R., Virji, M., Gray-Owen, S. D. Selection for a CEACAM Receptor-Specific Binding Phenotype during *Neisseria gonorrhoeae* Infection of the Human Genital Tract. *Infection and Immunity* (2015) 83, 1372-1383.
55. Gómez-Duarte, O. G., Dehio, M., Guzmán, C. A., Chhatwal, G. S., Dehio, C., Meyer, T. F. Binding of vitronectin to opa-expressing *Neisseria gonorrhoeae* mediates invasion of HeLa cells. *Infection and Immunity* (1997) 65, 3857-3866.
56. Duensing, T. D. and Putten, J. P. Vitronectin binds to the gonococcal adhesin OpaA through a glycosaminoglycan molecular bridge. *Biochem J* (1998) 334 (Pt 1), 133-9.
57. Klugman, K. P., Gotschlich, E. C., Blake, M. S. Sequence of the structural gene (*rmpM*) for the class 4 outer membrane protein of *Neisseria meningitidis*, homology of the protein to gonococcal protein III and *Escherichia coli* OmpA, and construction of meningococcal strains that lack class 4 protein. *Infect Immun* (1989) 57, 2066-71.
58. Judd, R. C., Strange, J. C., Pettit, R. K., Shafer, W. M. Identification and characterization of a conserved outer-membrane protein of *Neisseria gonorrhoeae*. *Mol Microbiol* (1991) 5, 1091-6.
59. Blake, M. S., Wetzler, L. M., Gotschlich, E. C., Rice, P. A. Protein III: structure, function, and genetics. *Clinical Microbiology Reviews* (1989) 2, S60-S63.
60. Serino, L., Nesta, B., Leuzzi, R., Fontana, M. R., Monaci, E., Mocca, B. T., Cartocci, E., Masignani, V., Jerse, A. E., Rappuoli, R., Pizza, M. Identification of a new OmpA-like protein in *Neisseria gonorrhoeae* involved in the binding to human epithelial cells and *in vivo* colonization. *Molecular Microbiology* (2007) 64, 1391-1403.
61. Copley, C. G. and MacFarlane, S. M. The production and characterization of monoclonal antibodies against the protein III of *Neisseria gonorrhoeae*. *J Gen Microbiol* (1988) 134, 1005-8.
62. Li, G., Xie, R., Zhu, X., Mao, Y., Liu, S., Jiao, H., Yan, H., Xiong, K., Ji, M. Antibodies with Higher Bactericidal Activity Induced by a *Neisseria gonorrhoeae* Rmp Deletion Mutant Strain. *PLoS ONE* (2014) 9, e90525.
63. Plummer, F. A., Chubb, H., Simonsen, J. N., Bosire, M., Slaney, L., MacLean, I., Ndinya-Achola, J. O., Waiyaki, P., Brunham, R. C. Antibody

to Rmp (outer membrane protein 3) increases susceptibility to gonococcal infection. *Journal of Clinical Investigation* (1993) 91, 339-343.

64. Rice, P. A., Vayo, H. E., Tam, M. R., Blake, M. S. Immunoglobulin G antibodies directed against protein III block killing of serum-resistant *Neisseria gonorrhoeae* by immune serum. *The Journal of Experimental Medicine* (1986) 164, 1735-1748.
65. Joiner, K. A., Scales, R., Warren, K. A., Frank, M. M., Rice, P. A. Mechanism of action of blocking immunoglobulin G for *Neisseria gonorrhoeae*. *Journal of Clinical Investigation* (1985) 76, 1765-1772.
66. Gulati, S., Mu, X., Zheng, B., Reed, G. W., Ram, S., Rice, P. A. Antibody to Reduction Modifiable Protein Increases the Bacterial Burden and the Duration of Gonococcal Infection in a Mouse Model. *Journal of Infectious Diseases* (2015) 212, 311-315.
67. Belcher, T., Rollier, C. S., Dold, C., Ross, J. D. C., MacLennan, C. A. Immune responses to *Neisseria gonorrhoeae* and implications for vaccine development. *Frontiers in Immunology* (2023) 14, 1248613.
68. Fowler, T., Caley, M., Johal, R., Brown, R., Ross, J. D. Previous history of gonococcal infection as a risk factor in patients presenting with gonorrhoea. *Int J STD AIDS* (2010) 21, 277-8.
69. Jones, R. A., Ramirez-Bencomo, F., Whiting, G., Fang, M., Lavender, H., Kurzyp, K., Thistlethwaite, A., Stejskal, L., Rashmi, S., Jerse, A. E., Cehovin, A., Derrick, J. P., Tang, C. M. Tackling immunosuppression by *Neisseria gonorrhoeae* to facilitate vaccine design. *PLOS Pathogens* (2024) 20, e1012688.
70. Fussenegger, M., Rudel, T., Barten, R., Ryll, R., Meyer, T. F. Transformation competence and type-4 pilus biogenesis in *Neisseria gonorrhoeae*--a review. *Gene* (1997) 192, 125-34.
71. Shaughnessy, J., Ram, S., Rice, P. A. (2019) Biology of the Gonococcus: Disease and Pathogenesis. Springer New York. 1-27.
72. Craig, L., Pique, M. E., Tainer, J. A. Type IV pilus structure and bacterial pathogenicity. *Nature Reviews Microbiology* (2004) 2, 363-378.
73. Jonsson, A. B., Rahman, M., Normark, S. Pilus biogenesis gene, *pilC*, of *Neisseria gonorrhoeae*: *pilC1* and *pilC2* are each part of a larger duplication of the gonococcal genome and share upstream and downstream homologous sequences with opa and pil loci. *Microbiology (Reading)* (1995) 141 (Pt 10), 2367-77.
74. Rudel, T., van Putten, J. P., Gibbs, C. P., Haas, R., Meyer, T. F. Interaction of two variable proteins (PilE and PilC) required for pilus-mediated adherence of *Neisseria gonorrhoeae* to human epithelial cells. *Mol Microbiol* (1992) 6, 3439-50.
75. Sparling, P. F., Cannon, J. G., So, M. Phase and antigenic variation of pili and outer membrane protein II of *Neisseria gonorrhoeae*. *J Infect Dis* (1986) 153, 196-201.
76. Muenzner, P. and Hauck, C. R. *Neisseria gonorrhoeae* Blocks Epithelial Exfoliation by Nitric-Oxide-Mediated Metabolic Cross Talk to Promote Colonization in Mice. *Cell Host & Microbe* (2020) 27, 793-808.e5.

77. Hill, S. A. and Davies, J. K. Pilin gene variation in *Neisseria gonorrhoeae*: reassessing the old paradigms. *FEMS Microbiology Reviews* (2009) 33, 521-530.
78. Cahoon, L. A. and Seifert, H. S. Focusing homologous recombination: pilin antigenic variation in the pathogenic *Neisseria*. *Molecular Microbiology* (2011) 81, 1136-1143.
79. Criss, A. K., Kline, K. A., Seifert, H. S. The frequency and rate of pilin antigenic variation in *Neisseria gonorrhoeae*. *Molecular Microbiology* (2005) 58, 510-519.
80. Kennouche, P., Charles-Orszag, A., Nishiguchi, D., Goussard, S., Imhaus, A. F., Dupré, M., Chamot-Rooke, J., Duménil, G. Deep mutational scanning of the *Neisseria meningitidis* major pilin reveals the importance of pilus tip-mediated adhesion. *The EMBO Journal* (2019) 38.
81. John, C. M., Phillips, N. J., Cardenas, A. J., Criss, A. K., Jarvis, G. A. Comparison of lipooligosaccharides from human challenge strains of *Neisseria gonorrhoeae*. *Frontiers in Microbiology* (2023) 14, 1215946.
82. Gulati, S., Shaughnessy, J., Ram, S., Rice, P. A. Targeting Lipooligosaccharide (LOS) for a Gonococcal Vaccine. *Frontiers in Immunology* (2019) 10, 321.
83. Lewis, L. A., Shafer, W. M., Dutta, R. T., Ram, S., Rice, P. A. Phosphoethanolamine Residues on the Lipid A Moiety of *Neisseria gonorrhoeae* Lipooligosaccharide Modulate Binding of Complement Inhibitors and Resistance to Complement Killing. *Infection and Immunity* (2013) 81, 33-42.
84. Packiam, M., Shell, D. M., Liu, S. V., Liu, Y.-B., McGee, D. J., Srivastava, R., Seal, S., Rest, R. F. Differential Expression and Transcriptional Analysis of the α-2,3-Sialyltransferase Gene in Pathogenic *Neisseria spp*. *Infection and Immunity* (2006) 74, 2637-2650.
85. Cardenas, A. J., Thomas, K. S., Broden, M. W., Ferraro, N. J., Pires, M. M., John, C. M., Jarvis, G. A., Criss, A. K. *Neisseria gonorrhoeae* scavenges host sialic acid for Siglec-mediated, complement-independent suppression of neutrophil activation. *mBio* (2024) 15:5, e0011924.
86. Ram, S., Shaughnessy, J., De Oliveira, R. B., Lewis, L. A., Gulati, S., Rice, P. A. Gonococcal lipooligosaccharide sialylation: virulence factor and target for novel immunotherapeutics. *Pathogens and Disease* (2017) 75:4, ftx049.
87. Workowski, K. A., Bachmann, L. H., Chan, P. A., Johnston, C. M., Muzny, C. A., Park, I., Reno, H., Zenilman, J. M., Bolan, G. A. Sexually Transmitted Infections Treatment Guidelines, 2021. *MMWR. Recommendations and Reports* (2021) 70, 1-187.
88. St. Cyr, S., Barbee, L., Workowski, K. A., Bachmann, L. H., Pham, C., Schlanger, K., Torrone, E., Weinstock, H., Kersh, E. N., Thorpe, P. Update to CDC's Treatment Guidelines for Gonococcal Infection, 2020. *MMWR. Morbidity and Mortality Weekly Report* (2020) 69, 1911-1916.
89. Workowski, K. A., Berman, S. Sexually transmitted diseases treatment guidelines, 2010. *MMWR Recomm Rep* (2010) 59, 1-110.

90. Blumer, J. L., Reed, M. D., Kaplan, E. L., Drusano, G. L. Explaining the poor bacteriologic eradication rate of single-dose ceftriaxone in group a streptococcal tonsillopharyngitis: a reverse engineering solution using pharmacodynamic modeling. *Pediatrics* (2005) 116, 927-32.
91. Moran, J. S. and Levine, W. C. Drugs of choice for the treatment of uncomplicated gonococcal infections. *Clin Infect Dis* (1995) 20 Suppl 1, S47-65.
92. Gaspari, V., Djusse, M. E., Morselli, S., Rapparini, L., Foschi, C., Ambretti, S., Lazzarotto, T., Piraccini, B. M., Marangoni, A. Non-pathogenic *Neisseria* species of the oropharynx as a reservoir of antimicrobial resistance: a cross-sectional study. *Frontiers in Cellular and Infection Microbiology* (2023) 13, 1343608.
93. Connolly, K. L., Eakin, A. E., Gomez, C., Osborn, B. L., Unemo, M., Jerse, A. E. Pharmacokinetic Data Are Predictive of *in vivo* Efficacy for Cefixime and Ceftriaxone against Susceptible and Resistant *Neisseria gonorrhoeae* Strains in the Gonorrhea Mouse Model. *Antimicrobial Agents and Chemotherapy* (2019) 63:3, e01644-18.
94. Golden, M. R., Whittington, W. L. H., Handsfield, H. H., Hughes, J. P., Stamm, W. E., Hogben, M., Clark, A., Malinski, C., Helmers, J. R. L., Thomas, K. K., Holmes, K. K. Effect of Expedited Treatment of Sex Partners on Recurrent or Persistent Gonorrhea or Chlamydial Infection. *New England Journal of Medicine* (2005) 352, 676-685.
95. Curry, S. J., Krist, A. H., Owens, D. K., Barry, M. J., Caughey, A. B., Davidson, K. W., Doubeni, C. A., Epling, J. W., Jr., Kemper, A. R., Kubik, M., Landefeld, C. S., Mangione, C. M., Silverstein, M., Simon, M. A., Tseng, C. W., Wong, J. B. Ocular Prophylaxis for Gonococcal Ophthalmia Neonatorum: US Preventive Services Task Force Reaffirmation Recommendation Statement. *JAMA* (2019) 321, 394-398.
96. Molina, J.-M., *et al*. Post-exposure prophylaxis with doxycycline to prevent sexually transmitted infections in men who have sex with men: an open-label randomised substudy of the ANRS IPERGAY trial. *The Lancet Infectious Diseases* (2018) 18, 308-317.
97. Traeger, M. W., Leyden, W. A., Volk, J. E., Silverberg, M. J., Horberg, M. A., Davis, T. L., Mayer, K. H., Krakower, D. S., Young, J. G., Jenness, S. M., Marcus, J. L. Doxycycline Postexposure Prophylaxis and Bacterial Sexually Transmitted Infections Among Individuals Using HIV Preexposure Prophylaxis. *JAMA Internal Medicine* (2025) 185, 273.
98. Robinson, L. R., McDevitt, C. J., Regan, M. R., Quail, S. L., Swartz, M., Wadsworth, C. B. Re-visiting the potential impact of doxycycline post-exposure prophylaxis (doxy-PEP) on the selection of doxycycline resistance in *Neisseria* commensals. *bioRxiv* (2025).
99. Luetkemeyer, A. F., Donnell, D., Dombrowski, J. C., Cohen, S., Grabow, C., Brown, C. E., Malinski, C., Perkins, R., Nasser, M., Lopez, C., Vittinghoff, E., Buchbinder, S. P., Scott, H., Charlebois, E. D., Havlir, D. V., Soge, O. O., Celum, C. Postexposure Doxycycline to Prevent Bacterial Sexually Transmitted Infections. *N Engl J Med* (2023) 388, 1296-1306.

100. Sokoll, P. R., Migliavaca, C. B., Doring, S., Traub, U., Stark, K., Sardeli, A. V. Efficacy of postexposure prophylaxis with doxycycline (Doxy-PEP) in reducing sexually transmitted infections: a systematic review and meta-analysis. *Sex Transm Infect* (2025) 101, 59-67.
101. Unemo, M., Lahra, M. M., Cole, M., Galarza, P., Ndowa, F., Martin, I., Dillon, J.-A. R., Ramon-Pardo, P., Bolan, G., Wi, T. World Health Organization Global Gonococcal Antimicrobial Surveillance Program (WHO GASP): review of new data and evidence to inform international collaborative actions and research efforts. *Sexual Health* (2019) 16, 412.
102. Unemo, M., Lahra, M. M., Escher, M., Eremin, S., Cole, M. J., Galarza, P., Ndowa, F., Martin, I., Dillon, J.-A. R., Galas, M., Ramon-Pardo, P., Weinstock, H., Wi, T. WHO global antimicrobial resistance surveillance for *Neisseria gonorrhoeae* 2017–18: a retrospective observational study. *The Lancet Microbe* (2021) 2, e627-e636.
103. Quilter, L. A. S., St Cyr, S. B., Hong, J., Asbel, L., Bautista, I., Carter, B., Casimir, Y., Denny, M., Ervin, M., Gomez, R., Harvey, A., Holderman, J. L., Johnson, K., Kohn, R. P., Learner, E. R., Mauk, K., Menza, T., Mettenbrink, C., Nettleton, W. D., Nicosia, K. R., Pham, C. D., Ried, C., Schlanger, K., Schneider, A., Soge, O. O., Tabidze, I., Taylor, S. N., Tilghman, W., Toler, C., Weinstock, H., Torrone, E. A. Antimicrobial Susceptibility of Urogenital and Extragenital *Neisseria gonorrhoeae* Isolates Among Men Who Have Sex With Men: Strengthening the US Response to Resistant Gonorrhea and Enhanced Gonococcal Isolate Surveillance Project, 2018 to 2019. *Sex Transm Dis* (2021) 48, S111-S117.
104. Costa-Lourenco, A., Barros Dos Santos, K. T., Moreira, B. M., Fracalanzza, S. E. L., Bonelli, R. R. Antimicrobial resistance in *Neisseria gonorrhoeae*: history, molecular mechanisms and epidemiological aspects of an emerging global threat. *Braz J Microbiol* (2017) 48, 617-628.
105. Unemo, M. and Shafer, W. M. Antimicrobial Resistance in *Neisseria gonorrhoeae* in the 21st Century: Past, Evolution, and Future. *Clinical Microbiology Reviews* (2014) 27, 587-613.
106. Centers for Disease Control and Prevention. Update to CDC's sexually transmitted diseases treatment guidelines, 2006: fluoroquinolones no longer recommended for treatment of gonococcal infections. *MMWR Morb Mortal Wkly Rep* (2007) 56, 332-6.
107. Kersh, E. N., Allen, V., Ransom, E., Schmerer, M., Cyr, S., Workowski, K., Weinstock, H., Patel, J., Ferraro, M. J. Rationale for a *Neisseria gonorrhoeae* Susceptible–only Interpretive Breakpoint for Azithromycin. *Clinical Infectious Diseases* (2020) 70, 798-804.
108. Chisholm, S. A., Wilson, J., Alexander, S., Tripodo, F., Al-Shahib, A., Schaefer, U., Lythgow, K., Fifer, H. An outbreak of high-level azithromycin resistant *Neisseria gonorrhoeae* in England. *Sex Transm Infect* (2016) 92, 365-7.
109. Centers for Disease Control and Prevention. Update to CDC's Sexually transmitted diseases treatment guidelines, 2010: oral cephalosporins no

longer a recommended treatment for gonococcal infections. *MMWR Morb Mortal Wkly Rep* (2012) 61, 590-4.

110. Ohnishi, M., Golparian, D., Shimuta, K., Saika, T., Hoshina, S., Iwasaku, K., Nakayama, S.-I., Kitawaki, J., Unemo, M. Is *Neisseria gonorrhoeae* Initiating a Future Era of Untreatable Gonorrhea?: Detailed Characterization of the First Strain with High-Level Resistance to Ceftriaxone. *Antimicrobial Agents and Chemotherapy* (2011) 55, 3538-3545.
111. Ohnishi, M., Saika, T., Hoshina, S., Iwasaku, K., Nakayama, S.-I., Watanabe, H., Kitawaki, J. Ceftriaxone-Resistant *Neisseria gonorrhoeae*, Japan. *Emerging Infectious Diseases* (2011) 17, 148-149.
112. Lan, P. T., Nguyen, H. T., Golparian, D., Thuy Van, N. T., Maatouk, I., Unemo, M. The WHO Enhanced Gonococcal Antimicrobial Surveillance Programme (EGASP) identifies high levels of ceftriaxone resistance across Vietnam, 2023. *Lancet Reg Health West Pac* (2024) 48, 101125.
113. Ouk, V., Say, H. L., Virak, M., Deng, S., Frankson, R., McDonald, R., Kersh, E. N., Wi, T., Maatouk, I., van Hal, S., Lahra, M. M. World Health Organization Enhanced Gonococcal Antimicrobial Surveillance Programme, Cambodia, 2023. *Emerg Infect Dis* (2024) 30, 1493-1495.
114. Taylor, S. N., Morris, D. H., Avery, A. K., Workowski, K. A., Batteiger, B. E., Tiffany, C. A., Perry, C. R., Raychaudhuri, A., Scangarella-Oman, N. E., Hossain, M., Dumont, E. F. Gepotidacin for the Treatment of Uncomplicated Urogenital Gonorrhea: A Phase 2, Randomized, Dose-Ranging, Single-Oral Dose Evaluation. *Clinical Infectious Diseases* (2018) 67, 504-512.
115. Perry, C. R., Scangarella-Oman, N. E., Millns, H., Flight, W., Gatsi, S., Jakielaszek, C., Janmohamed, S., Lewis, D. A. Efficacy and Safety of Gepotidacin as Treatment of Uncomplicated Urogenital Gonorrhea (EAGLE-1): Design of a Randomized, Comparator-Controlled, Phase 3 Study. *Infectious Diseases and Therapy* (2023) 12, 2307-2320.
116. Oyardi, O., Yilmaz, F. N., Dosler, S. Efficacy of Zoliflodacin, a Spiropyrimidinetrione Antibiotic, Against Gram-Negative Pathogens. *Current Microbiology* (2024) 81:8, 241.
117. Scangarella-Oman, N. E., Hossain, M., Perry, C. R., Tiffany, C., Powell, M., Swift, B., Dumont, E. F. Dose selection for a phase III study evaluating gepotidacin (GSK2140944) in the treatment of uncomplicated urogenital gonorrhoea. *Sexually Transmitted Infections* (2023) 99, 64-69.
118. Pascual, F., Au, C., Chikwari, C. D., Daram, P., Deal, C., Miranda, A. E., Grad, Y. H., Hook, E. W., Kittiyaowamarn, R., Luckey, A., Low, N., Maseko, V., Peters, R. P. H., Roberts, T., Unemo, M., Srinivasan, S. Recommendations for the optimal introduction of novel antibiotics to treat uncomplicated gonorrhoea in the face of increasing antimicrobial resistance: a case study with zoliflodacin. *BMC Global and Public Health* (2024) 2:1, 58.
119. Jacobsson, S., Golparian, D., Scangarella-Oman, N., Unemo, M. *In vitro* activity of the novel triazaacenaphthylene gepotidacin (GSK2140944)

against MDR *Neisseria gonorrhoeae*. *Journal of Antimicrobial Chemotherapy* (2018) 73, 2072-2077.

120. Rubin, D. H., Mortimer, T. D., Grad, Y. H. *Neisseria gonorrhoeae* diagnostic escape from a gyrA-based test for ciprofloxacin susceptibility and the effect on zoliflodacin resistance: a bacterial genetics and experimental evolution study. *Lancet Microbe* (2023) 4, e247-e254.
121. David, A., Golparian, D., Jacobsson, S., Stratton, C., Lan, P. T., Shimuta, K., Sonnenberg, P., Field, N., Ohnishi, M., Davies, C., Unemo, M. *In silico* gepotidacin target mining among 33213 global *Neisseria gonorrhoeae* genomes from 1928 to 2023 combined with gepotidacin MIC testing of 22 gonococcal isolates with different GyrA and ParC substitutions. *Journal of Antimicrobial Chemotherapy* (2024) 79, 2221-2226.
122. Shimuta, K., Ohama, Y., Ito, S., Hoshina, S., Takahashi, H., Igawa, G., Dorin Yamamoto, M., Akeda, Y., Ohnishi, M. Emergence of Ceftriaxone-Resistant *Neisseria gonorrhoeae* Through Horizontal Gene Transfer Among *Neisseria* Species. *The Journal of Infectious Diseases* (2025).
123. Djusse, M. E., Gaspari, V., Morselli, S., Rapparini, L., Foschi, C., Ambretti, S., Lazzarotto, T., Piraccini, B. M., Marangoni, A. Antimicrobial resistance determinants in the oropharyngeal microbiome of 'men having sex with men' attending an sexually transmitted infection clinic. *Int J STD AIDS* (2024) 35, 803-807.
124. Mlynarczyk-Bonikowska, B., Kowalewski, C., Krolak-Ulinska, A., Marusza, W. Molecular Mechanisms of Drug Resistance and Epidemiology of Multidrug-Resistant Variants of *Neisseria gonorrhoeae*. *International Journal of Molecular Sciences* (2022) 23, 10499.
125. Kaderabkova, N., Bharathwaj, M., Furniss, R. C. D., Gonzalez, D., Palmer, T., Mavridou, D. A. I. The biogenesis of β-lactamase enzymes. *Microbiology* (2022) 168:8, 001217.
126. Zapun, A., Morlot, C., Taha, M.-K. Resistance to β-Lactams in *Neisseria ssp*. Due to Chromosomally Encoded Penicillin-Binding Proteins. *Antibiotics* (2016) 5, 35.
127. Yahara, K., Ma, K. C., Mortimer, T. D., Shimuta, K., Nakayama, S.-I., Hirabayashi, A., Suzuki, M., Jinnai, M., Ohya, H., Kuroki, T., Watanabe, Y., Yasuda, M., Deguchi, T., Eldholm, V., Harrison, O. B., Maiden, M. C. J., Grad, Y. H., Ohnishi, M. Emergence and evolution of antimicrobial resistance genes and mutations in *Neisseria gonorrhoeae*. *Genome Medicine* (2021) 13:1, 51.
128. Mendes, A. C., De Souza, R. P., Bahia, D. The frequency of mutations in the *penA*, *mtrR*, *gyrA* and *parC* genes of *Neisseria gonorrhoeae*, the presence of *tetM* gene and antibiotic resistance/susceptibility: a systematic review and meta-analyses. *Frontiers in Microbiology* (2025) 15, 1414330.
129. Van Den Berg, B., Prathyusha Bhamidimarri, S., Dahyabhai Prajapati, J., Kleinekathöfer, U., Winterhalter, M. Outer-membrane translocation of bulky small molecules by passive diffusion. *Proceedings of the National Academy of Sciences* (2015) 112, E2991-E2999.

130. Brillet, K., Journet, L., Célia, H., Paulus, L., Stahl, A., Pattus, F., Cobessi, D. A β Strand Lock Exchange for Signal Transduction in TonB-Dependent Transducers on the Basis of a Common Structural Motif. *Structure* (2007) 15, 1383-1391.
131. Olesky, M., Zhao, S., Rosenberg, R. L., Nicholas, R. A. Porin-Mediated Antibiotic Resistance in *Neisseria gonorrhoeae*: Ion, Solute, and Antibiotic Permeation through PIB Proteins with *penB* Mutations. *Journal of Bacteriology* (2006) 188, 2300-2308.
132. Barry, P. M. and Klausner, J. D. The use of cephalosporins for gonorrhea: the impending problem of resistance. *Expert Opin Pharmacother* (2009) 10, 555-77.
133. Ohneck, E. A., Zalucki, Y. M., Johnson, P. J. T., Dhulipala, V., Golparian, D., Unemo, M., Jerse, A. E., Shafer, W. M. A Novel Mechanism of High-Level, Broad-Spectrum Antibiotic Resistance Caused by a Single Base Pair Change in *Neisseria gonorrhoeae*. *mBio* (2011) 2, e00187-11-e00187.
134. Ohneck, E. A., Goytia, M., Rouquette-Loughlin, C. E., Joseph, S. J., Read, T. D., Jerse, A. E., Shafer, W. M. Overproduction of the MtrCDE Efflux Pump in *Neisseria gonorrhoeae* Produces Unexpected Changes in Cellular Transcription Patterns. *Antimicrobial Agents and Chemotherapy* (2015) 59, 724-726.
135. Jerse, A. E., Sharma, N. D., Simms, A. N., Crow, E. T., Snyder, L. A., Shafer, W. M. A gonococcal efflux pump system enhances bacterial survival in a female mouse model of genital tract infection. *Infect Immun* (2003) 71, 5576-82.
136. Handing, J. W., Ragland, S. A., Bharathan, U. V., Criss, A. K. The MtrCDE Efflux Pump Contributes to Survival of *Neisseria gonorrhoeae* From Human Neutrophils and Their Antimicrobial Components. *Frontiers in Microbiology* (2018) 9, 2688.
137. Ram, S., Lewis, L. A., Rice, P. A. Infections of People with Complement Deficiencies and Patients Who Have Undergone Splenectomy. *Clinical Microbiology Reviews* (2010) 23, 740-780.
138. Sahu, S. K., Kulkarni, D. H., Ozanturk, A. N., Ma, L., Kulkarni, H. S. Emerging roles of the complement system in host-pathogen interactions. *Trends Microbiol* (2022) 30, 390-402.
139. Hastings, C. J., Syed, S. S., Marques, C. N. H. Subversion of the Complement System by *Pseudomonas aeruginosa*. *Journal of Bacteriology* (2023) 205:8, e0001823.
140. Abreu, A. G. and Barbosa, A. S. How *Escherichia coli* Circumvent Complement-Mediated Killing. *Frontiers in Immunology* (2017) 8, 452.
141. Hajishengallis, G., Reis, E. S., Mastellos, D. C., Ricklin, D., Lambris, J. D. Novel mechanisms and functions of complement. *Nat Immunol* (2017) 18, 1288-1298.
142. Mastellos, D. C., Hajishengallis, G., Lambris, J. D. A guide to complement biology, pathology and therapeutic opportunity. *Nature Reviews Immunology* (2024) 24, 118-141.

143. Liyayi, I. K., Forehand, A. L., Ray, J. C., Criss, A. K. Metal piracy by Neisseria gonorrhoeae to overcome human nutritional immunity. *PLOS Pathogens* (2023) 19, e1011091.
144. Tamarelle, J., Thiébaut, A. C. M., De Barbeyrac, B., Bébéar, C., Ravel, J., Delarocque-Astagneau, E. The vaginal microbiota and its association with human papillomavirus, *Chlamydia trachomatis*, *Neisseria gonorrhoeae* and *Mycoplasma genitalium* infections: a systematic review and meta-analysis. *Clinical Microbiology and Infection* (2019) 25, 35-47.
145. Lovett, A., Seña, A. C., MacIntyre, A. N., Sempowski, G. D., Duncan, J. A., Waltmann, A. Cervicovaginal Microbiota Predicts *Neisseria gonorrhoeae* Clinical Presentation. *Frontiers in Microbiology* (2022) 12, 790531.
146. Criss, A. K., Genco, C. A., Gray-Owen, S. D., Jerse, A. E., Seifert, H. S. Challenges and Controversies Concerning *Neisseria gonorrhoeae*-Neutrophil Interactions in Pathogenesis. *mBio* (2021) 12:3, e0072121.
147. Hedges, S. R., Mayo, M. S., Mestecky, J., Hook, E. W., Russell, M. W. Limited Local and Systemic Antibody Responses to *Neisseria gonorrhoeae* during Uncomplicated Genital Infections. *Infection and Immunity* (1999) 67, 3937-3946.
148. Franchi, N. and Ballarin, L. Immunity in Protochordates: The Tunicate Perspective. *Frontiers in Immunology* (2017) 8, 674.
149. Price, R. J. and Boettcher, B. The presence of complement in human cervical mucus and its possible relevance to infertility in women with complement-dependent sperm-immobilizing antibodies. *Fertil Steril* (1979) 32, 61-6.
150. Kopp, Z. A., Jain, U., Van Limbergen, J., Stadnyk, A. W. Do Antimicrobial Peptides and Complement Collaborate in the Intestinal Mucosa? *Frontiers in Immunology* (2015) 6, 17.
151. Bayly-Jones, C., Bubeck, D., Dunstone, M. A. The mystery behind membrane insertion: a review of the complement membrane attack complex. *Philosophical Transactions of the Royal Society B: Biological Sciences* (2017) 372, 20160221.
152. Kawa, S. (2016) The Immunobiology of Immunoglobulin G4 and Complement Activation Pathways in IgG4-Related Disease. Springer International Publishing. 61-73.
153. Schroeder, H. W. Jr. and Cavacini, L. Structure and function of immunoglobulins. *J Allergy Clin Immunol* (2010) 125, S41-52.
154. Taylor, R. P., Lindorfer, M. A., Cook, E. M., Beurskens, F. J., Schuurman, J., Parren, P., Zent, C. S., Van Der Meid, K. R., Burack, R., Mizuno, M., Morgan, B. P. Hexamerization-enhanced CD20 antibody mediates complement-dependent cytotoxicity in serum genetically deficient in C9. *Clin Immunol* (2017) 181, 24-28.
155. Bettoni, S., Shaughnessy, J., Maziarz, K., Ermert, D., Gulati, S., Zheng, B., Morgelin, M., Jacobsson, S., Riesbeck, K., Unemo, M., Ram, S., Blom, A. M. C4BP-IgM protein as a therapeutic approach to treat *Neisseria gonorrhoeae* infections. *JCI Insight* (2019) 4:23, e131886.

156. Gulati, S., Beurskens, F. J., de Kreuk, B. J., Roza, M., Zheng, B., De Oliveira, R. B., Shaughnessy, J., Nowak, N. A., Taylor, R. P., Botto, M., He, X., Ingalls, R. R., Woodruff, T. M., Song, W. C., Schuurman, J., Rice, P. A., Ram, S. Complement alone drives efficacy of a chimeric antigonococcal monoclonal antibody. *PLoS Biol* (2019) 17, e3000323.
157. Du Clos, T. W. Function of C-reactive protein. *Annals of Medicine* (2000) 32, 274-278.
158. Ma, Y. J. and Garred, P. Pentraxins in Complement Activation and Regulation. *Frontiers in Immunology* (2018) 19:9, 3046.
159. Noris, M. and Galbusera, M. The complement alternative pathway and hemostasis. *Immunol Rev* (2023) 313, 139-161.
160. Pangburn, M. K. Initiation of the alternative pathway of complement and the history of "tickover". *Immunol Rev* (2023) 313, 64-70.
161. Doorduijn, D. J., Rooijakkers, S. H. M., Heesterbeek, D. A. C. How the Membrane Attack Complex Damages the Bacterial Cell Envelope and Kills Gram-Negative Bacteria. *BioEssays* (2019) 41, 1900074.
162. Merle, N. S., Church, S. E., Fremeaux-Bacchi, V., Roumenina, L. T. Complement System Part I Molecular Mechanisms of Activation and Regulation. *Frontiers in Immunology* (2015) 6, 262.
163. Afshar-Kharghan, V. The role of the complement system in cancer. *Journal of Clinical Investigation* (2017) 127, 780-789.
164. Gavriilaki, E. and Brodsky, R. A. Complementopathies and precision medicine. *J Clin Invest* (2020) 130, 2152-2163.
165. Ricklin, D., Reis, E. S., Lambris, J. D. Complement in disease: a defence system turning offensive. *Nature Reviews Nephrology* (2016) 12, 383-401.
166. Zarantonello, A., Revel, M., Grunenwald, A., Roumenina, L. T. C3-dependent effector functions of complement. *Immunological Reviews* (2023) 313, 120-138.
167. Van Rees, D. J., Szilagyi, K., Kuijpers, T. W., Matlung, H. L., Van Den Berg, T. K. Immunoreceptors on neutrophils. *Seminars in Immunology* (2016) 28, 94-108.
168. Alemán, O. R. and Rosales, C. Human neutrophil Fc gamma receptors: different buttons for different responses. *J Leukoc Biol* (2023) 114, 571-584.
169. Small, A. G., Al-Baghdadi, M., Quach, A., Hii, C., Ferrante, A. Complement receptor immunoglobulin: a control point in infection and immunity, inflammation and cancer. *Swiss Med Wkly* (2016) 146, w14301.
170. Lim, J. and Hotchin, N. A. Signalling mechanisms of the leukocyte integrin αMβ2: Current and future perspectives. *Biology of the Cell* (2012) 104, 631-640.
171. Smirnov, A., Daily, K. P., Gray, M. C., Ragland, S. A., Werner, L. M., Brittany Johnson, M., Eby, J. C., Hewlett, E. L., Taylor, R. P., Criss, A. K. Phagocytosis via complement receptor 3 enables microbes to evade killing by neutrophils. *Journal of Leukocyte Biology* (2023) 114, 1-20.

172. Edwards, J. L. and Apicella, M. A. The Molecular Mechanisms Used by *Neisseria gonorrhoeae* To Initiate Infection Differ between Men and Women. *Clinical Microbiology Reviews* (2004) 17, 965-981.
173. Haas, P.-J. and Van Strijp, J. Anaphylatoxins. *Immunologic Research* (2007) 37, 161-175.
174. Metzemaekers, M., Gouwy, M., Proost, P. Neutrophil chemoattractant receptors in health and disease: double-edged swords. *Cell Mol Immunol* (2020) 17, 433-450.
175. Li, R., Coulthard, L. G., Wu, M. C., Taylor, S. M., Woodruff, T. M. C5L2: a controversial receptor of complement anaphylatoxin, C5a. *FASEB J* (2013) 27, 855-64.
176. Braun, L., Christophe, T., Boulay, F. Phosphorylation of Key Serine Residues Is Required for Internalization of the Complement 5a (C5a) Anaphylatoxin Receptor via a β-Arrestin, Dynamin, and Clathrin-dependent Pathway. *Journal of Biological Chemistry* (2003) 278, 4277-4285.
177. Gray, M. C., Thomas, K. S., Lamb, E. R., Werner, L. M., Connolly, K. L., Jerse, A. E., Criss, A. K. Evaluating vaccine-elicited antibody activities against *Neisseria gonorrhoeae*: cross-protective responses elicited by the 4CMenB meningococcal vaccine. *Infection and Immunity* (2023) 91:12, e0030923.
178. Gulati, S., Rice, P. A., Ram, S. Complement-Dependent Serum Bactericidal Assays for Neisseria gonorrhoeae. *Methods Mol Biol* (2019) 1997, 267-280.
179. Ispasanie, E., Muri, L., Schmid, M., Schubart, A., Thorburn, C., Zamurovic, N., Holbro, T., Kammüller, M., Pluschke, G. In vaccinated individuals serum bactericidal activity against B meningococci is abrogated by C5 inhibition but not by inhibition of the alternative complement pathway. *Frontiers in Immunology* (2023) 14, 1180833.
180. Matthias, K. A., Reveille, A., Dhara, K., Lyle, C. S., Natuk, R. J., Bonk, B., Bash, M. C. Development and validation of a standardized human complement serum bactericidal activity assay to measure functional antibody responses to *Neisseria gonorrhoeae*. *Vaccine* (2024) 43, 126508.
181. Joisel, F., Leroux-Nicollet, I., Lebreton, J. P., Fontaine, M. A hemolytic assay for clinical investigation of human C2. *J Immunol Methods* (1983) 59, 229-35.
182. Doorduijn, D. J., Bardoel, B. W., Heesterbeek, D. A. C., Ruyken, M., Benn, G., Parsons, E. S., Hoogenboom, B. W., Rooijakkers, S. H. M. Bacterial killing by complement requires direct anchoring of membrane attack complex precursor C5b-7. *PLOS Pathogens* (2020) 16, e1008606.
183. Doorduijn, D. J., Heesterbeek, D. A. C., Ruyken, M., De Haas, C. J. C., Stapels, D. A. C., Aerts, P. C., Rooijakkers, S. H. M., Bardoel, B. W. Polymerization of C9 enhances bacterial cell envelope damage and killing by membrane attack complex pores. *PLOS Pathogens* (2021) 17, e1010051.

184. Dudkina, N. V., Spicer, B. A., Reboul, C. F., Conroy, P. J., Lukoyanova, N., Elmlund, H., Law, R. H. P., Ekkel, S. M., Kondos, S. C., Goode, R. J. A., Ramm, G., Whisstock, J. C., Saibil, H. R., Dunstone, M. A. Structure of the poly-C9 component of the complement membrane attack complex. *Nature Communications* (2016) 7, 10588.
185. Menny, A., Serna, M., Boyd, C. M., Gardner, S., Joseph, A. P., Morgan, B. P., Topf, M., Brooks, N. J., Bubeck, D. CryoEM reveals how the complement membrane attack complex ruptures lipid bilayers. *Nature Communications* (2018) 9:1, 5216.
186. Serna, M., Giles, J. L., Morgan, B. P., Bubeck, D. Structural basis of complement membrane attack complex formation. *Nature Communications* (2016) 7, 10587.
187. Sharp, T. H., Koster, A. J., Gros, P. Heterogeneous MAC Initiator and Pore Structures in a Lipid Bilayer by Phase-Plate Cryo-electron Tomography. *Cell Reports* (2016) 15, 1-8.
188. Bhakdi, S., Kuller, G., Muhly, M., Fromm, S., Seibert, G., Parrisius, J. Formation of transmural complement pores in serum-sensitive *Escherichia coli*. *Infection and Immunity* (1987) 55, 206-210.
189. Sims, P. J. Complement pores in erythrocyte membranes. Analysis of C8/C9 binding required for functional membrane damage. *Biochim Biophys Acta* (1983) 732, 541-52.
190. Harriman, G. R., Esser, A. F., Podack, E. R., Wunderlich, A. C., Braude, A. I., Lint, T. F., Curd, J. G. The role of C9 in complement-mediated killing of Neisseria. *J Immunol* (1981) 127, 2386-90.
191. Preissner, K. P., Podack, E. R., Müller-Eberhard, H. J. SC5b-7, SC5b-8 and SC5b-9 complexes of complement: ultrastructure and localization of the S-protein (vitronectin) within the macromolecules. *European Journal of Immunology* (1989) 19, 69-75.
192. Morgan, B. P., Boyd, C., Bubeck, D. Molecular cell biology of complement membrane attack. *Semin Cell Dev Biol* (2017) 72, 124-132.
193. Moreland, A. S., Limwongyut, J., Holton, S. J., Bazan, G. C. Structural modulation of membrane-intercalating conjugated oligoelectrolytes decouples outer membrane permeabilizing and antimicrobial activities. *Chem Commun (Camb)* (2023) 59, 12172-12175.
194. Feingold, D. S., Goldman, J. N., Kuritz, H. M. Locus of the Action of Serum and the Role of Lysozyme in the Serum Bactericidal Reaction. *Journal of Bacteriology* (1968) 96, 2118-2126.
195. Taylor, P. W. Bactericidal and bacteriolytic activity of serum against gram-negative bacteria. *Microbiological Reviews* (1983) 47, 46-83.
196. Heesterbeek, D. A. C., Muts, R. M., Van Hensbergen, V. P., De Saint Aulaire, P., Wennekes, T., Bardoel, B. W., Van Sorge, N. M., Rooijakkers, S. H. M. Outer membrane permeabilization by the membrane attack complex sensitizes Gram-negative bacteria to antimicrobial proteins in serum and phagocytes. *PLOS Pathogens* (2021) 17, e1009227.

197. Nauser, C. L. and Sacks, S. H. Local complement synthesis—A process with near and far consequences for ischemia reperfusion injury and transplantation. *Immunological Reviews* (2023) 313, 320-326.
198. Figueroa, J., Andreoni, J., Densen, P. Complement deficiency states and meningococcal disease. *Immunol Res* (1993) 12, 295-311.
199. Nauser, C. L. and Sacks, S. H. Local complement synthesis-A process with near and far consequences for ischemia reperfusion injury and transplantation. *Immunol Rev* (2023) 313, 320-326.
200. Lubbers, R., Van Essen, M. F., Van Kooten, C., Trouw, L. A. Production of complement components by cells of the immune system. *Clinical and Experimental Immunology* (2017) 188, 183-194.
201. Chaudhary, N., Jayaraman, A., Reinhardt, C., Campbell, J. D., Bosmann, M. A single-cell lung atlas of complement genes identifies the mesothelium and epithelium as prominent sources of extrahepatic complement proteins. *Mucosal Immunology* (2022) 15, 927-939.
202. Potter, A. D., Edwards, V. L., D'Mello, A., Gray, M. C., Shetty, A. C., Forehand, A. L., Westlake, C. S., Lamb, E. R., Zhao, X., Ragland, S. A., Criss, A. K., Tettelin, H. Dual species transcriptomics reveals conserved metabolic and immunologic processes in interactions between human neutrophils and *Neisseria gonorrhoeae*. *PLOS Pathogens* (2024) 20, e1012369.
203. Suryawanshi, S., Huang, X., Elishaev, E., Budiu, R. A., Zhang, L., Kim, S., Donnellan, N., Mantia-Smaldone, G., Ma, T., Tseng, G., Lee, T., Mansuria, S., Edwards, R. P., Vlad, A. M. Complement Pathway Is Frequently Altered in Endometriosis and Endometriosis-Associated Ovarian Cancer. *Clinical Cancer Research* (2014) 20, 6163-6174.
204. Ram, S., Cullinane, M., Blom, A. M., Gulati, S., McQuillen, D. P., Boden, R., Monks, B. G., O'Connell, C., Elkins, C., Pangburn, M. K., Dahlback, B., Rice, P. A. C4BP binding to porin mediates stable serum resistance of *Neisseria gonorrhoeae*. *Int Immunopharmacol* (2001) 1, 423-32.
205. Werner, L. M. and Criss, A. K. Diverse Functions of C4b-Binding Protein in Health and Disease. *The Journal of Immunology* (2023) 211, 1443-1449.
206. Okusa, S., Takizawa, T., Imai, S., Oyama, M., Ishizuchi, K., Nakahara, J., Hori, S., Suzuki, S. Serious Bacterial Infections Associated with Eculizumab: A Pharmacovigilance Study. *Internal Medicine* (2024) 63, 1061-1066.
207. Crew, P. E., McNamara, L., Waldron, P. E., McCulley, L., Jones, S. C., Bersoff-Matcha, S. J. Unusual *Neisseria* species as a cause of infection in patients taking eculizumab. *Journal of Infection* (2019) 78, 113-118.
208. Lewis, L. A., Gulati, S., Zelek, W. M., Morgan, B. P., Song, W.-C., Zheng, B., Nowak, N., Deoliveira, R. B., Sanchez, B., Desouza Silva, L., Schuurman, J., Beurskens, F., Ram, S., Rice, P. A. Efficacy of an Experimental Gonococcal Lipooligosaccharide Mimitope Vaccine Requires Terminal Complement. *The Journal of Infectious Diseases* (2022) 225, 1861-1864.

209. Mantovani, A., Cassatella, M. A., Costantini, C., Jaillon, S. Neutrophils in the activation and regulation of innate and adaptive immunity. *Nature Reviews Immunology* (2011) 11, 519-531.
210. Ley, K., Hoffman, H. M., Kubes, P., Cassatella, M. A., Zychlinsky, A., Hedrick, C. C., Catz, S. D. Neutrophils: New insights and open questions. *Science Immunology* (2018) 3, eaat4579.
211. Burn, G. L., Foti, A., Marsman, G., Patel, D. F., Zychlinsky, A. The Neutrophil. *Immunity* (2021) 54, 1377-1391.
212. Yin, C. and Heit, B. Armed for destruction: formation, function and trafficking of neutrophil granules. *Cell and Tissue Research* (2018) 371, 455-471.
213. Nauseef, W. M. Human neutrophils ≠ murine neutrophils: Does it matter? *Immunological Reviews* (2023) 314, 442-456.
214. Futosi, K., Fodor, S., Mócsai, A. Neutrophil cell surface receptors and their intracellular signal transduction pathways. *Int Immunopharmacol* (2013) 17, 638-50.
215. Rocha-Gregg, B. and Huttenlocher, A. Signal integration in forward and reverse neutrophil migration: Fundamentals and emerging mechanisms. *Curr Opin Cell Biol* (2021) 72, 124-130.
216. Stevens, J. S., Gray, M. C., Morisseau, C., Criss, A. K. Endocervical and Neutrophil Lipoxygenases Coordinate Neutrophil Transepithelial Migration to Neisseria gonorrhoeae. *The Journal of Infectious Diseases* (2018) 218, 1663-1674.
217. Kolaczkowska, E. and Kubes, P. Neutrophil recruitment and function in health and inflammation. *Nature Reviews Immunology* (2013) 13, 159-175.
218. Grönloh, M. L. B., Arts, J. J. G., Van Buul, J. D. Neutrophil transendothelial migration hotspots – mechanisms and implications. *Journal of Cell Science* (2021) 134, jcs255653.
219. Parkos, C. A. Neutrophil-Epithelial Interactions. *The American Journal of Pathology* (2016) 186, 1404-1416.
220. Borregaard, N. Neutrophils, from Marrow to Microbes. *Immunity* (2010) 33, 657-670.
221. Hofman, P., Piche, M., Far, D. F., Le Negrate, G. L., Selva, E., Landraud, L., Alliana-Schmid, A., Boquet, P., Rossi, B. Increased *Escherichia coli* Phagocytosis in Neutrophils That Have Transmigrated across a Cultured Intestinal Epithelium. *Infection and Immunity* (2000) 68, 449-455.
222. Eun, J. C., Moore, E. E., Banerjee, A., Kelher, M. R., Khan, S. Y., Elzi, D. J., McLaughlin, N. J., Silliman, C. C. Leukotriene B4 and its metabolites prime the neutrophil oxidase and induce proinflammatory activation of human pulmonary microvascular endothelial cells. *Shock* (2011) 35, 240-4.
223. Mukhopadhyay, A., Tsukasaki, Y., Chan, W. C., Le, J. P., Kwok, M. L., Zhou, J., Natarajan, V., Mostafazadeh, N., Maienschein-Cline, M., Papautsky, I., Tiruppathi, C., Peng, Z., Rehman, J., Ganesh, B., Komarova, Y., Malik, A. B. trans-Endothelial neutrophil migration activates

bactericidal function via Piezo1 mechanosensing. *Immunity* (2024) 57, 52-67.e10.
224. Ramadass, M. and Catz, S. D. Molecular mechanisms regulating secretory organelles and endosomes in neutrophils and their implications for inflammation. *Immunological Reviews* (2016) 273, 249-265.
225. Lacy, P. and Eitzen, G. Control of granule exocytosis in neutrophils. *Front Biosci* (2008) 13, 5559-70.
226. Hurst, J. K. What really happens in the neutrophil phagosome? *Free Radical Biology and Medicine* (2012) 53, 508-520.
227. Brinkmann, V., Reichard, U., Goosmann, C., Fauler, B., Uhlemann, Y., Weiss, D. S., Weinrauch, Y., Zychlinsky, A. Neutrophil extracellular traps kill bacteria. *Science* (2004) 303, 1532-5.
228. Palmer, A. and Criss, A. K. Gonococcal Defenses against Antimicrobial Activities of Neutrophils. *Trends in Microbiology* (2018) 26, 1022-1034.
229. Deniset, J. F. and Kubes, P. Neutrophil heterogeneity: Bona fide subsets or polarization states? *Journal of Leukocyte Biology* (2018) 103, 829-838.
230. Ng, L. G., Ostuni, R., Hidalgo, A. Heterogeneity of neutrophils. *Nature Reviews Immunology* (2019) 19, 255-265.
231. Silvestre-Roig, C., Fridlender, Z. G., Glogauer, M., Scapini, P. Neutrophil Diversity in Health and Disease. *Trends Immunol* (2019) 40, 565-583.
232. Hedrick, C. C. and Malanchi, I. Neutrophils in cancer: heterogeneous and multifaceted. *Nature Reviews Immunology* (2022) 22, 173-187.
233. Wigerblad, G., Cao, Q., Brooks, S., Naz, F., Gadkari, M., Jiang, K., Gupta, S., O'Neil, L., Dell'Orso, S., Kaplan, M. J., Franco, L. M. Single-Cell Analysis Reveals the Range of Transcriptional States of Circulating Human Neutrophils. *The Journal of Immunology* (2022) 209, 772-782.
234. Schofield, C. J., Tirouvanziam, R., Garratt, L. W. OMIP-100: A flow cytometry panel to investigate human neutrophil subsets. *Cytometry Part A* (2024) 105, 81-87.
235. Park, L. M., Lannigan, J., Jaimes, M. C. OMIP-069: Forty-Color Full Spectrum Flow Cytometry Panel for Deep Immunophenotyping of Major Cell Subsets in Human Peripheral Blood. *Cytometry Part A* (2020) 97, 1044-1051.
236. Staser, K. W., Eades, W., Choi, J., Karpova, D., Dipersio, J. F. OMIP-042: 21-color flow cytometry to comprehensively immunophenotype major lymphocyte and myeloid subsets in human peripheral blood. *Cytometry Part A* (2018) 93, 186-189.
237. Lakschevitz, F. S., Hassanpour, S., Rubin, A., Fine, N., Sun, C., Glogauer, M. Identification of neutrophil surface marker changes in health and inflammation using high-throughput screening flow cytometry. *Exp Cell Res* (2016) 342, 200-9.
238. Mishra, H. K., Ma, J., Walcheck, B. Ectodomain Shedding by ADAM17: Its Role in Neutrophil Recruitment and the Impairment of This Process during Sepsis. *Frontiers in Cellular and Infection Microbiology* (2017) 7, 138.
239. Ivetic, A. A head-to-tail view of L-selectin and its impact on neutrophil behaviour. *Cell and Tissue Research* (2018) 371, 437-453.

240. Wang, Y., Wu, J., Newton, R., Bahaie, N. S., Long, C., Walcheck, B. ADAM17 cleaves CD16b (FcγRIIIb) in human neutrophils. *Biochim Biophys Acta* (2013) 1833, 680-5.
241. Wang, J., Chen, M., Li, S., Ye, R. D. Targeted Delivery of a Ligand-Drug Conjugate via Formyl Peptide Receptor 1 through Cholesterol-Dependent Endocytosis. *Mol Pharm* (2019) 16, 2636-2647.
242. Ganesh, K. and Joshi, M. B. Neutrophil sub-types in maintaining immune homeostasis during steady state, infections and sterile inflammation. *Inflammation Research* (2023) 72, 1175-1192.
243. McKenna, E., Mhaonaigh, A. U., Wubben, R., Dwivedi, A., Hurley, T., Kelly, L. A., Stevenson, N. J., Little, M. A., Molloy, E. J. Neutrophils: Need for Standardized Nomenclature. *Frontiers in Immunology* (2021) 12, 602963.
244. Allen, L. H. and Criss, A. K. Cell intrinsic functions of neutrophils and their manipulation by pathogens. *Curr Opin Immunol* (2019) 60, 124-129.
245. Soderholm, N., Vielfort, K., Hultenby, K., Aro, H. Pathogenic *Neisseria* hitchhike on the uropod of human neutrophils. *PLoS One* (2011) 6, e24353.
246. Johnson, M. B. and Criss, A. K. *Neisseria gonorrhoeae* phagosomes delay fusion with primary granules to enhance bacterial survival inside human neutrophils. *Cellular Microbiology* (2013) 15, 1323-1340.
247. Smirnov, A., Daily, K. P., Criss, A. K. Assembly of NADPH Oxidase in Human Neutrophils Is Modulated by the Opacity-Associated Protein Expression State of *Neisseria gonorrhoeae*. *Infection and Immunity* (2014) 82, 1036-1044.
248. Seib, K. L., Wu, H.-J., Kidd, S. P., Apicella, M. A., Jennings, M. P., McEwan, A. G. Defenses against Oxidative Stress in *Neisseria gonorrhoeae*: a System Tailored for a Challenging Environment. *Microbiology and Molecular Biology Reviews* (2006) 70, 344-361.
249. Ragland, S. A., Schaub, R. E., Hackett, K. T., Dillard, J. P., Criss, A. K. Two lytic transglycosylases in *Neisseria gonorrhoeae* impart resistance to killing by lysozyme and human neutrophils. *Cellular Microbiology* (2017) 19, e12662.
250. Ragland, S. A., Humbert, M. V., Christodoulides, M., Criss, A. K. *Neisseria gonorrhoeae* employs two protein inhibitors to evade killing by human lysozyme. *PLOS Pathogens* (2018) 14, e1007080.
251. Ragland, S. A., Gray, M. C., Melson, E. M., Kendall, M. M., Criss, A. K. Effect of Lipidation on the Localization and Activity of a Lysozyme Inhibitor in *Neisseria gonorrhoeae*. *Journal of Bacteriology* (2020) 202:8, e00633.
252. Atack, J. M., Ibranovic, I., Ong, C.-L. Y., Djoko, K. Y., Chen, N. H., Van den Hoven, R., Jennings, M. P., Edwards, J. L., McEwan, A. G. A Role for Lactate Dehydrogenases in the Survival of *Neisseria gonorrhoeae* in Human Polymorphonuclear Leukocytes and Cervical Epithelial Cells. *The Journal of Infectious Diseases* (2014) 210, 1311-1318.
253. Britigan, B. E., Klapper, D., Svendsen, T., Cohen, M. S. Phagocyte-derived lactate stimulates oxygen consumption by *Neisseria gonorrhoeae*.

An unrecognized aspect of the oxygen metabolism of phagocytosis. *Journal of Clinical Investigation* (1988) 81, 318-324.

254. Juneau, R. A., Stevens, J. S., Apicella, M. A., Criss, A. K. A thermonuclease of *Neisseria gonorrhoeae* enhances bacterial escape from killing by neutrophil extracellular traps. *J Infect Dis* (2015) 212, 316-24.
255. Ngampasutadol, J., Tran, C., Gulati, S., Blom, A. M., Jerse, E. A., Ram, S., Rice, P. A. Species-specificity of *Neisseria gonorrhoeae* infection: do human complement regulators contribute? *Vaccine* (2008) 26 Suppl 8, I62-6.
256. Adrian, J., Bonsignore, P., Hammer, S., Frickey, T., Hauck, C. R. Adaptation to Host-Specific Bacterial Pathogens Drives Rapid Evolution of a Human Innate Immune Receptor. *Current Biology* (2019) 29, 616-630.e5.
257. Miralda, I., Uriarte, S. M., McLeish, K. R. Multiple Phenotypic Changes Define Neutrophil Priming. *Frontiers in Cellular and Infection Microbiology* (2017) 7, 217.
258. London, D., Elhasid, R., Baron, S. Determination of reference intervals for neutrophil granular enzymes is affected by cell isolation techniques. *J Immunol Methods* (2022) 510, 113346.
259. Arko, R. J., Duncan, W. P., Brown, W. J., Peacock, W. L., Tomizawa, T. Immunity in infection with *Neisseria gonorrhoeae*: duration and serological response in the chimpanzee. *J Infect Dis* (1976) 133, 441-7.
260. Jerse, A. E., Wu, H., Packiam, M., Vonck, R. A., Begum, A. A., Garvin, L. E. Estradiol-Treated Female Mice as Surrogate Hosts for *Neisseria gonorrhoeae* Genital Tract Infections. *Frontiers in Microbiology* (2011) 2, 107.
261. Jerse, A. E. Experimental Gonococcal Genital Tract Infection and Opacity Protein Expression in Estradiol-Treated Mice. *Infection and Immunity* (1999) 67, 5699-5708.
262. Russell, M. W., Jerse, A. E., Gray-Owen, S. D. Progress Toward a Gonococcal Vaccine: The Way Forward. *Frontiers in Immunology* (2019) 10, 2517.
263. Packiam, M., Veit, S. J., Anderson, D. J., Ingalls, R. R., Jerse, A. E. Mouse Strain-Dependent Differences in Susceptibility to *Neisseria gonorrhoeae* Infection and Induction of Innate Immune Responses. *Infection and Immunity* (2010) 78, 433-440.
264. Deniset, J. F., Surewaard, B. G., Lee, W.-Y., Kubes, P. Splenic Ly6Ghigh mature and Ly6Gint immature neutrophils contribute to eradication of *S. pneumoniae*. *Journal of Experimental Medicine* (2017) 214, 1333-1350.
265. Rausch, P. G. and Moore, T. G. Granule enzymes of polymorphonuclear neutrophils: A phylogenetic comparison. *Blood* (1975) 46, 913-9.
266. Allen, L.-A. H. Closing the gap between murine neutrophils and neutrophil-like cell lines. *Journal of Leukocyte Biology* (2023) 114, 199-201.

267. Waltmann, A., Duncan, J. A., Pier, G. B., Cywes-Bentley, C., Cohen, M. S., Hobbs, M. M. (2021) Experimental Urethral Infection with *Neisseria gonorrhoeae*. Springer Nature Switzerland. 109-125.
268. Nudel, K., McClure, R., Moreau, M., Briars, E., Abrams, A. J., Tjaden, B., Su, X.-H., Trees, D., Rice, P. A., Massari, P., Genco, C. A. Transcriptome Analysis of *Neisseria gonorrhoeae* during Natural Infection Reveals Differential Expression of Antibiotic Resistance Determinants between Men and Women. *mSphere* (2018) 3:3, e00312.
269. Hobbs, M. M. and Duncan, J. A. (2019) Experimental Human Infection with *Neisseria gonorrhoeae*. Springer New York. 431-452.
270. Maurakis, S. A. and Cornelissen, C. N. Recent Progress Towards a Gonococcal Vaccine. *Frontiers in Cellular and Infection Microbiology* (2022) 12, 881392.
271. Waltmann, A., Chen, J. S., Duncan, J. A. Promising developments in gonococcal vaccines. *Curr Opin Infect Dis* (2024) 37, 63-69.
272. Song, W., Yu, Q., Wang, L.-C., Stein, D. C. Adaptation of *Neisseria gonorrhoeae* to the Female Reproductive Tract. *Microbiology Insights* (2020) 13, 117863612094707.
273. Lenz, J. D. and Dillard, J. P. Pathogenesis of *Neisseria gonorrhoeae* and the Host Defense in Ascending Infections of Human Fallopian Tube. *Frontiers in Immunology* (2018) 9, 2710.
274. Rest, R. F. and Frangipane, J. V. Growth of *Neisseria gonorrhoeae* in CMP-N-acetylneuraminic acid inhibits nonopsonic (opacity-associated outer membrane protein-mediated) interactions with human neutrophils. *Infection and Immunity* (1992) 60, 989-997.
275. Rest, R. F. and Shafer, W. M. Interactions of *Neisseria gonorrhoeae* with human neutrophils. *Clinical Microbiology Reviews* (1989) 2, S83-S91.
276. Reimer, A., Seufert, F., Weiwad, M., Ebert, J., Bzdyl, N. M., Kahler, C. M., Sarkar-Tyson, M., Holzgrabe, U., Rudel, T., Kozjak-Pavlovic, V. Inhibitors of macrophage infectivity potentiator-like PPIases affect Neisserial and Chlamydial pathogenicity. *Int J Antimicrob Agents* (2016) 48, 401-8.
277. Heydarian, M., Schweinlin, M., Schwarz, T., Rawal, R., Walles, H., Metzger, M., Rudel, T., Kozjak-Pavlovic, V. Triple co-culture and perfusion bioreactor for studying the interaction between *Neisseria gonorrhoeae* and neutrophils: A novel 3D tissue model for bacterial infection and immunity. *Journal of Tissue Engineering* (2021) 12, 204173142098880.
278. Xiao, S., Coppeta, J. R., Rogers, H. B., Isenberg, B. C., Zhu, J., Olalekan, S. A., McKinnon, K. E., Dokic, D., Rashedi, A. S., Haisenleder, D. J., Malpani, S. S., Arnold-Murray, C. A., Chen, K., Jiang, M., Bai, L., Nguyen, C. T., Zhang, J., Laronda, M. M., Hope, T. J., Maniar, K. P., Pavone, M. E., Avram, M. J., Sefton, E. C., Getsios, S., Burdette, J. E., Kim, J. J., Borenstein, J. T., Woodruff, T. K. A microfluidic culture model of the human reproductive tract and 28-day menstrual cycle. *Nature Communications* (2017) 8, 14584.

279. Pohlner, J., Halter, R., Beyreuther, K., Meyer, T. F. Gene structure and extracellular secretion of *Neisseria gonorrhoeae* IgA protease. *Nature* (1987) 325, 458-462.
280. Beck, S. C. and Meyer, T. F. IgA1 protease from *Neisseria gonorrhoeae* inhibits TNFα-mediated apoptosis of human monocytic cells. *FEBS Letters* (2000) 472, 287-292.
281. Senior, B. W., Stewart, W. W., Galloway, C., Kerr, M. A. Cleavage of the Hormone Human Chorionic Gonadotropin, by the Type 1 IgA1 Protease of *Neisseria gonorrhoeae*, and Its Implications. *The Journal of Infectious Diseases* (2001) 184, 922-925.
282. Lin, L., Ayala, P., Larson, J., Mulks, M., Fukuda, M., Carlsson, S. R., Enns, C., So, M. The *Neisseria* type 2 IgA1 protease cleaves LAMP1 and promotes survival of bacteria within epithelial cells. *Molecular Microbiology* (1997) 24, 1083-1094.
283. Li, L.-H., Lin, J.-S., Chiu, H.-W., Lin, W.-Y., Ju, T.-C., Chen, F.-H., Chernikov, O. V., Liu, M.-L., Chang, J.-C., Hsu, C.-H., Chen, A., Ka, S.-M., Gao, H.-W., Hua, K.-F. Mechanistic Insight Into the Activation of the NLRP3 Inflammasome by *Neisseria gonorrhoeae* in Macrophages. *Frontiers in Immunology* (2019) 10, 1815.
284. Liu, Y., Liu, W., Russell, M. W. Suppression of host adaptive immune responses by *Neisseria gonorrhoeae*: role of interleukin 10 and type 1 regulatory T cells. *Mucosal Immunology* (2014) 7, 165-176.
285. Pantelic, M., Kim, Y.-J., Bolland, S., Chen, I., Shively, J., Chen, T. *Neisseria gonorrhoeae* Kills Carcinoembryonic Antigen-Related Cellular Adhesion Molecule 1 (CD66a)-Expressing Human B Cells and Inhibits Antibody Production. *Infection and Immunity* (2005) 73, 4171-4179.
286. Gagliardi, M. C., Starnino, S., Teloni, R., Mariotti, S., Dal Conte, I., Di Carlo, A., Stefanelli, P. Circulating levels of interleukin-17A and interleukin-23 are increased in patients with gonococcal infection. *FEMS Immunology & Medical Microbiology* (2011) 61, 129-132.
287. Liu, Y., Hammer, L. A., Daamen, J., Stork, M., Egilmez, N. K., Russell, M. W. Microencapsulated IL-12 Drives Genital Tract Immune Responses to Intranasal Gonococcal Outer Membrane Vesicle Vaccine and Induces Resistance to Vaginal Infection with Diverse Strains of Neisseria gonorrhoeae. *mSphere* (2023) 8:1, e0038822.
288. Russell, M. W., Gray-Owen, S. D., Jerse, A. E. Editorial: Immunity to *Neisseria gonorrhoeae*. *Frontiers in Immunology* (2020) 11, 1375.
289. Cohen, M. S., Cannon, J. G., Jerse, A. E., Charniga, L. M., Isbey, S. F., Whicker, L. G. Human experimentation with *Neisseria gonorrhoeae*: rationale, methods, and implications for the biology of infection and vaccine development. *J Infect Dis* (1994) 169, 532-7.
290. Petousis-Harris, H., Paynter, J., Morgan, J., Saxton, P., McArdle, B., Goodyear-Smith, F., Black, S. Effectiveness of a group B outer membrane vesicle meningococcal vaccine against gonorrhoea in New Zealand: a retrospective case-control study. *Lancet* (2017) 390, 1603-1610.

291. Ruiz García, Y., Sohn, W.-Y., Seib, K. L., Taha, M.-K., Vázquez, J. A., De Lemos, A. P. S., Vadivelu, K., Pizza, M., Rappuoli, R., Bekkat-Berkani, R. Looking beyond meningococcal B with the 4CMenB vaccine: the *Neisseria* effect. *Vaccines* (2021) 6:1, 130.
292. Thng, C., Semchenko, E. A., Hughes, I., O'Sullivan, M., Seib, K. L. An open-label randomised controlled trial evaluating the efficacy of a meningococcal serogroup B (4CMenB) vaccine on *Neisseria gonorrhoeae* infection in gay and bisexual men: the MenGO study protocol. *BMC Public Health* (2023) 23:1, 607.
293. Semchenko, E. A., Tan, A., Borrow, R., Seib, K. L. The Serogroup B Meningococcal Vaccine Bexsero Elicits Antibodies to *Neisseria gonorrhoeae*. *Clin Infect Dis* (2019) 69, 1101-1111.
294. Leduc, I., Connolly, K. L., Begum, A., Underwood, K., Darnell, S., Shafer, W. M., Balthazar, J. T., MacIntyre, A. N., Sempowski, G. D., Duncan, J. A., Little, M. B., Rahman, N., Garges, E. C., Jerse, A. E. The serogroup B meningococcal outer membrane vesicle-based vaccine 4CMenB induces cross-species protection against *Neisseria gonorrhoeae*. *PLoS Pathog* (2020) 16, e1008602.
295. McQuillen, D. P., Gulati, S., Ram, S., Turner, A. K., Jani, D. B., Heeren, T. C., Rice, P. A. Complement processing and immunoglobulin binding to *Neisseria gonorrhoeae* determined *in vitro* simulates in vivo effects. *J Infect Dis* (1999) 179, 124-35.
296. Ross, S. C. and Densen, P. Opsonophagocytosis of *Neisseria gonorrhoeae*: interaction of local and disseminated isolates with complement and neutrophils. *J Infect Dis* (1985) 151, 33-41.
297. Podack, E. R. and Tschopp, J. Polymerization of the ninth component of complement (C9): formation of poly(C9) with a tubular ultrastructure resembling the membrane attack complex of complement. *Proc Natl Acad Sci U S A* (1982) 79, 574-8.
298. Shaughnessy, J., Ram, S., Bhattacharjee, A., Pedrosa, J., Tran, C., Horvath, G., Monks, B., Visintin, A., Jokiranta, T. S., Rice, P. A. Molecular Characterization of the Interaction between Sialylated *Neisseria gonorrhoeae* and Factor H. *Journal of Biological Chemistry* (2011) 286, 22235-22242.
299. Ram, S., MacKinnon, F. G., Gulati, S., McQuillen, D. P., Vogel, U., Frosch, M., Elkins, C., Guttormsen, H. K., Wetzler, L. M., Oppermann, M., Pangburn, M. K., Rice, P. A. The contrasting mechanisms of serum resistance of *Neisseria gonorrhoeae* and group B *Neisseria meningitidis*. *Mol Immunol* (1999) 36, 915-28.
300. Jarva, H., Ngampasutadol, J., Ram, S., Rice, P. A., Villoutreix, B. O., Blom, A. M. Molecular characterization of the interaction between porins of *Neisseria gonorrhoeae* and C4b-binding protein. *J Immunol* (2007) 179, 540-7.
301. Singh, B., Su, Y. C., Riesbeck, K. Vitronectin in bacterial pathogenesis: a host protein used in complement escape and cellular invasion. *Molecular Microbiology* (2010) 78, 545-560.

302. Xu, J. and Seifert, H. S. Analysis of Pilin Antigenic Variation in *Neisseria meningitidis* by Next-Generation Sequencing. *Journal of Bacteriology* (2018) 200:22, e00465.
303. Metruccio, M. M. E., Pigozzi, E., Roncarati, D., Berlanda Scorza, F., Norais, N., Hill, S. A., Scarlato, V., Delany, I. A Novel Phase Variation Mechanism in the Meningococcus Driven by a Ligand-Responsive Repressor and Differential Spacing of Distal Promoter Elements. *PLoS Pathogens* (2009) 5, e1000710.
304. Edwards, J. L., Jennings, M. P., Seib, K. L. *Neisseria gonorrhoeae* vaccine development: hope on the horizon? *Curr Opin Infect Dis* (2018) 31, 246-250.
305. Werner, L. M., Palmer, A., Smirnov, A., Belcher Dufrisne, M., Columbus, L., Criss, A. K. Imaging Flow Cytometry Analysis of CEACAM Binding to Opa-Expressing *Neisseria gonorrhoeae*. *Cytometry Part A* (2020) 97, 1081-1089.
306. Jensen, J. S. and Unemo, M. Antimicrobial treatment and resistance in sexually transmitted bacterial infections. *Nature Reviews Microbiology* (2024) 22, 435-450.
307. Nikaido, H. Molecular Basis of Bacterial Outer Membrane Permeability Revisited. *Microbiology and Molecular Biology Reviews* (2003) 67, 593-656.
308. Ghai, I. Electrophysiological Insights into Antibiotic Translocation and Resistance: The Impact of Outer Membrane Proteins. *Membranes (Basel)* (2024) 14:7, 161.
309. Heesterbeek, D. A. C., Martin, N. I., Velthuizen, A., Duijst, M., Ruyken, M., Wubbolts, R., Rooijakkers, S. H. M., Bardoel, B. W. Complement-dependent outer membrane perturbation sensitizes Gram-negative bacteria to Gram-positive specific antibiotics. *Scientific Reports* (2019) 9:1, 3074.
310. Bettoni, S., Maziarz, K., Stone, M. R. L., Blaskovich, M. A. T., Potempa, J., Bazzo, M. L., Unemo, M., Ram, S., Blom, A. M. Serum Complement Activation by C4BP-IgM Fusion Protein Can Restore Susceptibility to Antibiotics in *Neisseria gonorrhoeae*. *Frontiers in Immunology* (2021) 12, 726801.
311. Klobucar, K. and Brown, E. D. New potentiators of ineffective antibiotics: Targeting the Gram-negative outer membrane to overcome intrinsic resistance. *Curr Opin Chem Biol* (2022) 66, 102099.
312. Zhong, X., Deng, K., Yang, X., Song, X., Zou, Y., Zhou, X., Tang, H., Li, L., Fu, Y., Yin, Z., Wan, H., Zhao, X. Brevicidine acts as an effective sensitizer of outer membrane-impermeable conventional antibiotics for *Acinetobacter baumannii* treatment. *Frontiers in Microbiology* (2023) 14, 1304198.
313. Ramirez, D. M., Dhiman, S., Mukherjee, A., Wimalasekara, R., Schweizer, F. Application of tobramycin benzyl ether as an antibiotic adjuvant capable of sensitizing multidrug-resistant Gram-negative bacteria to rifampicin. *RSC Med Chem* (2024) 15, 1055-1065.

314. Benn, G., Bortolini, C., Roberts, D. M., Pyne, A. L. B., Holden, S., Hoogenboom, B. W. Complement-mediated killing of *Escherichia coli* by mechanical destabilization of the cell envelope. *The EMBO Journal* (2024) 43, 6152-6160.
315. Barratt-Due, A., Thorgersen, E. B., Lindstad, J. K., Pharo, A., Lissina, O., Lambris, J. D., Nunn, M. A., Mollnes, T. E. *Ornithodoros moubata* Complement Inhibitor Is an Equally Effective C5 Inhibitor in Pigs and Humans. *The Journal of Immunology* (2011) 187, 4913-4919.
316. Liao, M., Gong, H., Liu, H., Shen, K., Ge, T., King, S., Schweins, R., McBain, A. J., Hu, X., Lu, J. R. Combination of a pH-responsive peptide amphiphile and a conventional antibiotic in treating Gram-negative bacteria. *J Colloid Interface Sci* (2024) 659, 397-412.
317. Lapinska, U., Voliotis, M., Lee, K. K., Campey, A., Stone, M. R. L., Tuck, B., Phetsang, W., Zhang, B., Tsaneva-Atanasova, K., Blaskovich, M. A. T., Pagliara, S. Fast bacterial growth reduces antibiotic accumulation and efficacy. *Elife* (2022) 11, e74062.
318. Tomberg, J., Unemo, M., Ohnishi, M., Davies, C., Nicholas, R. A. Identification of Amino Acids Conferring High-Level Resistance to Expanded-Spectrum Cephalosporins in the *penA* Gene from *Neisseria gonorrhoeae* Strain H041. *Antimicrobial Agents and Chemotherapy* (2013) 57, 3029-3036.
319. Humphries, R., Bobenchik, A. M., Hindler, J. A., Schuetz, A. N. Overview of Changes to the Clinical and Laboratory Standards Institute Performance Standards for Antimicrobial Susceptibility Testing, M100, 31st Edition. *J Clin Microbiol* (2021) 59, e0021321.
320. Raccagni, A. R., Ranzenigo, M., Bruzzesi, E., Maci, C., Castagna, A., Nozza, S. *Neisseria gonorrhoeae* Antimicrobial Resistance: The Future of Antibiotic Therapy. *Journal of Clinical Medicine* (2023) 12, 7767.
321. Reichert, E. and Grad, Y. H. Effects of doxycycline post-exposure prophylaxis for prevention of sexually transmitted infections on gonorrhoea prevalence and antimicrobial resistance among men who have sex with men in the USA: a modelling study. *Lancet Microbe* (2024) 5, 100926.
322. Bachmann, L. H., Barbee, L. A., Chan, P., Reno, H., Workowski, K. A., Hoover, K., Mermin, J., Mena, L. CDC Clinical Guidelines on the Use of Doxycycline Postexposure Prophylaxis for Bacterial Sexually Transmitted Infection Prevention, United States, 2024. *MMWR Recomm Rep* (2024) 73, 1-8.
323. Ross, J. D. C., Brittain, C., Cole, M., Dewsnap, C., Harding, J., Hepburn, T., Jackson, L., Keogh, M., Lawrence, T., Montgomery, A. A., Roberts, T. E., Sprange, K., Tan, W., Thandi, S., White, J., Wilson, J., Duley, L. Gentamicin compared with ceftriaxone for the treatment of gonorrhoea (G-ToG): a randomised non-inferiority trial. *The Lancet* (2019) 393, 2511-2520.
324. Kirkcaldy, R. D., Weinstock, H. S., Moore, P. C., Philip, S. S., Wiesenfeld, H. C., Papp, J. R., Kerndt, P. R., Johnson, S., Ghanem, K. G., Hook, E. W., Newman, L. M., Dowell, D., Deal, C., Glock, J., Venkatasubramanian,

L., McNeil, L., Perlowski, C., Lee, J. Y., Lensing, S., Trainor, N., Fuller, S., Herrera, A., Carlson, J. S., Harbison, H., Lenderman, C., Dixon, P., Whittington, A., Macio, I., Priest, C., Jett, A., Campbell, T., Uniyal, A., Royal, L., Mejia, M., Vonghack, J., Tobias, S., Zenilman, J., Long, J., Harvey, A., Pettus, K., Sharpe, S. The Efficacy and Safety of Gentamicin Plus Azithromycin and Gemifloxacin Plus Azithromycin as Treatment of Uncomplicated Gonorrhea. *Clinical Infectious Diseases* (2014) 59, 1083-1091.

325. Bakheit, A. H., Al-Hadiya, B. M., Abd-Elgalil, A. A. Azithromycin. *Profiles Drug Subst Excip Relat Methodol* (2014) 39, 1-40.
326. Nam, K. H. Crystal Structure of Human Lysozyme Complexed with N-Acetyl-α-d-glucosamine. *Applied Sciences* (2022) 12, 4363.
327. Colvin, J. R. THE SIZE AND SHAPE OF LYSOZYME. *Canadian Journal of Chemistry* (1952) 30, 831-834.
328. Berends, E. T. M., Kuipers, A., Ravesloot, M. M., Urbanus, R. T., Rooijakkers, S. H. M. Bacteria under stress by complement and coagulation. *FEMS Microbiology Reviews* (2014) 38, 1146-1171.
329. Zhang, G., Meredith, T. C., Kahne, D. On the essentiality of lipopolysaccharide to Gram-negative bacteria. *Current Opinion in Microbiology* (2013) 16, 779-785.
330. Preston, A., Mandrell, R. E., Gibson, B. W., Apicella, M. A. The lipooligosaccharides of pathogenic gram-negative bacteria. *Crit Rev Microbiol* (1996) 22, 139-80.
331. Rahman, M. M., Kolli, V. S. K., Kahler, C. M., Shih, G., Stephens, D. S., Carlson, R. W. The membrane phospholipids of *Neisseria meningitidis* and *Neisseria gonorrhoeae* as characterized by fast atom bombardment mass spectrometry. *Microbiology* (2000) 146, 1901-1911.
332. Rowlett, V. W., Mallampalli, V. K. P. S., Karlstaedt, A., Dowhan, W., Taegtmeyer, H., Margolin, W., Vitrac, H. Impact of Membrane Phospholipid Alterations in *Escherichia coli* on Cellular Function and Bacterial Stress Adaptation. *Journal of Bacteriology* (2017) 199, JB.00849-16.
333. Sud, I. J. and Feingold, D. S. Phospholipids and fatty acids of *Neisseria gonorrhoeae*. *Journal of Bacteriology* (1975) 124, 713-717.
334. Hill, S. A. and Judd, R. C. Identification and characterization of peptidoglycan-associated proteins in *Neisseria gonorrhoeae*. *Infection and Immunity* (1989) 57, 3612-3618.
335. Cho, S.-H., Dekoninck, K., Collet, J.-F. Envelope-Stress Sensing Mechanism of Rcs and Cpx Signaling Pathways in Gram-Negative Bacteria. *Journal of Microbiology* (2023) 61, 317-329.
336. Wall, E., Majdalani, N., Gottesman, S. The Complex Rcs Regulatory Cascade. *Annu Rev Microbiol* (2018) 72, 111-139.
337. Lach, S. R., Kumar, S., Kim, S., Im, W., Konovalova, A. Conformational rearrangements in the sensory RcsF/OMP complex mediate signal transduction across the bacterial cell envelope. *PLoS Genet* (2023) 19, e1010601.

338. Criss, A. K. and Seifert, H. S. A bacterial siren song: intimate interactions between *Neisseria* and neutrophils. *Nature Reviews Microbiology* (2012) 10, 178-190.
339. Jerse, A. E., Bash, M. C., Russell, M. W. Vaccines against gonorrhea: Current status and future challenges. *Vaccine* (2014) 32, 1579-1587.
340. Rotman, E. and Seifert, H. S. The Genetics of *Neisseria* Species. *Annual Review of Genetics* (2014) 48, 405-431.
341. Dahlback, B. and Podack, E. R. Characterization of human S protein, an inhibitor of the membrane attack complex of complement. Demonstration of a free reactive thiol group. *Biochemistry* (1985) 24, 2368-74.
342. Mandrell, R., Schneider, H., Apicella, M., Zollinger, W., Rice, P. A., Griffiss, J. M. Antigenic and physical diversity of *Neisseria gonorrhoeae* lipooligosaccharides. *Infection and Immunity* (1986) 54, 63-69.
343. Parzych, E. M., Gulati, S., Zheng, B., Bah, M. A., Elliott, S. T. C., Chu, J. D., Nowak, N., Reed, G. W., Beurskens, F. J., Schuurman, J., Rice, P. A., Weiner, D. B., Ram, S. Synthetic DNA Delivery of an Optimized and Engineered Monoclonal Antibody Provides Rapid and Prolonged Protection against Experimental Gonococcal Infection. *mBio* (2021) 12:2, e00242.
344. Seifert, H. S., Ajioka, R. S., Marchal, C., Sparling, P. F., So, M. DNA transformation leads to pilin antigenic variation in *Neisseria gonorrhoeae*. *Nature* (1988) 336, 392-5.
345. Ozer, E. A., Prister, L. L., Yin, S., Ward, B. H., Ivanov, S., Seifert, H. S. PacBio Amplicon Sequencing Method To Measure Pilin Antigenic Variation Frequencies of *Neisseria gonorrhoeae*. *mSphere* (2019) 4:5, e00562.
346. Seifert, H. S., Wright, C. J., Jerse, A. E., Cohen, M. S., Cannon, J. G. Multiple gonococcal pilin antigenic variants are produced during experimental human infections. *Journal of Clinical Investigation* (1994) 93, 2744-2749.
347. Chen, A. and Seifert, H. S. Structure-Function Studies of the *Neisseria gonorrhoeae* Major Outer Membrane Porin. *Infection and Immunity* (2013) 81, 4383-4391.
348. Santos, G. F., Deck, R. R., Donnelly, J., Blackwelder, W., Granoff, D. M. Importance of Complement Source in Measuring Meningococcal Bactericidal Titers. *Clinical Diagnostic Laboratory Immunology* (2001) 8, 616-623.
349. Morgan, B. P. Complement Methods and Protocols. (2000).
350. Amjadi, F., Salehi, E., Mehdizadeh, M., Aflatoonian, R. Role of the innate immunity in female reproductive tract. *Advanced Biomedical Research* (2014) 3, 1.
351. Begg, E. J., Barclay, M. L., Kirkpatrick, C. J. M. The therapeutic monitoring of antimicrobial agents. *British Journal of Clinical Pharmacology* (1999) 47, 23-30.
352. Scheibenpflug, R., Obermuller, M., Reznicek, G., Neuper, O., Lamm, W. W., Raderer, M., Lagler, H. Azithromycin concentrations during long-term

regimen, a pilot study in patients with MALT lymphoma. *Sci Rep* (2021) 11, 18460.
353. Schleibinger, M., Steinbach, C. L., Töpper, C., Kratzer, A., Liebchen, U., Kees, F., Salzberger, B., Kees, M. G. Protein binding characteristics and pharmacokinetics of ceftriaxone in intensive care unit patients. *British Journal of Clinical Pharmacology* (2015) 80, 525-533.
354. Luckey, A., Alirol, E., Delhomme, S., O'Donnell, J., Bettiol, E., Mueller, J., O'Brien, S., Gillon, J. Y. Effect of food on the pharmacokinetics of zoliflodacin granules for oral suspension: Phase I open-label randomized cross-over study in healthy subjects. *Clinical and Translational Science* (2023) 16, 770-780.
355. Haaland, R. E., Fountain, J., Edwards, T. E., Dinh, C., Martin, A., Omoyege, D., Conway-Washington, C., Kelley, C. F., Heneine, W. Pharmacokinetics of single dose doxycycline in the rectum, vagina, and urethra: implications for prevention of bacterial sexually transmitted infections. *EBioMedicine* (2024) 101, 105037.
356. Cattaneo, D., Orlando, G., Cozzi, V., Cordier, L., Baldelli, S., Merli, S., Fucile, S., Gulisano, C., Rizzardini, G., Clementi, E. Linezolid plasma concentrations and occurrence of drug-related haematological toxicity in patients with gram-positive infections. *Int J Antimicrob Agents* (2013) 41, 586-9.
357. Kowalska-Krochmal, B. and Dudek-Wicher, R. The Minimum Inhibitory Concentration of Antibiotics: Methods, Interpretation, Clinical Relevance. *Pathogens* (2021) 10, 165.
358. Lacy, P. Control of granule exocytosis in neutrophils. *Frontiers in Bioscience* (2008) Volume, 5559.
359. Terstappen, L. W., Buescher, S., Nguyen, M., Reading, C. Differentiation and maturation of growth factor expanded human hematopoietic progenitors assessed by multidimensional flow cytometry. *Leukemia* (1992) 6, 1001-10.
360. Carulli, G. Applications of flow cytometry in the study of human neutrophil biology and pathology. *Hematopathol Mol Hematol* (1996) 10, 39-61.
361. Cowland, J. B. and Borregaard, N. Isolation of neutrophil precursors from bone marrow for biochemical and transcriptional analysis. *J Immunol Methods* (1999) 232, 191-200.
362. Aanei, C. M., Jacob, M. C., Veyrat-Masson, R., Picot, T., Rosenthal-Allieri, M. A., Lhoumeau, A. C., Ticchioni, M., Dumezy, F., Campos Catafal, L. Database-guided Flow-cytometry for Evaluation of Bone Marrow Myeloid Cell Maturation. *J Vis Exp* (2018) 141.
363. Evrard, M., Kwok, I. W. H., Chong, S. Z., Teng, K. W. W., Becht, E., Chen, J., Sieow, J. L., Penny, H. L., Ching, G. C., Devi, S., Adrover, J. M., Li, J. L. Y., Liong, K. H., Tan, L., Poon, Z., Foo, S., Chua, J. W., Su, I. H., Balabanian, K., Bachelerie, F., Biswas, S. K., Larbi, A., Hwang, W. Y. K., Madan, V., Koeffler, H. P., Wong, S. C., Newell, E. W., Hidalgo, A., Ginhoux, F., Ng, L. G. Developmental Analysis of Bone Marrow

Neutrophils Reveals Populations Specialized in Expansion, Trafficking, and Effector Functions. *Immunity* (2018) 48, 364-379.e8.
364. Ledderose, C., Hashiguchi, N., Valsami, E. A., Rusu, C., Junger, W. G. Optimized flow cytometry assays to monitor neutrophil activation in human and mouse whole blood samples. *J Immunol Methods* (2023) 512, 113403.
365. Masuda, S., Shimizu, S., Matsuo, J., Nishibata, Y., Kusunoki, Y., Hattanda, F., Shida, H., Nakazawa, D., Tomaru, U., Atsumi, T., Ishizu, A. Measurement of NET formation in vitro and in vivo by flow cytometry. *Cytometry Part A* (2017) 91, 822-829.
366. Alvarez-Larran, A., Toll, T., Rives, S., Estella, J. Assessment of neutrophil activation in whole blood by flow cytometry. *Clinical and Laboratory Haematology* (2005) 27, 41-46.
367. Stratmann, A. E. P., Wohlgemuth, L., Erber, M. E., Bernhard, S., Hug, S., Fauler, M., Vidoni, L., Mohamed, A. O. K., Thomaß, B. D., Münnich, F., Stukan, L., Föhr, K. J., Mannes, M., Huber-Lang, M. S., Messerer, D. A. C. Simultaneous Measurement of Changes in Neutrophil Granulocyte Membrane Potential, Intracellular pH, and Cell Size by Multiparametric Flow Cytometry. *Biomedicines* (2021) 9, 1504.
368. Timmer, K. D., Floyd, D. J., Scherer, A. K., Crossen, A. J., Atallah, J., Viens, A. L., Sykes, D. B., Mansour, M. K. Multiparametric Profiling of Neutrophil Function via a High-Throughput Flow Cytometry-Based Assay. *Cells* (2023) 12, 743.
369. Zhu, Y. P., Eggert, T., Araujo, D. J., Vijayanand, P., Ottensmeier, C. H., Hedrick, C. C. CyTOF mass cytometry reveals phenotypically distinct human blood neutrophil populations differentially correlated with melanoma stage. *Journal for ImmunoTherapy of Cancer* (2020) 8, e000473.
370. Meghraoui-Kheddar, A., Chousterman, B. G., Guillou, N., Barone, S. M., Granjeaud, S., Vallet, H., Corneau, A., Guessous, K., De Roquetaillade, C., Boissonnas, A., Irish, J. M., Combadière, C. Two New Neutrophil Subsets Define a Discriminating Sepsis Signature. *American Journal of Respiratory and Critical Care Medicine* (2022) 205, 46-59.
371. Zhang, T., Warden, A. R., Li, Y., Ding, X. Progress and applications of mass cytometry in sketching immune landscapes. *Clin Transl Med* (2020) 10, e206.
372. Behbehani, G. K. Applications of Mass Cytometry in Clinical Medicine: The Promise and Perils of Clinical CyTOF. *Clin Lab Med* (2017) 37, 945-964.
373. Robinson, J. P. and Rajwa, B. Spectral flow cytometry: Fundamentals and future impact. *Methods Cell Biol* (2024) 186, 311-332.
374. Marsh-Wakefield, F. M., Mitchell, A. J., Norton, S. E., Ashhurst, T. M., Leman, J. K., Roberts, J. M., Harte, J. E., McGuire, H. M., Kemp, R. A. Making the most of high-dimensional cytometry data. *Immunology & Cell Biology* (2021) 99, 680-696.

375. Parthasarathy, U., Kuang, Y., Thakur, G., Hogan, J. D., Wyche, T. P., Norton, J. E., Jr., Killough, J. R., Sana, T. R., Beakes, C., Shyong, B., Zhang, R. N., Gutierrez, D. A., Filbin, M., Christiani, D. C., Therien, A. G., Woelk, C. H., White, C. H., Martinelli, R. Distinct subsets of neutrophils crosstalk with cytokines and metabolites in patients with sepsis. *iScience* (2023) 26, 105948.
376. Kuang, Y., Parthasarathy, U., Martinelli, R. Protocol for density gradient neutrophil isolation and flow cytometry-based characterization from human peripheral blood. *STAR Protoc* (2023) 4, 102497.
377. Van Staveren, S., Ten Haaf, T., Klöpping, M., Hilvering, B., Tinnevelt, G. H., De Ruiter, K., Piacentini, M. F., Roelands, B., Meeusen, R., De Koning, J. J., Jansen, J. J., Vrisekoop, N., Koenderman, L. Multi-dimensional flow cytometry analysis reveals increasing changes in the systemic neutrophil compartment during seven consecutive days of endurance exercise. *PLOS ONE* (2018) 13, e0206175.
378. Becht, E., McInnes, L., Healy, J., Dutertre, C.-A., Kwok, I. W. H., Ng, L. G., Ginhoux, F., Newell, E. W. Dimensionality reduction for visualizing single-cell data using UMAP. *Nature Biotechnology* (2019) 37, 38-44.
379. Van der Maaten, L. and Hinton, G. Visualizing data using t-SNE. *Journal of machine learning research* (2008) 9:86, 2579-2605.
380. Konrad, F. M., Wohlert, J., Gamper-Tsigaras, J., Ngamsri, K.-C., Reutershan, J. How Adhesion Molecule Patterns Change While Neutrophils Traffic through the Lung during Inflammation. *Mediators of Inflammation* (2019) 2019, 1-16.
381. Ferrer-Font, L., Small, S. J., Hyde, E., Pilkington, K. R., Price, K. M. (2024) Panel Design and Optimization for Full Spectrum Flow Cytometry. Springer US. 99-124.
382. Foster, C. A. VCAM-1/α4-integrin adhesion pathway: Therapeutic target for allergic inflammatory disorders. *Journal of Allergy and Clinical Immunology* (1996) 98, S270-S277.
383. Hafeman, D. G., McConnell, H. M., Gray, J. W., Dean, P. N. Neutrophil activation monitored by flow cytometry: stimulation by phorbol diester is an all-or-none event. *Science* (1982) 215, 673-5.
384. Damascena, H. L., Silveira, W. A. A., Castro, M. S., Fontes, W. Neutrophil Activated by the Famous and Potent PMA (Phorbol Myristate Acetate). *Cells* (2022) 11, 2889.
385. Degroote, R. L., Weigand, M., Hauck, S. M., Deeg, C. A. IL8 and PMA Trigger the Regulation of Different Biological Processes in Granulocyte Activation. *Frontiers in Immunology* (2020) 10, 3064.
386. Videm, V. and Strand, E. Changes in Neutrophil Surface-Receptor Expression After Stimulation with FMLP, Endotoxin, Interleukin-8 and Activated Complement Compared to Degranulation. *Scandinavian Journal of Immunology* (2004) 59, 25-33.
387. Farrell, C. F. and Rest, R. F. Up-regulation of human neutrophil receptors for *Neisseria gonorrhoeae* expressing PII outer membrane proteins. *Infection and Immunity* (1990) 58, 2777-2784.

388. Brun, E. (2022) Investigating Human Neutrophil Phenotypes that Associate with *Neisseria gonorrhoeae*. University of Toronto. (2022) Thesis.
389. Tay, S. H., Celhar, T., Fairhurst, A. M. Low-Density Neutrophils in Systemic Lupus Erythematosus. *Arthritis & Rheumatology* (2020) 72, 1587-1595.
390. Jin, F. and Wang, F. The physiological and pathological roles and applications of sialyl Lewis x, a common carbohydrate ligand of the three selectins. *Glycoconj J* (2020) 37, 277-291.
391. Cao, H. and Crocker, P. R. Evolution of CD33-related siglecs: regulating host immune functions and escaping pathogen exploitation? *Immunology* (2011) 132, 18-26.
392. Spurgeon, B. E. J. and Naseem, K. M. Platelet Flow Cytometry: Instrument Setup, Controls, and Panel Performance. *Cytometry Part B: Clinical Cytometry* (2020) 98, 19-27.
393. Tung, J. W., Heydari, K., Tirouvanziam, R., Sahaf, B., Parks, D. R., Herzenberg, L. A., Herzenberg, L. A. Modern Flow Cytometry: A Practical Approach. *Clinics in Laboratory Medicine* (2007) 27, 453-468.
394. Wiesner, P. J. and Thompson, S. E. Gonococcal diseases. *Dis Mon* (1980) 26, 1-44.
395. Simons, M. P., Nauseef, W. M., Apicella, M. A. Interactions of *Neisseria gonorrhoeae* with Adherent Polymorphonuclear Leukocytes. *Infection and Immunity* (2005) 73, 1971-1977.
396. Criss, A. K., Katz, B. Z., Seifert, H. S. Resistance of *Neisseria gonorrhoeae* to non-oxidative killing by adherent human polymorphonuclear leucocytes. *Cellular Microbiology* (2009) 11, 1074-1087.
397. Németh, T. and Mócsai, A. Feedback Amplification of Neutrophil Function. *Trends in Immunology* (2016) 37, 412-424.
398. Kalafati, L., Hatzioannou, A., Hajishengallis, G., Chavakis, T. The role of neutrophils in trained immunity. *Immunological Reviews* (2023) 314, 142-157.
399. Xie, X., Shi, Q., Wu, P., Zhang, X., Kambara, H., Su, J., Yu, H., Park, S.-Y., Guo, R., Ren, Q., Zhang, S., Xu, Y., Silberstein, L. E., Cheng, T., Ma, F., Li, C., Luo, H. R. Single-cell transcriptome profiling reveals neutrophil heterogeneity in homeostasis and infection. *Nature Immunology* (2020) 21, 1119-1133.
400. Yin, S., Li, C., Zhang, Y., Yin, H., Fan, Z., Ye, X., Hu, H., Li, T. A Novel Tumor-Associated Neutrophil-Related Risk Signature Based on Single-Cell and Bulk RNA-Sequencing Analyses Predicts the Prognosis and Immune Landscape of Breast Cancer. *Journal of Cancer* (2024) 15, 5655-5671.
401. De Oliveira, S., Rosowski, E. E., Huttenlocher, A. Neutrophil migration in infection and wound repair: going forward in reverse. *Nature Reviews Immunology* (2016) 16, 378-391.

402. Zemans, R. L., Colgan, S. P., Downey, G. P. Transepithelial Migration of Neutrophils. *American Journal of Respiratory Cell and Molecular Biology* (2009) 40, 519-535.
403. Lee, W. Y., Chin, A. C., Voss, S., Parkos, C. A. In Vitro Neutrophil Transepithelial Migration. Humana Press. 205-216.
404. Johnson, M. B. and Criss, A. K. Fluorescence Microscopy Methods for Determining the Viability of Bacteria in Association with Mammalian Cells. *Journal of Visualized Experiments* (2013) 79, 50729.
405. Ayala, P., Wilbur, J. S., Wetzler, L. M., Tainer, J. A., Snyder, A., So, M. The pilus and porin of *Neisseria gonorrhoeae* cooperatively induce Ca2+ transients in infected epithelial cells. *Cellular Microbiology* (2005) 7, 1736-1748.
406. Källström, H., Islam, M. S., Berggren, P.-O., Jonsson, A.-B. Cell Signaling by the Type IV Pili of Pathogenic *Neisseria*. *Journal of Biological Chemistry* (1998) 273, 21777-21782.
407. Murakami, M. and Kudo, I. Phospholipase A2. *Journal of Biochemistry* (2002) 131, 285-292.
408. Shirai, Y. and Saito, N. Activation Mechanisms of Protein Kinase C: Maturation, Catalytic Activation, and Targeting. *Journal of Biochemistry* (2002) 132, 663-668.
409. Lamb, E. R., Glomski, I. J., Harper, T. A., Solga, M. D., Criss, A. K. High-dimensional spectral flow cytometry of activation and phagocytosis by peripheral human polymorphonuclear leukocytes. *Journal of Leukocyte Biology* (2025) e0014125.
410. Ray, J. C., Smirnov, A., Maurakis, S. A., Harrison, S. A., Ke, E., Chazin, W. J., Cornelissen, C. N., Criss, A. K. Adherence Enables *Neisseria gonorrhoeae* to Overcome Zinc Limitation Imposed by Nutritional Immunity Proteins. *Infection and Immunity* (2022) 90:3, e0000922.
411. Fichorova, R. N., Rheinwald, J. G., Anderson, D. J. Generation of Papillomavirus-Immortalized Cell Lines from Normal Human Ectocervical, Endocervical, and Vaginal Epithelium that Maintain Expression of Tissue-Specific Differentiation Proteins1. *Biology of Reproduction* (1997) 57, 847-855.
412. Rossi, R. M., Yum, L., Agaisse, H., Payne, S. M. Cardiolipin Synthesis and Outer Membrane Localization Are Required for *Shigella flexneri* Virulence. *mBio* (2017) 8:4, e01199.
413. Ragland, S. A. and Criss, A. K. From bacterial killing to immune modulation: Recent insights into the functions of lysozyme. *PLOS Pathogens* (2017) 13, e1006512.
414. Gao, J., Hu, X., Xu, C., Guo, M., Li, S., Yang, F., Pan, X., Zhou, F., Jin, Y., Bai, F., Cheng, Z., Wu, Z., Chen, S., Huang, X., Wu, W. Neutrophil-mediated delivery of the combination of colistin and azithromycin for the treatment of bacterial infection. *iScience* (2022) 25, 105035.
415. Langereis, J. D., Van Den Broek, B., Franssen, S., Joosten, I., Blijlevens, N. M. A., De Jonge, M. I., Langemeijer, S. Eculizumab impairs *Neisseria*

meningitidis serogroup B killing in whole blood despite 4CMenB vaccination of PNH patients. *Blood Advances* (2020) 4, 3615-3620.

416. Sprong, T., Brandtzaeg, P., Fung, M., Pharo, A. M., Høiby, E. A., Michaelsen, T. E., Aase, A., Van Der Meer, J. W. M., Van Deuren, M., Mollnes, T. E. Inhibition of C5a-induced inflammation with preserved C5b-9-mediated bactericidal activity in a human whole blood model of meningococcal sepsis. *Blood* (2003) 102, 3702-3710.
417. Granoff, D. M. Relative importance of complement-mediated bactericidal and opsonic activity for protection against meningococcal disease. *Vaccine* (2009) 27, B117-B125.